

Linking Rap to Rho:
Rap GTPases control ArhGAP29 in
endothelial barrier function

Anneke Post



ISBN/EAN: 978-90-393-6148-1 © Post, 2014

No part of this thesis may be reproduced in any form without prior written permission of the author.

Printed by: Gildeprint drukkerijen - Ede, the Netherlands.

Cover: "Molecule And Communication Background". © Milos Dizajn

The printing of this thesis was financially supported by:

Linking Rap to Rho: Rap GTPases control ArhGAP29 in endothelial barrier function

Rap aan Rho koppelen:

Rap GTPases reguleren de endotheliale barrière
functie via ArhGAP29

(met een samenvatting in het Nederlands)

Proefschrift

ter verkrijging van de graad van doctor aan de Universiteit Utrecht op
gezag van de rector magnificus, prof. dr. G. J. van der Zwaan, ingevolge
het besluit van het college voor promoties in het openbaar te verdedigen
op maandag 30 juni 2014 des middags te 2.30 uur

door

Anneke Post

geboren op 19 maart 1983 te Boston, MA, Verenigde Staten

Promotor: prof. dr. J.L. Bos

TABLE OF CONTENTS

Chapter 1	General introduction Linking Rap to Rho GTPases: Hierarchical communication and spatial regulation of cytoskeletal driven processes	7
	Thesis outline	23
Chapter 2	Ezrin is required for efficient Rap1-induced cell spreading	25
Chapter 3	ERM proteins integrate Rap1 up- and downstream signaling by binding Epac1 and Radil to regulate cell spreading	51
Chapter 4	Rasip1 mediates Rap1 regulation of Rho in endothelial barrier function through ArhGAP29	61
Chapter 5	Rap1 spatially controls ArhGAP29 to inhibit Rho signaling during endothelial barrier regulation	83
Chapter 6	Rap1 signaling in endothelial barrier control	99
Chapter 7	Restriction of apical brush border localization by PTPL1	111
Chapter 8	Discussion	125
Appendices	References	138
	Nederlandse Samenvatting	155
	Curriculum Vitae	160
	Publications	161
	Dankwoord	162

CHAPTER

GENERAL INTRODUCTION

LINKING RAP TO RHO GTPASES:
HIERARCHICAL COMMUNICATION
AND SPATIAL REGULATION OF
CYTOSKELETON-DRIVEN PROCESSES

1

ABSTRACT

The main function of the small GTPase Rap1 is to translate spatial and temporal cues at the plasma membrane into localized actin dynamics, through which it regulates actin cytoskeleton-driven processes, such as cell adhesion, migration and polarity. These spatial and temporal cues control when and where Rap1 is activated, by impinging on RapGEFs. Once activated, Rap1 modulates Rho GTPase signaling, the master regulators of actin cytoskeletal dynamics. It does so by recruiting various RhoGEFs and GAPs, either through direct binding or through adaptor proteins, to the sites of action. In this review I summarize the evidence for the interaction between Rap1 and Rho GTPase signaling and discuss the outstanding questions. Following a brief general introduction on Rap and Rho GTPases, I will discuss how Rap may regulate Rho GTPase signaling per biological processes they are involved in, e.i. cell spreading, cell-cell adhesion, cell migration, polarity and neuron development. Furthermore, I will briefly discuss the interconnectivity between Rap and Rho GTPase signaling from an evolutionary point of view.

INTRODUCTION

Small GTPases are important signaling molecules, involved in a plethora of biological processes. By cycling between an inactive, GDP-bound state and active, GTP-bound state, small GTPases can quickly change their on/off state. Spatiotemporal control of this cycling is regulated by guanine nucleotide exchange factors (GEFs) and GTPase activating proteins (GAPs). GEFs activate small GTPases by displacing bound GDP from the nucleotide-binding pocket, allowing binding of the more abundant GTP in the cell. Binding of GTP induces a conformational change, creating a binding interface for effector proteins, thus referred to as the 'on' state. The intrinsic hydrolyzing activity of small GTPases is very low, therefore efficient inactivation of GTPases requires GAPs, which increase the hydrolysis rate (reviewed in ¹) (Fig. 1).

The amount of GEFs and GAPs greatly outnumbers the small GTPases and it is becoming clear that the cellular distribution and activation mechanisms of these GEFs and GAPs control when and where GTPases are activated, thereby determining the biological outcome. Typically, GEFs and GAPs are multidomain structures, comprising a catalytic domain and regulatory regions. Protein-protein or protein-lipid interactions, second messenger binding and posttranslational modifications may affect their catalytic activity and/or their subcellular localization, temporally and spatially regulating their target GTPases, an important feature of GTPase signaling ¹.

Over 60 different small GTPases exist in mammals and can be roughly divided into five families: Ras, Rho, Rab, Arf and Ran ². The Rho family of small GTPases are key regulators of cytoskeletal dynamics, thereby regulating morphogenetic events, such as cell adhesion and spreading, cell-cell adhesion, cell migration, cell polarity, axonal guidance, vesicle trafficking and cell division. Although Rap GTPases belong to the Ras family, they are involved in distinct biological processes. Rap proteins are best known for their role in integrin-based cell adhesion and spreading, cell-cell adhesion, cell migration and axonal guidance, however Rap proteins have been implicated in many other biological functions. Interestingly, most biological processes regulated by Rap proteins involve modulation of the actin cytoskeleton. Even the widely studied activation of integrins by Rap proteins involves only the population of integrins linked to the actin cytoskeleton ³⁻⁷. Due to the high overlap of biological processes affected by both Rap and Rho GTPases, a picture emerges in which the one family may impinge on the other. Indeed, over the past years a vast amount of data confirming crosstalk between Rap and Rho GTPases has arisen. Here we discuss when, where and how Rap and Rho GTPases communicate with each other during various biological processes, including cell spreading, cadherin-based cell-cell adhesion, polarity and neuron development. This results in a picture in which Rap proteins function upstream of Rho GTPases in a Rac/Cdc42-activating and Rho-inhibiting manner.

RAP AND RHO GTPASES – A SHORT INTRODUCTION

Rap GTPases

The Rap family comprises two Rap1 (Rap1A and Rap1B) and three Rap2 (Rap2A, Rap2B and Rap2C) proteins. Rap1 and Rap2 share 60% sequence identity and signal through distinct signaling pathways. Within the subfamilies, however, the Rap1 proteins show 95% sequence homology and the Rap2 proteins show 85% sequence homology, resulting in common effectors ⁸. The majority of the sequence variation can be found in the C-terminus, which is thought to affect protein localization. Although there is a high level of redundancy within the subfamilies, some subtype specificity does exist, ascribed to spatial regulation and differential tissue distribution. However, for simplicity matters we will refer to them as Rap1 and Rap2.

Rap proteins are membrane-anchored proteins, found at the plasma membrane (PM) ⁹⁻¹², vesicles ^{9,12-16}, nuclear envelope ^{17,18} and the Golgi ^{11,19-21}. Membrane anchorage is achieved through

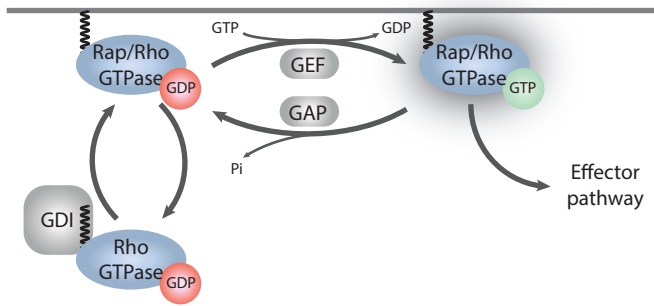


Figure 1: Activity cycle of Rap and Rho small GTPases.

Rap and Rho small GTPases cycle between a GTP-bound, active state, and a GDP-bound inactive state. This is catalyzed by Guanine nucleotide exchange factors (GEFs) and GTPase activating proteins (GAPs), respectively. Rho small GTPases display a third activity state, in which they are bound to guanine-nucleotide dissociation inhibitors (GDIs), which prevent the exchange of GDP to GTP. GDI-bound Rho GTPases reside in the cytoplasm.

v-Ki-Ras^{25,26}. Rap and Ras are highly similar in their effector-binding region⁸, and it was therefore thought that Rap opposed Ras signaling by sequestering Ras effectors in an inactive complex²⁷⁻²⁹. By now it has become evident that rather than opposing Ras signaling, Rap is involved in a plethora of Ras-independent processes, such as cell-extracellular matrix (ECM) adhesion^{4,30}, cell-cell adhesion^{31,32}, cell migration³³⁻³⁶ and cell polarity³⁷, and that the reverting effect of Rap on Ras signaling is through these biological processes.

Rho GTPases

The Rho GTPase family in mammals comprises ~20 proteins, which can be divided into classical and atypical Rho GTPases. Whereas the classical Rho GTPases cycle between the GTP- and GDP-bound forms (Fig. 1), atypical Rho GTPases are thought to be constitutively bound to GTP and therefore regulated in a GEF- and GAP-independent manner. The classical Rho GTPases can be subdivided into the Rho-family, Rac-family, Cdc42-family and a family consisting of RhoF (RIF) and RhoD³⁸. Of the classical Rho GTPases RhoA, Rac1 and Cdc42 have been the most extensively studied and have been ascribed to be involved in a plethora of biological functions, mostly processes involving the cytoskeleton³⁹. Herein, the dogma is that RhoA induces stress fiber formation and actomyosin-based contractility, whereas Rac1 and Cdc42 induce actin polymerization resulting in lamellipodia and filopodia formation, respectively. For this review we will restrict ourselves to these three Rho GTPases. RhoA induces cellular tension via modulation of actomyosin contraction. This is reflected by the observation that on soft substrates activation of RhoA results in shrinkage of matrices, whereas on rigid substrates it results in the commonly described formation of stress fibers. Several Rho-effectors have been described, with Diaphanous-related formin 1 (Diaph1) and the Rho-kinases RockI and RockII being the most elaborately studied. RockI and RockII share 65% identity and 92% identity in their kinase domain, owing to a high degree of common substrates and therefore research frequently does not distinguish between the two. Activation of Rho-kinase induces actomyosin contraction via both the direct diphosphorylation (Thr19/Ser19) of the myosin subunit myosin light chain 2 (MLC2), responsible for contraction, and indirectly via inactivation of myosin light chain phosphatase 1 (MYPT1), which dephosphorylates MLC2. Simultaneously, Rock phosphorylates and activates LIM kinase (LIMK). LIMK in turn phosphorylates cofilin, thereby inhibiting its actin depolymerizing function, thus overall resulting in actin filament stability⁴⁰. Diaph1 is involved in stress fiber formation

lipid modification of the C-terminal tail. Differences in the C-terminal tail sequence of the Rap orthologs results in alternative lipid modification, resulting in distinct cellular localization²². Alternatively, post-translational modifications and effector binding has also been demonstrated to affect protein localization^{23,24}.

The small GTPase Rap1 was originally characterized to be a Ras-revertant, capable of reverting the oncogenic transformation induced by

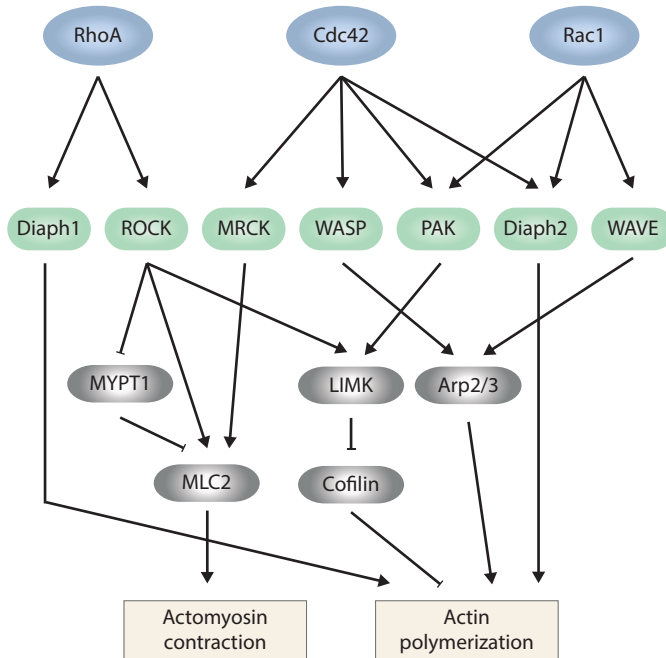


Figure 2: Effectors of Rho GTPases.

Rho GTPases regulate a variety of cellular processes, including actin cytoskeletal remodeling. The best-characterized Rho GTPases are RhoA, Cdc42 and Rac1, which all affect the actin cytoskeleton, partially by impinging on the same signaling cascades. Depicted are their main effectors involved in actin dynamics. Diaph1 and Diaph 2, Protein diaphanous homolog 1 and 2; ROCK, Rho-kinase; MRCK, myotonic dystrophy kinase-related CDC42-binding kinase; WASP, Wiskott–Aldrich syndrome protein; PAK, p21-activated kinases; WAVE, WASP-family verprolin-homologous protein.

by inducing polymerization of unbranched actin⁴¹ (Fig. 2).

Rac1 and Cdc42 are regarded to oppose RhoA by inducing actin polymerization and stability, frequently achieved through regulating common signaling cascades (Fig. 2). The Cdc42-effector WASP (Wiskott–Aldrich Syndrome Protein) and the Rac1-effector WAVE (Wiskott–Aldrich Syndrome Protein family member 1) both activate the Arp2/3 (Actin-related protein 2 and 3) complex, resulting in actin nucleation and branching, thereby inducing actin polymerization⁴². Actin stabilization can be achieved through the common Cdc42- and Rac1-effector, PAK1. Intriguingly, PAK1 phosphorylates LIMK, thereby inhibiting actin depolymerization by cofilin⁴³, thereby impinging on the same signaling cascade as Rock does. Furthermore, the Cdc42-effector MRCK (Myotonic dystrophy kinase-related CDC42-binding kinase alpha) also phosphorylates MLC2, however, in contrast to Rock, this results in MLC2 monophosphorylation (Ser19)⁴⁴ (Fig. 2).

As described for Rap GTPases, Rho GTPases also acquire lipid modifications regulating membrane localization. Also here differential lipid modifications, other posttranslational modifications and specific protein-protein interactions determine cellular localization. Moreover, Rho GTPases can interact with guanine nucleotide dissociation inhibitors (GDIs), a feature so far not found for Rap GTPases, preventing their interaction with membranes by masking the prenyl group, and their interaction with downstream effectors (Fig. 1).

CROSSTALK BETWEEN RAP AND RHO GTPASES

Rap and Rho GTPases are involved in many common biological processes, therefore it is not surprising that signaling by the two families can converge. However, intricate crosstalk also occurs within the Rho GTPase family, with RhoA opposing Rac1 and Cdc42 signaling, and vice versa (reviewed in⁴⁵). Due to this feedback mechanism, changes in RhoA-, Rac1- or Cdc42-GTP levels by Rap1 signaling can be indirect and results should be interpreted with caution. However, several signaling cascades have been elucidated directly linking Rap1 to either Rho-GAPs or Rac1/Cdc42-GEFs (Fig. 3). We will describe how Rap and Rho GTPases are implicated in various biological processes, followed by the signaling cascades

linking the two during these processes.

Adhesion and cell spreading

Cell spreading is a multistep process involving the interaction of integrins with the extracellular matrix (ECM), reorganization of the actin cytoskeleton and stabilization of cell-matrix interactions by linking the actin cytoskeleton to focal adhesions^{46,47}. The small GTPase Rap1 has been identified as a key component in the regulation of cell spreading and has been found to modulate several steps of the spreading process^{48,49}. The first step in cell spreading is the formation of contacts between the cell and the extracellular matrix (ECM), mediated by integrins. Rap1 can activate integrins by increasing integrin affinity and inducing integrin clustering (increased avidity), which is mediated through the Rap1-effectors Riam^{50,51} and RapL⁵².

Upon engagement of cell-ECM interactions, cells start to spread, resulting in new contact surfaces and the formation of new integrin-based adhesions. During this phase, cytoskeletal rearrangements occur, generating protrusive activity through actin polymerization and releasing tension generated by actomyosin contraction⁴⁶. Activation of Rac1 and Cdc42 induces lamellipodia and filopodia formation, respectively, together responsible for membrane protrusive activity, whereas RhoA opposes this through the induction of stress fibers formation and actomyosin contraction^{53,54}. Indeed, inhibition of RhoA through siRNA-mediated depletion of RhoA, dominant negative overexpression of RhoA, or chemical inhibition of RhoA increases and accelerates cell spreading⁵⁵⁻⁵⁷. During the early phases of cell spreading, after cell-ECM contacts have been formed, RhoA activity is inhibited in an integrin-Src kinase dependent manner allowing cells to spread⁵⁸⁻⁶⁰. In contrast, Rac is activated in an integrin-Src kinase dependent manner, further supporting cell spreading⁶¹⁻⁶³. Thus, in a simplified view, Rac1 and Cdc42 account for cell spreading, which is opposed by RhoA.

Cycles of cell protrusion and retraction occur locally under normal spreading conditions^{49,64}. Interestingly, Rap1 induces spreading by increasing the spreading rate and reducing cell retraction, resulting in increased total spread area⁴⁹, suggesting that there is interplay between Rap1 and the Rho GTPases. Moreover, Rap1 accomplishes this in a Src-independent manner, since Src inhibition does not affect Rap1-induced spreading⁴⁹. This indicates that reduction of actomyosin contraction by Rap1 is not merely a consequence of the increased cell-ECM adhesion induced by Rap1, but suggests a direct effect of Rap1 on the Rac1-Cdc42/RhoA balance.

There are a variety of examples of modulation of the activity of Rho GTPases by Rap1 during cell spreading. Already a decade ago Rac was proposed to be a downstream effector of Rap1 during cell spreading⁶⁵, which has been confirmed in various biological settings^{10,66}. Arthur and colleagues demonstrated that specifically the inhibition of Rac abolished cell spreading of HeLa cells by an active Rap1 mutant, Rap1AE63, whereas inhibition of Cdc42 or RhoA had no effect. In contrast, inhibition of cell spreading by inactivation of Rap1 was rescued by an active Rac1 mutant, placing Rac1 downstream of Rap1. Also here, this effect was not mediated by increased cell adhesion, since similar results were obtained on poly-L-lysine substrates⁶⁵, suggesting that Rap1 can directly affect Rac1 signaling. Indeed, the authors found that Rap1 could bind to the RacGEFs Vav2 and Tiam1.¹⁰ Interestingly, Rap1 did not affect the activity of these RacGEFs, but rather affected their subcellular localization, necessary for cell spreading⁶⁵. In the same year the Arf- and RhoGAP ARAP3 was identified as a novel Rap1-effector. Binding of Rap1 to ARAP3 specifically induces the RhoGAP activity of ARAP3, without affecting the ArfGAP activity⁶⁷. Overexpression of ARAP3 induces filipodia and membrane extensions in a Rap1- and RhoGAP-dependent manner^{67,68}, suggesting that apart from activating Rac1, Rap1 induces cell spreading through the inhibition of RhoA. Later it was demonstrated that ARAP3 is essential for PDGF-induced lamellipodium formation in both an ArfGAP and RhoGAP dependent manner⁶⁹, possibly through the activation of Rap1 by PDGF stimulation¹⁰. Over time other Rap1-regulated RhoGAPs and

RacGEFs have been implicated in cell adhesion and spreading. The ARAP3 family member, ARAP1, has also been demonstrated to be regulated by Rap1 and mediates lamellipodia formation, stress fiber reduction and RhoA inactivation by active Rap1⁷⁰. Furthermore, the RhoGAP ArhGAP29 has been demonstrated to mediate Rap1-induced cell spreading. In contrast to ARAP3, Rap1 does not interact directly with ArhGAP29, but affects it through the Rap-effectors Radil and Rasip1⁷¹. Whether Rap1 affects the activity of ArhGAP29 is unknown, however, as has been demonstrated for Vav2 and Tiam1, Rap1, through Radil, affects the subcellular localization of ArhGAP29 (described in chapter 5), recruiting it to the plasma membrane. Intriguingly, Rap2 can directly interact with ArhGAP29, which, based on the spreading phenotype, was suggested to inhibit RhoGAP activity⁷². Through this Rap2 could oppose Rap1 signaling. Indeed, opposing biological effects of Rap1 and Rap2 have been found in both cell spreading (unpublished data, A. Post and J.L. Bos) and endothelial barrier function⁷³.

Cell-cell adhesion

The presence and regulation of cell-cell contacts is of utmost importance for both epithelial and endothelial monolayers, since they act as a physical barrier between body compartments, controlling paracellular transport from and to underlying tissues. The junctional region is composed of two main adhesion complexes: the tight junction (TJ) and adherens junction (AJ), both linked to the actin cytoskeleton. In epithelial cells the TJ is located apically of the AJ, whereas in endothelial cells this distribution is less defined (Fig. 4). The core component of AJs is the transmembrane cadherin protein. Several cadherin family members exist, and expression is cell type dependent, with N-cadherin expressed in neurons, E-cadherin expressed in epithelia and VE-cadherin expressed in endothelial cells. Cadherins contain an extracellular domain responsible for homophilic trans-interaction, and a cytoplasmic tail, interacting with various adaptor proteins. The core interactors are p120-catenin, interacting with the junctamembrane region and affecting cadherin transport to and stability at the PM, and β -catenin, interacting with the C-terminus and functioning as a scaffold for α -catenin (Fig. 4). α -catenin links cadherins to the actin cytoskeleton and serves as a docking site for several cadherin complex-associated proteins. Apart from these core cadherin-catenin complex components, various other proteins have been found at cadherin-based cell junctions, however their presence is more dynamic and seems to depend on the junctional status, e.g. whether junctions are being formed, remodeled or are matured. The junctional status closely correlates with the organization and contractility of the actin cytoskeleton and many actin binding and remodeling proteins are present at the junction, including the Rho GTPase-regulated ena/VASP, Arp2/3 and formins. Indeed, Rho GTPases play essential roles during adherens junction formation, maintenance and remodeling. As for cell spreading, RhoA and Rac1/Cdc42 are regarded to have opposing effects on epithelial and endothelial permeability, with RhoA increasing permeability and Cdc42 and Rac reducing it^{71,74-76}. However, contradictory findings have been reported. Whereas activation of Cdc42 in epithelial monolayers increases junctional actin and E-cadherin localization at cell junctions⁷⁴, both active and inactive Rac1 and RhoA may result in AJ disassembly^{75,77-79}, suggesting that spatiotemporal control of these GTPases is essential for proper barrier function. Indeed, several GEFs and GAPs for both GTPases have been found at AJs.

The effect of Rap1 signaling on AJs seems more straightforward; activation of Rap1 increases barrier function, whereas loss of Rap1 activity reduces barrier function. Supporting this, using a FRET-based Rap1 biosensor, an active Rap1 pool can be found at newly formed cell-cell junction⁸⁰. Rap1 has been reported to increase barrier function by both directly affecting cadherin proteins, either by increasing cadherins levels at the junction⁸¹⁻⁸³ or by stabilizing cadherins at the junction^{84,85}, as well as affecting the actin cytoskeleton linked to the junctions.

Constant remodeling occurs at the cell-cell junction to maintain its state. This is emphasized by the

finding that junctional actin is highly dynamic, even in matured cell-cell contacts ^{86,87}. Especially in endothelial barriers there is a significant importance for junction remodeling, as it not only functions to prevent excessive leakage into underlying tissues, but must also allow controlled transendothelial migration of leukocytes into underlying tissues, thus calling for dissemination and reformation of cell-cell junctions. This is reflected by the gross changes in actin cytoskeleton morphology upon Rho GTPase or Rap1 signaling ^{31,71,88,89}. Activation of RhoA results in the formation of thick actin cables orientated perpendicular to the cell-cell junction and referred to as radial stress fibers ^{90,91}. Actomyosin contraction of these radial stress fibers is thought to exert tension on the junction, thereby inducing endothelial permeability ^{90,91}. Activation of Cdc42, on the other hand, results in the accumulation of actin at the cell-cell junctions, orientated parallel to the junction, and is thought to increase barrier function, referred to as circumferential actin bundles ⁸⁸.

These different actin cytoskeletal statuses are less obvious in epithelial cell layers –mainly displaying a thick, junctional associated actin ring – likely because junction dissemination is not a favorable feature under normal physiological conditions. However, during epithelial-mesenchymal transition, when cells must disrupt their cell-cell contacts, radial stress fibers are formed, thought to exert pulling forces on the junction ^{92,93}.

Activation of Rap1 in endothelial cells reduces radial stress fibers content and increases circumferential actin bundles ^{31,71,88,89}, suggesting that it affects Rho GTPase activity. Indeed, Rap1-induced inhibition of RhoA ^{71,89,94-96} and activation of Cdc42 ^{88,97,98} and Rac1 ^{77,94,95,99} activity has frequently been suggested to mediate Rap1-induced barrier function, however only few direct signaling routes have been elucidated. It was recently demonstrated that the RhoGAP ArhGAP29 mediates Rap1-induced endothelial barrier function, by reducing radial stress fibers and phospho-MLC2 levels, suggestive of decreased Rho activity ⁷¹. This is mediated by the Rap1-effectors Radil and Rasip1, which can interact with ArhGAP29 ^{100,101}. Activation of Rap1 induces the translocation of Radil, which through its interaction

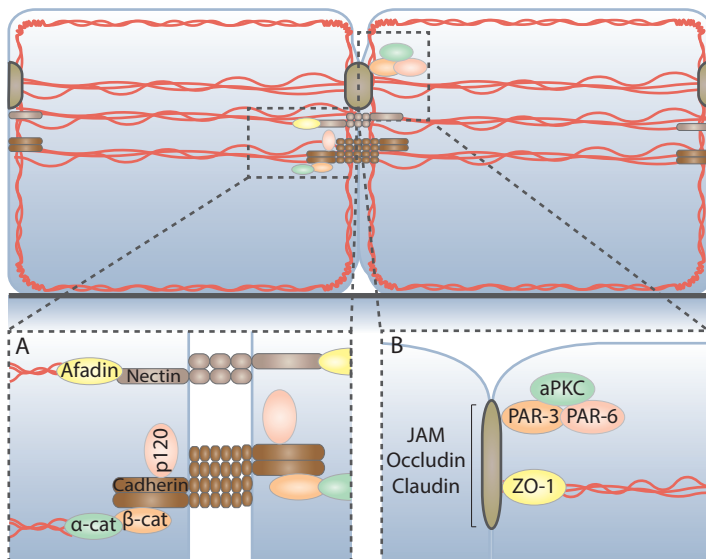


Figure 4: Schematic overview of junctional region.

Simplified schematic overview of the junctional region with in (A) an enlargement of the adherens junction zone, with the most relevant proteins complexes and in (B) an enlargement of the tight junction zone with the most relevant proteins complexes and the PAR polarity complex.

with ArhGAP29, causes ArhGAP29 to translocate to the PM (chapter 5). Independently, Rasip1 is recruited by active Rap1 to the PM (¹⁰², chapter 5), where it can interact with the Radil-ArhGAP29 complex, together forming a functional signaling complex (Chapter 5). Apart from Rasip1 and Radil, the Rap1-effector Krit1/CCM1 has been demonstrated to localize to cell-cell junctions and mediate Rap1-induced endothelial barrier function ¹⁰³. Also Krit1/CCM1 has been suggested to reduce RhoA activity and subsequent MLC2 phosphorylation ^{96,104,105}. However, the molecular mechanism through which Krit1/CCM1 regulates RhoA activity is currently unknown.

Secondly, activation of Cdc42 has been implicated in Rap1-induced AJ regulation. Activation of Cdc42 induces the formation of a junctional actin ring, a feature also observed by Rap1 activation ⁸⁸. Recently, it was demonstrated that Rap1 could induce CAB formation through Cdc42 activation. For this, Rap1 induced the translocation of the Cdc42GEF, FGD5, to cell-cell junctions, resulting in the subsequent translocation and activation of Cdc42 and N-WASP. This signaling cascade mediated Rap1-induced endothelial barrier function. Intriguingly, whereas the double phosphorylation of MLC2 on Thr18 and Ser19, known to be regulated through Rho-Rock signaling, was reduced by Rap1, activation of Cdc42 resulted in a single phosphorylation of MLC2 on Ser19, mediated by MRCK. This shift in phosphorylation status of MLC2 was essential for barrier function ⁸⁸.

Thirdly, Rap1 has been suggested to induce endothelial barrier function through activation of Rac1, however the molecular mechanism for this has not been fully elucidated. During cell spreading, in HeLa cells, Rap1 can bind and recruit the RacGEFs Tiam1 and Vav2 ⁶⁵, and E-cadherin-induced outside-in signaling has been demonstrated to activate Rac1 through a Rap1-PI3K-Vav2 signaling cascade ¹⁰⁶. Furthermore, depletion of Vav2 or Tiam1 has been demonstrated to abrogate endothelial barrier function in a similar manner as depletion of Rap1 does ⁹⁹, making these GEFs likely candidates for mediating Rap1-signaling during cell-cell contact regulation, although this remains to be demonstrated directly.

Most research on the control of cell-cell junction by Rap1 has focused on its effect on cadherin-based cell-cell contacts. However, this field of research is being expanded to two other junctional components, e.i. nectins and TJs. Nectins are another type of trans-interacting junctional proteins, mostly reported to regulate cadherin-based junctions. Although not completely understood yet, some suggest that through the ligation of nectins Rap1 gets activated at newly forming cell-cell junctions ^{97,98,107}. This activation of Rap1 subsequently regulates the cadherin status, in part by affecting Rho GTPase activity ^{97,107}. Furthermore, Rap1 has also been reported to affect TJ formation. However, since TJ formation relies on the prior formation of AJs, much of the defects in TJ assembly, resulting from interference with Rap1-signaling, can be attributed to aberrant AJ formation ⁹⁸. Thus, Rap1 is at the cross road between nectin- and cadherin-based cell-cell contacts and the subsequent TJ formation.

Migration

Cell migration is a multifaceted process depending on cytoskeletal reorganization, integrating the modulation of cell-cell adhesion, cell-ECM adhesion and actin-driven protrusion and retraction. Coordinated spreading at the leading edge and retraction at the rear assures proper migration. Cell retraction requires actomyosin mediated retractile forces. Simultaneously, actomyosin contraction induces cell-cell contact dissemination in order to allow cells to migrate away from the cells they are attached to. Emphasized by the dependency on actin cytoskeleton modulation, Rho GTPases play fundamental roles in cell migration regulation. For a long time it was thought that cell migration was regulated by the concerted actions of Rac1 and Cdc42 at the leading edge, and RhoA activity at the rear, however recent studies with RhoA, Rac1 and Cdc42 bioprobes, allowing visualization of the local activity of small GTPases, has revealed spatial activity of RhoA at the leading edge as well ¹⁰⁸, emphasizing the importance of spatial control of Rho GTPases. Of note, also here RhoA and Rac1/

Cdc42 activity were mutually exclusive.

Since Rap1 regulates cell spreading and adhesion, it inevitably influences cell migration. In line with a positive role of Rap1 activity on cell migration, stable expression of active Rap1 in prostate and breast cancer cells enhances metastasis and extravasation, respectively^{33,34}. Furthermore, overexpression of Rap1GAP inhibits cell migration, invasion and metastasis both *in vitro* and *in vivo*^{35,36}. Although no activating mutations of Rap1 have been reported in tumors, Rap1GAP down regulation has been reported in various tumors¹⁰⁹⁻¹¹¹. Colon tumor cells with reduced levels of Rap1GAP have been suggested to shift their migratory phenotype from RhoA-Rock mediated amoeboid-like migration to Rac1-dependent mesenchymal cell migration. Indeed, inhibition of Rac1 signaling inhibits cell migration in these cells, suggesting that Rap1 induces cell migration through increased activation of Rac1¹¹¹. Also in human microvascular endothelial cells loss of Rap1 reduces directional migration, which also correlated to increased Rac1-GTP levels¹¹². Possibly, this is regulated through the local accumulation of Rac1 and the Rac1GEF Vav2 at the lamellipodium in a Rap1-dependent manner, as has been demonstrated for PDGF-induced cell migration of NIH3T3 cells. Consistently, overexpression of Rap1GAP as well as depletion of Rap1 itself reduces the ability of NIH3T3 cells to form lamellipodia upon PDGF stimulation, which correlates with a reduced migratory capacity¹⁰. Furthermore, ARAP3 has been demonstrated to mediate PDGF-induced lamellipodium formation in pig aortic endothelial cells, necessary for persistent cell migration⁶⁹, thus regulating cell migration by inhibiting RhoA. Whereas the mechanism of shifting the RhoA/Rac1 balance by Rap1 in response to PDGF could be cell type specific, another possibility is that PDGF signaling converges at ARAP3 and Vav2. ARAP3 has been demonstrated to directly interact with Vav2 upon EGF stimulation¹¹³. It is plausible that PDGF can similarly induce interaction between ARAP3 and Vav2. Through such an interaction Rap1 may simultaneously induce Rac1 activity, while inhibiting RhoA activity.

Since cell migration relies on cell spreading, signaling cascades regulating the latter may also affect cell migration. Indeed, as described above, Vav2 and ARAP3 are implicated in both processes. Also ARAP1 is implicated in directed cell migration. Here it is thought that local activation of Rap1 recruits the Rap1-effector Afadin – or AF-6 – which stabilizes Rap1-activity and has been suggested to facilitate the interaction between Rap1 and the RhoGAP ARAP1, thereby enhancing directed cell migration^{70,114}. In contrast, Afadin has also been suggested to integrate Rap1 and Rac1 activity during directed cell migration¹¹⁴ and loss of Afadin in breast cancer is associated with a poor outcome, likely due to increased cell migration and invasiveness¹¹⁵. Whereas ArhGAP29 has thus far not been implicated in cell migration directly, both Rasip1 and Radil, which regulate ArhGAP29 during cell spreading, are involved in cell migration^{100,116-118}. Also Tiam1 plays a well-documented role in cell migration¹¹⁹, however, Rap1 has never been implicated in this role of Tiam1.

Since spatial confinement of the activity of the Rho GTPases is imperative to cell migration¹⁰⁸, Rap1 likely spatially restricts the activity of the GEFs and GAPs described here. Indeed, spatial regulation of the various signaling cascades has been suggested^{10,70,100,102,108,114}, however the precise molecular events are largely elusive.

PAR-complex based polarity

Cell polarity, referring to the asymmetrical distribution of proteins, is key to proper functioning of any cell type, be it epithelial cells, endothelial cells, lymphocytes or neurons. For instance, apico-basal polarity of epithelial and endothelial cells distinguishes between the apical cell surface, in most tissues facing the luminal space, and the basolateral cell surface, responsible for the communication and interaction between the epithelial or endothelial cells and the underlying tissues. On the other hand, polarity of lymphocytes, such as T-cell polarity described below, is necessary for directed cell migration in response to chemokine signaling, and neuronal polarity is essential during axon specification and

outgrowth. A common feature of these different polarity processes is the formation of polarity complexes. Three main polarity complexes assemble, referred to as the partitioning defective (PAR), Scribble and Crumbs complexes, with the PAR polarity complex having the broadest function and controlling most polarization processes. In epithelial tissues, the PAR polarity complex, comprising Par-3, Par-6 and atypical PKC (aPKC), localizes to the apical membrane and TJs and displays intricate cross-regulation with Rho GTPases (Fig. 4). Active Cdc42 and Rac1 both reinforce polarity establishment through their interaction with Par-6, resulting in the activation of aPKC, key to functioning of the PAR polarity complex¹²⁰. Loss of Cdc42, through siRNA-mediated depletion of Cdc42, prevents the polarized distribution of the PAR polarity proteins, resulting in aberrant polarity in *C. elegans*^{121,122}. Increased RhoA activity, on the other hand, results in polarity reversion, as exemplified in 3D cyst cultures¹²³. The exact molecular events responsible for this are unknown, but Rock has been demonstrated to phosphorylate Par-3 and disrupt the Par polarity complex¹²⁴, possibly resulting in aberrant polarity. Thus, RhoA has an adverse effect on the PAR polarity complex.

For studying apico-basal polarity, *Drosophila* embryogenesis is a superb model, allowing one to study the establishment of apico-basal polarity prior to cell-cell junction formation occurring. Using this model system, Rap1 has been found to play an important role during the early steps of polarity establishment. In this, the Rap1-effector Cno (Cno), homologue of mammalian Afadin plays an essential role in apico-basal polarity establishment. Rap1-Cno signaling forms the spatial cue at the apical membrane, positioning Bazooka (homologue to Par-3) and AJ complex components at the apical membrane, prior to cell-cell contact formation¹²⁵. However, once cell-cell junctions are being formed this hierarchical signaling cascade is less defined.

In the textbook model, apico-basal cell polarity, most pronounced in epithelial sheets, succeeds cell-cell contact formation. Whereas cadherins promote TJ formation, TJs in turn are thought to induce apico-basal polarity formation by preventing free lateral movement of plasma membrane components, maintaining differential apical and basolateral membrane composition. However, the sequential induction of AJs, TJs and subsequent polarization is not as straightforward as frequently portrayed. Data from endothelial cells support a direct role for cadherin in polarity establishment¹²⁶. Indeed, VE-cadherin can directly interact with Par-3¹²⁷. Moreover, early events of epithelial cell polarity occur prior to the establishment of TJs^{123,128}, suggesting that AJs may function prior to, parallel with or redundantly with TJs in polarity establishment and maintenance. Furthermore, interference in the PAR polarity complex results in disrupted cell-cell contacts, suggesting that there is two-way communication between the PAR polarity complex and cell-cell junctions. For instance, aPKC λ null mice do not form neuroepithelial AJs¹²⁹ whereas loss of the Par-3 homologue Bazooka in *Drosophila* results in mislocalized E-cadherin^{130,131}. Since cell-cell adhesion and polarity are such interconnected processes, the two cannot simply be dissected. Therefore, we will discuss the interconnectivity between Rap1, Rho GTPases and the PAR polarity proteins, without distinguishing between the effects on cell-cell junction formation or polarity establishment.

At the cell-cell junction Afadin interacts with nectins^{132,133} and forms a platform for communication between the various cell-cell contact structures, the PAR polarity complex and the actin cytoskeleton, allowing the relevant players to cross-regulate each other. Loss of Afadin during embryoid body formation results loss of polarity, reflected by aberrant localization of Par-3 and Par-6 and reduced activation of aPKC. The reduced activity of aPKC is likely due to the decreased activity of Cdc42 found in Afadin-null embryoid bodies. This coincides with aberrant localization of both adherens and tight junctional proteins¹³⁴. Possibly the loss of proper junction formation upon loss of Afadin accounts for the abnormal polarity in these embryoid bodies. Alternatively, loss of Afadin may result in aberrant

PAR polarity complex positioning, as occurs during embryogenesis¹²⁵, thereby perturbing junctional localization. Furthermore, it has been suggested that the PAR complex regulates in the interaction of Afadin with nectins, upon which cadherin-mediated cell-cell contacts form¹³⁵, accounting for a third mechanism through which Afadin and the PAR polarity complex can communicate.

Also in endothelial lumen formation, Rap1 has also been suggested to be involved in the regulation of apico-basal polarity. Loss of Rap1 resulted in mislocalized Par-3, aPKC ζ and the RacGEF, Tiam1. This was suggested to be due to abnormal VE-cadherin based cell-cell junction formation, since knockdown of the Rap1-effector KRIT-1/CCM1, resulted in a similar phenotype¹²⁶. Furthermore, loss of Rasip1 both in vivo and in vitro disrupts proper vascular lumen formation and results in aberrant localization of VE-cadherin and the apical marker podocalyxin¹⁰¹. Since both KRIT-1/CCM1 and Rasip1 result in reduced Rho activity^{71,101,104}, this implies that Rap1 mediates lumen formation by reducing Rho activity. However, since both Rasip1 and KRIT-1/CCM1 also mediate Rap1-induced cadherin-based cell-cell adhesion, polarity disruption in these cases may be the direct consequence of aberrant junction formation.

Thus, it seems that cell-cell contact proteins and the polarity complex cross-communicate through Rap1 and Rho GTPases, to maintain each other's function, however the precise order of events is still unclear.

T-cell polarity, which requires dramatic cytoskeletal rearrangements, also depends on Rap1 and the PAR polarity complex. Chemokine stimulation activates Rap1, which is thought to be the initial event in T-cell polarization. Active Rap1 subsequently recruits the RacGEF Tiam1, which co-recruits PAR3. Tiam1 and PAR3 interact in a Rap1-independent manner. Furthermore, PAR3 assures the recruitment of the other two complex members, PAR6 and aPKC ζ . While recruiting Tiam1, Rap1 also activates Cdc42 through a currently unknown mechanism. Through Cdc42 activation, active Rap1 induces the kinase activity of aPKC ζ , which subsequently phosphorylates Tiam1, thereby activating its GEF activity. Ultimately, this results in Rac1 activation, thought to be responsible for the cytoskeletal rearrangements necessary for T-cell polarity¹³⁶. Thus Rap1 translates chemokine stimulation into local actin rearrangements to assure proper cell migration. Whether this signaling cascade is also involved in apicobasal polarity is currently unknown, however, all components, including Tiam1, have been implicated in apico-basal polarity, making this plausible scenario.

Neurons

Neuronal development is a multistep process, depending on polarity establishment to define axon specification, followed by lamellipodial and filopodial protrusion and cell migration to control axon outgrowth. Not surprisingly, small GTPases of the Rho family function during various stages of neuron differentiation. Immature neurons continuously project and retract neurites from their cell body until one becomes dominant and differentiates into an axon. The remaining neurites will develop into dendrites. Whereas neurite protrusion and axonal differentiation relies on Rac1 and Cdc42 activity, activation of RhoA induces neurite retraction and inhibits axon formation¹³⁷.

Rap1B plays an essential role in early steps of axonal differentiation. During axon specification Rap1B, originally localized at the tips of all neurites, becomes restricted to the tip of the future axon. A similar shift in distribution is observed for Cdc42, however this succeeds Rap1B restriction. Overexpression of active Rap1B or a fast-cycling Cdc42 mutant results in an increased number of forming axons, whereas depletion of either GTPase inhibits axon formation, indicating that both are essential for axonal differentiation. Moreover, expression of fast-cycling Cdc42 rescues the loss of axon outgrowth upon Rap1B depletion, placing Cdc42 downstream of Rap1B³⁷. How Rap1B regulates Cdc42 in axon differentiation remains to be determined.

Axonal growth requires the localized activity of Rac1 and Cdc42 at the growth cone, whereas RhoA must be inhibited since active RhoA induces growth cone collapse and neurite retraction¹³⁷. Thus, inhibition of RhoA during axonal growth is a favorable event. Indeed, several RhoGAPs have been reported to localize to the axon, locally inhibiting RhoA activity. Two of these RhoGAPs, RA-RhoGAP and Arap3, are regulated by Rap1.

During neurite sprouting and extension, Rap1B down regulates the activity of RhoA through activation of the RhoGAP, RA-RhoGAP. RA-RhoGAP contains an RA-domain, which interacts with GTP-bound Rap1B. Binding of Rap1B to the RA-domain increases the GAP-activity of RA-RhoGAP towards RhoA and depletion of RA-RhoGAP inhibits Rap1-induced neurite outgrowth¹³⁸. Whereas Rap1-induced activation of RA-RhoGAP is essential for neurite sprouting, RA-RhoGAP also interacts with, and can be activated by, phosphatidic acid (PA), resulting in the translocation of RA-RhoGAP to the PM. The interaction with PA can induce neurite extension, but is not sufficient for neurite sprouting.

Secondly, the Arf- and RhoGAP ARAP3 has been demonstrated to mediate Rap1-induced neurite extension^{139,140}. Also here, Rap1 directly interacts with ARAP3 to specifically induce its RhoGAP activity, without affecting its ArfGAP activity⁶⁷. Interestingly, ARAP3 also interacts with PI(3,4,5)P3 at the PM, through which it can be activated. Similar to the PA-binding by RA-RhoGAP, this interaction recruits ARAP3 to the PM¹⁴¹. Moreover, an ARAP3 mutant incapable of interaction with PI(3,4,5)P3 cannot be activated by Rap1⁶⁷. Possibly, phospholipids in this case function as a landmark, tethering the RhoGAPs to specific micro-domains, where Rap1 can then activate them. Intriguingly, PI3K induces local production of PI(3,4,5)P3 at the prospective axon¹⁴², thereby recruiting proteins necessary for axonal growth. Possibly, ARAP3 is one of these proteins recruited by PI3K activity to the growth cone.

Crosstalk between Rap-GTPases and Rho-GTPases is an evolutionary conserved feature – lessons from the budding yeast

Spatiotemporal control of Rho GTPase activity by Rap GTPases is an evolutionary conserved feature, demonstrated by its functionality in the budding yeast, *S. cerevisiae*. Polarized growth in the budding yeast is essential for both mating and budding, and depends on the spatial control of actin dynamics. Bud site determination is a strictly regulated process, directed by the bud scar from the previous division, creating landmark cues at the future bud site. The Rap ortholog Bud1/Rsr1 plays a crucial role in bud site positioning. The Bud1/Rsr1 GEF, Bud5, and GAP, Bud2, are targeted to the future bud site, by interacting with the landmark cues. There they locally regulate the activity of Bud1/Rsr1.

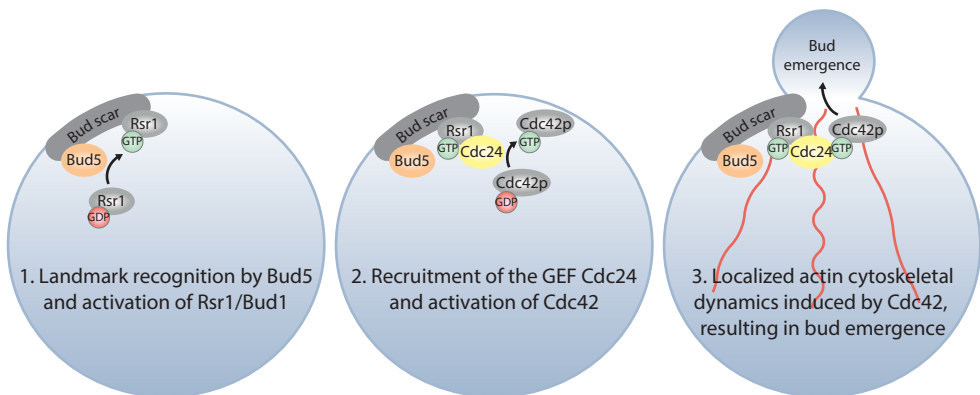


Figure 5: Regulation of Cdc42 by Rap in *S. cerevisiae* during bud formation.

Human orthologous: Bud5, Epac1; Rsr1, Rap; Cdc24 is a Cdc42GEF; Cdc42p, Cdc42.

Loss of either Bud1/Rsr1, Bud5 or Bud2 results in randomized bud location. Once activated, Bud1/Rsr1 recruits Cdc24, a GEF for Cdc42, which then recruits and activates Cdc42. Activation of Cdc42 induces bud site emergence through the regulation of the actin cytoskeleton, septins and by directing exocytosis. In contrast to loss of Rsr1/Bud1, loss of Cdc42 gives rise to large, round, unbudded cells^{143,144}. Thus, Bud1/Rsr1 translates cortical landmarks into restricted Cdc42 activity, resulting in localized actin dynamics (Fig. 5).

DISCUSSION

Here we have reviewed and discussed several direct signaling cascades between Rap1 and Rho GTPases. From this a picture emerges in which Rap1 functions upstream of the Rho family, spatiotemporally regulating its activity to modulate actin cytoskeletal dynamics. Through this, Rap1 controls a variety of biological processes, including cell spreading, cell-cell adhesion, migration, polarity and neuron development (Fig. 3).

Intriguingly, apart from Tiam1, only for those Rap1-effectors containing an RA-domain, e.g. ARAP3, ARAP1 and RA-RhoGAP, Rap1 has been demonstrated to regulate the activity of the proteins, for all other GEFs and GAPs, Rap1 has been reported to determine the cellular localization of the protein, thus spatially controlling Rho GTPase activity.

Also from an evolutionary point of view, Rap1 functions upstream of the Rho GTPases, as exemplified in the budding yeast. And also here this occurs through spatially controlling the localization of the Cdc42GEF, Cdc24, thereby spatially regulating actin dynamics, emphasizing the conservation of this cross talk between Rap1 and Rho GTPases.

In the discussed biological processes, several RacGEFs, Cdc42GEFs and RhoGAPs, regulated by Rap1, have been implicated in the same biological process (Fig. 3), raising the question what the need is of having several proteins mediating the same biological process. Whether this is the result of cell type specificity or the biological context they are put in, is unclear. Also for Rap1 several GEFs have been implicated in the same biological process. For instance, the RapGEFs C3G, PDZ-GEF1 and 2 and Epac1 have all been implicated in endothelial barrier function. However, we are now starting to understand that the biological context, and thus the input signal, determines which GEF is necessary. Whereas PDZ-GEF1 and 2 are necessary to sustain basal barrier integrity, C3G comes into action during barrier recovery, while Epac1 is necessary when enhanced barrier function is required (reviewed in chapter 6). Possibly, a similar situation explains the seeming high level of functional overlap between the Rap1-regulated RacGEFs, Cdc42GEFs and RhoGAPs, where the spatial or temporal cue activating Rap1 determines which GEF or GAP is subsequently regulated. Alternatively, the need for several GEFs and GAPs in the same biological process may be explained by the recent findings that several GEFs and GAPs of the Rho GTPase family are directly linked to a specific downstream effector of the GTPase¹⁴⁵⁻¹⁴⁷. Determined by the input signal, Rap1 may be directed to a specific GEF or GAP depending on the downstream effector the particular GEF or GAP is linked to, thereby determining which particular downstream signaling cascade is activated or inactivated.

In all biological processes discussed here, Rap1 has been reported to induce Rac1 or Cdc42 and inhibit RhoA activity. Most likely both occur simultaneously, be it direct or indirect. This implies that upon activation of Rap1 the cell switches from a more contracted to a protrusive state, through actomyosin relaxation and actin polymerization.

Cross talk between Rap1 and Rho GTPases has mostly been reported to occur through the regulation of Rho GTPase activity, through affecting its GEFs and GAPs. Alternatively, cross talk between Rap and Rho GTPases could also occur through GEF- and GAP-independent mechanisms, by regulating

each other's expression or stability and impinging on each other's downstream effectors. For instance, depletion of KRIT1/CCM1 induces the translocation of its binding partner β -catenin, to the nucleus, where it can regulate transcription¹⁴⁸. Moreover, KRIT-1/CCM1 itself can also translocate to the nucleus¹⁴⁹, potentially pointing towards a role for KRIT1/CCM1 itself in transcriptional regulation. Indeed, not only changes in Rho activity, but also in Rho expression have been identified upon KRIT1/CCM1 depletion^{105,150}. Furthermore, hypothetically Rap1 and Rac1/Cdc42 signaling can also converge through regulation of common effectors such as IQGAP1¹⁵¹⁻¹⁵³ and PI3K^{154,155}.

Although from an evolutionary point of view Rap1 functions upstream of the Rho module, few exceptions have been reported. For instance, chemokine-induced integrin activation in lymphocytes, mediated through JAK tyrosine kinases, has been demonstrated to activate Rap1A in a RhoA-PLD1-dependent manner¹⁵⁶. And also Rac1-induced actin polymerization has been demonstrated to spatially regulate the RapGEF CalDAG-GEFI, targeting it to membrane ruffles, thereby localizing Rap1 activity¹⁵⁷.

Although several direct routes between Rap1 and Rho GTPases have been elucidated, frequently only a change in Rac1, Cdc42 or RhoA activity is reported, without elucidating the molecular mechanism mediating this. Cross talk within the Rho GTPase family itself challenges research focused on the signaling between Rap and Rho GTPases. With few exceptions, Rac and Rho are considered to negatively regulate each other's activity, whereas several biological effects of Cdc42 have been attributed to the activation of Rac (extensively reviewed in⁴⁵). Due to the positive and negative feedback loops within the Rho GTPase family, effects found on the activity of either one upon activation of Rap proteins, should be interpreted with caution. For instance, depletion of ARAP3 has not only been demonstrated to increase RhoA-GTP levels, but also reduce Rac1-GTP levels⁶⁹. Thus, without unraveling the signaling cascade through which Rap proteins directly affect one of the Rho GTPases, focus should be on the modulation of the Rac:Rho ratio by Rap proteins and how this affects the biological outcome of interest.

SCOPE OF THIS THESIS

In this thesis we have investigated downstream signaling of Rap1 in endothelial barrier control and related cytoskeletal driven processes.

Chapter 2 describes the development of an siRNA screening tool, to identify downstream signaling cascades of Rap1. For this we analyzed the induction of cells spreading upon Epac1-Rap1 activation. This resulted in the identification of the Rap1-effector, Radil, as a mediator of Rap1-induced cell spreading. Furthermore, the plasma membrane-actin linker, Ezrin, was identified as a crucial component of Rap1-induced cell spreading, but not cell adhesion. The interconnectivity between these two proteins has been investigated and described in **chapter 3**, identifying ERM proteins as a potential scaffold for Rap1-signaling, integrating upstream signaling by binding Epac1, and downstream signaling by binding Radil.

In **chapter 4**, we have identified a novel Rap1-effector, Rasip1, which is a homologue of Radil. We confirmed that it functions downstream of Rap1, and modulates the actin cytoskeletal driven processes of cell spreading and endothelial barrier control. Moreover, we identified that in concert with Radil, Rasip1 modulates the actin cytoskeleton through the RhoGAP ArhGAP29, thus impinging on Rho signaling. In **chapter 5**, we have elucidated how this signaling cascade functions mechanistically. Here we reveal that Rap1 regulates Radil, Rasip1 and ArhGAP29 by inducing their dynamic translocation to the plasma membrane, where they form a multimeric complex. Elucidating the pathway through which Rap1 induces endothelial barrier control through the modulation of Rho, together with other reports, has led us to develop a dual tension model in the control of endothelial barrier function, described in **chapter 6**.

Finally, in **chapter 7** we identify a Rap1-Radil-Rasip1-independent function of ArhGAP29. Rather than Rap1, this module incorporates Rap2 signaling, suggesting that besides a Rap1-Rho axis, there also is a Rap2-Rho axis. Integration of this axis is achieved through the tyrosine phosphatase PTPL1.

Of note, **chapters 3, 5 and 7** all identify potential spatial cues for Rap-Rho signaling axes in various cytoskeletal driven processes.

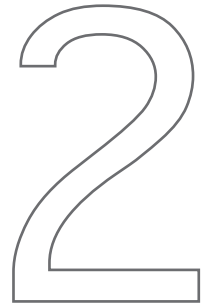
From the research presented in this thesis, and from the research on Rap-biology over the past decade, we have created a picture in which Rap translates cortical landmark cues into localized modulation of the actin cytoskeleton, by spatially and temporally regulating the Rho GTPase family, the master regulators of the actin cytoskeleton.

CHAPTER

EZRIN IS REQUIRED FOR EFFICIENT RAP1-INDUCED CELL SPREADING

Sarah H. Ross, Anneke Post[†],
Judith H. Raaijmakers[†], Ingrid Verlaan,
Martijn Gloerich and Johannes L. Bos

Journal of Cell science. 2011; 124(11): 1808-1818

A large, hollow outline of the number '2' is positioned on the right side of the page, partially overlapping a vertical line that runs down the page.

[†] These authors contributed equally to this work

ABSTRACT

The Rap family of small GTPases regulate the adhesion of cells to extracellular matrices. Several Rap-binding proteins have been shown to function as effectors which mediate Rap-induced adhesion. However, little is known regarding the relationships between these effectors, or about other proteins which are downstream of or act in parallel to the effectors. To establish if an array of effectors was required for Rap-induced cell adhesion and spreading, and to find new components involved in Rap-signal transduction, we performed a small-scale siRNA screen in A549 lung epithelial cells. Of the Rap effectors we tested, only Radil blocked Rap-induced spreading. Additionally, we identified a novel role for Ezrin downstream of Rap1. Ezrin was necessary for Rap-induced cell spreading, but not Rap-induced cell adhesion or basal adhesion processes. Furthermore, Ezrin depletion inhibited Rap-induced cell spreading in several cell lines, including primary human umbilical vein endothelial cells. Interestingly, Radixin and Moesin, two proteins with high homology to Ezrin, are not required for Rap-induced cell spreading and cannot compensate for loss of Ezrin to rescue Rap-induced cell spreading. Here, we present a novel function for Ezrin in Rap1-induced cell spreading and evidence of a non-redundant role of an ERM family member.

INTRODUCTION

The response of cells following contact with an extracellular matrix, either for spreading or for migration, requires the tightly controlled regulation of cell adhesion, actin polymerisation and force generation¹⁵⁸. Co-ordination of these processes is ensured by signals which derive from inside the cell (inside-out signalling) and those which are received through interactions with the extracellular environment (outside-in signalling)¹⁵⁹⁻¹⁶¹.

The small GTPase, Rap1, is strongly implicated in the regulation of inside-out signalling of cell-matrix adhesion^{162,163}. Within cells, levels of active Rap-GTP are spatially and temporally controlled through the activity of GTPase activating proteins (GAPs) and guanine nucleotide exchange factor (GEFs), such as the cAMP-regulated Epac proteins. Studies where Rap has been selectively activated in cells, either by overexpression of constitutively active Rap proteins, or by the specific activation of endogenous Rap using the Epac-specific cAMP analogue, 8-pCPT-2'-O-Me-cAMP (also called 007), have demonstrated that Rap activation has the capacity both to increase the affinity of integrins for their ligand⁴⁻⁶ and to promote integrin clustering^{162,164-166}. Along with this, Rap can regulate the cytoskeleton, as exemplified by the induction of cortical actin formation in endothelial cells^{31,89,167,168} and the inhibition of membrane protrusion in migrating cells¹⁶⁹. These functions of Rap are fundamental for the control of basal adhesion¹⁷⁰ as well as for activation of integrins in response to a number of external stimuli, including Mn²⁺¹⁷¹.

Although the outcome of Rap activation on cell adhesion and actin remodelling is well established, the mechanisms by which these occur are less well understood, but are beginning to be elucidated. A number of proteins, including Riam

^{50,51,172,173}, RapL^{52,174-177}, Arap3^{67,178}, Tiam1¹⁷⁹, AF6^{180,181}, and Radil^{117,182} have been proposed to be Rap effector proteins that mediate aspects of Rap-induced changes to integrins or the cytoskeleton^{165,183}. Most of these proteins have been identified by their ability to bind to Rap-GTP via RA domains¹⁸⁴. However, with the exception of Riam and RapL, which can regulate integrin complexes^{51,52,172-177}, it is unclear how most of these different proteins bring about Rap induced changes. Furthermore, it is not yet understood how the functions of these individual proteins relate to one another. In a particular cell type, Rap-regulated adhesion and cytoskeletal changes may require activation of a single effector protein. Alternatively, a number of proteins may be regulated by Rap concurrently or sequentially, performing separate functions, which are all required downstream of Rap.

In order to determine if an array of proteins is required for Rap-induced focal adhesion formation and cell spreading, we performed a limited siRNA screen in A549 cells, using a small library of siRNAs against putative Rap effectors and other proteins indirectly implicated in Rap-mediated adhesion. As expected, core regulators of focal adhesions and cellular tension were required for both basal and Rap-stimulated cell spreading. In the Rap signalling pathway, we found that, although both Rap1A and Rap1B are expressed in these cells, only siRNA against Rap1A blocked the changes in cellular morphology induced by activation of the Epac-Rap signalling pathway. Moreover, of the Rap effectors investigated in the screen, depletion of Radil had the biggest inhibitory effect on Rap-induced spreading. Interestingly, we identified that Ezrin, one of the Ezrin-Radixin-Moesin (ERM) family proteins, played a specific role in Rap1-induced spreading changes. Our results indicate that Ezrin is not critical for the initial phase of Rap-induced adhesion, but rather functions during later stages of Rap-dependent spreading processes. Moreover, this function of Ezrin does not appear to be shared by Radixin and Moesin. Here, we report on our findings which demonstrate a specific role of an ERM family protein in Rap-regulated cellular spreading.

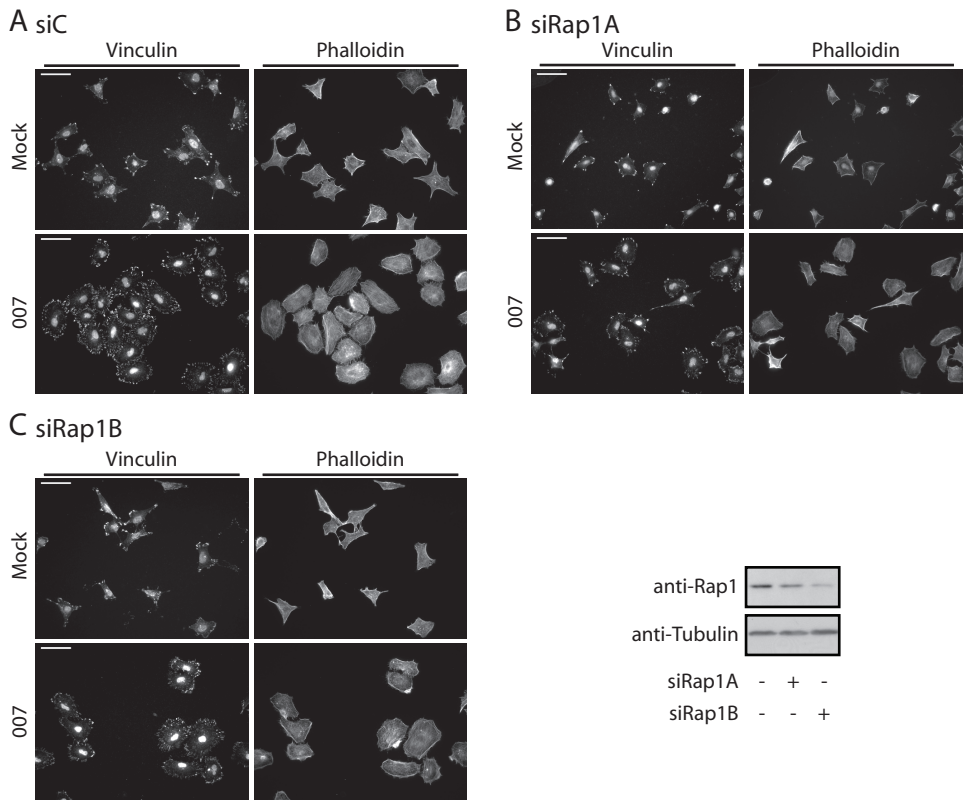


Figure 1: Activation of the Epac1-Rap signalling pathway by the cAMP analogue, 8-pCPT-2'-O-Me-cAMP, stimulates cell spreading, rounding and focal adhesion formation.

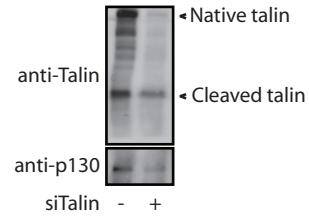
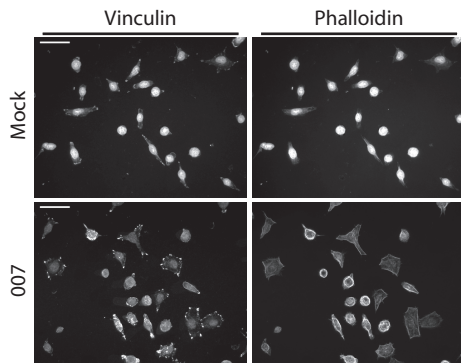
A549-Epac cells treated with scrambled siRNA (A) or siRNA against Rap1A (B) or Rap1B (C) for 48 hours were replated and allowed to adhere to fibronectin for 3 hours with or without 100 μ M 007. Following adhesion and spreading, cells were fixed and anti-vinculin antibodies were used to detect focal adhesions and phalloidin was used to detect F-actin by immunofluorescence. The scale bars represent 50 μ m. Western blot analysis to confirm knockdown of Rap1A and Rap1B is shown alongside. The antibody used recognises both Rap1A and Rap1B isoforms.

RESULTS

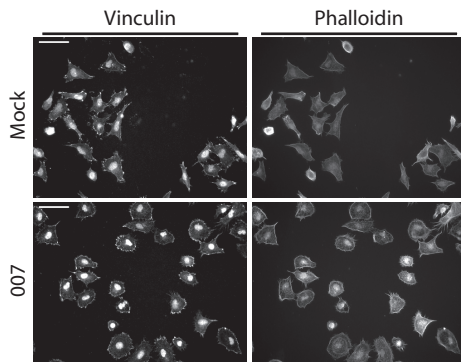
Knockdown of Ezrin and of core components of cell adhesion inhibits cell spreading following activation of the Rap signal transduction pathway

To analyse the activation of the Rap signalling pathway, we used A549-Epac1 cells, and activated the endogenous Rap proteins through the exchange factor, Epac1, using the cAMP analogue, 007. We then used immunofluorescence to monitor changes to focal adhesions, the cytoskeleton and cell shape. Following 3 hours of adhesion and spreading on fibronectin with Rap activation, cells showed a marked difference in overall morphology compared to cells which had spread under control conditions. Treatment of cells with 007 stimulated the spreading of cells, and promoted an increase in the number of focal adhesions around the periphery of individual cells (Fig. 1A and supplementary material Fig. S1). This increase in focal adhesions resulted in the Rap-stimulated cells taking on a pronounced rounded morphology, quite unlike the angularly-shaped control cells (Fig. 1A and supplementary material Fig. S1). This rounded cell morphology was not shown by mock treated cells which were allowed to spread on fibronectin for longer than 3 hours. This suggests that prolonged activation of the Rap signalling pathway induced a distinctive type of cell spreading.

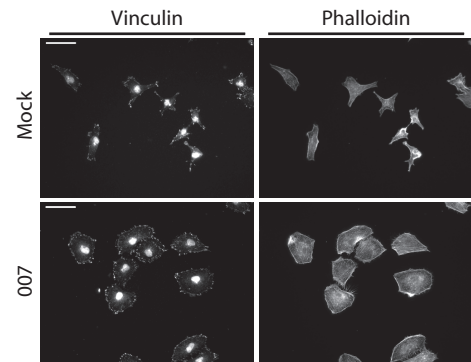
A siTalin



B siRadil



C siRiam



D siAF6

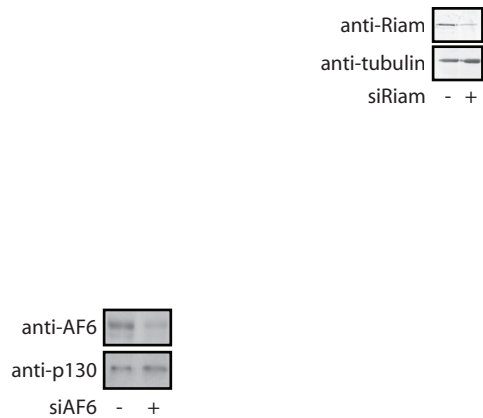
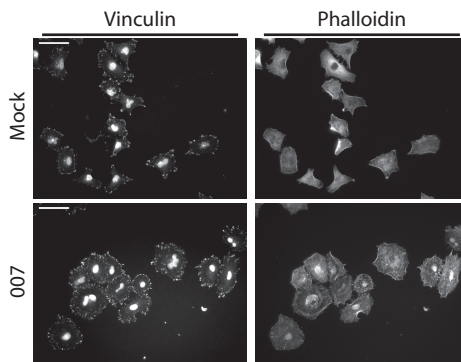


Figure 2: Knockdown of Talin and the Rap effector, Radil, inhibits cell spreading stimulated by activation of Epac. A549-Epac cells treated with siRNA against (A) Talin, (B) Radil, (C) Riam or (D) AF6 were replated and allowed to adhere to fibronectin for 3 hours with or without 100 μ M 007. Following adhesion and spreading, cells were fixed and focal adhesions and the cytoskeleton were visualized by immunofluorescence. The scale bars represent 50 μ m. Western blot analysis of protein levels to confirm knockdown of the proteins by siRNA is shown alongside.

To confirm that the 007-phenotype was due to stimulation of the Epac-Rap signalling pathway, we blocked activation of the pathway using siRNA against Rap and Epac proteins. We found that siRNA against Rap1A (Fig. 1B and supplementary material Fig. S2) and Epac1 (supplementary material Table S1) inhibited the basal spreading of cells and blocked the response of cells to 007. Interestingly, siRNA against Rap1B (Fig. 1C and supplementary material Fig. S2) and the Rap2 proteins (supplementary material Table S1) did not block 007-induced spreading, suggesting that the changes in cell morphology that we observed were induced specifically by Rap1A. These data validated that the distinctive phenotype induced by 007 resulted from activation of the Epac-Rap pathway, and that monitoring these morphological changes could be used to screen for components and mediators of 007-induced adhesion.

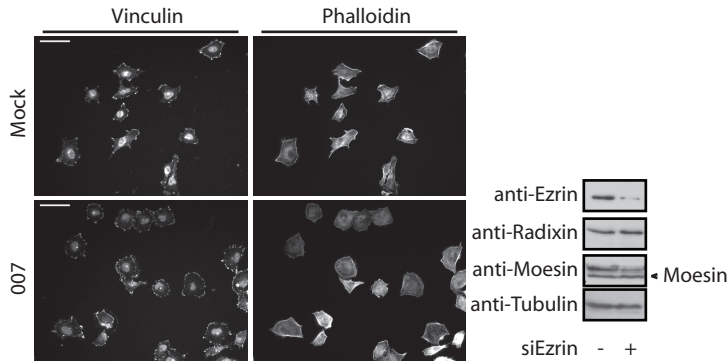
Our screen used a custom siRNA library which targeted proteins that have been previously described to be Rap effectors, as well as other proteins linked to Rap function, regulation of the cytoskeleton, focal adhesions and cell polarity. We found that siRNA against most of the proteins targeted in our screen did not block the 007 effect (supplementary material Table S1). However, knockdown of both Talin (Fig. 2A and supplementary material Fig. S2) and RockII (supplementary material Table S1) inhibited basal and 007-induced adhesion and spreading, consistent with their essential function in regulating integrins and cell spreading. Of the reported Rap effectors, only knockdown of Radil (also known as AF6-L) caused an inhibition of 007-induced cell spreading in approximately 70% of the replated cells (Fig. 2B and supplementary material Fig. S2). This result was corroborated by two single siRNAs against Radil, and confirms previous reports of a role for Radil in Rap-induced cell adhesion^{117,182}. In comparison, other Rap effector proteins, such as Riam (Fig. 2C and supplementary material Fig. S2), did not block the 007 effect. This suggests that, in the A549-Epac cells, Radil plays a more critical role in 007-induced spreading and focal adhesion formation than other Rap effectors. Knockdown of AF6 (Fig. 2D and supplementary material Fig. S2) increased the spreading of A549-Epac cells in response to 007, which is consistent with its previously described role as a negative regulator of Rap function¹⁸¹. Although Radil is known as AF6-L, because, like AF6, it contains RA and DIL domains, the divergence of these two genes predates the emergence of animals (T.J.P. van Dam, personal communication). Such a long evolutionary distance between AF6 and Radil may account for their different functions downstream of Rap activation.

Work from our group has demonstrated that ERM proteins play a redundant role as an anchor which localises Epac1 at the plasma membrane. This interaction regulates cell adhesion, as simultaneous knockdown of all three ERM proteins decreased but did not block completely Epac1-induced cell adhesion¹⁸⁵. Interestingly, although all three ERM family members are expressed in A549-Epac1 cells,

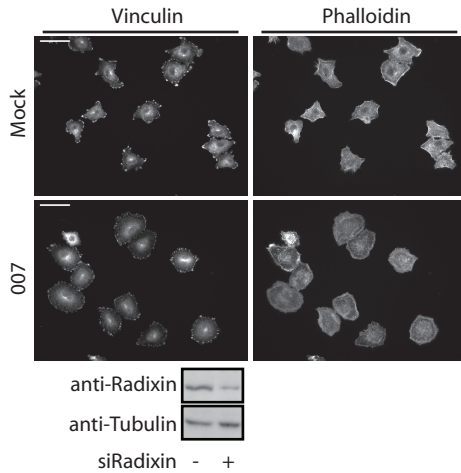
Figure 3: Knockdown of Ezrin, but not Radixin and Moesin, inhibits Epac-induced cell spreading.

A549-Epac cells treated with siRNA against (A) Ezrin, (B) Radixin or (C) Moesin were replated and allowed to spread on fibronectin for 3 hours with or without 100 μ M 007, and the focal adhesions and the actin cytoskeleton were visualised by immunofluorescence. The scale bars represent 50 μ m. Knockdown of each ERM protein was confirmed by western blot. The anti-Moesin antibody also recognises Ezrin and Radixin, which have a higher molecular weight, as indicated. In (D), the spreading of at least 25 cells from each condition from four separate experiments was measured and quantified using ImageJ. The spreading index was calculated by using the mean size of the control cells which had spread in the absence of 007 as the standard. The graph shows the mean of four experiments \pm the standard error of the means. The P value was obtained by performing a paired Student's t-test. In (E), the spreading of cells from a single representative experiment subjected to non-targeting siRNA, C, the SMARTpool, Sp, siRNA against Ezrin, and the single siRNAs, oligos 8-11 from the SMARTpool, were quantified. The mean of the average cell size per field of view is shown \pm the standard deviation. Five fields of view were analysed per condition. The ability of these siRNAs to decrease the cellular levels of the Ezrin protein is shown alongside. In (F), cells transfected with siRNA against Ezrin, Radixin, Moesin or all three ERM proteins together were lysed and the knockdown of each ERM protein and their contribution to the active pool of ERM proteins were analysed by western blot.

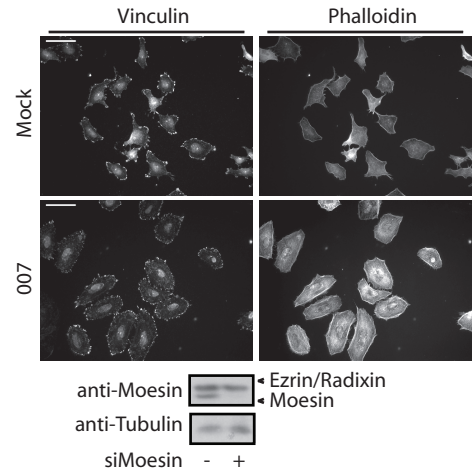
A siEzrin



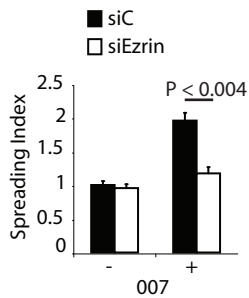
B siRadixin



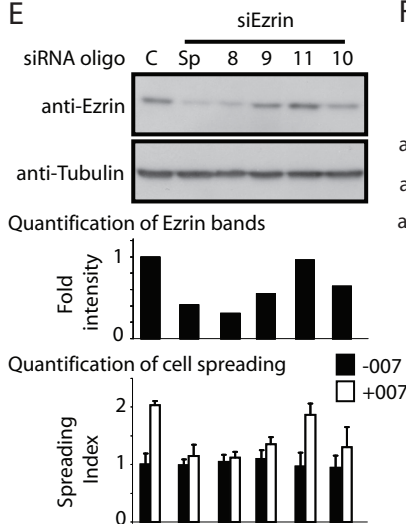
C siMoesin



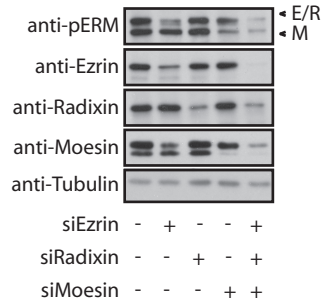
D



E



F



we found that depletion of Ezrin blocked the 007 effect in more than 70% of cells (Fig. 3A), similar to siRNA targeting Rap1A and Radil. However, knockdown of Radixin (Fig. 3B and supplementary material Fig. S2) and Moesin (Fig. 3C and supplementary material Fig. S2) did not block cell spreading. Importantly, siRNA against Ezrin neither inhibited the spreading of cells under basal conditions nor depleted the levels of the Radixin and Moesin protein (Fig. 3A). To confirm our visual observations of the immunofluorescence studies, correct regulation of Rap signalling was analysed by quantifying the area of A549-Epac1 cells under different conditions, using ImageJ software, as an indication of cell spreading. Using this method, we confirmed that Ezrin knockdown caused a significant decrease in the Rap-induced spreading response (Fig. 3D). To validate that the siRNA was, indeed, targeting Ezrin specifically, we used single siRNAs against Ezrin (Fig. 3E). We found that the level of depletion of Ezrin protein by each siRNA corresponded to the inhibition of 007-induced spreading.

The block in the 007-reponse could be consistent with Ezrin being required to localise Epac1 for signal transduction. Western blot analysis of the pool of active ERM proteins in A549-Epac1 cells revealed that siRNA against Ezrin and Moesin had the biggest effect on depletion of the phospho-ERM levels (Fig. 3F). However, as depletion of Moesin had a similar effect on the levels of phospho-ERM proteins, but did not block Rap-induced spreading, our findings suggested that Ezrin had another function downstream of Rap.

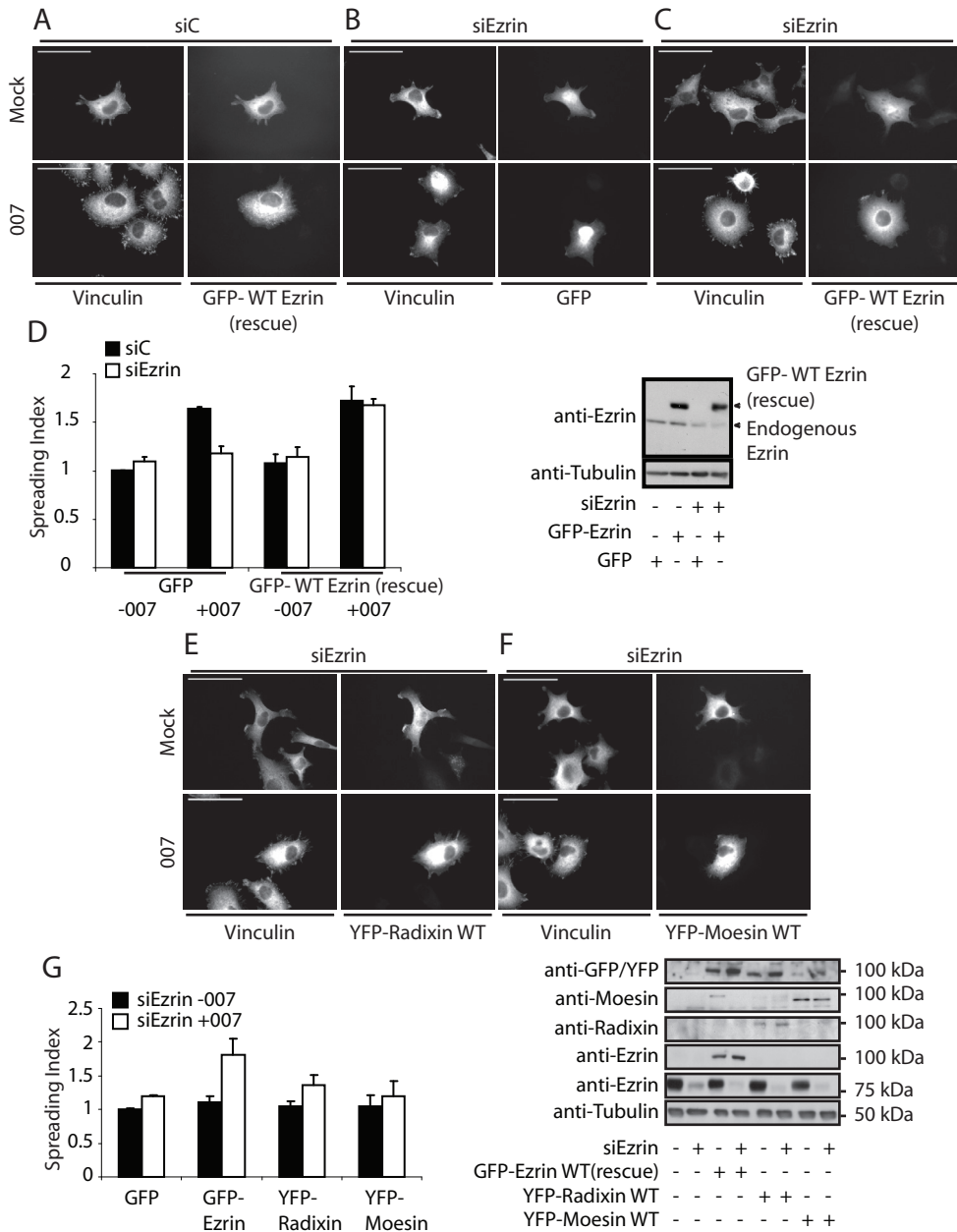
Overexpression of an Ezrin resistant to a single siRNA can rescue the inhibition of cell spreading caused by Ezrin depletion

To confirm that depletion of Ezrin itself caused the defects in 007-induced spreading which we observed, we made a GFP-Ezrin wild-type (WT) construct, GFP-WT Ezrin (rescue), which was resistant to one of the single siRNAs that depleted Ezrin protein levels and blocked 007-induced spreading (Fig. 3E). A549-Epac1 cells which were transfected with scrambled siRNA and expressed GFP-empty vector control or GFP-WT Ezrin (rescue), spread normally under mock and 007-stimulated conditions (Fig. 4A and 4E). Importantly, GFP-WT Ezrin (rescue) did not seem to alter the basal spreading of the cells. In cells which had been transfected with siRNA against Ezrin, GFP-empty vector-expressing cells did not respond to 007 (Fig. 4B and 4E), whereas cells expressing the GFP-WT Ezrin (rescue) protein showed an increase in their spreading comparable to the spreading observed in the control cells (Fig. 4C and 4E).

The recovery of the 007-induced phenotype by re-introducing Ezrin into siEzrin treated cells confirmed that the effects on spreading were due to the depletion of the endogenous Ezrin protein, and were not due to off-target effects of the siRNA. Depletion of Ezrin caused a substantial loss of the active pool of ERM proteins (Fig. 3F). To determine if overexpression of another ERM protein could restore 007-induced spreading in Ezrin-depleted cells, we performed similar rescue experiments, but overexpressed YFP-Radixin (Fig. 4E) or YFP-Moesin (Fig. 4F). In order to approximate for equal protein expression, cells of equal fluorescence to those expressing GFP-WT Ezrin (rescue) were imaged and quantified (Fig. 4G). Cells expressing YFP-Radixin or YFP-Moesin were not sufficient to recover the 007-induced spreading (Fig. 4D, 4F and 4G). Hence, our data strongly suggest that the Ezrin protein, specifically, is required for 007-induced cell spreading.

Figure 4: The inhibition of the 007-phenotype in knockdown of Ezrin can be recovered by overexpression of siRNA-resistant Ezrin.

To rescue the effects of Ezrin knockdown, cells were transfected with siRNA for 8 hours before being transfected with GFP-empty vector (Ev), GFP-WT Ezrin (rescue), YFP-Radixin or YFP-Moesin. Images of representative cells were captured (A-C and E-F), and the scale bars represent 50 μm . The spreading of individual cells expressing



GFP, GFP-WT Ezrin (rescue), YFP-Radixin or YFP-Moesin transfected with either scrambled siRNA or siRNA against Ezrin, was quantified using ImageJ. For each experiment, 20 cells were analysed per condition. In order to take into account differences in transfection efficiencies and to try to standardise for equal overexpression of each of the ERM proteins in individual cells, cells of equal YFP fluorescence were selected for quantification. In (D), the graph shows the average spreading for three individual experiments \pm standard error of the means. Western blot analysis from a representative experiment confirming knockdown of endogenous Ezrin and overexpression of the GFP-WT Ezrin (rescue) construct is shown alongside. In (G), the graph shows the median spreading value for two individual experiments \pm the range of the means. Western blot analysis to confirm depletion of Ezrin and overexpression of YFP-Radixin and YFP-Moesin is shown alongside.

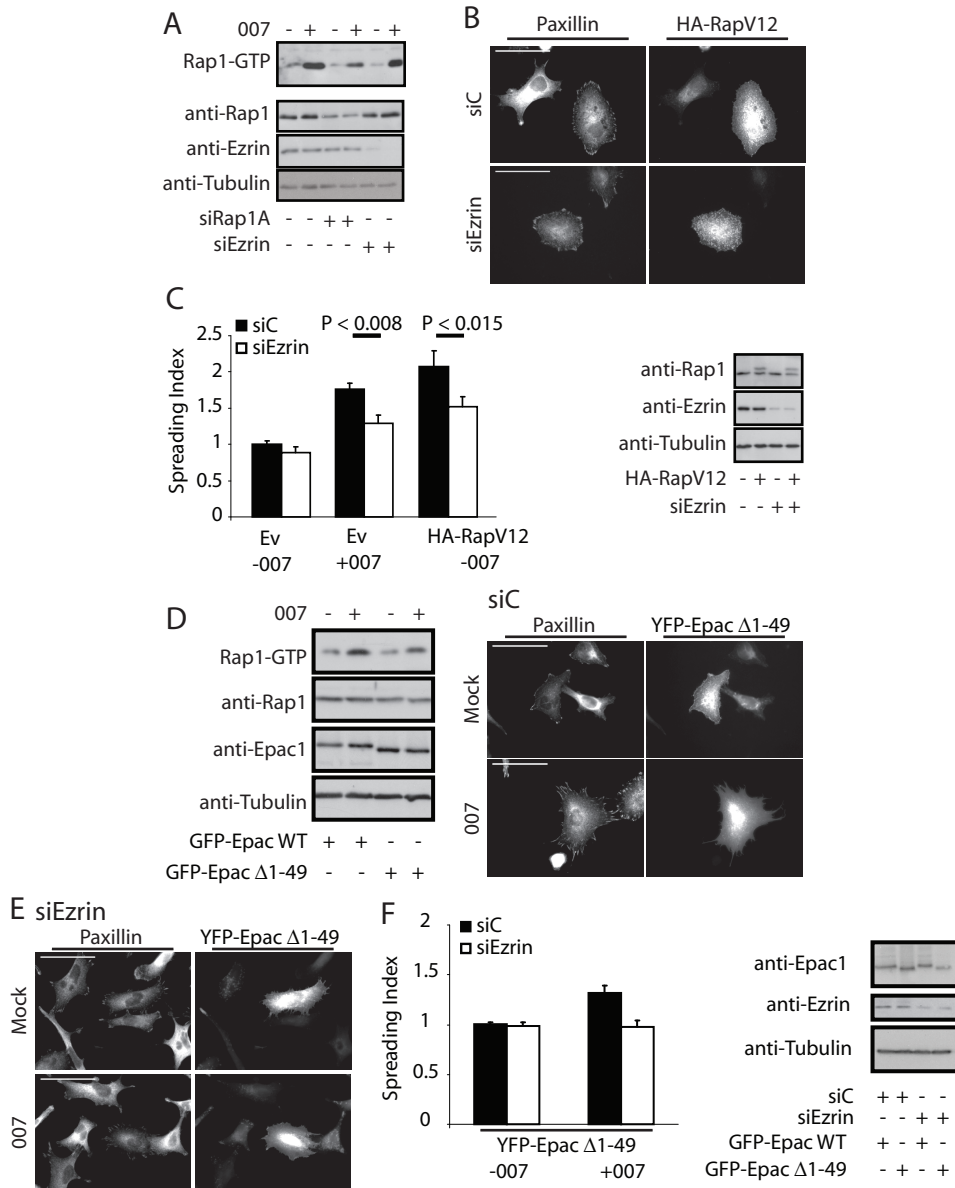


Figure 5: Ezrin functions downstream of Rap in the signal transduction pathway.

(A) A549-Epac cells were transfected with scrambled siRNA or siRNA against Rap and Ezrin for 48 hours before being exposed to mock or 100 μ M 007 for 15 minutes. Pull down of Rap-GTP, by the RalGDS Rap-binding domain, and knockdown of Rap1A and Ezrin were detected by western blot. In (B), cells were transfected with scrambled or Ezrin siRNA for 8 hours before being transfected with HA-RapV12. After 48 hours, cells were replated on fibronectin and allowed to adhere and spread for 3 hours. Cells were fixed and stained as described in Materials and methods. Images in (B) are representative cells, with the scale bars representing 50 μ m. In (C), the spreading of cells transfected with empty vector (Ev) or expressing HA-RapV12, were quantified using ImageJ. The graph shows the mean size of cells from four separate experiments \pm standard error of the mean. In each experiment, at least 50 cells were analysed per condition. The P values were calculated using a paired Student's t-test. Western blots confirming the overexpression of HA-Rap1A and knockdown of Ezrin are shown alongside. In (D) and (E), A549 cells which had been subjected to

Ezrin is required downstream of Rap activation to regulate cellular spreading

As our group has demonstrated that active ERM family proteins can localise Epac1, and hence can regulate Epac-mediated cell adhesion¹⁸⁵, it is possible that the major defect caused by Ezrin depletion occurs via disruption or mislocalisation of Epac1-Rap signalling complexes. To investigate whether Epac1-Rap1 signal transduction was still intact in cells depleted of Ezrin, we analysed the levels of Rap1-GTP which were stimulated in response to 007 in cells transfected with siRNA against Ezrin. We found that Rap1 was activated robustly in the presence of Ezrin knockdown (Fig. 5A).

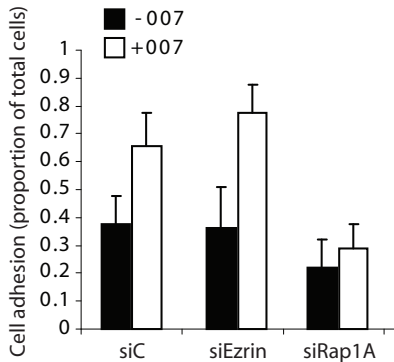
Then, to determine whether the effects of Ezrin depletion on Rap-induced cell spreading were independent from its function as an anchor for Epac, we used the constitutively active RapV12 protein to induce cell spreading in the A549-Epac1 cells. Indeed, in cells which had been transfected with scrambled siRNA, overexpression of the HA-RapV12 protein caused an increase in the number of focal adhesions and promoted spreading of these cells in the absence of 007 (Fig. 5B and 5C) which was comparable to the spreading induced by 007 (Fig. 5C). In comparison, in cells transfected with siRNA against Ezrin, the focal adhesion formation and cell spreading induced by RapV12 overexpression was inhibited (Fig. 5B and 5C). Quantification of the cells expressing HA-RapV12 confirmed that Ezrin depletion caused a significant reduction in RapV12-induced spreading (Fig. 5C) and demonstrated that Ezrin is required for the focal adhesion formation and cell spreading induced by Rap activation, and would suggest its role in spreading is not entirely upstream, via localisation of Epac1¹⁸⁵, but also downstream of Rap1.

To strengthen our conclusion that the Ezrin was performing a function independent of its ability to bind to Epac1, we investigated whether depletion of Ezrin could block spreading regulated by YFP-Epac1 $\Delta 49$. In this protein, the first 49 amino acids that mediate the interaction with ERM proteins are deleted, producing a protein which is still activated by 007 and can induce cell adhesion, although to a lesser extent than the WT protein, but with any upstream regulation of Epac1-Rap1 signalling by Ezrin being abolished¹⁸⁵. Therefore, if Ezrin regulated cell spreading only by localising the Epac-Rap signalling complex, depletion of Ezrin would have no effect on the spreading which was induced by activation of YFP-Epac1 $\Delta 49$ with 007. In A549 cells, which lack endogenous Epac proteins¹⁶⁹, overexpression of YFP-Epac1 $\Delta 49$ stimulated the formation of Rap1-GTP (Fig. 5D) and permitted cells to spread in response 007 (Fig. 5D and 5F). In cells treated with siRNA against Ezrin, the basal spreading of cells expressing YFP-Epac1 $\Delta 49$ was not repressed, but the 007-induced spreading was inhibited (Fig. 5E and 5F). Together, these data demonstrate that the Ezrin protein functions downstream of Rap activation to regulate 007-induced spreading.

Depletion of Ezrin blocks the spreading of A549-Epac1 cells in response to 007, specifically, without inhibiting the increase in Rap-stimulated initial adhesion

As cell spreading requires the co-ordinated regulation of both integrin activity and cytoskeletal changes, it is possible that depletion of Ezrin blocked the initial adhesion of cells to fibronectin, which resulted in the cells not being able to spread properly. To gain understanding of how Ezrin may be functioning during spreading, we used a short-term adhesion assay to analyse whether the ability of cells to adhere to fibronectin was reduced by Ezrin knockdown.

scrambled siRNA or siRNA against Ezrin for 8 hours were then transfected with YFP-Epac1 $\Delta 49$ for 48 hours before being allowed to adhere under mock or 007 stimulated conditions for 3 hours. The ability of YFP-Epac1 $\Delta 49$ to increase Rap-GTP levels in response to 007 in A549 cells, in the absence of siRNA transfection, is shown alongside. The spreading of the YFP-Epac1 $\Delta 49$ expressing cells was measured using ImageJ and the graph shows the mean spreading of cells from 3 experiments \pm standard error of the means (F). At least 20 cells were analysed per condition in each experiment. Western blot analysis, shown alongside, confirmed the overexpression of the truncated YFP-Epac1 $\Delta 49$ protein and the knockdown of Ezrin.



performed in quadruplicate. The graph shows the mean adhesion for three experiments \pm standard error of the means. A representative western blot analysis, to confirm the knockdown of Rap1A and Ezrin in the cells used in the alkaline phosphatase adhesion assay, is shown alongside.

Over a 30 minute period, 007 induced an approximately 2-fold increase in cell adhesion in cells treated with scrambled siRNA (Fig. 6). Depletion of Rap1A from the cells decreased basal adhesion and inhibited 007-induced adhesion. Interestingly, depletion of Ezrin did not affect initial adhesion of cells, with or without 007 treatment. This suggests that Ezrin does not play a role in the initial adhesion of A549-Epac1 cells to fibronectin, but is involved in the cellular changes that occur to produce the increase in focal adhesions and spreading that we observed following adhesion of cells in the presence of 007.

Depletion of Ezrin using a validated siRNA blocks 007-induced spreading in a number of cell lines

To determine if Ezrin blocks 007-induced spreading in cells other than the A549-Epac1 cell line, we performed the spreading assay with MDA MB231 breast cancer cell line (Fig. 7A), which stably overexpressed Epac1, and with human umbilical vein endothelial cells (Fig. 7B), which have endogenous Epac. We found that depletion of Ezrin in these cells blocked 007-induced spreading changes (Fig. 7A and 7B). This suggests the role of Ezrin is not limited to cells overexpressing Epac1, or restricted to a particular cell type. Ezrin, therefore, may have a wide-spread role in Rap-induced cellular changes.

Ezrin is not sufficient to produce the spreading and morphology changes associated with Rap activation in A549 cells

To determine if Ezrin alone is sufficient to induce the 007 effect in A549-Epac1 cells, we overexpressed either GFP-Ezrin WT or the open, constitutively active GFP-Ezrin T567D mutant protein^{186,187} in A549-Epac1 cells. Using a short-term adhesion assay to measure the ability of cells to adhere to fibronectin, we observed that overexpression of Ezrin WT did not stimulate initial cell adhesion. However, overexpression of the Ezrin T567D mutant caused an increase in the adhesion of the A549-Epac1 cells comparable to the effects of 007 (Fig. 8A). This overexpression study suggests that although Ezrin is not required in the initial adhesion induced by Rap, Ezrin can regulate adhesion processes, which may be required by Rap during the spreading response.

To observe if this ability to regulate adhesion caused an increase in cell spreading, we monitored GFP-Ezrin overexpressing cells by immunofluorescence. As observed with the Ezrin rescue experiments, GFP-Ezrin WT did not stimulate the spreading of A549-Epac1 cells (Fig. 8B and 8C). In contrast, GFP-Ezrin T567D-expressing cells were significantly more spread in the absence of 007 (Fig. 8B and 8C).

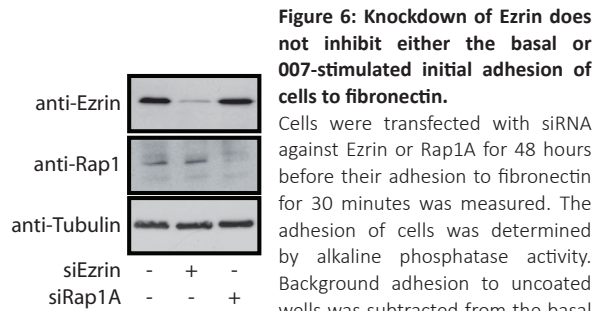


Figure 6: Knockdown of Ezrin does not inhibit either the basal or 007-stimulated initial adhesion of cells to fibronectin.

Cells were transfected with siRNA against Ezrin or Rap1A for 48 hours before their adhesion to fibronectin for 30 minutes was measured. The adhesion of cells was determined by alkaline phosphatase activity. Background adhesion to uncoated wells was subtracted from the basal and 007-induced adhesion and expressed as a proportion of the total cells added per well. For each experiment, each condition was

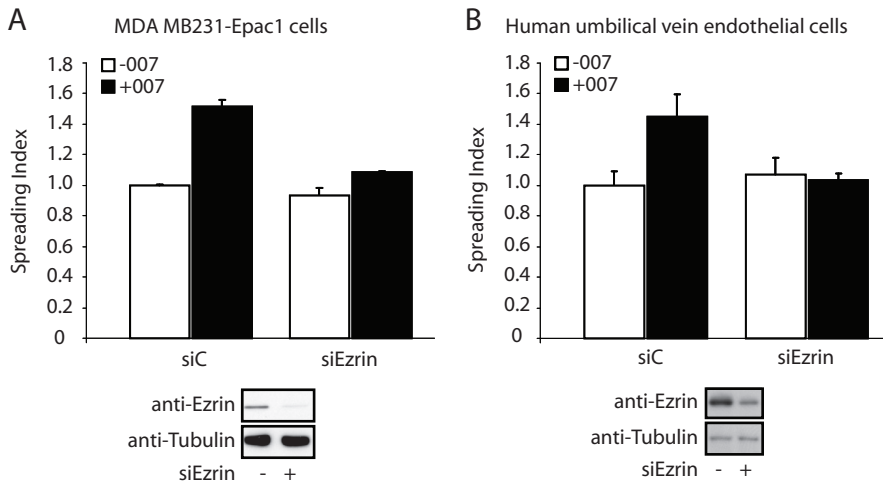


Figure 7: Knockdown of Ezrin blocks Rap-induced spreading of a number of cell lines.

MDA MB321-Epac1 cells (A) or human umbilical vein endothelial cells (B) transfected with scrambled siRNA or siRNA against Ezrin for 48 hours were replated and allowed to adhere to fibronectin for 3 hours with or without 100 μ M 007. Following adhesion and spreading, cells were fixed and visualized by immunofluorescence, and the spreading of the cells was quantified using ImageJ. The graph shows the mean spreading for two experiments \pm the range of the means. Twenty cells were analysed per condition in each experiment. Western blot analyses to confirm the knockdown of Ezrin in each cell type are shown alongside.

Critically, the spreading which was induced by GFP-Ezrin T567D was different from the spreading which was induced by 007, as the cells did not show an increase in focal adhesions compared to GFP-Ev mock treated cells (Fig. 8B and 8D) and they did not display the rounded morphology characteristic of Rap-induced spreading. To analyse this morphology difference, we quantified the shapes of the cells by determining the convex hull of individual cells (Fig. 8E). Then, to give an indication of the shape, the total area between the cell and the edges which joined up the outermost parts of the cell was measured. We found that, consistent with being round in shape, GFP-expressing cells treated with 007 had less area outside of the cell (Fig. 8E). However, in accordance with being different in shape from 007-treated cells, cells overexpressing GFP-Ezrin T567D without 007 stimulation had consistently more area outside of the cell (Fig. 8E). This difference in shape corresponded to the cells overexpressing GFP-Ezrin T567D having fewer focal adhesions than cells which had spread to a similar size with 007 (Fig. 8D). This suggests that, although GFP-Ezrin T567D regulates spreading adhesion processes, it cannot initiate the focal adhesion formation and cellular morphology changes sufficient to produce the 007 phenotype.

As the open form of Ezrin can mediate these effects, we performed a time course of 007 treatment on adherent cells to determine if Rap activation stimulates phosphorylation of the ERM pool at the threonine residue responsible for stabilising the open conformation of the proteins. We found that Rap activation does not stimulate the phosphorylation of the total pool of ERM proteins in the cell (Fig. 8F).

DISCUSSION

The small GTPase Rap is involved in inside-out control of cell adhesion processes which can be monitored as changes to cell spreading and focal adhesion formation. This paper presents evidence that the ERM family member, Ezrin, is critical for spreading and morphology changes induced by

Rap activation. Our screen identified that knockdown of Ezrin had a similar effect on 007-induced spreading as depletion of either Rap1A or the Rap effector, Radil. Furthermore, we have identified that Ezrin is required for Rap-induced cellular spreading in both epithelial and endothelial cells.

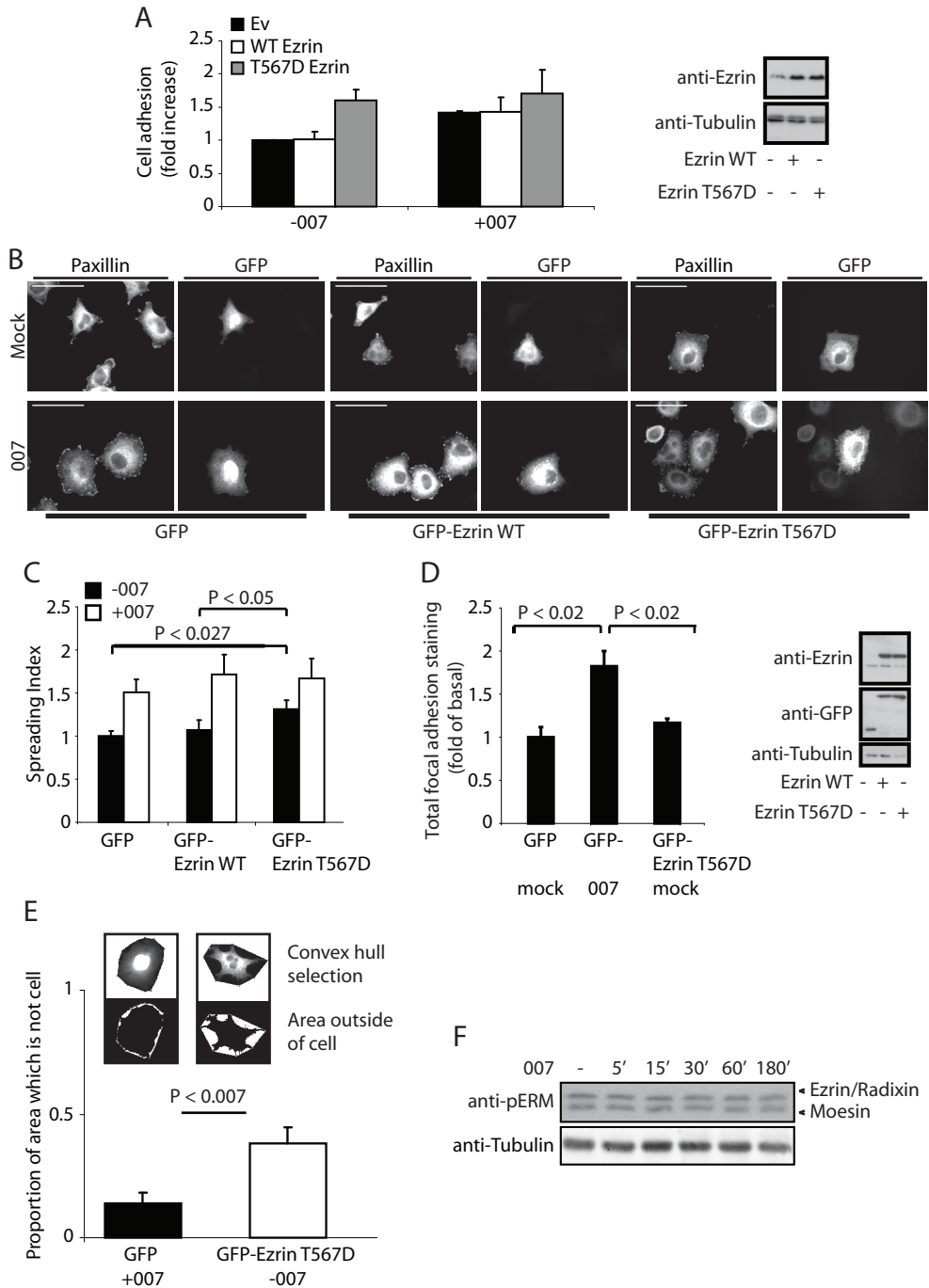
Interestingly, although the homologous ERM proteins, Radixin and Moesin, are co-expressed in the A549-Epac1 cells, their depletion did not block Rap-induced spreading. Previous work from our lab has found that ERM proteins can localise Epac1 at the plasma membrane. In this case, the function of ERM proteins did seem to be redundant, as all three ERM proteins had to be depleted in to order block Epac-induced cell adhesion¹⁸⁵. In this study, through our analysis of the spreading induced by HA-RapV12 and YFP-Epac1 Δ 49, we have shown that Ezrin has an additional role downstream of Rap activation, independent from its ability to bind to Epac1. Moreover, overexpression of YFP-Radixin or YFP-Moesin could not rescue the 007-induced spreading of Ezrin knockdown cells. Therefore, the role of Ezrin in cell spreading downstream of active Rap appears to be a novel example of a non-redundant function of a single ERM protein.

Our data suggest that Ezrin is critical during Rap-dependent cell spreading of replated cells, without being necessary for the initial cell adhesion steps. Interestingly, we found that knockdown of the Rap effector, Radil, also inhibited Rap-induced cell spreading, but not adhesion. Together these data indicate that Rap1 regulates two independent steps during adhesion and spreading, with both Ezrin and Radil being required during the second spreading step. In a similar way, the Rap effector protein, RapL, does not mediate the Rap-dependent rolling arrest of T cells, but is required for their Rap-dependent stable interaction with ICAM-1¹⁷⁴.

The activity of Ezrin is regulated by phosphorylation of Thr567^{186,187}, with phosphorylation of other tyrosine residues also being implicated in the function of the protein^{186,188,189}. Currently, we do not have evidence that Rap1 can induce activation of Ezrin. For instance, treatment of cells with 007 did not result in an increase in Thr567 phosphorylation. Although overexpression of the open, active form of Ezrin, Ezrin T567D, did induce cell adhesion and spreading, it did not mimic the activation of Rap1 in cells. Specifically, Ezrin did not increase the number of focal adhesions to the same extent as activation of Rap1 and did not induce the rounded cell morphology. This implies that although Ezrin is required for Rap1-induced spreading, other Rap1-mediated changes are necessary as well. Indeed, from

Figure 8: Overexpression of Ezrin is not sufficient to produce the 007 phenotype.

(A) Empty vector (Ev), Flag-His-Ezrin WT or VSVG-Ezrin T567D was co-transfected with a luciferase construct into A549-Epac1 cells for 48 hours prior to cells being replated on fibronectin for 30 minutes. Cells which had adhered were measured by luciferase assay. The background adhesion of cells to uncoated wells was subtracted from the basal and 007-induced adhesion. Each condition was standardised to the basal adhesion of Ev-expressing cells. The graph shows the mean adhesion of four separate experiments \pm standard error of the means. Overexpression of Ezrin was confirmed by western blot. (B) GFP-Ev, GFP-Ezrin WT or GFP-T567D Ezrin was overexpressed in the A549-Epac1 cells for 48 hours before the cells were replated and allowed to adhere and spread on fibronectin for 3 hours; they were then fixed, and focal adhesions were detected using an antibody against paxillin. The scale bars represent 50 μ m. The spreading of cells (C) and the total area of cells which stained for paxillin (D) in cells overexpressing GFP-Ev, GFP-Ezrin WT or GFP Ezrin T567D were quantified using ImageJ. The graphs show the average size of cells from 3 experiments \pm standard error of the means. At least 20 cells were analysed per condition in each experiment. Western blot analysis confirmed overexpression of Ezrin. To analyse the shape of GFP-Ev cells treated with 007 and cells overexpressing Ezrin T567D, the convex hull of individual cells was determined using ImageJ (E). The outermost points of the cell were joined up to create a shape, and the size of the shape was measured. Then, the area between the outside of the cell and the edge of the shape was measured, as indicated by the white areas in the bottom panel. The proportion of the shape that was outside the cell was calculated. The graph shows the mean proportion for 3 experiments \pm the standard error of the means. Ten cells were analysed per experiment. A rounder cell gives rise to a lower proportion of the shape outside of the cell. (F) To determine if Rap activation could regulate the activity of ERM proteins, adherent cells were stimulated with 007 for different times, lysed, and then the levels of the open, active conformation of Ezrin were detected using a phospho-ERM antibody by western blot.



our screen, we found that knockdown of the previously identified Rap-effector, Radil, blocked Rap-induced spreading of A549-Epac1 cells. The function of Radil, therefore, may be needed along with Ezrin to induce the 007-phenotype in cells. Recently, it has been shown that G_{βγ} subunits co-ordinate and localise the complex of active Rap and Radil which is critical for cell-matrix adhesion following activation of G-protein coupled receptors via fMLP¹⁸². Therefore, downstream of Rap activation, Ezrin may be a critically important signalling scaffold, localising complexes of proteins, including Epac1, active Rap1A and effectors, such as Radil. However, thus far we have been unable to demonstrate an interaction of Radil with Ezrin or a synergism between Ezrin and Radil in cell spreading.

Like the other ERM family members, Ezrin acts to link the cytoskeleton to the plasma membrane by binding to actin and PtdIns(4,5)P₂¹⁹⁰ or to membrane proteins like ICAM-1/2, CD44 and syndecan-2¹⁹¹⁻¹⁹⁷. By creating such a linkage, ERM proteins can perform both structural and regulatory functions in cells. For instance, ERM proteins are able to control cell shape by organising actin filaments and regulating cortical stiffness¹⁹⁸⁻²⁰⁰. Regulation of the interaction of ERM proteins with the actin cytoskeleton is required to alter T cell morphology^{201,202} and to control the membrane diffusion and signalling of the B cell receptor²⁰³. Therefore, Ezrin may be able to create discreet and dynamically regulated compartments within the plasma membrane, in order to organise and localise transmembrane proteins, such as adhesion molecules. Indeed, Ezrin has been implicated in cell-cell and cell-substrate adhesion²⁰⁴⁻²⁰⁷, stabilisation of β4 integrins²⁰⁸ and modulation of cell spreading^{204,205}. However, these studies give conflicting reports on the effects of Ezrin on cell adhesion. It is possible that by regulating the diffusion of adhesion molecules and by controlling cellular shape changes, Ezrin may either increase or limit adhesion and spreading in different cell types. In addition, by linking the co-receptor, CD44v6, to the actin cytoskeleton, Ezrin can organise signalling complexes which enable signal transduction from the c-Met receptor²⁰⁹ and the VEGFR-2 receptor²¹⁰. Ezrin may function downstream of Rap as a multipurpose molecule, controlling cell architecture, by regulating the tension changes in actin and the localisation of adhesion molecules, as well as by co-ordinating signalling processes.

Our finding that Ezrin is required for Rap-induced cell spreading suggests that, in combination with the modulation of the integrin-actin linkage, Rap may regulate a link between the plasma membrane and the cytoskeleton. Thus, during cell spreading, in parallel to changes to focal adhesions, Rap may modulate cellular rigidity through signalling complexes controlled by Ezrin. Mapping the protein-protein interactions of Rap-induced Ezrin signalling complexes may give insights into why Ezrin, specifically, is required in Rap signal transduction. Such studies may lead to the discovery of other unique roles for ERM family proteins in cells.

ACKNOWLEDGEMENTS

We would like to thank Jelena Linnemann for help with culturing the human umbilical vein endothelial cells and Johan de Rooij for discussions and critical reading of the manuscript. SHR was supported by a FEBS Long-Term Fellowship. AP and JHR were funded by grants (2003–2956 and 2009-4317) from the Dutch Cancer Society (KWF Kankerbestrijding), while MG was funded by a grant from Chemical Sciences of the Netherlands Organization for Scientific Research (NWO). This work was further supported by the Netherlands Genomics Initiative of the Netherlands Organization for Scientific Research.

MATERIALS AND METHODS

Cell Lines and Culture

The lung A549 cell line and the derivative monoclonal Epac1-expressing A549-Epac1 cell line, which has been described previously¹⁶⁹, were cultured in RPMI supplemented with L-glutamine, antibiotics, and 10% FCS. Stable expression of Epac1 in the MDA MB231 breast cancer cell line was achieved using amphotropic retroviruses. Single Epac1-expressing colonies were isolated following zeocin selection, and cultured in DMEM supplemented with L-glutamine, antibiotics, and 10% FCS. Human umbilical vein endothelial cells were cultured using standard

procedures³¹.

Reagents and Antibodies

8-pCPT-2'-O-Me-cAMP (007) was obtained from MP biochemicals. Antibodies were from Santa Cruz (Rap1, p130), BD Biosciences (Paxillin, Ezrin, Radixin, Moesin, AF6), Cell Signaling Technology (phospho-Ezrin[Thr567]/Radixin[Thr564]/Moesin[588]), Roche (GFP), Chemicon (α -Tubulin), Sigma-Aldrich (Vinculin, Talin) and Covance (monoclonal HA antibody, HA11). Anti-Riam antibody was a gift from M. Krause. The monoclonal anti-Epac1 5D3 antibody has been described before²¹¹. siRNAs were obtained from Dharmacon. The initial screen was performed using ON-targetplus SMARTpool siRNA oligos, with Ezrin, Radil, Riam, AF6 and Radixin knockdowns being confirmed with single siRNAs.

DNA Constructs

The HA-RapV12 construct has been described previously²¹². cDNA for Ezrin (EZR, Homo sapiens, GI: 161702985), Radixin (RDX, Homo sapiens, GI: 62244047) and Moesin (MSN, Homo sapiens, GI: 53729335), were obtained from RZPD (Berlin, Germany). The ERM proteins were cloned to express an N-terminal Flag-His tag or VSVG tag in a pCDNA3 vector, or GFP or YFP in a modified pLV CMVbc vector, or pCDNA3.1, respectively, using the Gateway system (Invitrogen) as described previously¹⁸⁵. Site-directed mutagenesis was used to make the Ezrin T567D mutant, and a rescue producing a WT protein sequence not targeted by the single Dharmacon siRNA (sequence GCGCAAGGAGGAUGAAGUU) was made using the primers 5'-CCTGGAATGTATGGCATAAATTACTTTGAAATAAAAAACAAG-3' and 5'-CTGTTTTTTATTTCAAAGTAATTATGCCATACATTTCAGG-3'

Epac1 (RapGEF3, Homo sapiens, GI: 3978530) was cloned N-terminally to a YFP tag in a pCDNA3 vector. Epac1 Δ 1-49 was generated by site-directed mutagenesis as described previously¹⁸⁵.

Cell transfection

For knockdown experiments, A549-Epac1 and MDA MB231 cells were seeded sparsely for 24 hours prior to transfection with 50 nM ON-targetplus SMARTpool siRNA oligos (Dharmacon) using oligofectamine (Invitrogen) according to the manufacturer's protocol. HUVEC cells with transfected with 50 nM siRNAs using Dharmafect 1 reagent. For overexpression of proteins, sparsely seeded A549-Epac cells were transfected with RapV12 or Ezrin constructs using FuGENE 6 (Roche) according to the manufacturer's instructions. For rescue experiments or experiments where cells were subjected to siRNA and overexpression constructs, A549-Epac cells were seeded sparsely and transfected with siRNA for 8 hours before transfection of the RapV12, Ezrin or Epac1 constructs.

Immunofluorescence and spreading assay

Cells were trypsinised 48 hours after transfection, washed once with the appropriate media with 10% FCS and then kept in suspension for 1.5 hours at 37 °C in media containing 0.5 % FCS, glutamine, antibiotics and 20 mM Hepes, to allow surface proteins to recover. The cells were maintained in 0.5% serum, as the A549 cells failed to adhere and spread adequately in the absence of serum. For the spreading assay using human umbilical vein endothelial cells, all steps were carried out in full media. Following recovery, cells (2×10^4 cells/ml) were plated onto coverslips, which had been coated with fibronectin overnight at 4 °C. The cells were allowed to adhere and spread for 3 hours in the presence or absence of 100 μ M O07. In the knockdown experiments, after 3 hours, the coverslips were washed in PBS, then cytoskeletal buffer (0.5% Triton X-100, 10 mM Pipes, pH 7, 50 mM KCl, 2 mM CaCl₂, 2 mM MgCl₂, 300 mM sucrose) and then cells were fixed in 4% (v/v) paraformaldehyde for 15 minutes. In experiments where cytosolic proteins were overexpressed, after cells had been allowed to adhere, the coverslips were washed in PBS, fixed with 4% (v/v) paraformaldehyde and permeabilised with 0.1% Triton X-100 for 5 minutes. In all experiments, the coverslips were blocked overnight in 2% (w/v) BSA in PBS at 4 °C. Focal adhesions were detected using a monoclonal anti-vinculin antibody and the Alexa 568-coupled secondary antibody. Actin was visualized using phalloidin coupled to Alexa 488 (Invitrogen) or Alexa 568 (for experiments where GFP had been overexpressed). Images were acquired using a Zeiss Axioskop 2 microscope fitted with a Zeiss Axioacam CCD camera and 40x and 100x Plan APO objective lenses. ImageJ (NIH) was used to quantify cell spreading and focal adhesion staining. For the siRNA screening experiments, at least 20 cells per condition were analysed. To avoid bias, all of the cells imaged in a single field of view taken through the 40x objective were analysed. Measurements were taken from at least 3 different fields of view with a minimum of 6 cells per field. Cells were selected using the threshold function, to either measure the whole area of the cell, or the areas stained for focal adhesion proteins. Areas were measured in pixels and the spreading index for individual experiments was determined by standardising the spreading of cells under each condition to the mean size of cells under control conditions. Focal adhesions were analysed by measuring the total area per cell which stained for vinculin or paxillin, as individual focal adhesions could not always be easily distinguished. Focal adhesion staining was standardised to the mean area of focal adhesion staining measured

under basal conditions. To analyse the cell shape, ImageJ was used to determine the convex hull of the cells. To do this, the outermost points of the cell were manually selected then joined up using the convex hull selection tool of ImageJ. The area of the resulting shape, the size of cell, and the size of the region outside the cell, between the cell edges and the edge of the shape, were measured in pixels. To standardise results, the proportion of the shape filled with cell and the proportion of the shape that was outside of the cell was calculated. By this method, the more circular the cell, the lower the proportion of the shape is present outside the edges of the cell. Statistical differences in cell size, to calculate the P value, were determined by carrying out paired, two-tailed Student's t-tests.

Short-term adhesion assays

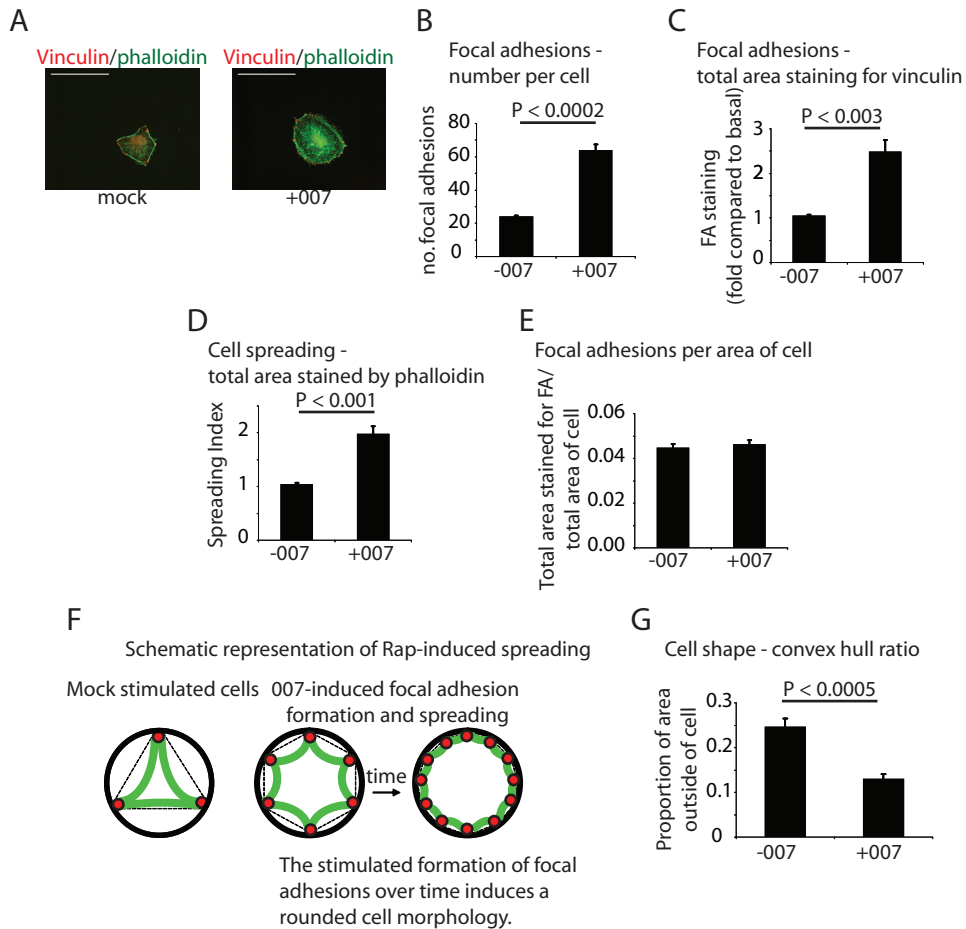
A549-Epac1 cells were transfected with siRNA or co-transfected with Ezrin and luciferase expression vectors for 48 hours before cells were trypsinised, washed once in RPMI containing 10% FCS, and kept in suspension for 1.5 hours in RPMI containing 0.5% FCS, glutamine, antibiotics, and 10 mM Hepes, pH 7.4, at 37 °C to allow recovery of surface proteins. 96-well plates were coated with fibronectin overnight at 4 °C, followed by a blocking step with heat-denatured BSA for 1 hour at 37 °C. Following recovery, cells were plated into the fibronectin-coated wells and allowed to adhere for 30 minutes at 37 °C in the presence or absence of 100 µM O07. Every condition was done in quadruplicate. After 30 minutes, non-adherent cells were removed and adherent cells were washed once with pre-warmed PBS. For siRNA transfections, cells were lysed in alkaline phosphatase buffer (0.4% Triton X-100, 50 mM sodium citrate, and 10 mg/ml phosphatase substrate (Sigma-Aldrich)). In cells where Ezrin constructs were co-expressed with a luciferase construct, cells were lysed in luciferase assay buffer (25 mM Tris phosphate pH 7.8, 10% glycerol, 2% Triton X-100, 8 mM MgCl₂ and 1 mM DTT). Total cells added per well were determined by taking aliquots of the cell-suspension added to each well, then pelleting the cells before lysis in the appropriate buffer. The total amount of cells adhering was determined by either phosphatase assay²¹³, or luciferase assay²¹⁴.

Isolation and analysis of Rap-GTP

Cells were transfected with siRNA for 48 hours and then stimulated with mock or 100 µM O07 for 15 minutes. Cells were lysed in Ral buffer (50 mM Tris.HCl pH 7.5, 200 mM NaCl, 2 mM MgCl₂, 1% (v/v) NP40, 10% (v/v) glycerol, 1 mM PMSF, 1 µM leupeptin, 0.1 µM aprotinin), and the lysates were pre-cleared by centrifugation. The Rap-GTP was captured using the RaGDS-RBD, pre-bound to Glutathione agarose, for 45 minutes as described previously²¹⁵. Endogenous Rap was detected following western blotting with polyclonal anti-Rap1 antibody.

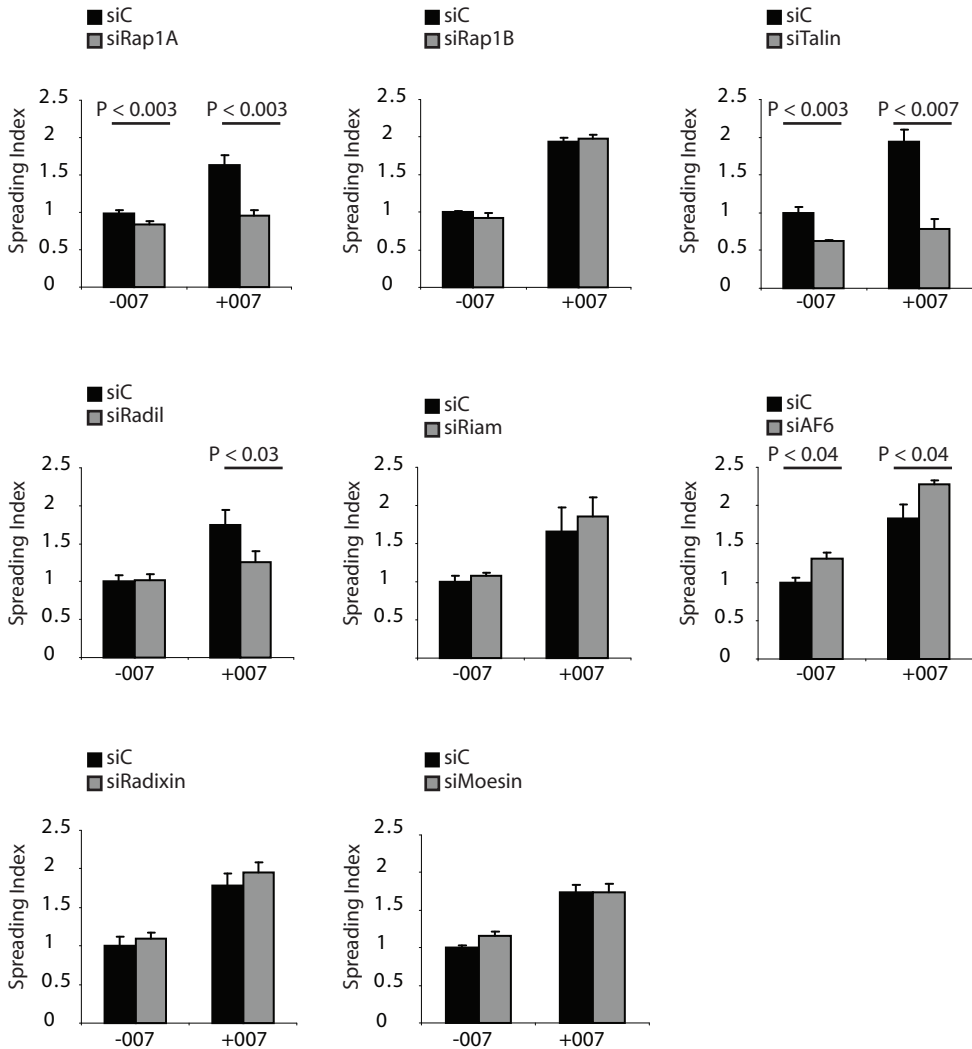
Western blotting

Cells were lysed using Laemmli sample buffer and proteins were separated using SDS-PAGE. Proteins were transferred to PVDF membranes (Immobilion) and blocked in 2% milk/2% BSA for 1 hour and then probed with the appropriate primary antibody. The antibodies were detected by anti-mouse or anti-rabbit conjugated to HRP and proteins were detected by ECL.



Supplementary Figure S1. Analysis and quantification of the 007 phenotype.

To obtain detailed analysis of the changes induced by 007, cells were allowed to spread before being fixed and stained for focal adhesions and actin. Representative images are shown in (A). Bars represent 50 μm . The images were analysed to determine the number of focal adhesions (FA) per cell (B), the area of the cell staining for focal adhesions (C), and the cell spreading (D). To determine the proportion of each cell consisting of focal adhesions, the area (in pixels) of focal adhesions was divided by the total area of the cell (E). A schematic representation of the change in cell morphology caused by 007-induced focal adhesions and spreading is shown in (F). Focal adhesions are shown in red, with actin stress fibres joining the adhesions in green. The cellular morphology is governed by the focal adhesions and stress fibres present in the cell. Under basal conditions, with few focal adhesions, the stress fibres generate the angular morphology. Following 007 stimulation, an increase in the number of focal adhesions results in smaller stress fibres between contact sites, thus generating a rounder cell morphology. To analyse cell shape, the convex hull of cells was generated by joining the outermost points of the cells with straight lines (represented by black dashes in F) as described in Materials and methods. Cells which are more angular in shape have more area between the dashed black lines forming the convex hull and the edges of the cell. In (G), the graph shows the proportion of the convex hull area of individual cells which lies outside of the cell. For each experiment, 10 representative cells from each condition were measured. The graphs show mean data for 6 separate experiments \pm the standard error of the means. The P values were obtained by performing a paired Student's t-test.



Supplementary Figure S2. Quantification of the effect of selected siRNAs on Rap-induced spreading.

For the indicated siRNAs, images of cells were captured through the x40 objective and the spreading of at least 20 cells from each condition was measured and quantified using ImageJ. For each siRNA, the graphs show the mean of 3 experiments \pm the standard error of the means. The P values were obtained by performing a paired Student's t-test.

Protein	Spreading and focal adhesion (FA) induction	Actin phenotype
α -catenin	Normal	Normal
AF6	Normal. Following 007, many cells showed increased spreading with more FAs. Focal adhesions were no longer restricted to the periphery of the cell.	Normal
AF6-L/Radil	Partial defect in the 007-induced spreading and FA formation.	Mixed
α PKC	Normal	Normal
Arap1	Normal	Normal
Arap3	Small defect in basal adhesion and spreading, but a normal response to 007.	Normal
ARHGAP20	Small defect in basal adhesion and spreading, but a normal response to 007.	Normal
β -catenin	Unstimulated cells were elongated and displayed an increase in cell protrusions. Spreading and FAs were stimulated by 007, but the cells remained elongated.	Increase in thin actin fibers.
C3G	Cells displayed a defect in basal spreading, which was rescued and further induced by 007.	Normal
CCM1	Normal	Normal
CCM2	Many cells showed increased FAs. Focal adhesions were no longer restricted to the periphery of the cell.	Increase in stress fibers.
CCM3	Unstimulated knockdown cells were more spread than control cells, and showed many cellular protrusions. Cells still spread and formed FAs with 007.	Increase in stress fibers.
CDC42	Normal	Normal
DGKQ	Normal	Normal
DLG5	Normal	Normal
EBP50	Normal	Normal
E-cadherin	Normal	Normal
Epac1	Cells did not spread or form FAs with 007.	Normal
Epac2	Normal	Normal
Exoc2	Normal	Normal
Exoc8	Unstimulated cells were already spread, with small FAs. 007 still induced spreading but FAs remained small.	Increase in actin protrusions/filopodia in basal conditions. 007 induced small stress fibers throughout cells.
Ezrin	Cells displayed a defect in spreading and FA induction in response to 007.	Mixed

Protein	Spreading and focal adhesion (FA) induction	Actin phenotype
FRMPD1	Normal	Normal
ICAP	Normal	Normal
IQGAP	Normal	Normal
Lamellipodin	Normal	Thin unorganized actin fibers throughout cells.
LIMK	Normal	Normal
Moesin	Normal	Normal
Occludin	Normal	Normal
p120-catenin	Normal	Normal
Par3	Normal	Normal
Par6	Normal	Normal
PDZGEF1	Mixed effect. Some unstimulated cells showed the 007-phenotype, although this was not reproducible. The response to 007 was normal.	Some unstimulated cells showed the 007-phenotype, although this was not reproducible.
PDZGEF2	Normal. Following 007, some cells showed an increase in FAs. Focal adhesions were no longer restricted to the periphery of the cell.	Increase in small stress fibers throughout cells.
PDZK10	Normal	Normal
Rac1	Normal	Normal
Radixin	Normal	Normal
RalA	Normal	Normal
RalB	Normal	Normal
RalGDS	Normal	Normal
Rap1A	Cells displayed a defect in basal spreading. There was no spreading or FA induction upon 007.	Normal
Rap1B	Normal	Normal
Rap1GAP1	Normal. Following 007, some cells showed an increase in FAs. Focal adhesions were no longer restricted to the periphery of the cell.	Increase in small stress fibers throughout cells.
Rap1GAP2	Normal	Normal
Rap2A	Normal	Normal
Rap2B	Normal	Normal
Rap2C	Normal	Normal
RapL	Normal	Increase in small stress fibers throughout cells.

Protein	Spreading and focal adhesion (FA) induction	Actin phenotype
RasGRP1	Normal. Following 007, some cells showed an increase in FAs. Focal adhesions were no longer restricted to the periphery of the cell.	Normal
RasGRP2	Normal	Normal
RasGRP3	Normal	Normal
Rgl1	Normal. Following 007, some cells showed an increase in FAs. Focal adhesions were no longer restricted to the periphery of the cell.	Normal
RhoA	Normal	Normal
Riam	Normal	Increase in small stress fibers throughout cells.
Rin1	Normal. Following 007, some cells showed an increase in FAs. Focal adhesions were no longer restricted to the periphery of the cell.	Normal
Rock1	Normal	Normal
RockII	Basal adhesion of cells was decreased. The spreading and FA induction defect in response to 007 was inhibited.	Mixed
R-Ras	Normal	Normal
Sec15L1	Normal	Normal
Sec15L2	Normal	Normal
Sec8	Normal	Normal
SHIP2	Normal	Normal
Spa1	Normal	Normal
Talin1	Cells showed a defect in basal adhesion and spreading, which was not rescued by 007.	Normal actin phenotype, although the cells did not spread well
Talin2	Normal	Normal
Tiam1	Normal	Normal
Vasp	Normal	Normal
Vav1	Normal	Normal
Vav2	Normal. Cells did not become very round with 007.	Normal
Vav3	Normal	Normal
ZAK	Normal	Increase in small actin fibers.

Table S1. Overview of siRNA screen results.

The effect of siRNA depletion of proteins on focal adhesion (FA) formation and spreading under basal conditions, or when the Epac1-Rap signal transduction pathway had been activated, was determined by visual inspection of replated cells.

CHAPTER

ERM PROTEINS INTEGRATE RAP1 UP- AND
DOWNSTREAM SIGNALING BY BINDING
EPAC1 AND RADIL TO REGULATE
CELL SPREADING

A. Post, M. J. Vliem, I. Verlaan, J. L. Bos

3

ABSTRACT

When and where small GTPases become activated has profound implications for the biological outcome. Previously, we have demonstrated that active ERM proteins function as membrane-bound anchors for the RapGEF Epac1, localizing Rap1 activation. Moreover, we have found that the ERM protein Ezrin also functions downstream of Rap1 in cell spreading. In addition, the Rap1-effector Radil also mediates Rap1-induced cell spreading. Here, we demonstrate that Radil and ERM proteins form a complex. Open, active ERM proteins recruit Radil to the plasma membrane in an Epac1-Rap1-dependent manner. Subsequently, they form an anchor for Radil, resulting in clustering of Radil at the plasma membrane. We conclude that ERM proteins may function as scaffolds, integrating Rap1 up- and downstream signaling, to assure efficient cell spreading.

INTRODUCTION

When and where small GTPases become activated has profound implications for the biological outcome. Accordingly, spatio-temporal control of GTPase activity is an important component of small GTPase biology. For the small GTPase Rap1, spatial regulation can be achieved through tethering its specific guanine nucleotide exchange factors (GEFs) and GTPase activating proteins (GAPs) to micro domains ²¹⁶. GEFs typically are multi-domain proteins consisting of a catalytic domain and several regulatory domains, which are not only responsible for regulating the activity of the GEF but also the localization of the GEF by binding phospholipids or anchoring proteins ^{18,185,217-221}. A well-studied GEF for Rap1 is Epac1. Several localization cues for Epac1 exist and can either positively or negatively affect the activity of Epac1 towards Rap1 ^{18,185,217-221}. One such localization cue is through the activation of ERM (Ezrin, Radixin, Moesin) proteins ¹⁸⁵. ERM proteins reside in the cytoplasm in their inactive conformation, achieved by the binding of its N-terminal FERM-domain to its C-terminal actin-binding domain (ABD). Binding of PIP2 at the plasma membrane by the FERM-domain and phosphorylation of a threonine in the ABD induces the open conformation of the protein, allowing the ABD to bind actin and thereby linking the plasma membrane to the actin cytoskeleton ^{222,223}. Once open, ERM proteins can function as scaffolding proteins, creating docking sites for a variety of signaling cascades. Previously, we have demonstrated that the N-terminal 49 amino acids of Epac1 can directly interact with ERM proteins in their open conformation, resulting in clustering of Epac1 at the plasma membrane ¹⁸⁵. Apart from their role in localizing Epac1 and thus Rap1 activity, ERM proteins also mediate signaling downstream of Rap1. More specifically, Rap1-induced cell spreading is dependent on the ERM protein Ezrin, independent of its scaffolding function for Epac1. Although the open, active conformation of Ezrin is necessary for Rap1-induced spreading, it is not sufficient ⁴⁸. This suggests that additional proteins are required for Rap1-induced spreading and that ERM proteins may function as scaffolds in this process. Indeed, the Rap1-effector Radil is crucial for Rap1-induced cell spreading and is demonstrated to translocate to the PM upon Rap1 activation ^{48,182}.

Here we demonstrate that ERM proteins function as anchoring proteins for Radil at the plasma membrane. Radil is recruited to the plasma membrane in an Epac1-Rap1-dependent manner and once there, Radil may interact with open, active ERM proteins.

We postulate that ERM proteins function as scaffold proteins, integrating up- and downstream signaling of Rap1 by binding Epac1 and Radil, which is required for efficient cell spreading.

RESULTS

Radil and ERM proteins interact to mediate Rap1-induced cell spreading

We previously demonstrated that ERM proteins are required for Rap1-induced cell spreading both upstream of Rap1, by tethering Epac1 to the plasma membrane ¹⁸⁵, and downstream of Rap1 ⁴⁸, through an unknown mechanism. Downstream of Rap1 we found that specifically Ezrin mediated Rap1-induced cell spreading in a non-redundant manner. Furthermore, we demonstrated that the Rap1-effector Radil is also essential for Rap1-induced cell spreading ⁴⁸. Depletion of ERM proteins or Radil affects Rap1-induced cell spreading in a similar manner, specifically mediating the actin cytoskeletal driven spreading phase and not the Rap1-induced initial adhesion ^{48,71}. To investigate a possible link between ERM proteins and Radil we first simultaneously depleted Ezrin and Radil and performed spreading assays, to investigate the possibility of parallel pathways. Simultaneous depletion of Ezrin and Radil did not reduce Rap1-induced cell spreading to a greater extent than depletion of either one alone (Fig. 1A), indicating a possibility of the two proteins being involved in the same signaling cascade. Next, we investigated whether ERM proteins and Radil form a complex. For this we transfected 293T cells with V5-Radil, Flag-tagged Ezrin, Radixin or Moesin and cotransfected HA-Epac1 as a positive control. Indeed, Radil was able to coimmunoprecipitate with all ERM protein family members (Fig. 1B). Active

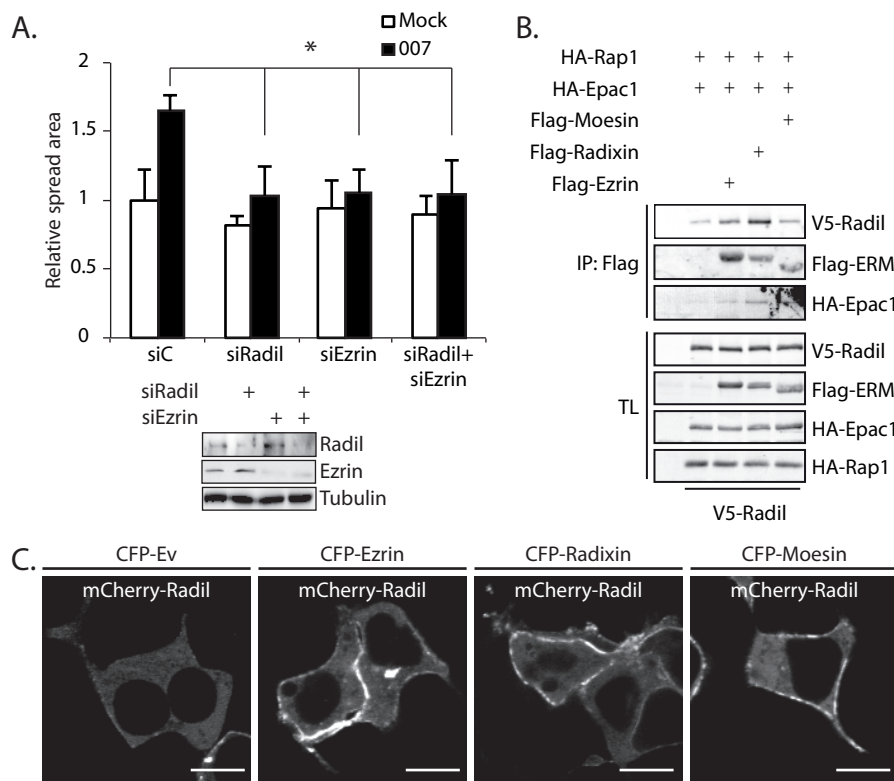


Figure 1: Radil and ERM proteins interact to mediate Rap1-induced cell spreading.

(A) Spreading of A549-Epac1 cells transfected with scrambled siRNA (siC) or siRNA targeting Radil (siRadil), Ezrin (siEzrin) or both (siRadil+siEzrin). Cells were replated for 3h on fibronectin-coated coverslips in the absence (-) or presence (+) of 100 μ M 007. Cells were fixed and the actin cytoskeleton was stained with phalloidin. Quantification of cell area as quantified using ImageJ. Depicted is average spreading area \pm s.d. of three individual experiments and a minimum of 10 cells per experiment, normalized to unstimulated, siC transfected cells. Statistical analysis was obtained by performing a paired Student's t-test. * $P < 0.05$. Knockdown efficiency was determined by Western blot. (B) Coimmunoprecipitation of V5-Radil and HA-Epac1 with Flag-Ezrin, Flag-Radixin or Flag-Moesin expressed in HEK293T cells. (C) Live cell imaging of mCherry-Radil in HEK293T cells, coexpressed with HA-Epac1, HA-Rap1, and the indicated ERM proteins or empty vector (ev).

ERM proteins are bound to PIP2 at the plasma membrane (PM), where they form an anchor for Epac1¹⁸⁵. To test whether ERM proteins also function as an anchor for Radil we cotransfect 293T cells with mCherry-Radil, HA-Epac1 and HA-Rap1, with or without CFP-tagged Ezrin, Radixin or Moesin. In the absence of ERM proteins Radil resided in the cytoplasm, whereas it translocated to the PM upon cotransfection with either of the ERM protein family members (Fig. 1C).

Thus, Radil and Ezrin mediate Rap1-induced cell spreading and form a complex at the PM. Since the ERM proteins show high sequence similarity and Radil binds all three family members, we have chosen to use Ezrin as a representative family member for further investigation of the interaction between Radil and ERM proteins.

Radil interacts with activate ERM proteins at the plasma membrane

ERM proteins reside in the cytoplasm in a closed, inactive conformation, achieved by the binding of its N-terminal FERM domain to its C-terminal ABD. Binding of PIP2 at the PM and phosphorylation

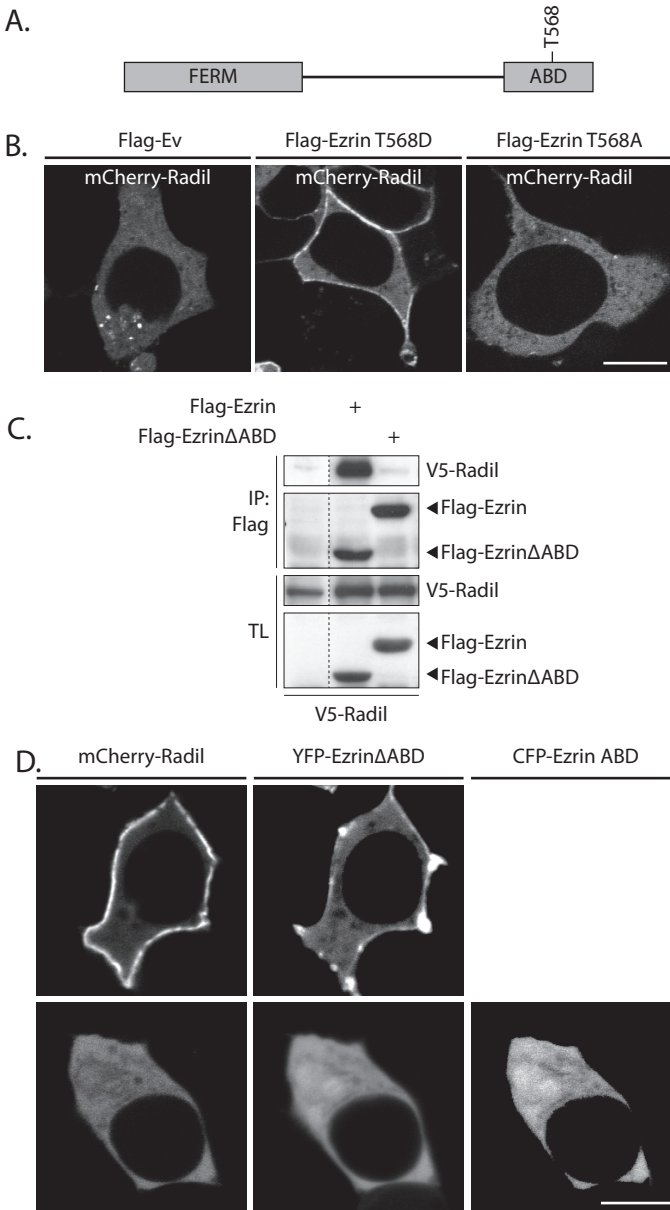


Figure 2: ERM proteins require an open conformation to recruit Radil.

(A) Domain structure of Ezrin containing a FERM-domain capable of interacting with PI(4,5)P₂ and a actin-binding domain (ABD). An intramolecular interaction between the FERM domain and the ABD results in an inactive conformation. Phosphorylation of threonine 568 releases this interaction, thereby activating the protein. (B) Live imaging of mCherry-Radil in HEK293T cells in the presence of YFP-empty vector, YFP-Ezrin(T568D) or YFP-Ezrin (T568A). (C) Coimmunoprecipitation of V5-Radil with Flag-tagged wild-type ezrin or ezrin lacking the ABD (Flag-ezrinΔABD, residues 1 to 492) in A549-Epac1 cells. (D) Live imaging of Radil in HEK293T cells in the presence of YFP-empty vector, YFP-EzrinΔABD or in the presence of YFP-EzrinΔABD and CFP-ezrin ABD.

of a threonine in the ABD induces the open conformation²²³ (Fig. 2A). Since only open, active ERM proteins are bound to the PM, the results in Fig. 1C may reflect a fraction of active ERM proteins under basal conditions, tethering Radil at the PM. To confirm that Radil is recruited to the PM by active ERM proteins we cotransfected 293T cells with mCherry-Radil and Flag-ev, the constitutively active Flag-Ezrin T568D, mimicking the threonine phosphorylation, or the inactive Flag-Ezrin T568A, preventing threonine phosphorylation. Radil was localized to the PM only in the presence of Ezrin T568D (Fig. 2B), indicating that Radil is indeed recruited by open, active ERM proteins. Furthermore, coexpression of a truncated mutant of Ezrin lacking the ABD (EzrinΔABD), thus not autoinhibited,

readily coimmunoprecipitated Radil, indicating that Radil binds the N-terminal part of Ezrin (Fig. 2C). Moreover, this interaction was greater than with wild type Ezrin, suggesting that the ABD inhibits the interaction of Radil and Ezrin. Coexpression of the ABD with Ezrin Δ ABD in 293T cells, indeed, prevented the PM recruitment of Radil, indicating that the ABD masks the binding site for Radil (Fig. 2D).

Thus, Radil is recruited to the plasma membrane by open, active ERM proteins.

Radil must be recruited by active Rap1 to interact with ERM proteins

We next investigated whether the translocation of Radil to the PM by overexpression of Ezrin is dependent on the binding of Radil to Rap1. Since ERM proteins in their active conformation can recruit Epac1¹⁸⁵, overexpression of ERM proteins may create a local increase in the amount of active Epac1 and thus active Rap1, which may be responsible for the recruitment of Radil.

Whereas coexpression of Ezrin, Epac1, and Rap1 induces PM localization of Radil, the absence of either

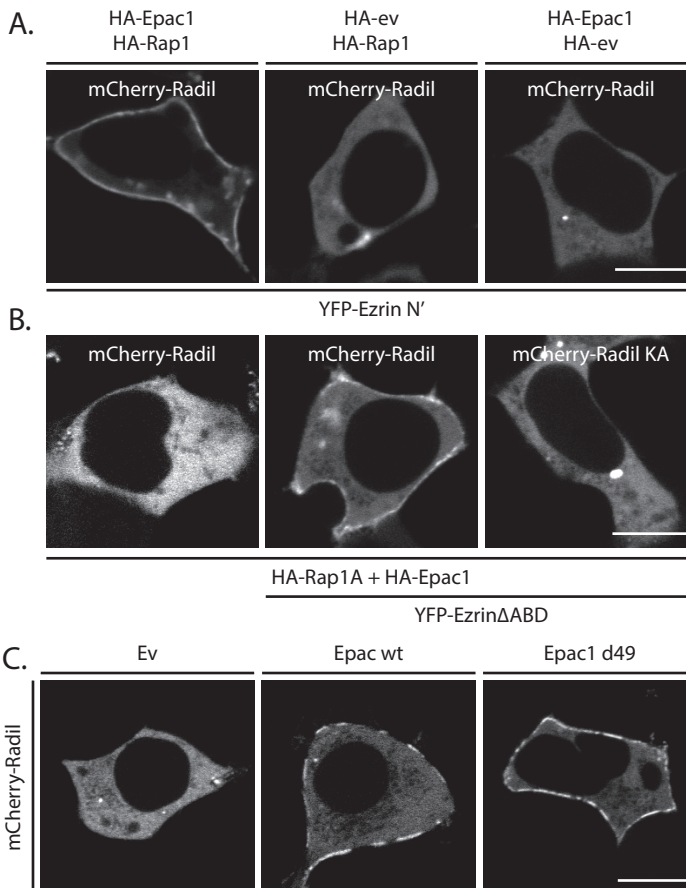


Figure 3: Recruitment of Radil by ERM proteins requires Epac1-Rap1 signaling.

(A) Live imaging of mCherry-Radil in HEK293T cells in the presence of YFP-Ezrin and either HA-Epac1 and HA-Rap1A together, HA-Rap1A alone or HA-Epac1 alone. (B) Live imaging of HEK293T cells expressing HA-Epac1 and HA-Rap1 in the presence or absence of YFP-Ezrin Δ ABD, either transfected with wild-type mCherry-Radil or a mutant incapable of binding Rap1 (mCherry-Radil (K76A)).

Epac1 or Rap1 greatly reduces the amount of Radil at the PM (Fig. 3A), suggesting that recruitment of Radil to the PM requires active Rap1. This is supported by the fact that expression of Radil containing a point mutation in its RA-domain, rendering it incapable of binding Rap1, does not localize to the PM upon expression of Ezrin (Fig. 3B). Furthermore, not only ERM-localized Epac1 could induce the translocation of Radil to the PM, but also expression of an Epac1 mutant lacking its first 49 amino acids, thus incapable of interacting with ERM proteins, could induce the translocation of Radil to the PM (Fig. 3C). Thus Radil is recruited to the PM through Epac1-Rap1 signaling, for which ERM proteins are not necessary.

However, Radil did coprecipitate with ERM proteins (Fig. 1C), suggesting that they are in one complex. To determine whether ERM proteins could function as an anchor for Radil once it is localized at the PM, we induced PM translocation of Radil by the active Rap1 mutant, Rap1AV12 (Fig. 4A), thereby eliminating the Epac1-mediated effects of ERM proteins on Radil localization. Coexpression of Radil, Rap1AV12 and Ezrin resulted in localization of Radil along the plasma membrane (Fig. 4A). Coexpression of the catalytic DHPH-domain of the RhoGEF p190RhoGEF, resulting in phosphorylation and clustering of ERM proteins¹⁸⁵, induced a clustered localization of Radil at the PM (Fig. 4A). Expression of a construct constituting the first 49 amino acids of Epac1 (Epac1 1-49), which binds active ERM proteins, but lacks other regulatory or catalytic domains, was coexpressed to visualize

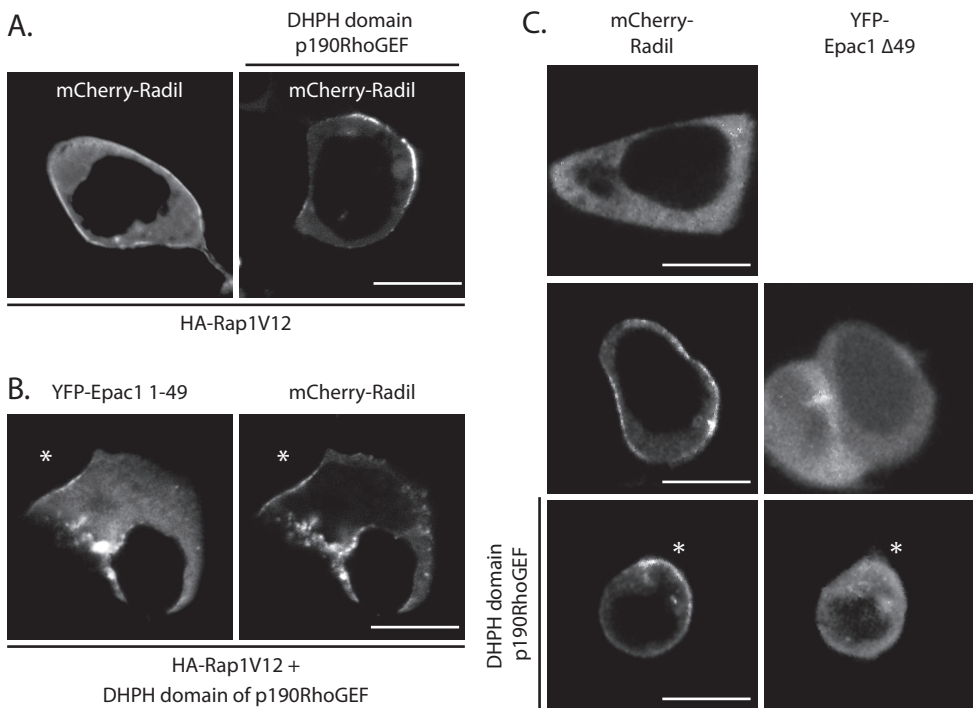


Figure 4: ERM proteins induce clustering of plasma membrane localized Radil.

(A) Live imaging of HEK293T cells expressing mCherry-Radil, HA-Rap1AV12 and CFP-Ezrin, in the presence or absence of the catalytic domain of p190-RhoGEF. (B) Live imaging of HEK293T cells expressing mCherry-Radil, HA-Rap1AV12, CFP-Ezrin and the first 49 amino acids of Epac1 (YFP-Epac1 1-49), in the presence or absence of the catalytic domain of p190-RhoGEF. (C) Live imaging of HEK293T cells expressing mCherry-Radil, HA-Rap1A, CFP-Ezrin and Epac1 lacking the first 40 amino acids (YFP-Epac1Δ49), in the presence or absence of the catalytic domain of p190-RhoGEF.

where active ERM proteins were present. Indeed, Radil colocalized with Epac1 1-49 in a polarized fashion (Fig. 4B). Furthermore, expression Epac1 Δ 49, which localizes to the PM through phosphatidic acid²¹⁷, but cannot bind ERM proteins, also induces translocation of Radil to the PM (Fig. 4C). Again, coexpression of DHPH-p190RhoGEF induces a clustered colocalization of Radil and Ezrin, whereas Epac1 Δ 49 is uniformly distributed (Fig. 4C).

Altogether, these results indicate that Radil must bind active Rap1 to translocate to the PM, where ERM proteins then function as an anchor, creating confined regions of Radil localization.

DISCUSSION

Spatial regulation of small GTPase activity determines the biological outcome of small GTPase signaling and a considerable amount of research has focused on the spatial cues and anchors, responsible for this effect. Although GTPases themselves are spatially regulated, mostly through lipid membrane anchoring²²⁻²⁴, it frequently are the respective GEFs and GAPs of a particular GTPase which are regulated in space^{18,185,217-221}. However, spatial determination of small GTPase signaling can also be achieved by spatially restricting the downstream effectors.

Recently, we have identified the ERM protein, Ezrin, and the Rap1-effector, Radil, as components of a signaling cascade downstream of Rap1, involved in Rap1-induced cell spreading⁴⁸. Here, we suggest that ERM proteins function as plasma membrane localized scaffolds, integrating Rap1 up- and downstream signaling by binding both the RapGEF, Epac1, and Radil. Radil is recruited to the PM in a Rap1-dependent manner, after which it can interact with ERM proteins in their open, active conformation. Similarly, we have previously demonstrated that Epac1 is recruited to the plasma membrane by active ERM proteins¹⁸⁵. From these findings that we propose that ERM proteins function as scaffolds for Rap1 signaling, capable of directly coupling Epac1-mediated activation of Rap1 to Radil-mediated signaling output.

ERM proteins function as membrane anchors for Epac1 in a redundant manner. Ezrin, Radixin and Moesin can all recruit Epac1 to the plasma membrane, suggesting that Epac1 binds to a conserved region of the proteins¹⁸⁵. In contrast, we have found that Ezrin non-redundantly mediates Rap1-induced cell spreading downstream of Rap1⁴⁸. This observation cannot be explained by its scaffolding function for Epac1 and Radil, since Radil also binds all three ERM proteins, suggesting that other Ezrin-specific interactors are involved in Rap1-induced cell spreading.

As ERM proteins need to be in their open conformation to function as scaffolds for Epac1-Rap1-Radil signaling during cell spreading, it functions as a point of convergence for signals activating ERM proteins and Epac1. RhoA signaling has a prominent role in ERM activation. Both direct phosphorylation of the ABD through the Rho-effector Rock¹⁸⁷, as well as increased PIP2 production, via activation of PIP5K²²⁴, results in the open conformation of ERM proteins. Intriguingly, we have recently proposed that Radil may regulate cell spreading through the RhoGAP ArhGAP29⁷¹. Thus, the scaffolding function of ERM proteins for Rap1-signaling may comprise a direct feedback loop, reducing RhoA activity and ERM phosphorylation. It has been reported that the cyclical phosphorylation of ERM proteins is necessary for efficient lamellipodium formation^{225,226}, a form of cell spreading, possibly explaining the need for this feedback loop. Indeed, we found that the phosphorylation-mimicking mutant of Ezrin did not readily phenocopy Rap1-induced cell spreading⁴⁸, possibly due to the constitutive active conformation. Furthermore, waves of RhoA activation and inactivation are present at the protruding membrane^{49,64,108,227}, and it is an intriguing thought that this could possibly be linked to the findings described here. Further research needs to confirm this possible feedback loop.

In summary, our findings suggest that ERM proteins can integrate and confine Epac1-Rap1-Radil signaling, which is necessary for efficient Epac1-Rap1-induced cells spreading. Direct linkage of up- and downstream signaling is also being reported for other small GTPases¹⁴⁵⁻¹⁴⁷, possibly reflecting a

key, but currently underappreciated, component of small GTPase biology.

MATERIALS AND METHODS

Reagents and antibodies.

007 (8-pCPT-2'-O-Me-cAMP) was from Biolog Life Sciences (Bremen, Germany) and used at concentrations of 100 μ M (1). Sphingosine 1-phosphate (S1P) was obtained from Sigma-Aldrich. Antibodies were from Invitrogen (V5, fluorescently-labeled Phalloidin and secondary antibodies), Roche (GFP), Chemicon (α -tubulin), Sigma-Aldrich (Flag; M2), Covance (HA; HA11), Cell Signaling Technology (phospho-ERM (ezrin T567, radixin T564, moesin T558)) BD Biosciences (Ezrin), ProteinTech (Radil) and Cell Signaling (Epac1; 5D3). siRNA SMARTpools were used for Radil and Ezrin using ON-Target Plus siRNA (Dharmacon).

DNA constructs.

Ezrin, radixin, moesin, Epac1, Radil, Rap1A, the ezrin actin binding domain (ABD; amino acids 492 to 584), and Ezrin Δ ABD (amino acids 1 to 492), the ERM-binding domain of Epac1 (Epac1 1-49) or an Epac1 construct lacking the ERM-binding domain (Epac1 Δ 49) were cloned N-terminally to either YFP, mCherry, CFP, V5 or a Flag-His tag using a pCDNA3 vector or to a hemagglutinin (HA) tag using a PMT2 vector with the Gateway system (Invitrogen). The ERM and Epac1 constructs have previously been described in (2), the Rap1A and Rap1AV12 constructs have previously been described in (3) and Radil was subcloned from pMT2-HA-Radil described in (4).

Cell culture.

HEK293T (human embryonic kidney) cells were cultured in Dulbecco's modified Eagle medium (DMEM), A549-Epac1 cells (lung carcinoma cell line stably expressing Epac1, previously described in (5)), were cultured in RPMI. Both were supplemented with L-glutamine, antibiotics and 10% Fetal Bovine Serum (FBS). OvCar3 cells were grown in RPMI containing 20% FBS, insulin, L-glutamine and antibiotics.

siRNA transfections were performed 72 hours before experiments with 40 nM ON-TARGETplus SMARTpools or single siRNAs (Dharmacon Inc.) targeting indicated proteins using HiPerfect (Qiagen). 293T cells were transfected using X-tremeGENE 9 (Roche Inc.) 24 hours prior to live imaging or 48h prior to immunoprecipitation experiments.

Spreading assay and immunofluorescence.

For spreading assays, A549-Epac1 cells or OvCar3 cells were trypsinized, resuspended and kept in suspension for 1.5 h in RPMI medium containing 0.5% FBS, glutamine, antibiotics and 10 mM HEPES, pH 7.4, at 37°C to allow surface proteins to recover. Coverslips were coated with fibronectin overnight in a 24-well plate at 4°C. After recovery, 2.5×10^4 cells were plated per well in the absence or presence of 100 μ M 007 and allowed to adhere for 3 hours at 37 °C. Cells were fixed with 4% formaldehyde in cytoskeletal buffer (0.5% Triton X-100, 10 mM PIPES pH 7, 50 mM KCl, 2mM CaCl₂, 2 mM MgCl₂, 300 mM sucrose) for 10 min. Subsequently, cells were stained with phalloidin coupled to Alexa Fluor 488 (Invitrogen) for 30 min. Cells were mounted onto glass slides and examined on an Axioskop 2 plus microscope (Zeiss) fitted with a Zeiss Axiocam CCD camera and 40x Plan APO objective immersion oil lenses. ImageJ (NIH) was used to quantify cell spreading. For the cell spreading experiments, at least 15 cells per condition were analyzed, from at least five fields of view. To avoid bias, all of the cells imaged in a single field of view taken through the 40x objective were analyzed. Cells were selected using the threshold function to measure the whole area of the cell. Areas were measured in pixels per cell and the relative spreading area for individual experiments was determined by standardizing the spreading of cells under each condition to the mean size of cells under control conditions. P-values were determined by Student's t-test (two-tailed, paired).

Immunoprecipitations.

HEK293T cells were cultured in 6-cm dishes and lysed 48h after transfection. Lysates were made using a buffer containing 0,5% NP-40, 20 mM Tris, pH 7.5, 150 mM NaCl, 20 mM MgCl₂, 10% glycerol and protease and phosphatase inhibitors. Cell lysates were cleared by centrifugation, and lysates were incubated with protein A-agarose beads (Pharmacia) coupled to the appropriate antibody. After extensive washing with lysis buffer, bound proteins were eluted in Laemmli buffer and analyzed by SDS-PAGE.

Live cell imaging.

For confocal live-imaging, cells were seeded overnight in glass-bottom wells (WillCo Wells) and examined in L-15 Leibovitz medium (Invitrogen) at 37 °C on an inverted Zeiss LSM510 confocal microscope equipped with 63x magnification objective lens (N.A. 1.4; Leica). Postacquisition image adjustments for brightness and contrast enhancement were performed using ImageJ software (NIH).

CHAPTER

4

RASIP1 MEDIATES RAP1 REGULATION OF
RHO IN ENDOTHELIAL BARRIER FUNCTION
THROUGH ARHGAP29

Anneke Post, Willem-Jan Pannekoek,
Sarah H. Ross, Ingrid Verlaan,
Patricia M. Brouwer, Johannes L. Bos

PNAS. 2013; 110(28): 11427-11432

ABSTRACT

Ras-related protein 1 (Rap1) is a small GTPase regulating cell-cell adhesion, cell-matrix adhesion and actin rearrangements, all processes dynamically coordinated during cell spreading and endothelial barrier function. Here, we identify the adaptor protein Ras-interacting protein 1 (Rasip1) as a Rap1-effector involved in cell spreading and endothelial barrier function. Using Förster resonance energy transfer, we show that Rasip1 interacts with active Rap1 in a cellular context. Rasip1 mediates Rap1-induced cell spreading through its interaction partner Rho GTPase-activating protein 29 (ArhGAP29), a GAP for Rho proteins. Accordingly, the Rap1-Rasip1 complex induces cell spreading by inhibiting Rho signaling. The Rasip1-ArhGAP29 pathway also functions in Rap1-mediated regulation of endothelial junctions, which controls endothelial barrier function. In this process Rasip1 cooperates with its close relative Ras-associating and dilute domain-containing protein (Radil) to inhibit Rho-mediated stress fiber formation and induces junctional tightening. These results demonstrate how Rap1 can modulate Rho signaling and actin dynamics, through which Rap1 modulates endothelial barrier function.

INTRODUCTION

The small GTPase, Ras-related protein 1 (Rap1), regulates both integrin-mediated and cadherin-mediated adhesions. Rap1 can increase cell adhesion by inducing the allosteric activation and clustering of integrins thereby increasing cell-extracellular matrix (ECM) adhesion⁵⁰⁻⁵². Upon cell-ECM engagement, Rap1 induces cell spreading, due to increased cell protrusion and decreased cell contraction, indicating changes in actin dynamics^{49,169}. In addition, Rap1 regulates both epithelial and endothelial cell-cell adhesion^{31,228-232}. Particularly the role of Rap1 in controlling endothelial cell junctions is important, as weakening of the endothelial barrier can result in pathologies such as chronic inflammation, atherosclerosis and vascular leakage²³³⁻²³⁵. Activation of Rap1 in endothelial cells results in stabilization of junctions and consequently increased barrier function through the recruitment of β -catenin, resulting in stabilization of vascular endothelial (VE)-cadherin at cell-cell junctions^{85,148,236,237} and rearrangements of the actin cytoskeleton^{31,167,228,238,239}. These rearrangements of the actin cytoskeleton includes the disruption of radial stress fibers and the induction of cortical actin bundles, and consequently a switch from discontinuous, motile junctions into linear, stable junctions^{31,167,228,229}. Rap1 achieves this at least in part by regulating Rho-signaling^{31,167,228,231,238}. The molecular mechanism of how Rap1 regulates Rho however remains largely elusive, although the Rap1-effector Krev interaction trapped protein 1 (Krit-1)/cerebral cavernous malformations 1 protein (CCM1) has been proposed to be involved^{104,148,236}.

In this study, we identified a Rap1-signaling cascade, comprising the Ras interacting protein 1 (Rasip1), Ras-associating and dilute domain-containing protein (Radil) and Rho GTPase-activating protein 29 (ArhGAP29), affecting both cell spreading and endothelial barrier function by regulating the Rho-signaling cascade.

RESULTS

Rasip1 mediates Rap1-induced spreading without affecting adhesion

To investigate whether Rasip1 is involved in Rap1-induced cell spreading, we used A549 cells stably expressing the cAMP responsive Rap1GEF, Epac1⁴⁹. When treated with the Epac1-specific cAMP analog, 8-pCTP-2'-O-Me-cAMP (hereafter referred to as 007), to activate endogenous Rap, cells showed a 2-fold increase in cell area compared to untreated cells, as determined by pixels per cell, 3hr after replating on fibronectin (Fig. 1A). Previously, we established that this effect is mainly mediated by Rap1A⁴⁸. siRNA-mediated depletion of Rasip1 significantly reduced 007-induced spreading (Fig. 1A). This result was obtained with both a pool of siRNAs (spRasip1) as well as with four single siRNAs targeting Rasip1 (siRasip1 #1-4) (Fig. 1A). Furthermore, add back of a YFP-Rasip1 construct to cells treated with siRNA targeting the 3'UTR of Rasip1 mRNA (siRasip1 #2), rescued siRNA-mediated depletion of endogenous Rasip1 (Fig. 1B), excluding an off-target effect of the siRNAs. Interestingly, overexpression of YFP-Rasip1 itself did not induce cell spreading, but required Rap1-activation to promote cell spreading (Fig. 1B).

To assess whether Rasip1 affects 007-induced spreading by regulating the activity of Rap1, we measured the amount of GTP-bound Rap1 after depletion of Rasip1. Whereas depletion of Epac1 reduced the amount of Rap1-GTP after 007 treatment, depletion of Rasip1 had no effect on Rap1-GTP levels (Fig. 1C), ruling out that Rasip1 mediates 007-induced spreading by affecting Rap1-activity. To exclude any possibility that Rasip1 mediates a Rap1-independent effect of Epac1, we induced spreading by overexpression of a constitutively active Rap1 mutant. Overexpression of HA-Rap1AV12 potently induced a nearly 2-fold increase in cell area (Fig. S1A). Depletion of Rasip1 abolished this effect (Fig. S1A), indicating that Rasip1 mediates Rap1A-induced cell spreading. To investigate whether Rasip1 is selective for Rap1-induced spreading, we induced spreading independently of Rap1 by expression of constitutively active T-lymphoma invasion and metastasis-inducing protein 1 (Tiam1) (C1199), a

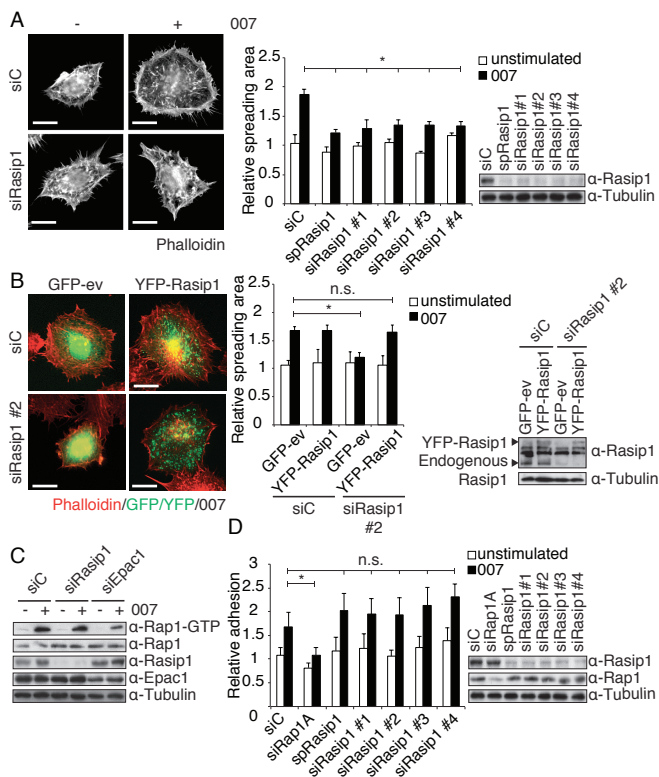


Figure 1: Rasip1 mediates Rap1-induced cell spreading.

(A) Left panel: Spreading of A549-Epac1 cells transfected with scrambled siRNA (siC) or a SMARTpool of siRNAs targeting Rasip1 (spRasip1). Cells were replated for 3h on fibronectin-coated coverslips in the absence (-) or presence (+) of 100 μ M 007. Cells were fixed and the actin cytoskeleton was stained with phalloidin. Right panel: Quantification of cell area of A549-Epac1 cells transfected with scrambled siRNA (siC), a SMARTpool siRNAs targeting Rasip1 (spRasip1) or single siRNAs targeting Rasip1 (siRasip1 #1-4) in the absence (unstimulated) or presence (007) of 007, as quantified using ImageJ. Depicted is average spreading area \pm s.d. of three individual experiments and a minimum of 10 cells per experiment, normalized to unstimulated, siC transfected cells. Statistical analysis was obtained by performing a paired Student's t-test. * $P < 0.05$. Knockdown efficiency was determined by Western blot. (B) Recovery of Rasip1 depletion by an siRNA resistant YFP-Rasip1 construct. A549-Epac1 cells were treated with siC or siRasip1#2 16h before cotransfection with either GFP-empty vector (GFP-ev) or siRNA-resistant YFP-Rasip1 construct. Cells were replated, treated and quantified as for A. Depicted is average spreading area \pm s.d. of three individual experiments normalized to unstimulated siC transfected cells. * $P < 0.02$. (C) Pull-down of Rap1-GTP from A549-Epac1 cells, either unstimulated (-) or upon 15 min stimulation with 100 μ M 007 (+), transfected with siC, siRasip1 or siEpac1. (D) Adhesion of A549-Epac1 cells transfected with siC, siRasip1 or single siRNAs targeting Rasip1 (siRasip1#1-4). Cells were replated onto fibronectin-coated surfaces for 25 minutes in the absence (unstimulated) or presence (007) of 100 μ M 007. Non-adherent cells were washed off and adherent cells were quantified by measuring endogenous phosphatase activity. Depicted is mean data \pm s.d. of five individual experiments normalized to unstimulated siC transfected cells. * $P < 0.03$. All statistical analyses were obtained by performing a paired Student's t-test. Bars are 20 μ m.

GEF for Rac1. This resulted in a 1.5-fold increase in cell area (Fig. S1B). However, this increase was insensitive to depletion of either Rap1A or Rasip1 (Fig. S1B). Together, these results indicate that Rasip1 functions specifically downstream of Rap1 in cell spreading.

As described previously, cell spreading is a multistep process including the initiation and formation of cell-ECM contacts and induction of cytoskeletal rearrangements. Rap1 has been reported to

both increase integrin affinity and induce integrin clustering, resulting in increased cell adhesion⁵⁰⁻⁵². We, therefore, investigated whether Rasip1 affects Rap1-induced cell spreading by mediating Rap1-induced cell-ECM interactions. Firstly, we tested whether Rasip1 is involved in Rap1-induced adhesion. For this, we assessed the amount of cells adherent to fibronectin over a 25-minute period in the presence or absence of 007. In scrambled siRNA treated cells, 007 induced a 1.5-fold increase in cell adhesion (Fig. 1D). As expected, siRap1A abolished this effect. However, depletion of Rasip1 did not affect 007-induced adhesion (Fig. 1D). These results indicate that in A549-Epac1 cells Rasip1 specifically mediates cell spreading without affecting cell adhesion. Importantly, focal adhesions formed and matured normally as determined by paxillin, pY118-paxillin and vinculin staining (Fig. S1C), suggesting that depletion of Rasip1 does not affect cell spreading through inhibiting of the focal adhesion maturation.

Full length Rasip1 interacts with active Rap1

Mitin et al.²⁴⁰ showed that the RA-domain of Rasip1 can interact with the constitutively active Rap1A63E mutant in vitro. Furthermore, both Rap1 and Rasip1 have been reported to localize to the perinuclear region (Fig. 1B and^{11,240}). Together with our results that show that Rasip1 functions downstream from Rap1, this prompted us to investigate whether full length Rasip1 and Rap1 interact in vivo. To that end, we measured Rasip1-Rap1 interaction by Förster resonance energy transfer (FRET), using the acceptor photobleaching technique. Cells were transfected with GFP-Rasip1 and either the constitutively active mCherry-Rap1V12 or inactive mCherry-Rap1N17. FRET was observed between GFP-Rasip1 and mCherry-Rap1V12 (Fig. 2A) with an efficiency of ~19% versus an efficiency of ~2.5% for GFP-Rasip1 and mCherry-Rap1N17 (Fig. 2B), indicating that Rasip1 and active Rap1 indeed interact within the cell.

Rasip1 mediates Rap1-induced spreading by affecting Rho-signaling through the RhoGAP ArhGAP29

Rasip1 has previously been reported to inhibit RhoA signaling through interaction with the RhoGAP ArhGAP29¹⁰¹. We were able to confirm this interaction (Fig. S2) and we, therefore, determined

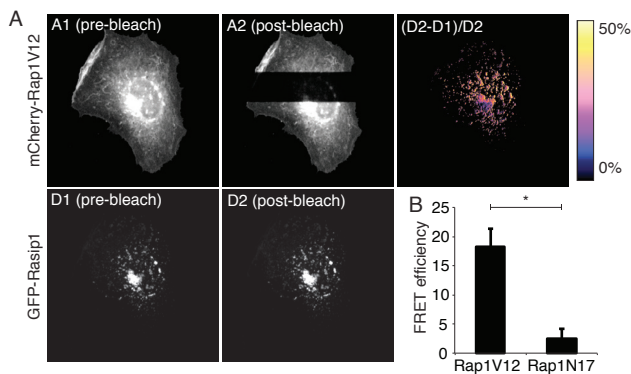


Figure 2: Rasip1 interacts with active Rap1.

Analysis of FRET between GFP-Rasip1 and mCherry-Rap1V12 or mCherry-Rap1N17 using acceptor photobleaching. (A) Scans of GFP-Rasip1 (donor) and mCherry-Rap1V12 (acceptor) were taken prior to (pre) and after (post) photobleaching and FRET efficiency was calculated by $E = (\text{Donor}_{\text{post}} - \text{Donor}_{\text{pre}}) / \text{Donor}_{\text{post}}$. (B) Average FRET efficiency calculated for GFP-Rasip1 and mCherry-Rap1V12 or GFP-Rasip1 and mCherry-Rap1N17. Intensities were calculated with ImageJ within a defined region of interest (ROI). Per cell 3 ROIs were taken of both the bleached area and unbleached area for background correction and values were averaged. 3 cells per experiment were visualized. Graph depicts the mean FRET efficiency of 3 individual experiments \pm s.d. Statistical analysis was obtained by performing a paired Student's t-test. * $P < 0.01$.

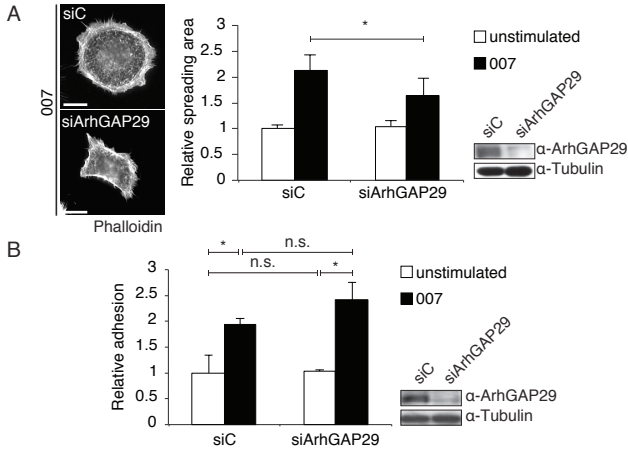


Figure 3: ArhGAP29 mediates Rap1-induced spreading.

(A) Spreading of A549-Epac1 cells treated with scrambled siRNA (siC) or siRNA targeting ArhGAP29 (siArhGAP29). Cells were replated, treated and quantified as for fig. 1A. Depicted is average spreading area \pm s.d. of five individual experiments normalized to unstimulated siC transfected cells. Knockdown efficiency was determined by Western blot. * $P < 0.005$. (B) Adhesion of A549-Epac1 cells transfected with siC or siArhGAP29. Cells were replated, treated and quantified as for fig. 1D. Depicted is mean data \pm s.d. of three individual experiments normalized to unstimulated, siC-transfected cells. * $P < 0.01$. All statistical analyses were obtained by performing a paired Student's t-test. Bars are 20 μ M.

whether Rap1-induced cell spreading also requires ArhGAP29. Indeed, depletion of ArhGAP29 also inhibited 007-induced spreading of A549-Epac1 cells (Fig. 3A). Furthermore, as we have demonstrated for Rasip1, depletion of ArhGAP29 does not abolish 007-induced initial adhesion (Fig. 3B). These results indicate that Rap1-induced cell spreading requires the Rasip1-ArhGAP29 complex.

ArhGAP29 has been shown to have predominant GAP activity towards RhoA over Rac1 and Cdc42²⁴¹. Activation of Rho results in increased activity of its effector Rho-associated protein kinase (ROCK), which phosphorylates MLC2 and MYPT1, resulting in increased actomyosin contraction. During the process of cell spreading, cell contraction must be reduced to allow cell spreading to occur^{55,242}. To assess whether Rap1 induces cell spreading by reducing cell contraction, A549-Epac1 cells, adherent to fibronectin, were stimulated with 007 for 30 minutes. Cells were lysed and assessed for pMLC2 levels. 007 treatment reduced the levels of pMLC2, and depletion of either Rasip1 or ArhGAP29 attenuated the 007-induced reduction of pMLC2 (Fig. 4A). These results indicate that Rap1 induces cell spreading by reducing the amount of phosphorylated MLC2. Furthermore, since Rasip1 and ArhGAP29 depletion attenuate this effect, we concluded that this effect is achieved through reduction of Rho activity.

To address the notion that the Rap1-Rasip1-ArhGAP29 pathway affects cell spreading through modulation of Rho activity, we hypothesized that if the effect of Rasip1 and ArhGAP29 depletion on Rap1-induced spreading is due to increased levels of Rho activity, inhibition of Rho activity should alleviate the inhibitory effects of Rasip1 and ArhGAP29 depletion on Rap1-induced spreading. We, therefore, treated A549-Epac1 cells with the Rho-inhibitor C3 transferase. Indeed, whereas depletion of Rasip1 or ArhGAP29 inhibited 007-induced spreading, treatment with C3 transferase, not only induced cell spreading on its own, but also relieved the inhibitory effect of depletion of Rasip1 or ArhGAP29 on 007-induced spreading (Fig. 4B, 4C, S2B and S2C). Furthermore, the ROCK-inhibitor Y27623 relieved the inhibitory effect of ArhGAP29 depletion on 007-induced cell spreading (Fig. 4C and S2C). Conversely, overexpression of a constitutively active RhoA (RhoAQ63L) mutant inhibited 007-induced spreading (Fig. S2D), indicating that RhoA activity must be reduced to allow Rap1-induced spreading to occur. Taken together, we conclude that Rap1, through Rasip1 and ArhGAP29 reduces Rho activity and consequently actomyosin-induced tension.

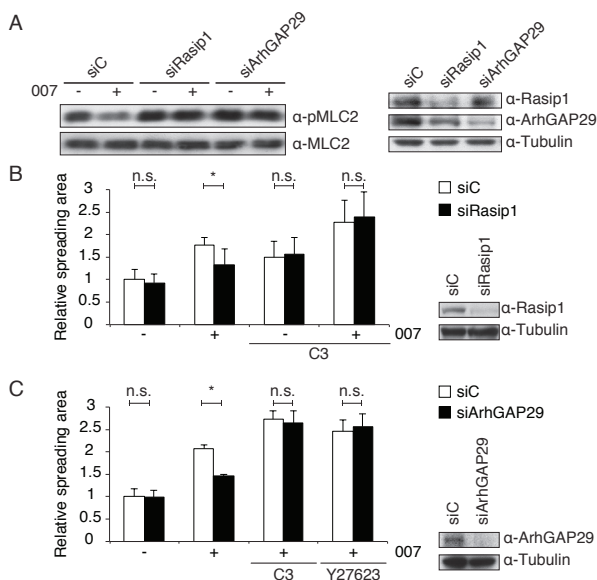


Figure 4: Rap1 modulates Rho activity through Rasip1 and ArhGAP29.

(A) phosho-MLC2 (pMLC2) levels in A549-Epac1 cells transfected with siC, siRasip1 or siArhGAP29. Upon 30 min stimulation with 100 μ M 007 (+) cells were lysed and lysates were subjected to Western blotting. Minus depicts untreated cells. Western blot is a representative of four individual experiments. (B) Quantification of spreading of A549-Epac1 cells transfected with siC or siRasip1 in the presence or absence of 007 and C3 transferase (C3). Cells were replated, fixed and quantified as for fig. 1A. Depicted is average spreading area \pm s.d. of four individual experiments normalized to unstimulated siC transfected cells. Knockdown efficiency was determined by Western blot. * $P < 0.008$. (C) Quantification of spreading of A549-Epac1 cells transfected with siC or siArhGAP29 in the presence or

absence of 007 and C3 transferase (C3) or a ROCK-inhibitor (Y27623). Cells were replated, fixed and quantified as for fig. 1A. Depicted is average spreading area \pm s.d. of three individual experiments normalized to unstimulated siC transfected cells. Knockdown efficiency was determined by Western blot. * $P < 0.005$.

Rasip1 and ArhGAP29 mediate Rap1-induced endothelial barrier function

To investigate the physiological relevance of the Rap1-Rasip1-ArhGAP29 signaling pathway, we investigated its involvement in Rap1-induced endothelial barrier function. First, we determined whether Rasip1 and ArhGAP29 were also involved in cell spreading in endothelial cells. In human umbilical vein endothelial cells (HUVECs), depletion of either Rasip1 or ArhGAP29 abrogated 007-induced spreading (Fig. S3A), demonstrating that the Rap1-Rasip1-ArhGAP29 pathway is conserved in endothelial cells. Previously, it was demonstrated that depletion of Rap1 in HUVECs results in both reduced basal and 007-induced endothelial barrier function, as measured by electrical impedance to evaluate the junctional resistance (R_j)^{229,230}. In a confluent monolayer of HUVECs, we found that depletion of ArhGAP29 decreased basal resistance and 007-induced resistance as compared to scrambled siRNA treated cells (Fig. 5A), thereby phenocopying previous results for Rap1 knockdown^{229,230}. Epac1 has been shown to regulate endothelial barrier function in a Rap1-dependent and -independent manner^{229,239}. To determine whether ArhGAP29 mediates the Rap1-dependent component of Epac1-regulated barrier function, we induced endothelial barrier function in an Epac1-independent, Rap1A-dependent manner. For this, we transduced HUVECs with the constitutively active mutant of Rap1A, Rap1AV12. Overexpression of Rap1AV12 increased the impedance compared to empty vector-transfected cells (Fig. 5B). When ArhGAP29 was depleted, overexpression of Rap1AV12 was no longer able to increase the electrical impedance (Fig. 5B), confirming that ArhGAP29 mediates Rap1A-induced endothelial barrier function.

Depletion of Rasip1 also significantly reduced the basal endothelial barrier function, but the effect was clearly much less dramatic than depletion of ArhGAP29 (Figure 5C). This suggested that Rasip1 might not be the only mediator of Rap1 controlling ArhGAP29. Indeed, recently Radil, a close relative of Rasip1, was found to interact with ArhGAP29 in a mass spectrometry analysis²²⁹. In addition, Radil is also identified as an effector of Rap1 required for Rap1-induced cell spreading^{(48,182} and Fig. S3A and B) and like Rasip1 and ArhGAP29, is dispensable for 007-induced cell adhesion (Fig. S3C). We therefore

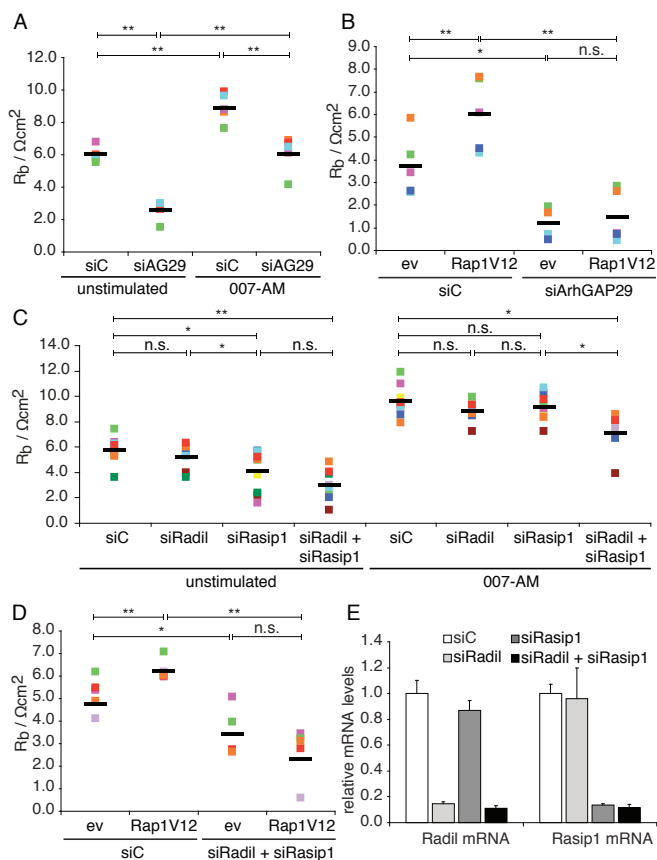


Figure 5: Rasip1, Radil and ArhGAP29 mediate Rap1-induced endothelial barrier function.

(A) Endothelial barrier (R_b) of control HUVEC monolayers (siC) and HUVEC monolayers depleted of ArhGAP29 (siAG29), as determined by ECIS, both before and after the addition of $1 \mu\text{M}$ 007-AM. Different colors represent independent experiments ($n=5$). Averages are indicated by the black line. (B) Endothelial barrier (R_b) of control HUVEC monolayers (siC) and HUVEC monolayers depleted of ArhGAP29 (siArhGAP29), transduced with control lentivirus or Rap1AV12 containing lentivirus. Different colors represent independent experiments ($n=5$). Averages are indicated by the black line. (C) Endothelial barrier (R_b) of control HUVEC monolayers (siC) and HUVEC monolayers depleted of Radil (siRadil), Rasip1 (siRasip1) or both (siRadil + siRasip1), both before and after the addition of $1 \mu\text{M}$ 007-AM. Different colors represent independent experiments ($n=10$). Averages are indicated by the black line. (D) Endothelial barrier (R_b) of control HUVEC monolayers (siC) and HUVEC monolayers depleted of both Radil and Rasip1 (siRadil + siRasip1), transduced with control lentivirus or Rap1AV12 containing lentivirus. Different colors represent independent experiments ($n=6$). Averages are indicated by the black line. (E) HUVECs depleted of Radil (siRadil), Rasip1 (siRasip1) or both (siRadil + siRasip1) were grown to confluency, after which RNA was extracted and mRNA levels were assessed by real-time PCR. The histogram shows Radil and Rasip1 expression within one of the experiments represented in 6C. Expression was correlated to the expression in siC transfected cells. Error bars indicate standard deviation between PCR triplicates. All statistical analyses were obtained by performing a paired Student's t-test. ** $P > 0.01$, * $P > 0.05$, n.s. = not significant.

investigated the contribution of Radil to Rap1-induced endothelial barrier function. Whereas depletion of Radil did not significantly affected endothelial barrier function, simultaneous depletion of Rasip1 and Radil did reduce the endothelial barrier resistance to a similar level as depletion of ArhGAP29, both in the absence or presence of 007 (Fig. 5C and 5E). Furthermore, simultaneous depletion of Rasip1 and Radil prevented the induction of resistance by the overexpression of Rap1AV12 (Fig. 5D),

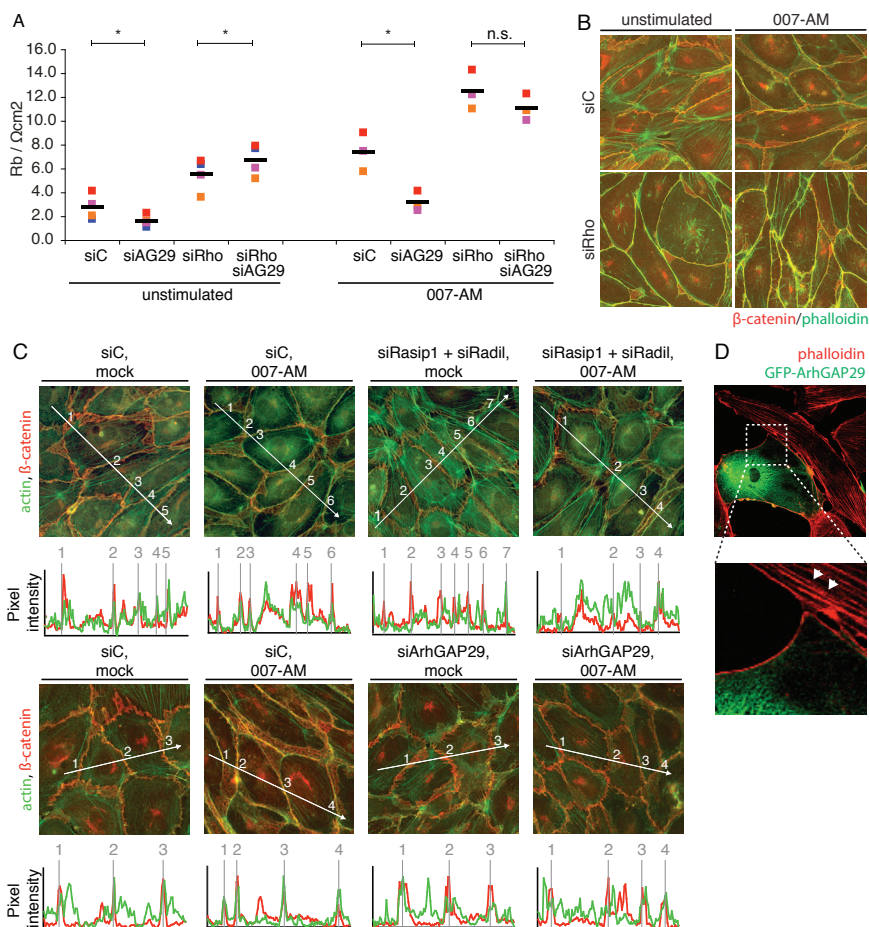


Figure 6: Rasip1, Radil and ArhGAP29 mediate Rap1-regulation of Rho in endothelial barrier function.

(A) Endothelial barrier (R_b) of control HUVEC monolayers (siC) and HUVEC monolayers depleted of ArhGAP29 (siAG29), RhoA, RhoB and RhoC (siRho) or ArhGAP29 and RhoA, RhoB and RhoC (siAG29 + siRho), both before and after the addition of 1 μ M 007-AM. Different colors represent independent experiments (n=4). Averages are indicated by the black line. A Western blot to determine knockdown efficiency is depicted in Fig. S4B. (B) Immunofluorescence of confluent HUVEC monolayers transfected with control (siC) or RhoA, RhoB and RhoC (siRho) siRNA. Monolayers were stimulated with or without 007-AM (1 μ M, 10 minutes) and stained for F-actin (phalloidin, green) and β -catenin (red). (C) Upper panel: Immunofluorescence of confluent HUVEC monolayers transfected with control (siC), Rasip1 and Radil (siRasip1 + siRadil) or ArhGAP29 (siArhGAP29) siRNA. Monolayers were stimulated with or without 007-AM (1 μ M, 10 minutes) and stained for F-actin (phalloidin, green) and β -catenin (red). Lower panel: The graphs show profiles of fluorescence signal intensities along the line scan of phalloidin (green) and β -catenin (red) staining. Grey lines and numbers indicate where the line scan crosses an AJ. (D) Immunofluorescence of HUVECs transduced with GFP-ArhGAP29 containing lentivirus. Cells were fixed and the actin cytoskeleton was stained with phalloidin (red). Arrowheads depict radial stress fibers.

indicating that Rasip1 and Radil together specifically mediate the Rap1-dependent component of Epac1-induced endothelial barrier function.

Rap1-Rasip1-ArhGAP29 axis induces endothelial barrier function through Rho

To confirm that the Rap1-Rasip1-ArhGAP29 signaling pathway regulates endothelial barrier function

through Rho signaling, we investigated whether depletion of Rho could alleviate the endothelial barrier dysfunction caused by ArhGAP29 depletion. Depletion of either RhoA, RhoB or RhoC slightly increased endothelial barrier resistance, however, simultaneous depletion of RhoA, RhoB and RhoC resulted in a robust increase in endothelial barrier function (Fig. S4A), indicating that a reduction of Rho activity increases endothelial barrier function. The reduction in endothelial barrier resistance upon ArhGAP29 depletion, both in the absence and presence of 007, was completely restored by simultaneous depletion of Rho (Fig. 6A).

The induction of endothelial barrier function by activation of the Epac1-Rap1 signaling pathway is accompanied by actin cytoskeletal rearrangements, including induction of junctional actin formation and reduction of radial stress fibers^{31,167,228,229}. Radial stress fibers attach to and exert tension on adherence junctions (AJs), resulting in irregular junctions, which is regulated by the Rho-Rock signaling pathway^{90,91}. Indeed, depletion of RhoA, RhoB and RhoC resulted in the loss of radial stress fibers and induced linear AJs, which was visualized by staining of β -catenin (Fig. 6B). As reported previously^{31,167,228,229}, activation of Epac1 also resulted in a transition from irregular to more linear junctions, accompanied by a reduction of radial stress fibers (Fig. 6C). Interestingly, simultaneous knockdown of Rasip1 and Radil or depletion of ArhGAP29 resulted in an increased number of irregular junctions and showed an increased stress fiber profile (Fig. 6C, S4C and S4D), suggesting increased tension on the AJs. Moreover, cells overexpressing ArhGAP29 lacked radial stress fibers (Fig. 6D), thereby phenocopying Rho depletion. Together, these results show that ArhGAP29 mediates Rap1-induced endothelial barrier function through Rho signaling, thereby reducing actomyosin-induced tension on AJs.

DISCUSSION

Here we identified a signaling cascade regulated by Rap1, through which Rap1 regulates Rho signaling and actomyosin-induced tension, resulting in cell spreading and endothelial barrier function. Specifically, we identified Rasip1 as a Rap1-effector, interacting with active Rap1 and mediating Rap1-induced cell spreading and endothelial barrier function. Furthermore, we found that the Rasip1 homologue and Rap1-effector, Radil, was similarly involved in Rap1-induced endothelial barrier function. The common binding partner of both Rasip1¹¹⁸ and Radil¹⁰⁰, ArhGAP29, was also required for Rap1-mediated cell spreading and endothelial barrier function, indicating that this protein is part of the effector complex regulated by Rap1. ArhGAP29 has GAP activity towards RhoA²⁴¹ and was previously found to inhibit Rho signaling¹⁰¹. Indeed, Rap1 activation resulted in reduced phospho-MLC2 levels and this required Rasip1 and ArhGAP29. Inhibition of Rho or Rho kinase activity attenuated the 007-induced spreading defect in cells depleted of Rasip1 or ArhGAP29. Furthermore, simultaneous depletion of Rho proteins rescued the effect of ArhGAP29 depletion on endothelial barrier function. We were, however, unable to demonstrate consistent reduction in Rho-GTP levels upon Rap1 activation (Fig. S5), perhaps because Rho activity is only locally affected. Indeed, several recent reports emphasize the importance of spatiotemporal regulation of Rho activity in a variety of biological processes, including endothelial barrier function^{108,147,227,243,244}.

Previously, it has been described that Rho-induced formation and contraction of radial stress fibers, attached to VE-cadherin based AJs, induces irregular, highly dynamic junctions, resulting in increased endothelial permeability^{90,91}. Compatible with this notion, depletion of ArhGAP29 or Rasip1 and Radil increased the amount of stress fibers and irregular junctions. In contrast, overexpression of ArhGAP29 resulted in complete loss of radial stress fibers, thereby phenocopying cells devoid of RhoA, RhoB and RhoC. We therefore conclude that Rasip1 is an effector of Rap1 that together with Radil, controls Rho signaling through ArhGAP29 in cell spreading and endothelial barrier function, and that this is achieved by the reduction of actomyosin-induced tension (Fig. S6).

In apparent contrast to previous reports^{101,182}, we find that Rasip1, Radil and ArhGAP29 are dispensable for Rap1-induced initial cell adhesion, suggesting that Rap1 can differentially regulate cell adhesion and cell spreading (Fig. S6). However, we did observe that the number of focal adhesions was reduced in Rasip1 or Radil depleted cells (Fig. S1C and⁴⁸), possibly accounting for the reduced amount of active integrins found previously when depleting Rasip1¹⁰¹ or Radil¹⁸². Our finding that Rasip1 and Radil did not affect Rap1-induced initial adhesion does imply that other Rap1 effectors are involved in this process. Several different Rap effectors have been identified that play a role in Rap1-induced cell adhesion and integrin regulation, such as Rap1-GTP-interacting adaptor molecule (Riam) and Ras-association domain-containing protein 5 (RapL). For the B14 cells, however, the effector for Rap1-induced initial adhesion is currently elusive.

The interplay between Rasip1 and Radil requires further investigation. Interestingly, Radil might interact with ArhGAP29 through its PDZ (PSD-95/Dlg/ZO1) domain¹⁰⁰, a domain not present in Rasip1. Perhaps Radil and Rasip1 form a complex, with Radil as the ArhGAP29 binding partner.

Endothelial junctions are regulated by a number of signaling pathways, one of which is the Rap1-Rasip1/Radil-ArhGAP29-Rho pathway. However, Rap1 may use additional routes for controlling these junctions. As already indicated, the Krit-1/CCM1 route may be one of them. Furthermore, in epithelial cells Rap1 localizes non-muscle myosin II-B to cortical actin bundles in a Rho-independent manner²⁴⁵.

ACKNOWLEDGEMENTS

We thank Prof. Dr. K. Kariya, Dr. J. de Rooij and Dr. J. G. Collard for providing DNA constructs and members of the Bos lab for discussions. A.P. and W.J.P. were funded by grants from the Dutch Cancer Society (KWF Kankerbestrijding). S.H.R. was supported by a FEBS Long-Term Fellowship. This work was further supported by the Netherlands Genomics Initiative of the Netherlands Organization for Scientific Research.

MATERIALS AND METHODS

A detailed description of the experimental procedures and of all compounds used can be found in SI Material and Methods.

Spreading assays, short-term adhesion assays and immunofluorescence

Cells were trypsinized and kept in suspension for 1.5 h to allow surface proteins to recover. For spreading assays, cells were replated onto fibronectin-coated coverslips and allowed to adhere for 3 hours at 37 °C. Cells were fixed and incubated with appropriate antibodies and immunofluorescent images were obtained. For short-term adhesion assays, cells were replated onto fibronectin-coated cell culture dishes and allowed to adhere for 25 min at 37 °C. Unbound cells were discarded by washing with phosphate-buffered saline (PBS) after which adhered cells were lysed in alkaline phosphatase buffer and the total amount of cellular protein was determined by measuring absorption at 405 nm. For evaluation of confluent HUVEC monolayers, HUVECs were plated onto fibronectin-coated glass coverslips and grown to confluency. After stimulation, cells were fixed and incubated with appropriate antibodies and immunofluorescent images were obtained. ImageJ (NIH) was used to quantify images. P-values were determined by Student's t-test (two-tailed, paired).

Rap activation assay

Cells were stimulated for 15 min with 100 μM O07, and subsequently lysed in Ralbuffer. Active Rap was precipitated with a GST fusion protein of the Ras-binding domain of Ral guanine nucleotide dissociation stimulator precoupled to glutathione-Sepharose beads. Bound proteins were eluted in Laemmli buffer and analyzed by SDS-PAGE and Western blotting.

Acceptor-photobleaching-based FRET detection

Cells expressing mCherry-Rap1V12, mCherry-Rap1N17 or GFP-Rasip1 were plated onto fibronectin-coated coverslips as described for the spreading assays. FRET efficiency was determined by the acceptor-photobleaching method. A series of pre-bleaching and post-bleaching fluorescence intensities of GFP (donor) were recorded and

the energy transfer efficiency (E) was calculated from the equation: $E = (D_{\text{post}} - D_{\text{pre}}) / D_{\text{post}}$. Intensities were calculated with ImageJ. Statistical analysis was obtained by performing a paired Student's t-test.

Endothelial barrier measurements

Endothelial barrier was assessed by ECIS measurements. HUVECs were plated onto fibronectin-coated electrodes and grown to confluency. The impedance was measured at multiple frequencies within the range of 62.5 Hz to 16000 Hz at 37°C. These frequency scans were used to calculate endothelial barrier (R_b). P-values were calculated by student's t-test (two-tailed, paired).

SI MATERIALS AND METHODS

Reagents and antibodies

007 (8-pCPT-2'-O-Me-cAMP) and 007-AM (8-pCPT-2'-O-Me-cAMP-AM) were from Biolog Life Sciences (Bremen, Germany) and used at concentrations of 100 μ M and 1 μ M, respectively²⁴⁶. C3 transferase protein (CT03) was from Cytoskeleton Inc. and Y27623 was from Sigma-Aldrich. Antibodies were from Invitrogen (V5, fluorescently-labeled Phalloidin and secondary antibodies), Santa Cruz Biotechnology (Ras-related protein 1 (Rap1)), BD Biosciences (β -catenin, Paxillin), Roche (GFP), Chemicon (α -tubulin), Sigma-Aldrich (Vinculin), Abcam (Radil), Abgent (Rasip1), Cell Signalling Technology (phospho-MLC2 T18/S19, MLC2, Epac1, phospho-Paxillin Y118), Novus Biologicals (Rho GTPase-activating protein 29 (ArhGAP29)) and Covance (HA). All knockdowns were performed using ON-Target Plus siRNA (Dharmacon). siRNA SMARTpools were used for Rap1A, Rasip1, ArhGAP29, Radil, RhoA, RhoB and RhoC. Knockdowns for Rasip1, ArhGAP29 and Radil were confirmed using single siRNAs.

DNA constructs

pBluescript-Rasip1 was purchased from Source Bioscience LifeSciences (Clone: IRATp970H03101D). The HA-RapV12 construct has been described previously²¹². Rasip1 and Rap1 were N-terminally cloned to either citrine YFP or GFP in a pcDNA3 vector or mCherry in a modified pLV-CMVbc vector using the Gateway system (Invitrogen). Site-directed mutagenesis was used to make the Rap1N17 mutant. GFP-Tiam C1199 was a gift from J.G. Collard (Netherlands Cancer Institute, the Netherlands). GFP-RhoAQ63L was a gift from J. de Rooij (Hubrecht Institute, the Netherlands). pLV-GFP-ArhGAP29 was cloned from pCleo-HA-ArhGAP29 (a kind gift from prof. K. Kariya, University of the Ryuky, Japan) into the Gateway cloning system (Invitrogen).

Cell culture and transfections

The lung carcinoma A549 cell line and the derivative monoclonal Epac1-expressing A549-Epac1 cell line, previously described in¹⁶⁹ were cultured in RPMI supplemented with L-glutamine, antibiotics and 10% FCS. HEK293T cells, used for production of lentivirus, were cultured at 37°C and 6% CO₂ in Dulbecco's Modified Eagle Medium supplemented with 10% fetal bovine serum, 2 mM L-glutamine and antibiotics. Human Umbilical Vein Endothelial Cells (HUVECs) (Lonza) were grown at 37°C and 6% CO₂ on tissue culture dishes coated with 0.5% Gelatin in EBM-2 culture medium (Lonza) supplemented with EGM-2 SingleQuots (EGF, hydrocortisone, fetal bovine serum, VEGF, FGF-B, R3-IGF-1, ascorbic acid, GA-100, heparin) (Lonza). HUVECs were cultured maximally 14 days before experiments. siRNA transfections were performed 72 hours before experiments with 50 nM ON-TARGETplus SMARTpools or single siRNAs (Dharmacon Inc.) targeting indicated proteins using HiPerfect (Qiagen) for A549-Epac1 cells or Dharmafect-1 (Dharmacon Inc.) for HUVECs, according to manufacturers protocol. A549-Epac1 cells were transfected with expression plasmids 48h before performing experiments using FuGENE 6 (Roche) according to the manufacturer's protocol. A549-Epac1 cells were transfected with siRNA 16 hours before transfection of the expression plasmid. Overexpression of proteins in HUVECs was established by lentiviral transduction. For lentivirus production, the growth medium of HEK293T cells was replaced by EBM-2 growth medium, upon which these cells were transfected with pLV-CMV-V5-V12Rap1A-bc-GFP or an empty vector control together with third-generation packaging constructs using FuGene6 (Roche). HUVECs were infected 48 hours before experiments using the undiluted growth medium of virus-producing HEK293T cells supplemented with 8 mg/l polybrene.

Spreading assay and immunofluorescence

For spreading assays, A549-Epac1 cells were trypsinized, washed once in RPMI medium containing 10% FCS, and kept in suspension for 1.5 h in RPMI medium containing 0.5% FCS, glutamine, antibiotics and 10 mM HEPES, pH 7.4, at 37°C to allow surface proteins to recover. For the spreading assay using human umbilical vein endothelial cells, all steps were carried out in full media. Coverslips were coated with fibronectin overnight in a 24-well plate at 4°C. After recovery, 2.5×10^4 cells were plated per well in the absence or presence of 100 μ M 007 and allowed to adhere for 3 hours at 37 °C. Cells transfected with siRNA only were fixed with 4% formaldehyde in cytoskeletal

buffer (0.5% Triton X-100, 10 mM PIPES pH 7, 50 mM KCl, 2mM CaCl₂, 2 mM MgCl₂, 300 mM sucrose) for 10 min. In experiments where proteins were overexpressed, cells were fixed with 4% formaldehyde and permeabilised with 0.1% Triton X-100 for 5 minutes. Subsequently, cells were incubated with indicated primary antibodies for 2 hours and secondary antibodies or phalloidin coupled to Alexa Fluor 488 or Alexa Fluor 568 (Invitrogen) for 30 min. Cells were mounted onto glass slides and examined on an Axioskop 2 plus microscope (Zeiss) fitted with a Zeiss Axiocam CCD camera and 40x and 100x Plan APO objective immersion oil lenses. ImageJ (NIH) was used to quantify cell spreading. For the cell spreading experiments, at least 10 cells per condition were analysed, from at least four fields of view. To avoid bias, all of the cells imaged in a single field of view taken through the 40x objective were analysed. Cells were selected using the threshold function to measure the whole area of the cell. Areas were measured in pixels per cell and the relative spreading area for individual experiments was determined by standardizing the spreading of cells under each condition to the mean size of cells under control conditions. Quantification of foal adhesion staining was performed as previously described⁴⁹. A minimum of 3 cells per experiment was analyzed. P-values were determined by Student's t-test (two-tailed, paired).

For evaluation of confluent HUVEC monolayers, HUVECs were plated onto fibronectin-coated glass coverslips in 24-well plates (2x10⁵ cells/well) and grown to confluency for another 24 hours. After 10 minutes stimulation with 1 μM 007-AM, cells were fixed with 4% formaldehyde for 20 minutes, permeabilized with 0.1% Triton X-100 for 3 minutes and blocked with 1% BSA for at least 2 hours. Next, cells were incubated with indicated primary antibodies for 1 hour, secondary antibody for 30 minutes and mounted onto glass slides, which were subsequently examined on an Axioskop 2 plus microscope (Zeiss) fitted with a Zeiss Axiocam CCD camera and 40x immersion oil lens. Original images were used to create line scans in ImageJ. The graphs show profiles of signal intensities along the line scan. To allow easy visual comparison between channels, signal intensities in both channels were normalized to the minimal and maximal intensity along the line scan.

Short-term adhesion assay

The adhesion of A549-Epac1 cells was measured as described previously⁴⁸. In brief, 48-well polystyrene cell culture dishes were coated with fibronectin overnight at 4 °C and subsequently blocked with 1% heat-denatured BSA for 1 hour at 37 °C. Cells were trypsinized, washed once in RPMI medium containing 10% FCS, and kept in suspension for 1.5h in RPMI medium containing 0.5% FCS, glutamine, antibiotics and 10 mM HEPES, pH 7.4, at 37°C to allow surface proteins to recover. Subsequently, 5.0x10⁴ cells were plated per well in the absence or presence of 100 μM 007 and allowed to adhere for 25 min at 37 °C. Unbound cells were discarded by washing with phosphate-buffered saline (PBS) after which adhered cells were lysed in alkaline phosphatase buffer (0.4% Triton X-100, 50 mM sodium citrate, and 10 mg/ml phosphatase substrate (Sigma-Aldrich)). The reaction mixture was incubated at RT, and the total amount of cellular protein was determined by measuring absorption at 405 nm.

Rap activation assay

Rap activity was assayed as described previously²⁴⁷. In brief, A549-Epac1 cells were stimulated for 15 min with 100 μM 007, and subsequently lysed in Ralbuffer (1% NP-40, 150 mM NaCl, 50 mM Tris-HCl, pH 7.4, 10% glycerol, 2 mM MgCl₂, and protease and phosphatase inhibitors). Lysates were cleared by centrifugation, and active Rap was precipitated with a GST fusion protein of the Ras-binding domain of Ral guanine nucleotide dissociation stimulator precoupled to glutathione–Sepharose beads. Bound proteins were eluted in Laemmli buffer and analyzed by SDS-PAGE and Western blotting with polyclonal anti-Rap1 antibody.

Acceptor-photobleaching-based FRET detection

A459-Epac1 cells transfected with GFP-Rap1V12, GFP-Rap1N17 or mCherry-Rasip1 were plated onto fibronectin-coated coverslips for 3 hours and fixed with 4% formaldehyde for 10 min. Mounted slides were examined using a confocal laser-scanning microscope (Axioskop2; Carl Zeiss; 40x magnification lenses, NA 1.4). The GFP and mCherry were excited at 488 nm and 561 nm, respectively. To determine FRET efficiency we used the acceptor-photobleaching method. For acceptor-photobleaching a 20s pulse of high intensity laser excitation of 561 nm was applied to bleach a region of interest (ROI) within a cell. A series of pre-bleaching and post-bleaching fluorescence intensities of GFP (donor) were recorded. When FRET occurred an increase in donor fluorescence could be measured after acceptor-photobleaching due to the loss of quenching by the acceptor. The energy transfer efficiency (E) was calculated from the equation: $E = (D_{\text{post}} - D_{\text{pre}}) / D_{\text{post}}$, where D_{pre} and D_{post} represent the fluorescence intensities of the donor before and after acceptor photobleaching, respectively. Intensities were calculated with ImageJ within a defined region of interest (ROI). Per cell 3 ROIs were taken of both the bleached area and unbleached area for background correction and values were averaged. 3 cells per experiment were visualized. Statistical analysis was obtained by performing a paired Student's t-test.

Endothelial barrier measurements

Endothelial barrier was assessed by ECIS measurements. 48 hours after siRNA transfection and/or 24 hours after lentiviral infection, HUVECs were plated onto L-cysteine reduced, fibronectin-coated 8W10E electrodes (Applied Biophysics) at a density of 1×10^5 cells/well and grown to confluency for another 24 hours. The impedance was measured at multiple frequencies within the range of 62.5 Hz to 16000 Hz at 37°C and 6% CO₂ using a 1600R Electrical Cell Impedance Sensing (ECIS) system (Applied Biophysics) both before and after the addition of 007-AM. These frequency scans were used to calculate endothelial barrier (R_b) with ECIS software (v1.2.50.0 PC) from Applied Biophysics. The graphs show multiple independent experiments represented by different colors. P-values were calculated by student's t-test (two-tailed, paired).

Real-time quantitative polymerase chain reaction

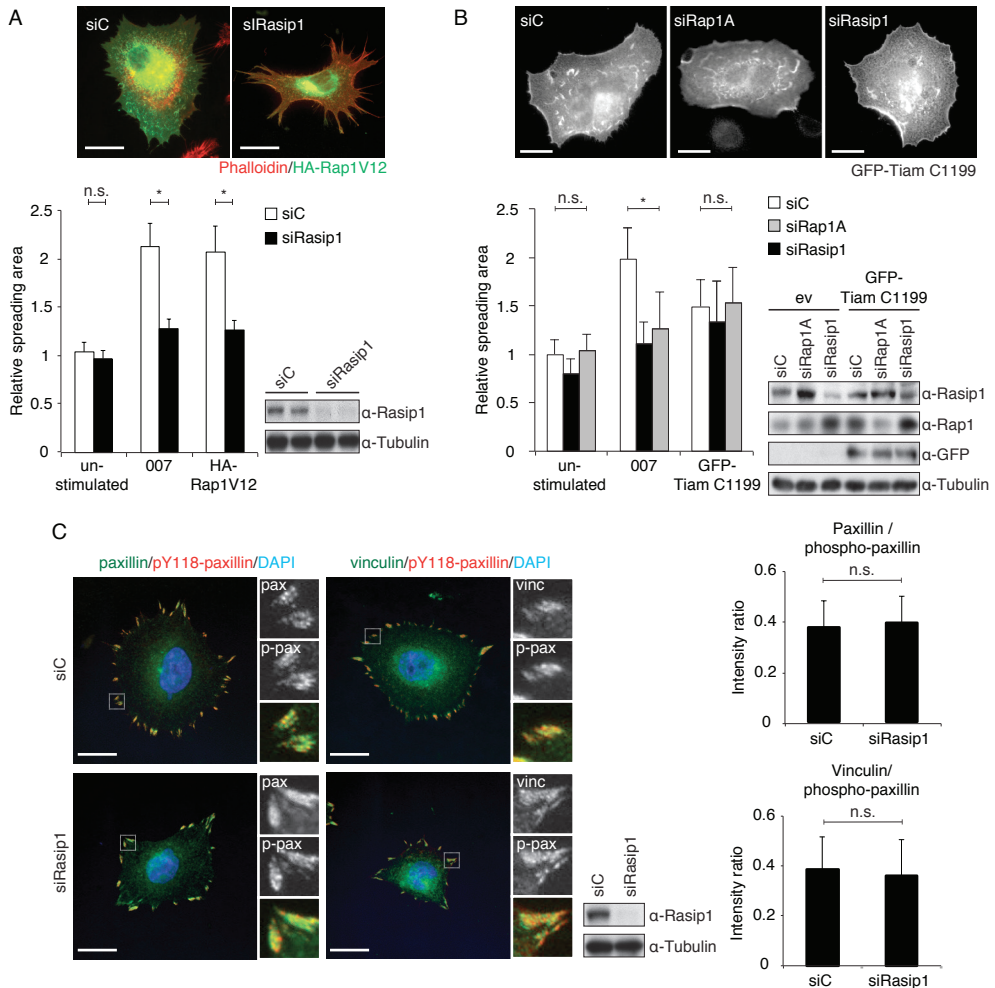
8×10^5 HUVEC cells were plated 48 hours after siRNA transfection onto Fibronectin-coated 6 cm dishes and grown for another 24 hours. Total RNA was isolated using the RNeasy Mini Kit (Qiagen) and transcribed into cDNA using the iScript cDNA Synthesis Kit (BIO-RAD). cDNA levels were quantified by SYBR green real-time PCR on a C1000 Thermal Cycler (BIO-RAD) using the following primers: CTGGACATCACAGGCTCGAA (Radil-forward), TTGGAGACATAGTAGCGCAC (Radil-reverse), TCAGCCAGAAAACCACCTGA (Rasip1-forward), CAGCACCTTCTCCTGCACAAA (Rasip1-reverse). Nonspecific signals were excluded based on non-template control samples. Amplification of the HPRT1 gene was used as a control for sample loading. Expression levels were normalized to the siScrambled control. Error bars indicate standard deviation (n=3).

Co-immunoprecipitations

HEK293T cells were transfected using X-tremeGENE 9 (Roche Inc.) and lysed 48h after transfection using a buffer containing 1% NP-40, 20 mM Tris, pH 7.5, 150 mM NaCl, 20 mM MgCl₂, 10% glycerol and protease and phosphatase inhibitors. Cell lysates were cleared by centrifugation, and lysates were incubated with protein A-agarose beads (Pharmacia) coupled to the appropriate antibody. After extensive washing with lysis buffer, bound proteins were eluted in Laemmli buffer and analyzed by SDS-PAGE.

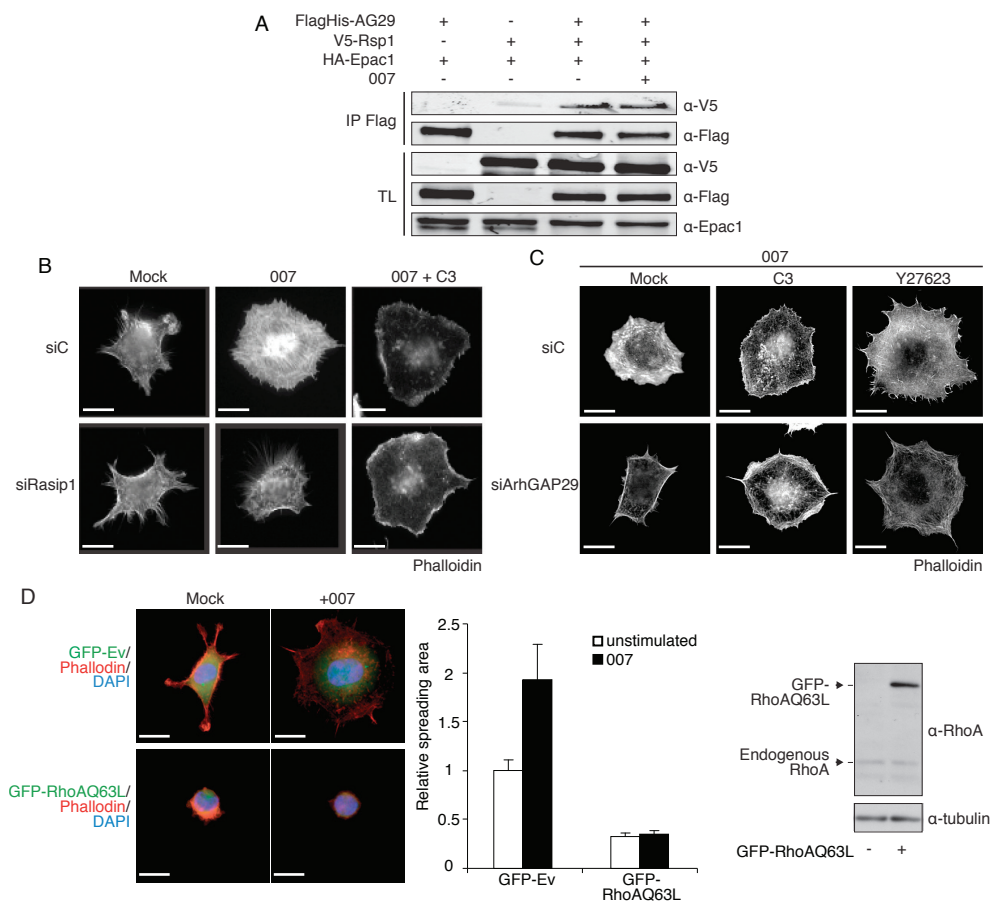
Rho activation assay

Rho activity was assayed using an Active Rho Pull-down and Detection kit from Thermo Scientific, and performed according to manufacturers protocol. In brief, A549-Epac1 cells were stimulated for 15 min with 100 μM 007 or 4 hours with C3 transferase protein, and subsequently lysed. Lysates were cleared by centrifugation, and active Rho was precipitated with a GST fusion protein of the Ras-binding domain of Rhotekin. Bound proteins were eluted in Laemmli buffer and analyzed by SDS-PAGE and Western blotting with anti-Rho antibody.



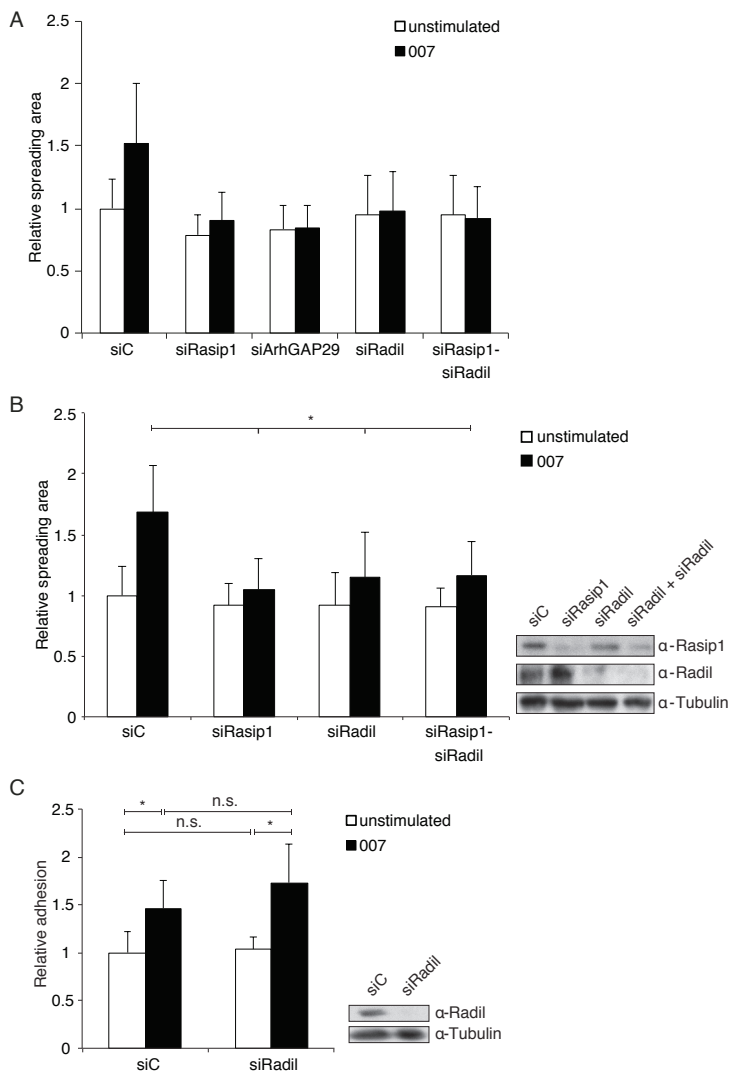
Supplemental figure 1: Rasip1 specifically mediates Rap1-induced spreading without affecting focal adhesion dynamics.

(A) Spreading of A549-Epac1 cells transfected with scrambled siRNA (siC) or siRNAs targeting Rasip1 (siRasip1) 16h prior to transfection with HA-ev or HA-Rap1V12. Cells were replated, treated and quantified as described for fig. 1A. Depicted is average spreading area \pm s.d. of three individual experiments normalized to unstimulated siC transfected cells. * $P < 0.05$. (B) Spreading of A549-Epac1 cells transfected with scrambled siRNA (siC), Rap1A targeting siRNA (siRap1A) or Rasip1 targeting siRNA (siRasip1) 16h prior to transfection with GFP-ev or GFP-Tiam C1199. Cells were replated, treated as and quantified for fig. 1A. Depicted is average spreading area \pm s.d. of four individual experiments normalized to unstimulated siC transfected cells. * $P < 0.007$. (C) Focal adhesion composition of siC or siRasip1 treated cells. Cells were replated onto fibronectin-coated coverslips for 3h in the presence of 100 μ M 007. Left panel: Cells were fixed and stained for paxillin, pY118-paxillin and vinculin. Enlargements of focal adhesions are shown on the right of each overview picture. Right panel: The ratios of paxillin to pY118-paxillin and vinculin to pY118-paxillin were calculated. Depicted is the average ratio \pm s.d. of three individual experiments. All statistical analyses were obtained by performing a paired Student's t-test. Bars are 20 μ M.



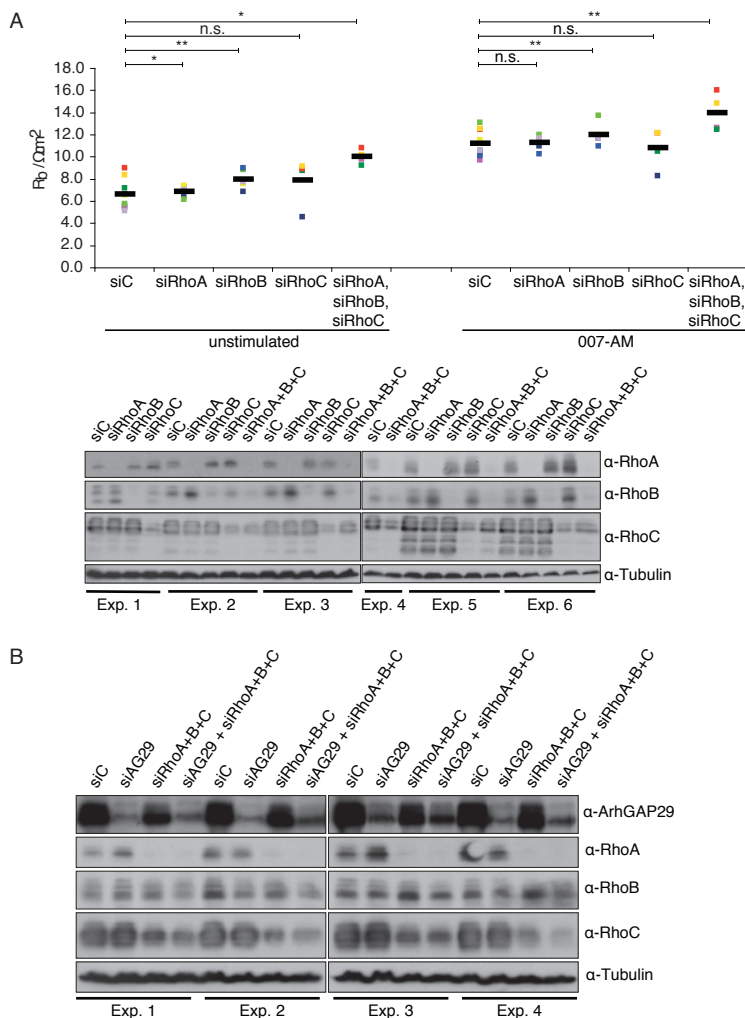
Supplemental figure 2: Rasip1 interacts with the RhoGAP ArhGAP29 to modulate Rho signaling.

(A) Co-immunoprecipitation of FlagHis-ArhGAP29 (IP) with V5-Rasp1 in HEK293T cells. Cells were cotransfected with HA-Epac1 and either not stimulated (-) or stimulated with 100 μ M 007 (+) for 15 minutes. Complex formation was assessed by immunoprecipitation using a Flag antibody followed by Western blotting. Total cell lysates (TL) show protein expression. (B) Spreading of A549-Epac1 cells transfected with siC or siRasp1 in the presence or absence of C3 transferase (C3). Cells were replated for 3h onto fibronectin-coated coverslips in the absence or presence of 100 μ M 007 and absence or presence of C3 transferase. Cells were fixed and the actin cytoskeleton was visualized by phalloidin staining (For quantification see fig. 4B). (C) Spreading of A549-Epac1 cells transfected with siC or siArhGAP29 in the presence or absence of C3 transferase (C3) or a ROCK-inhibitor (Y27623). Cells were replated for 3h onto fibronectin-coated coverslips in the absence or presence of 100 μ M 007, C3 transferase and/or Y27623. Cells were fixed and the actin cytoskeleton was visualized by phalloidin (For quantification see fig. 4C). (D) Spreading of A549-Epac1 cells transfected with a constitutively active RhoA construct. 48h after transfection with GFP-empty vector (GFP-ev) or GFP-RhoAQ63L, cells were replated for 3h onto fibronectin-coated coverslips prior to fixation. The actin cytoskeleton was stained with phalloidin and transfected cells were visualized by immunofluorescence. The cell areas of transfected cells were quantified, and the graph shows the average results of three experiments \pm s.e.m. The Western blot shows RhoA protein expression. All statistical analyses were obtained by performing a paired Student's t-test. Bars are 20 μ M.



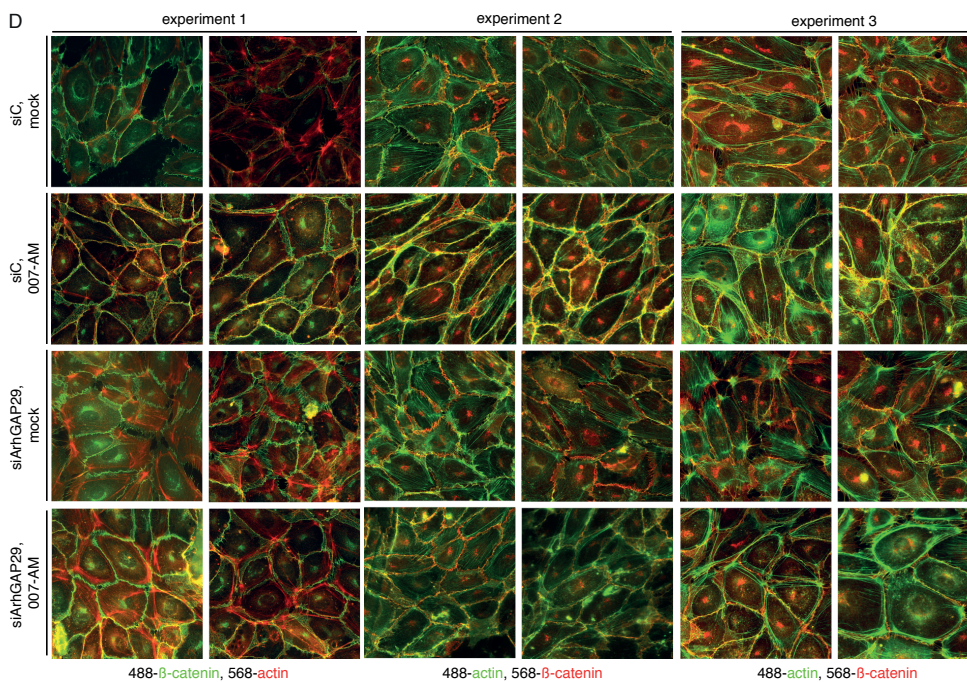
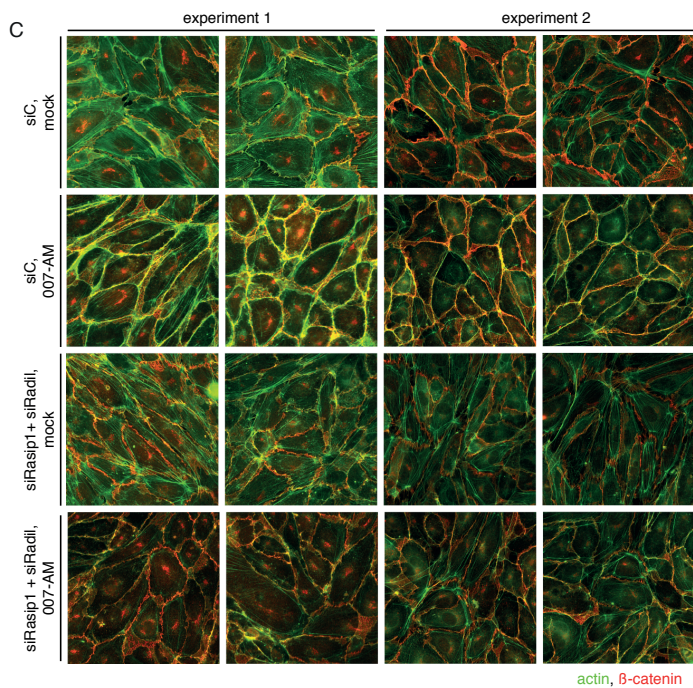
Supplemental figure 3: The Rap1-effector Radil is essential for Rap1-induced spreading in conjunction with Rasip1.

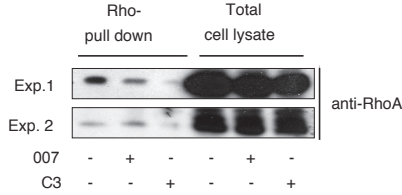
(A) Spreading of HUVECs transfected with control siRNA (siC) or siRNA targeting Rasip1 (siRasip1), Radil (siRadil), both (siRasip1 + siRadil) or ArhGAP29 (siArhGAP29). Cells were replated on fibronectin-coated coverslips and treated and quantified as for fig. 1A. Depicted is average spreading area \pm s.d. of two individual experiments normalized to unstimulated siC transfected cells. (B) Spreading of A549-Epac1 cells transfected with control siRNA (siC) or siRNA targeting Rasip1 (siRasip1), Radil (siRadil), both (siRasip1 + siRadil) or ArhGAP29 (siArhGAP29). Cells were replated on fibronectin-coated coverslips and treated and quantified as for fig. 1A. Depicted is average spreading area \pm s.d. of three individual experiments normalized to unstimulated siC transfected cells. * $P < 0.005$. (C) Adhesion of A549-Epac1 cells transfected with siC or siRadil. Cells were replated, treated and quantified as for fig. 1D. Depicted is mean data \pm s.d. of five individual experiments normalized to unstimulated siC transfected cells. * $P < 0.02$. All statistical analyses were obtained by performing a paired Student's t-test. Bars are 20 μ M.



Supplemental figure 4: Rasip1, Radil and ArhGAP29 mediate Rap1-induced cytoskeletal changes.

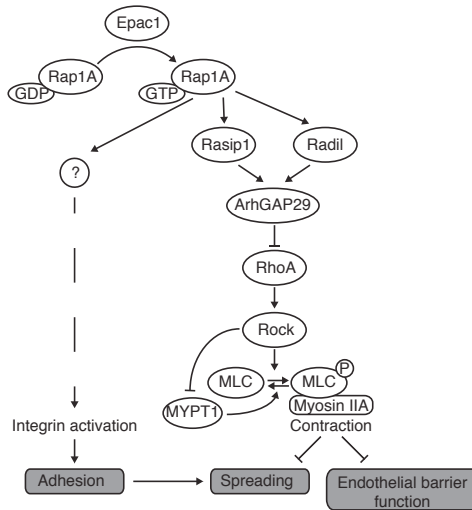
(A) Endothelial barrier (R_b) of control HUVEC monolayers (siC) and HUVEC monolayers depleted of RhoA (siRhoA), RhoB (siRhoB), RhoC (siRhoC) or all three Rho isoforms simultaneously (siRho), both before and after the addition of $1 \mu M$ 007-AM. Different colors represent independent experiments ($n=6$). Averages are indicated by the black line. Knockdown efficiency was determined by Western blot. (B) Western blot of the knockdown efficiency of individual experiment depicted in Fig. 6A. (C and D, see next page) Immunofluorescence of confluent HUVEC monolayers transfected with control (siC), Rasip1 and Radil (siRasip1 + siRadil) or ArhGAP29 (siArhGAP29) siRNA. Monolayers were stimulated with or without 007-AM ($1 \mu M$, 10 minutes) and stained for F-actin (phalloidin) and β -catenin. Per experiment two fields are depicted.





Supplemental figure 5: Inhibition of RhoA activity by Rap1 does not affect global RhoA activity.

A549-Epac1 cells were either not stimulated, stimulated for 15 min with 100 μM 007 or 4h with the Rho inhibitor C3 transferase, after which cells were lysed and lysates were subjected to Rhotekin-Rho binding domain pull-down to isolate Rho-GTP. Rho protein levels in the Rho pull-down and total cell lysates were assessed by Western blotting.



Supplemental figure 6: Schematic representation of how Rap1 regulates spreading and endothelial barrier function through the Rasip1-ArhGAP29 pathway.

Actomyosin-induced contraction inhibits cell spreading and exerts tension on AJs resulting in an increased permeability of the endothelial monolayer. Through Rasip1, Radil and ArhGAP29, Rap1 inhibits Rho signaling resulting in reduced actomyosin contraction, thereby inducing cell spreading and endothelial barrier function.

CHAPTER

RAP1 SPATIALLY CONTROLS ARHGAP29 TO INHIBIT RHO SIGNALING DURING ENDOTHELIAL BARRIER REGULATION

A. Post, W. J. Pannekoek, B. Ponsioen,
M. J. Vliem, J. L. Bos

To be submitted

5

ABSTRACT

The small GTPase Rap1 controls the actin cytoskeleton by regulating Rho GTPase signaling. We have recently established that in the processes of epithelial cell spreading and endothelial barrier function the Rap1 effectors Radil and Rasip1, and the Rho GTPase activating protein ArhGAP29, mediate Rap1-induced inhibition of Rho signaling. Here we show that Rap1 induces the independent translocation of Rasip1 and a Radil-ArhGAP29 complex to the plasma membrane. This results in the formation of a multimeric protein complex required for Rap1-induced inhibition of Rho signaling and increased endothelial barrier function. Together with the previously reported spatiotemporal control of the Rap guanine nucleotide exchange factor, Epac1, this elucidates a signaling pathway for spatiotemporal control of Rho signaling, that operates by successive protein translocations to and complex formation at the plasma membrane.

INTRODUCTION

The small GTPase Rap1 controls many processes linked to actin cytoskeletal dynamics, including integrin-mediated and cadherin-mediated cell adhesion. As such Rap1 appears to be a master regulator of tissue integrity, to which end it translates spatial and temporal information into actin cytoskeleton modulation. This spatiotemporal information is received by Rap1 guanine nucleotide exchange factors (GEFs), such as Epac1 and PDZ-GEF. For instance, Epac1 responds to cAMP by catalytic activation and translocation to specific sites at the plasma membrane resulting in the local activation of Rap1. Subsequently, actin cytoskeletal rearrangements occur, as exemplified in endothelial barrier regulation.

The endothelial barrier is under tight control to allow passage of fluids, solutes and immune cells, without losing tissue integrity and barrier function²³³⁻²³⁵. Rap1 plays an important role in this by enhancing the endothelial barrier function^{31,228,229,231,248}. It does so by impinging on the family of Rho GTPases, the master regulators of the actin cytoskeleton. Once activated, Rap1 inhibits the small GTPase Rho, resulting in the relaxation and disappearance of stress fibers^{71,88,104,236}, and activates the small GTPase Cdc42, resulting in the formation of junctional actin bundles⁸⁸. As a result barrier function is enhanced. Indeed, Rho GTPases are important players in adherens junction formation and maintenance, necessary to sustain barrier integrity of both epithelial and endothelial monolayers²⁴⁹⁻²⁵¹.

Recently, we have elucidated that one way for Rap1 to regulate Rho activity in endothelial barrier function is through the RhoGAP ArhGAP29. Rap1 does so through its effectors Radil and Rasip1⁷¹. Importantly, this same pathway also controls cell spreading of epithelial cells, indicating that the pathway is not cell type specific.

Here we have addressed the question how Rasip1, Radil and ArhGAP29 cooperate with Rap1 to regulate Rho signaling. We demonstrate that Rap1 induces the translocation of ArhGAP29 to the plasma membrane in a highly dynamic manner, thereby spatially regulating Rho activity. It does so by recruiting Radil, which forms a stable complex with ArhGAP29. Rasip1 can be recruited by Rap1 to the plasma membrane independently of the Radil-ArhGAP29 complex. However, enhanced by active Rap1, Rasip1 interacts with the Radil-ArhGAP29 complex, necessary for the functionality of this complex. From these results we conclude that upon Rap1 activation, Rasip1 and a complex of Radil and ArhGAP29 are independently recruited to the plasma membrane to form a multimeric complex, through which Rap1 spatially restricts Rho signaling, necessary for endothelial barrier potentiation.

RESULTS

ArhGAP29 is recruited to the plasma membrane upon activation of Epac1 and Rap1

To investigate how ArhGAP29 is regulated downstream of Epac1-Rap1 signaling we first studied the subcellular localization of ArhGAP29 by expressing GFP-ArhGAP29 in HUVECs. GFP-ArhGAP29 localized predominantly to the cytoplasm under resting conditions, with some localization to the plasma membrane. Upon activation of Epac1 by 007-AM, GFP-ArhGAP29 largely redistributed to the plasma membrane (Fig. 1A), as compared to GFP-ev (Fig. 1B). This translocation was abrogated by depletion of Rap1 (Fig. 1C), indicating that Rap1 induces the translocation of ArhGAP29 to cell-cell junctions.

Similar results were obtained when we reconstituted the signaling cascade in 293T cells by coexpressing CFP-Epac1, HA-Rap1 and YFP-ArhGAP29, together with HA-Radil and HA-Rasip1, the Rap1 effectors involved in this process⁷¹. Stimulation with 8-CPT-2'OMe-cAMP-AM (007-AM), a selective agonist for Epac1²⁵², readily induced the translocation of YFP-ArhGAP29 to the PM (Fig. 1D, movie 1), which closely followed Epac1 translocation to the PM (movie 1).

To confirm that the translocation of ArhGAP29 to the plasma membrane was Rap1-mediated, we transfected 293T cells with YFP-ArhGAP29, HA-Radil, HA-Rasip1 and CFP-Rap1AV12, an active

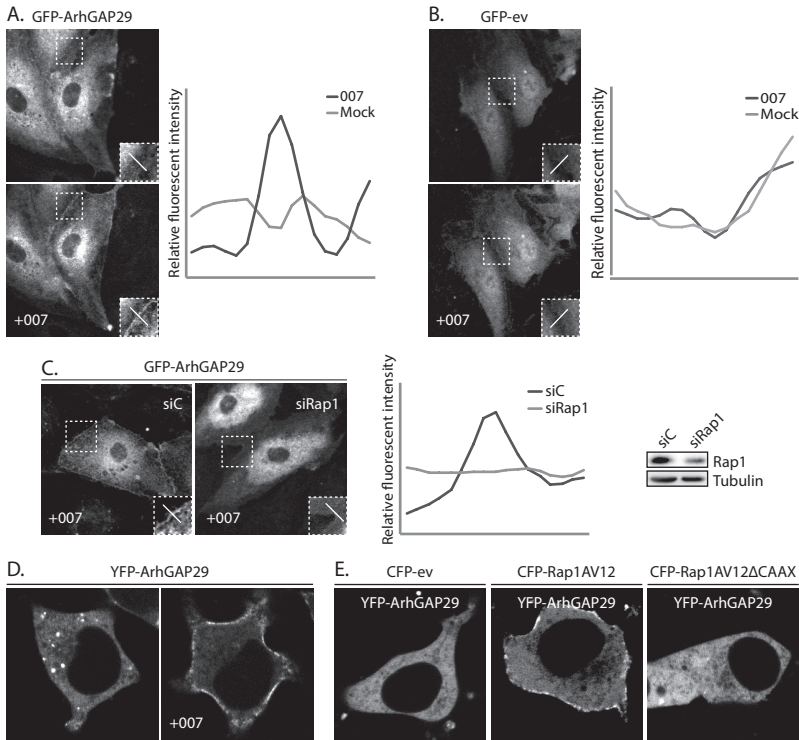
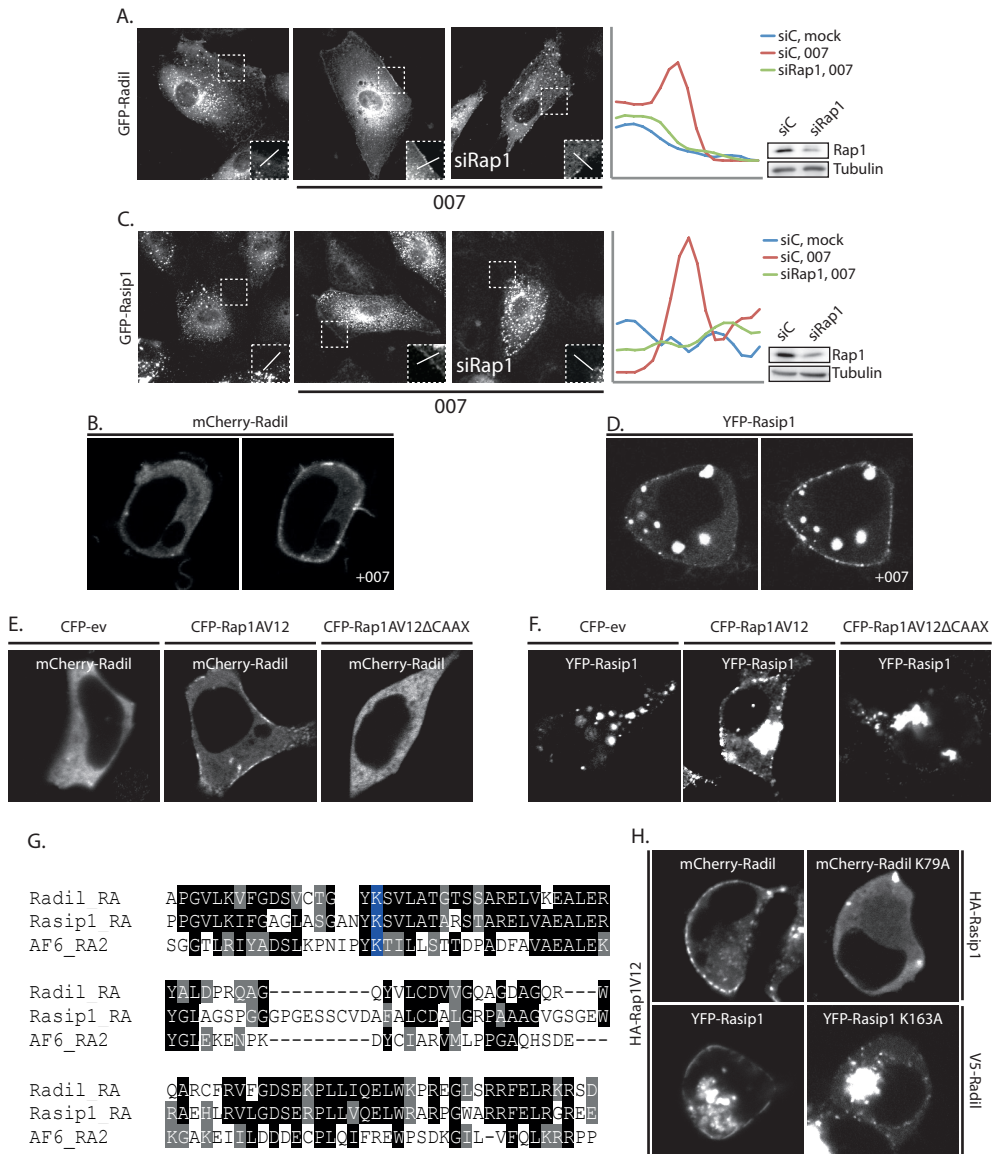


Figure 1: Active Rap1 recruits ArhGAP29 to the plasma membrane.

(A) Left panel: Live imaging of confluent monolayers of HUVECs infected with GFP-ArhGAP29. Cells were imaged prior to or 15 min after stimulation with 007-AM. Boxed areas of cell-cell contacts are enlarged in the insets. Right panel: Graph showing relative intensity profiles of fluorescent signal intensities along the line scans depicted in the boxed area. (B) Left panel: Live imaging of confluent monolayers of HUVECs infected with GFP-ev. Cells were imaged prior to or 15 min after stimulation with 007-AM. Boxed areas of cell-cell contacts are enlarged in the insets. Right panel: Graph showing relative intensity profiles of fluorescent signal intensities along the line scans depicted in the boxed area. (C) Left panel: Live imaging of GFP-ArhGAP29 infected HUVECs, treated with control siRNA (siC) or siRNA targeting Rap1A and Rap1B (siRap1). Cells were grown to confluence and stimulated with 007-AM 15 minutes prior to imaging. Boxed areas are enlarged in insets. Right panel: Graph showing relative intensity profiles of fluorescent signal intensities along the line scans depicted in the boxed area. (D) Western blot depicting protein expression of Rap1 in the HUVECs analysed in figure C. (E) Live imaging of 293T cells transiently transfected with HA-Epac1, HA-Rap1A, V5-Radil, Flag-Rasip1 and YFP-ArhGAP29, imaged prior to and 10 min after stimulation with 007-AM. (F) Imaging of YFP-ArhGAP29 in 293T cells transfected with V5-Radil, Flag-Rasip1, YFP-ArhGAP29 and either with CFP-ev, CFP-Rap1AV12 or CFP-Rap1AV12ΔCAAX. Experiments were repeated at least 3 times and representative images were chosen.

Figure 2: Active Rap1 recruits Radil and Rasip1 to the plasma membrane.

(A) Left panel: Live imaging of confluent monolayers of HUVECs infected with GFP-Radil and treated with control siRNA (siC) or siRNA targeting Rap1A and Rap1B (siRap1). Cells were imaged prior to or 15 min after stimulation with 007-AM. Boxed areas of cell-cell contacts are enlarged in the insets. Right panel: Graph showing relative intensity profiles of fluorescent signal intensities along the line scans depicted in the boxed area. Knockdown efficiency was assessed by Western blot. (B) Stills corresponding to the live imaging (movie 2) of 293T cells transiently transfected with HA-Epac1, HA-Rap1A, mCherry-Radil, Flag-Rasip1 and HA-ArhGAP29 stimulated with 007-AM. (C) Left panel: Live imaging of confluent monolayers of HUVECs infected with GFP-Rasip1 and treated with control siRNA (siC) or siRNA targeting Rap1A and Rap1B (siRap1). Cells were imaged prior to or 15 min after stimulation with 007-AM. Boxed areas of cell-cell contacts are enlarged in the insets. Right panel: Graph showing relative intensity profiles of



fluorescent signal intensities along the line scans depicted in the boxed area. Knockdown efficient was assessed by Western blot. (D) Stills corresponding to the live imaging (movie 3) of 293T cells transiently transfected with HA-Epac1, HA-Rap1A, V5-Radil, YFP-Rasip1 and HA-ArhGAP29, imaged prior to and 10 min after stimulation with 007-AM. (E) Live imaging of mCherry-Radil in 293T cells transfected with mCherry-Radil, Flag-Rasip1, HA-ArhGAP29 and either with CFP-ev, CFP-Rap1AV12 or CFP-Rap1AV12ΔCAAX. (F) Live imaging of YFP-Rasip1 in 293T cells transfected with YFP-Rasip1, V5-Radil, HA-ArhGAP29 and either with CFP-ev, CFP-Rap1AV12 or CFP-Rap1AV12ΔCAAX. (G) Alignment of the RA-domains of Radil, Rasip1 and the second RA-domain of AF6. Highlighted by blue is the conserved lysine, essential for interaction with GTP-loaded Rap1. (H) Live imaging of wild type versus RA-mutant mCherry-Radil (upper panels) and wild type versus RA-mutant YFP-Rasip1 (lower panels) in 293T cells transfected with Flag-Rasip1, HA-ArhGAP29 and HA-Rap1AV12 together with mCherry-Radil, mCherry-Radil K79A, YFP-Rasip1 or YFP-Rasip1 K163A. Experiments were repeated at least 3 times and representative images were chosen.

Rap1A mutant. Indeed, expression of CFP-Rap1V12 resulted in PM localized YFP-ArhGAP29 (Fig. 1E). Transfection of a CFP-Rap1AV12-CAAX mutant (unable to associate with the PM), did not result in PM recruitment of YFP-ArhGAP29 (Fig. 1E), indicating that Rap1 functions as the PM anchor for ArhGAP29. From these results we conclude that activation of Epac1 results in PM recruitment of ArhGAP29 to active Rap1, in both HUVECs and 293T cells.

Radil and Rasip1 translocate to the plasma membrane by binding active Rap1

We next investigated the localization of Radil and Rasip1 upon activation of Epac1-Rap1 signaling. In HUVECs and 293T cells we found that both Radil (Fig. 2A and B) and Rasip1 (Fig. 2C and D) translocate

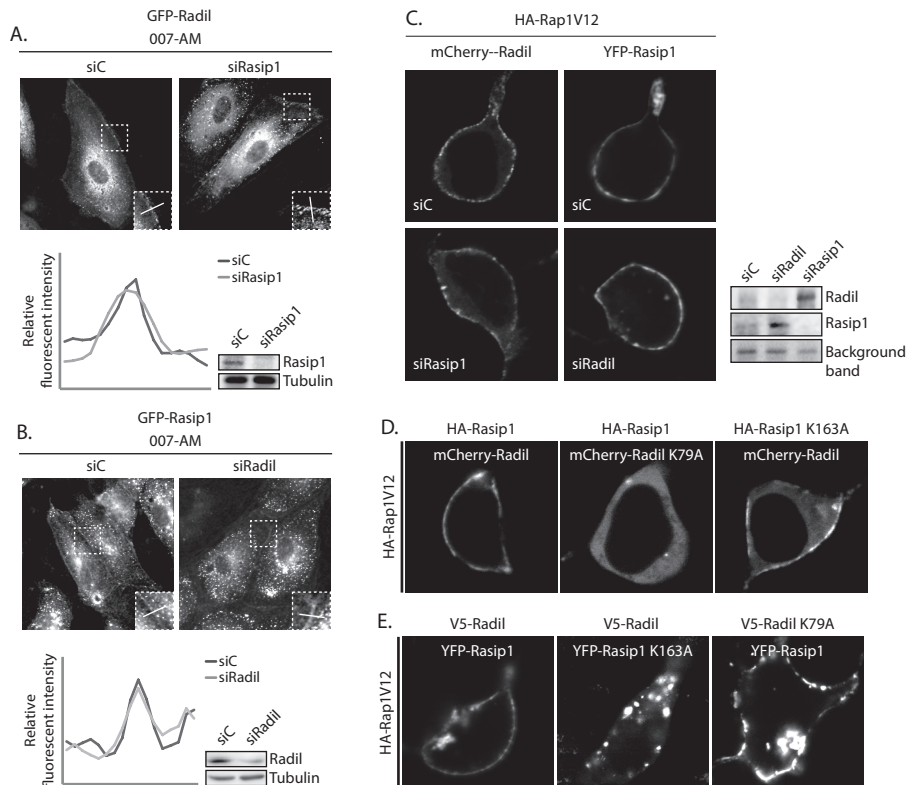


Figure 3: Rasip1 and Radil translocate to the plasma membrane independently.

(A) Upper panel: Live imaging of GFP-Radil infected HUVECs, treated with control siRNA (siC) or siRNA targeting Rasip1 (siRasip1). Cells were grown to confluence and stimulated with 007-AM 15 minutes prior to imaging. Boxed areas are enlarged in insets. Lower panel: Graph showing relative intensity profiles of fluorescent signal intensities along the line scans depicted in the boxed area. Knockdown efficient was assessed by Western blot. (B) Upper panel: Live imaging of GFP-Rasip1 infected HUVECs, treated with control siRNA (siC) or siRNA targeting Radil (siRadil). Cells were grown to confluence and stimulated with 007-AM for 15 minutes prior to imaging. Boxed areas are enlarged in insets. Lower panel: Graph showing relative intensity profiles of fluorescent signal intensities along the line scans depicted in the boxed area. Knockdown efficient was assessed by Western blot. (C) Live imaging of mCherry-Radil or YFP-Rasip1 in 293T cells transfected with HA-Rap1AV12 and mCherry-Radil and YFP-Rasip1 (upper panels), mCherry-Radil and siRNA targeting Rasip1 (lower left panel) or YFP-Rasip1 and siRNA targeting Radil (lower right panel). (D) Live imaging of wild or mutant mCherry-Radil (as indicated) in 293T cells transfected with HA-Rap1AV12 and either mCherry-Radil or mCherry-Radil K79A, together with either Flag-Rasip1 or Flag-Rasip1 K163A. (E) Live imaging of wild or mutant YFP-Rasip1 (as indicated) in 293T cells transfected with HA-Rap1AV12 and either YFP-Rasip1 or YFP-Rasip1 K163A, together with either V5-Radil or V5-Radil K79A.

to the PM upon activation of Epac1 by 007-AM. As for ArhGAP29, this translocation is dependent on Rap1 since depletion of Rap1 abrogated this translocation in HUVECs (Fig. 2A and C), whereas overexpression of CFP-Rap1AV12 resulted in PM localization of mCherry-Radil (Fig. 2E) and YFP-Rasip1 (Fig. 2F) in 293T cells. Furthermore, the CFP-Rap1AV12 Δ CAAX mutant could not recruit Radil (Fig. 2E) or Rasip1 (Fig. 2F) to the PM, demonstrating that both Radil and Rasip1 are recruited to an active pool of Rap1 at the plasma membrane. To test whether Radil and Rasip1 directly bind active Rap1 at the PM we mutated a conserved lysine (Fig. 2G) to an alanine in the RA-domains of Radil and Rasip1. A similar mutation in the Rap1-effector AF6 was shown to abolish Rap1 interaction²⁵³. As expected Radil K79A and Rasip1 K163A did not translocate to the PM in the presence of CFP-Rap1AV12 (Fig. 2H). We conclude that activation of Rap1 results in the translocation of Radil and Rasip1 to the PM by directly interacting with active Rap1.

Rasip1 and Radil translocate to the plasma membrane independently

Next, we investigated whether the translocation of Radil and Rasip1 to the PM depend on each other. Rap1-induced PM localization of Radil in HUVECs or 293T was unaffected by depletion of Rasip1 (Fig. 3A and C). Vice versa, Rap1-induced PM localization of Rasip1 in HUVECs or 293T cells was unaffected by depletion of Radil (Fig. 3B and C). Moreover, wild type Radil did not co-recruit mutant Rasip1, nor

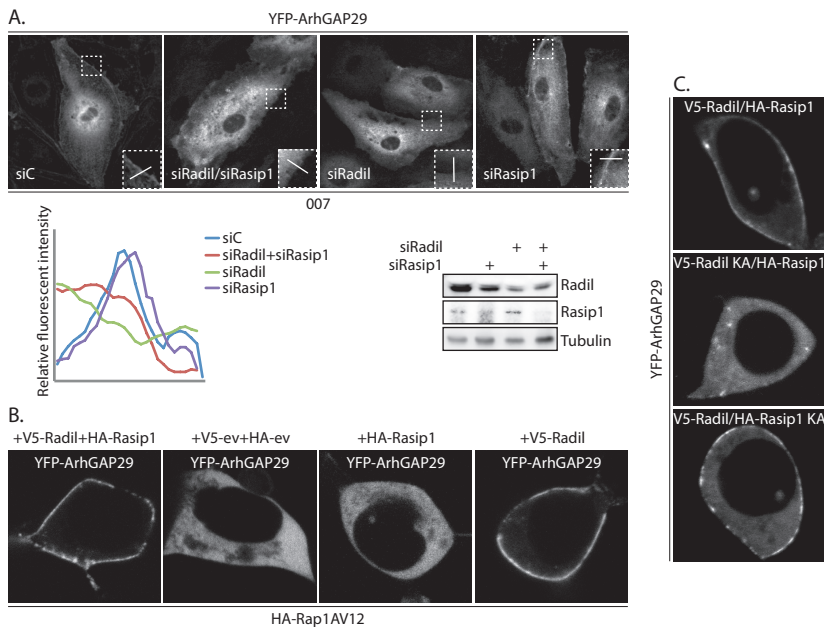


Figure 4: Rap1 recruits ArhGAP29 to the plasma membrane through Radil.

(A) Upper panel: GFP-ArhGAP29 expressing HUVECs were treated with control siRNA (siC), siRNA targeting Radil and Rasip1 (siRadil + siRasip1), Radil (siRadil) or Rasip1 (siRasip1). Cells were grown to confluence and treated with 007-AM for 15 min. Boxed areas of cell-cell contacts are enlarged in the insets. Lower panel: Graph showing relative intensity profiles of fluorescent signal intensities along the line scans depicted in the boxed area. Knockdown efficiency was assessed by Western blot. (B) Live imaging of YFP-ArhGAP29 in 293T cells transfected with HA-Rap1AV12 and YFP-ArhGAP29 upon cotransfection with either V5-Radil and Flag Rasip1 (panel 1), empty vector only (panel 2), Flag-Rasip1 supplemented with empty vector (panel 3) or V5-Radil supplemented with empty vector (panel 4). (C) Live imaging of YFP-ArhGAP29 in 293T cells transfected with HA-Rap1AV12 and YFP-ArhGAP29 upon cotransfection with either V5-Radil and Flag-Rasip1 (panel 1), V5-Radil K79A and Flag-Rasip1 (panel 2) or V5-Radil and Flag-Rasip1 K163A (panel 3). Experiments were repeated at least 3 times and representative images were chosen.

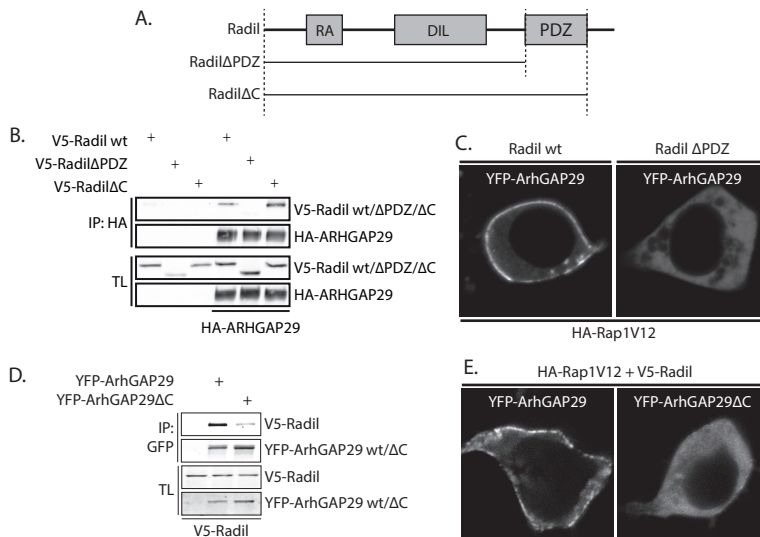


Figure 5: ArhGAP29 binds the PDZ-domain of Radil through its C-terminus.

(A) Domain architecture of Radil and the truncation mutants used for the assays depicted in Fig. 4B and C. RA: Ras Association domain; DIL: dilute domain; PDZ: PSD-95/Dlg1/ZO-1. (B) Coimmunoprecipitation of V5-Radil truncation mutants with HA-ArhGAP29 expressed in 293T cells. Western blot is representative of three independent experiments. (C) Live imaging of YFP-ArhGAP29 in 293T cells transfected with YFP-ArhGAP29 and HA-Rap1AV12 in the presence of V5-Radil or V5-RadilΔPDZ. Experiments were repeated 4 times and representative images were chosen. (D) Coimmunoprecipitation of V5-Radil with YFP-tagged full length ArhGAP29, or ArhGAP29 lacking its last four amino acids (ArhGAP29ΔC) expressed in 293T. Western blot is representative of two independent experiments. (E) Live imaging of YFP-ArhGAP29 in 293T cells transfected with YFP-ArhGAP29 or YFP-ArhGAP29ΔPQFV with HA-Rap1AV12 and V5-Radil. Experiments were repeated 4 times and a representative image was chosen.

did mutant Rasip1 prevent the translocation of wild type Radil, and vice versa (Fig. 3D and E). These results indicate that Rasip1 and Radil translocate to active Rap1 at the PM independent of each other.

ArhGAP29 recruitment to the plasma membrane is dependent on Radil but not Rasip1

We next investigated whether Rap1-induced translocation of ArhGAP29 was dependent on Radil and/or Rasip1. Depletion of both Radil and Rasip1 simultaneously abrogated Epac1-Rap1 induced translocation of ArhGAP29 to the PM both in HUVECs and in 293T cells (Fig. 4A and B). Interestingly, depletion of Radil alone, but not Rasip1 alone, is sufficient to abrogate ArhGAP29 translocation to the PM upon activation of Epac1 with 007-AM, both in HUVECs and 293T cells (Fig. 4A and B). This suggests that the translocation of ArhGAP29 to the PM is solely dependent on Radil. Indeed, in 293T cells expressing CFP-Rap1AV12 and YFP-ArhGAP29, co-expression of V5-Radil K79A and Flag-Rasip1, did not result in the translocation of YFP-ArhGAP29 to the PM, whereas YFP-ArhGAP29 normally localized to the PM when coexpressed with CFP-Rap1AV12, V5-Radil and Flag-Rasip1 K179A (Fig. 4C). We conclude that Radil and not Rasip1 mediates Rap1-induced translocation of ArhGAP29 to the PM.

ArhGAP29 directly interacts with the PDZ domain of Radil

Recently, in a mass spectrometry screen for proteins interacting with the PDZ domain of Radil, ArhGAP29 was identified¹⁰⁰. Indeed, wild type Radil co-precipitated with ArhGAP29, whereas a truncation mutant lacking the PDZ-domain and the neighbouring C-terminal tail (RadilΔPDZ) did not (Fig. 5B).

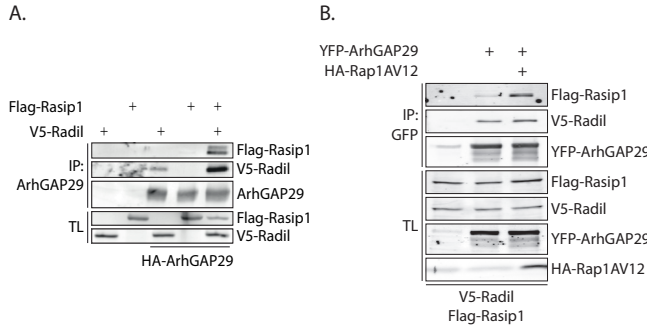


Figure 6: Rasip1 forms a multimeric complex with ArhGAP29 and Radil.

(A) Coimmunoprecipitation of Flag-Rasip1 with YFP-ArhGAP29 in the presence or absence of V5-Radil in 293T cells. (B) Coimmunoprecipitation of Flag-Rasip1 and V5-Radil with YFP-ArhGAP29 in the presence or absence of HA-Rap1AV12 in 293T cells. Experiments were repeated at least four times.

This lack of binding is fully attributed to the missing PDZ-domain, as a truncation mutant lacking only the C-terminus directly after the PDZ-domain (Radil Δ C) normally interacted with ArhGAP29 (Fig. 5B). Furthermore, PM localization of ArhGAP29 in 293T cells by CFP-Rap1AV12 was abrogated when cells were co-transfected with mCherry-tagged Radil Δ PDZ instead of wild type Radil (Fig. 5C). PDZ-domains usually interact with the C-terminal amino acids. ArhGAP29 contains an unconventional PDZ-binding motif (PBM) at its C-terminus, comprising P-Q-F-V. To determine whether this motif was responsible for the interaction with Radil we created a truncation mutant of ArhGAP29 (ArhGAP29 Δ C) lacking the last four amino acids. Whereas Radil readily co-precipitated with ArhGAP29 in 293T cells, far less Radil precipitated with ArhGAP29 Δ C (Fig. 5D). As expected, this truncation mutant exhibited reduced PM localization by Rap1AV12-Radil signaling (fig. 5E). These results indicate that Radil, through its PDZ-domain, directly interacts with the C-terminus of ArhGAP29 and that this interaction is essential for the PM localization of ArhGAP29 by Epac1-Rap1 signaling.

Rasip1 forms a ternary complex with Radil and ArhGAP29

As both Rasip1 and Radil are required for Rap1 induced barrier function (21) and Rasip1 was found to interact with ArhGAP29^{71,101}, we investigated whether the three proteins form a trimeric complex when expressed in 293T cells. Precipitation of ArhGAP29 was capable of simultaneously co-precipitating Radil and Rasip1. Importantly, the precipitation of Rasip1 was most pronounced when Radil was coexpressed (Fig. 6A). Furthermore, Rap1AV12 increased the interaction between Rasip1 and ArhGAP29, whereas the interaction between Radil and ArhGAP29 was unaffected (Fig. 6B). These results strongly suggest that Rasip1 forms a complex with Radil and ArhGAP29 after binding to Rap1 at the PM.

Both Rasip1 and Radil are required for Rap1- induced inhibition of Rho signaling and endothelial barrier function

Previously, we demonstrated that Epac1-induced or Rap1AV12-induced endothelial barrier function is dependent on both Radil and Rasip1⁷¹. The formation of a multimeric complex of Rasip1, Radil and ArhGAP29 by Rap1, suggests that Radil and Rasip1 mediate Rap1AV12-induced endothelial barrier function in a non-redundant manner. Indeed, depletion of either Rasip1 or Radil inhibited Rap1AV12-induced endothelial barrier function (Fig. 7A and B). Furthermore, the reduction of radial stress fibers, a hallmark of Rho signaling, in HUVECs by 007-AM was abrogated by the depletion of either Rasip1 or Radil (Fig. 7C). From these results we conclude that Rasip1 forms a functional complex with Radil and ArhGAP29 to mediate Rap1-induced inhibition of Rho signaling.

DISCUSSION

Previously we have shown that Rap1 induces cell spreading and endothelial barrier function by

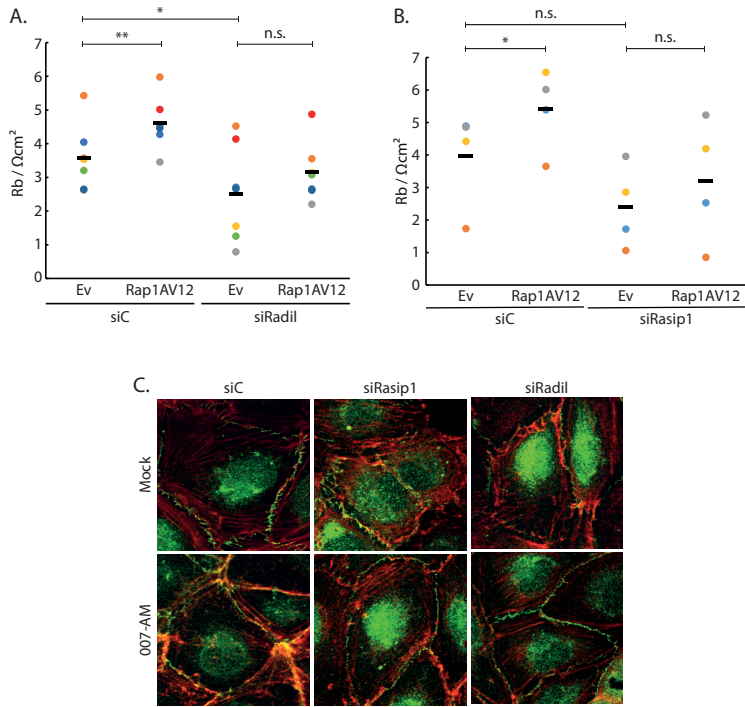


Figure 7: Rasip1 and Radil are required for Rap1-induced endothelial barrier function.

(A) Endothelial barrier (R_b) of control HUVEC monolayers (siC) and HUVEC monolayers depleted of Radil (siRadil), transduced with control lentivirus or Rap1AV12 containing lentivirus. Different colors represent independent experiments ($n=4$). Averages are indicated by the black line. * $P<0.05$, ** $P<0.01$. (For expression levels see supplemental figure 1A) (B) Endothelial barrier (R_b) of control HUVEC monolayers (siC) and HUVEC monolayers depleted of Rasip1 (siRasip1), transduced with control lentivirus or Rap1AV12 containing lentivirus. Different colors represent independent experiments ($n=5$). Averages are indicated by the black line. * $P<0.05$. (For expression levels see supplemental figure 1B) (C) Immunofluorescence of HUVECs transfected with control siRNA (siC), siRNA targeting Rasip1 (siRasip1) or siRNA targeting Radil (siRadil) were grown to confluence and either not stimulated or stimulated with 007-AM 15 min prior to fixation. Cells were stained for VE-cadherin (green) and actin (red).

inhibiting Rho signaling through its effectors Rasip1 and Radil and their binding partner, the RhoGAP ArhGAP29^{71,100,101}. We now show that activation of Rap1 induces the dynamic translocation of all three components, Radil, Rasip1 and ArhGAP29, to the plasma membrane. Importantly, the translocation of ArhGAP29 is dependent on Radil, whereas Rasip1 is dispensable for this. Supporting this, we find Radil to form a stable complex with ArhGAP29 by binding with its PDZ-domain to the C-terminus of ArhGAP29. Although Rasip1 is not necessary for the translocation of ArhGAP29, Rasip1 does form a ternary complex with Radil and ArhGAP29, which is enhanced by active Rap1. From this we conclude that upon Rap1 activation, Rasip1 and a complex of Radil and ArhGAP29 are independently recruited to the plasma membrane to form a multimeric complex. Formation of this complex mediates the modulation of Rho activity, demonstrated by the effects on the actin cytoskeleton, and their subsequent roles in Rap1-induced endothelial barrier potentiation.

How Rasip1 affects the ternary complex is currently unclear. However, since Rasip1 is in a complex with ArhGAP29 it is plausible that Rasip1 affects the activity of ArhGAP29. Indeed, depletion of Rasip1 prevents the reduction of radial stress fibers by Rap1^{71,102}, suggesting that Rasip1 is required for the regulation of Rho signaling. Furthermore, depletion of Rasip1 has been demonstrated to result

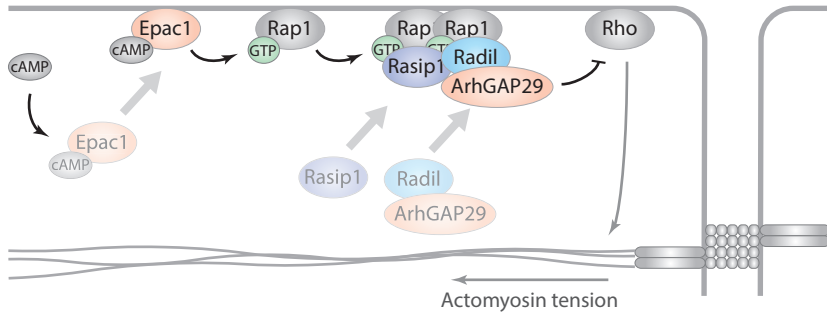


Figure 8: Sequential translocation in Rap1 signaling.

Upon cAMP-binding of Epac1, Epac1 is activated and translocates to the plasma membrane where it binds phosphatidic acid. There Epac1 activates Rap1. Rap1, in turn, recruits both Rasip1 and Radil, which is in complex with ArhGAP29, to form a multimeric complex. Subsequently, Rho activity is reduced to release actomyosin-induced tension, and thus tension exerted on the cell-cell junctions.

in increased Rho-GTP levels in 3D HUVEC cultures ¹⁰¹, although this could not be confirmed in 2D HUVEC cultures ^{71,102}. However, Epac1-Rap1-induced reduction of phospho-MLC2 levels was inhibited by Rasip1 depletion in lung epithelial cells ⁷¹. Although Rasip1 clearly mediates Rap1-induced actin cytoskeletal dynamics, its exact mode of action remains to be elucidated.

Apart from Rasip1 and Radil, the Rap1-effector Krit1/CCM1 has been demonstrated to mediate Rap1-induced endothelial barrier function ¹⁰³. Furthermore, loss of Krit1/CCM1 results in increased MLC2 phosphorylation, which can be rescued by the inhibition of Rho-kinase ^{96,104,105}. However, the molecular mechanism through which Krit1/CCM1 regulates Rho activity is currently unknown, possibly this could be indirect through the regulation of β -catenin ²³⁶.

Spatiotemporal regulation of Rho activity is key to tissue homeostasis. Supporting this, it has been visualized that the spatial activity of Rho is highly dynamic ^{108,254}. In comparison the localization of its GEFs and GAPs are frequently semi-static. Through anchoring proteins, RhoGEFs and -GAPs are linked to cellular structures, such as focal adhesions and tight junctions. The lifetime and location of these structures seem to determine when and where a particular RhoGEF or -GAP is localized. Our finding that Rap1 can dynamically regulate the localization of the RhoGAP ArhGAP29 reveals an additional manner of regulating Rho activity in time and space, in a highly dynamic manner.

Also upstream of Rap1 the RapGEF Epac1 can translocate to the plasma membrane in a highly dynamic manner. Binding of cAMP to Epac1 results in Epac1 activation, as well as its dynamic translocation to the plasma membrane where it can interact with phosphatidic acid ^{217,221}. Together with our current results, this elucidates a signaling pathway, which operates by successive protein translocations to the plasma membrane, spatially restricting Rho activity and subsequent actin cytoskeletal dynamics (Fig. 8). Parallel to this, Rap1 has been demonstrated to activate Cdc42 through the recruitment of the Cdc42GEF FGD5 to cell-cell junctions, resulting in cortical actin bundle formation. However, which Rap1-effector mediates this translocation is still elusive ⁸⁸.

Spatial regulation of actin dynamics seems to be a conserved feature in Rap-biology. In the budding yeast *S. cerevisiae*, the Rap-orthologue Bud1/Rsr1 is involved in bud site determination. Here, landmarks at the bud scar from the previous division recruit the Bud1/Rsr1 GEF, Bud5, to locally activate Bud1/Rsr1. Subsequently, Bud1/Rsr1 recruits Cdc24, a GEF for Cdc42, which then recruits and activates Cdc42, resulting in bud site emergence through the regulation of the actin cytoskeleton, septins and by directing exocytosis. ^{143,144}. Thus, Bud1/Rsr1 translates cortical landmarks into restricted Cdc42 activity, resulting in localized actin dynamics. Also in intestinal cells, apical brush border formation is regulated

by Rap2. Again phosphatidic acid recruits a RapGEF, in this case PDZGEF, resulting in localized Rap2 activation. Through the activation of Rap2, and successive translocation of the kinases TNIK and Mst4, Ezrin is phosphorylated, linking the actin cytoskeleton to the plasma membrane, thereby inducing brush border formation. These findings together create a picture in which Rap-proteins translate spatial cues in local actin cytoskeletal dynamics, mediated through successive protein translocation. Whereas Rap1 achieves this through modulation of Rho GTPases, Rap2 impinges on a kinase module, although Rap2 can also directly bind ArhGAP29, suggested to inhibit its activity. Through this, Rap2 may oppose Rap1-signaling to fine tune actin cytoskeleton modulation. Indeed, Rap1 and Rap2 have opposing effects on endothelial barrier function.

MATERIAL AND METHODS

Reagents and antibodies

007-AM (8-pCPT-2'-O-Me-cAMP-AM) was from Biolog Life Sciences (Bremen, Germany) and used at concentrations of 1 μM ²⁴⁶. Antibodies were from Invitrogen (V5, fluorescently-labeled Phalloidin and secondary antibodies), Santa Cruz Biotechnology (Ras-related protein 1 (Rap1)), Roche (GFP), Chemicon (α -tubulin), ProteinTech (Radil), Abgent (Rasip1), Cell Signalling Technology (phospho-MLC2 T18/S19, MLC2), Novus Biologicals (Rho GTPase-activating protein 29 (ArhGAP29)), BD-bioscience (VE-cadherin, Rap2), Sigma-Aldrich (Flag; M2) and Covance (HA; HA11). All knockdowns were performed using ON-Target Plus siRNA (Dharmacon). siRNA SMARTpools were used for Rap1A, Rap1B, Rap2A, Rap2B, Rap2C, Rasip1, ArhGAP29 and Radil.

DNA constructs

Rasip1, Radil and ArhGAP29 were cloned into the Gateway system (Invitrogen) as described previously⁷¹. Using this system constructs were N-terminally cloned to a Flag-His, V5, CFP or citrine YFP tag using a pcDNA3 vector, or an HA tag using a pMT2 vector or an mCherry or GFP tag using a modified pLV-CMVbc vector. Site-directed mutagenesis was used to create Rasip1 K163A, Radil K79A and a premature stop-codon for ArhGAP29 Δ C (P1258*). Radil Δ PDZ (1-965) and Radil Δ C (1-1058) were cloned into the Gateway system and subsequently N-terminally tagged.

Cell culture and transfections

HEK293T cells were cultured at 37°C and 6% CO₂ in Dulbecco's Modified Eagle Medium supplemented with 10% fetal bovine serum, 2 mM L-glutamine and antibiotics. Human Umbilical Vein Endothelial Cells (HUVECs) (Lonza) were grown at 37°C and 6% CO₂ on tissue culture dishes coated with 0.5% Gelatin in EBM-2 culture medium (Lonza) supplemented with EGM-2 SingleQuots (EGF, hydrocortisone, fetal bovine serum, VEGF, FGF-B, R3-IGF-1, ascorbic acid, GA-100, heparin) (Lonza). HUVECs were cultured maximally 14 days before experiments. siRNA transfections were performed 72 hours before experiments with 40 nM ON-TARGETplus SMARTpools (Dharmacon Inc.) targeting indicated proteins using HiPerfect (Qiagen) or Dharmafect-1 (Dharmacon Inc.), according to manufacturers protocol. HEK293T cells were transfected with expression plasmids 24-48h before performing experiments using X-tremeGENE 9 (Roche) according to the manufacturer's protocol. Overexpression of proteins in HUVECs was established by lentiviral transduction. For lentivirus production, the growth medium of HEK293T cells was replaced by EBM-2 growth medium, upon which these cells were transfected with the appropriate expression vector together with third-generation packaging constructs using X-tremeGENE 9 (Roche). HUVECs were infected 48-72h before experiments using the undiluted growth medium of virus-producing HEK293T cells supplemented with 8 mg/l polybrene. siRNA transfections occurred 16 hours prior to transfection or infection of the expression plasmid.

Cell imaging

For confocal live-imaging, HEK293T cells were seeded overnight in glass-bottom wells (WillCo Wells). For HUVECs glass-bottom wells (WillCo Wells) were coated with Fibronectin prior to seeding. HUVECs were grown to confluence prior to imaging. Cells examined in L-15 Leibovitz medium (Invitrogen) at 37 °C on an inverted Zeiss LSM510 confocal microscope equipped with 63 \times magnification objective lens (N.A. 1.4; Leica). Postacquisition image adjustments for brightness and contrast enhancement were performed using ImageJ software (NIH). Images of HUVECs were taken prior to and 15 minutes after 007-AM stimulation.

Immunofluorescence

HUVECs were plated onto Fibronectin coated glass coverslips either 48 h after transfection and grown to confluency for another 24 h. After 15 min stimulation with 1 μM 007-AM, cells were fixed with 4% formaldehyde for 15 min,

permeabilized with 0.1% TX-100 for 5 min and blocked with 1% BSA for at least 30 minutes. Next, cells were incubated with indicated primary antibodies for 1 h, secondary antibody for 30 min and mounted onto glass slides, which were subsequently examined on an Axioskop 2 mot plus microscope (Zeiss) with a 40× or 100× immersion oil objective and AxioCam camera. Original images were used to create line scans in ImageJ. The graphs show profiles of signal intensities along the line scan. To allow easy visual comparison between channels, signal intensities were normalized to the mean.

Co-immunoprecipitations

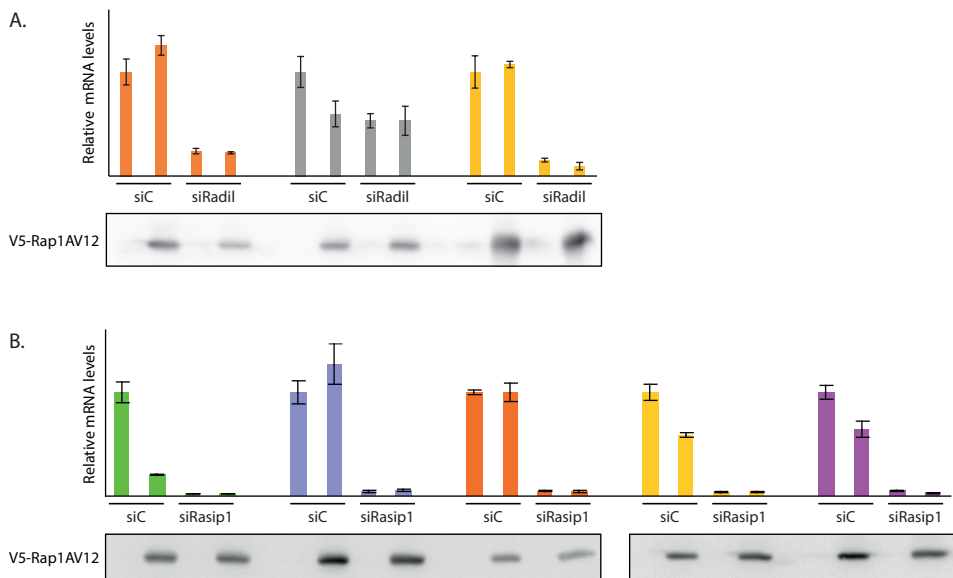
HEK293T cells were transfected using X-tremeGENE 9 (Roche Inc.) and lysed 48h after transfection using a buffer containing 0.5% NP-40, 20 mM Tris, pH 7.5, 150 mM NaCl, 20 mM MgCl₂, 10% glycerol and protease and phosphatase inhibitors. Cell lysates were cleared by centrifugation, and lysates were incubated with protein A-agarose beads (Pharmacia) coupled to the appropriate antibody. After extensive washing with lysis buffer, bound proteins were eluted in Laemmli buffer and analyzed by SDS-PAGE.

Endothelial barrier measurements

Endothelial barrier was assessed by ECIS measurements. 48 hours after siRNA transfection and/or 24 hours after lentiviral infection, HUVECs were plated onto L-cysteine reduced, fibronectin-coated 8W10E electrodes (Applied Biophysics) at a density of 1x10⁵ cells/well and grown to confluency for another 24 hours. The impedance was measured at multiple frequencies within the range of 62.5 Hz to 16000 Hz at 37°C and 6% CO₂ using a 1600R Electrical Cell Impedance Sensing (ECIS) system (Applied Biophysics) both before and after the addition of 007-AM. These frequency scans were used to calculate endothelial barrier (R_b) with ECIS software (v1.2.50.0 PC) from Applied Biophysics. The graphs show multiple independent experiments represented by different colors. P-values were calculated by student's t-test (two-tailed, paired).

Real-time quantitative polymerase chain reaction

8x10⁵ HUVEC cells were plated 48 hours after siRNA transfection onto Fibronectin-coated 6 cm dishes and grown for another 24 hours. Total RNA was isolated using the RNeasy Mini Kit (Qiagen) and transcribed into cDNA using the iScript cDNA Synthesis Kit (BIO-RAD). cDNA levels were quantified by SYBR green real-time PCR on a C1000 Thermal Cycler (BIO-RAD) using the following primers: CTGGACATCACAGGCTCGAA (Radil-forward), TTGGAGACATAGTAGACGCAC (Radil-reverse), TCAGCCAGAAAACCACCTGA (Rasip1-forward), CAGCACCTTCTCTGCACAAA (Rasip1-reverse). Nonspecific signals were excluded based on non-template control samples. Amplification of the HPRT1 gene was used as a control for sample loading. Expression levels were normalized to the siScrambled control. Error bars indicate standard deviation (n=3).



Supplemental figure 1: Knockdown efficiency of experiments 7A and 7B.

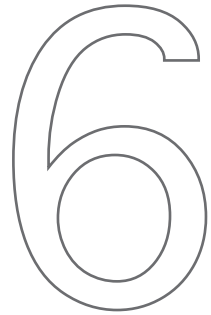
(A) Measurement of the expression levels of Radil and V5-Rap1AV12 in HUVECs treated with control siRNA (siC) or depleted of Radil (siRadil) and transduced with control lentivirus or Rap1AV12 containing lentivirus, used in the experiments depicted in Fig. 7A. Upper panel: RNA expression levels of Radil assessed by real-time PCR. Lower graph: V5-Rap1AV12 protein expression levels as assessed by Western blot. (B) Measurement of the expression levels of Rasip1 and V5-Rap1AV12 in HUVECs treated with control siRNA (siC) or depleted of Rasip1 (siRasip1) and transduced with control lentivirus or Rap1AV12 containing lentivirus, used in the experiments depicted in Fig. 7B. Upper panel: RNA expression levels of Rasip1 assessed by real-time PCR. Lower graph: V5-Rap1AV12 protein expression levels as assessed by Western blot. Expression was correlated to the expression in siC transfected cells. Error bars indicate standard deviation between PCR triplicates. Colors correlate to the individual experiments depicted in Fig. 7A and B.

CHAPTER

RAP1 SIGNALING IN ENDOTHELIAL BARRIER CONTROL

W. J. Pannekoek, A. Post, J. L. Bos

Cell Adh. Migr. 2014; 8(2)



ABSTRACT

The small G-protein Rap1 plays an important role in the regulation of endothelial barrier function, a process controlled largely by cell-cell adhesions and their connection to the actin cytoskeleton. During the various stages of barrier dynamics, different guanine nucleotide exchange factors (GEFs) control Rap1 activity, indicating that Rap1 integrates multiple input signals. Once activated, Rap1 induces numerous signaling cascades, together responsible for the increased endothelial barrier function. Most notably, Rap1 activation results in the inhibition of Rho to decrease radial stress fibers and the activation of Cdc42 to increase junctional actin. This implies that Rap regulates endothelial barrier function by dual control of cytoskeletal tension. The molecular details of the signaling pathways are becoming to be elucidated.

INTRODUCTION

The Rap1 protein, comprising the two highly homologous isoforms Rap1A and Rap1B (95% sequence homology), is a Ras-like small G-protein that was heralded 25 years ago as an inhibitor of Ras-induced cell transformation²⁵. By now it is recognized that Rap1 has one main function: induction of cell adhesion, either to other cells or to extracellular matrix^{164,183,255}. Many other effects reported to occur downstream of Rap1, including inhibition of Ras-induced cell transformation, can likely be attributed to the effect of Rap1 on cell adhesion. Cell adhesion dynamics are of vital importance for many processes, including platelet coagulation, lymphocyte homing, angiogenesis and endothelial barrier function. Genetic interference with Rap1 signaling in diverse model systems has solidly implicated Rap1 in all of these processes²⁵⁶. Multiple regulators and effectors of Rap1 have been identified for single events, raising an important question: why are multiple activators and effectors simultaneously important to relay signaling? We are now starting to understand the conjunctive function of Rap1 regulators and effectors due to novel insights into Rap1 signaling in the regulation of the endothelial barrier function.

The endothelium is a specific layer of cells that forms the inner lining of the entire vascular system. As such, it functions as the main control system to dynamically regulate the passage of fluids, solutes and cells through the vessel wall, a process referred to as endothelial barrier function²⁵⁷. Regulated transport through endothelial cells (transcellular permeability) is of significant importance, although transport through intercellular cell-cell junctions (paracellular permeability) forms the most conventional mode of barrier regulation: the tighter cell-cell adhesion, the less leakage through the monolayer. Two molecular complexes regulate endothelial cell-cell adhesion: Tight Junctions (TJs) and Adherens Junctions (AJs). At TJs, the extracellular domains of transmembrane proteins such as Claudin and Occludin of neighbouring cells interact in a homophilic manner. The cytosolic tails of these proteins interact with the zonula occludens (ZO) adaptor proteins to link to the actin cytoskeleton. The AJ is conceptually similar, although different in protein composition: VE-cadherin transmembrane proteins interact homophilically in the intercellular cleft and intracellularly bind Catenin adaptor proteins to link to the actin cytoskeleton²⁵⁸. As such, TJs and AJs connect the actin cytoskeletons of neighbouring cells, thereby conferring monolayer rigidity, but also allowing dynamic adhesion regulation, as will become evident below.

Rap1 is a small G-protein that cycles between an active, GTP-bound, state and an inactive, GDP-bound, state. Guanine nucleotide exchange factors (GEFs) bind Rap1 and stimulate the dissociation of GDP, thereby allowing abundant GTP to bind, activating Rap1. GTPase activating proteins (GAPs) enhance the intrinsic GTP-hydrolyzing activity of Rap1 to inactivate the G-protein¹. The importance of Rap1 in controlling the endothelial barrier was recognized upon the finding that barrier tightening agents generally act by elevating the levels of cAMP, but do not solely increase barrier function by activating the cAMP-activated kinase PKA. Instead, cAMP-induced barrier tightening can be recapitulated by specifically activating the cAMP-responsive RapGEF Epac1^{31,167,228,231}. Consistently, the barrier function of endothelial monolayers *in vitro* can be decreased by overexpression of RapGAP^{167,231} or depletion of Rap1^{230,259,260}. Specific activation of Epac1-Rap1 protects isolated rat venular microvessels against platelet activating factor (PAF)-induced permeability²⁶¹ and *in vivo* Epac1-Rap1 protects against VEGF-induced dermal leakage¹⁶⁷ and ventilator-induced lung injury²³⁸.

In terms of expression levels, Rap1B is the major Rap1 isoform in endothelial cells²⁶². However, loss of one Rap1A allele in mice severely enhances embryonic pathology of endothelial-specific Rap1B deletion (unpublished data mentioned in²⁵⁶). Furthermore, the barrier function of HUVEC monolayers

is more sensitive to depletion of Rap1A rather than Rap1B^{230,259}. A different subcellular localization of Rap1A and Rap1B may explain this discrepancy. When overexpressed in HUVEC, Rap1A, but not Rap1B, colocalizes with VE-cadherin at cell-cell junctions and coimmunoprecipitates the junctional Rap1 effector AF6²³⁰. The localization of Ras-like G-proteins depends on lipid modifications and charged residues within the C-terminal hypervariable region²⁶³. Both Rap1A and Rap1B are geranylgeranylated, but subtle differences exist in their C-terminal hypervariable regions, which are likely to direct different localizations. Furthermore, differentially localized pools of Rap1 isoforms may exist. As will become evident below, Rap1 controls endothelial barrier function by regulating several downstream pathways. It is conceivable that these pathways are controlled by different localized pools of Rap1, although data to support this theory are lacking at the moment.

ENDOTHELIAL BARRIER IS CONTROLLED BY MULTIPLE RAPGEFS

The endothelial monolayer is subjected to permeability-inducing agents and permeability-decreasing agents and it will dynamically adjust its barrier function based on the relative presence of these stimuli²⁶⁴. Rap1 activity is important during different stages of permeability dynamics (figure 1): (1) Endothelial monolayers maintain a certain baseline, steady-state level of permeability (also referred to as normal permeability)²⁶⁵, which we will hereafter refer to as ‘basal barrier function’. Basal barrier function is decreased in cells depleted of Rap1^{230,259}. (2) Hyperpermeability can be induced by growth factors or agents like VEGF or thrombin upon request of the underlying tissue. Once the need for hyperpermeability declines, barrier is restored to basal, which we will call ‘barrier recovery’. In monolayers depleted of Rap1, barrier recovery is prolonged²⁶⁶. (3) Lastly, high levels of barrier can be achieved by cAMP-inducing agents, which we will refer to as ‘barrier tightening’. Absolute barrier levels upon tightening are decreased when Rap1 is depleted²⁵⁹.

It can be hypothesized that barrier levels during these stages are regulated by the same permeability-promoting and –antagonizing signaling pathways, the relative strengths of which will determine absolute barrier levels²⁶⁵. However, it appears that there is a differential requirement of the RapGEFs C3G, PDZ-GEF and Epac1 during different stages of permeability based on the hierarchical effects they have on barrier regulation (figure 1): C3G is not required for basal barrier function (our unpublished results) but is implicated in barrier recovery after hyperpermeability²⁶⁶. In contrast, depletion of PDZ-

6

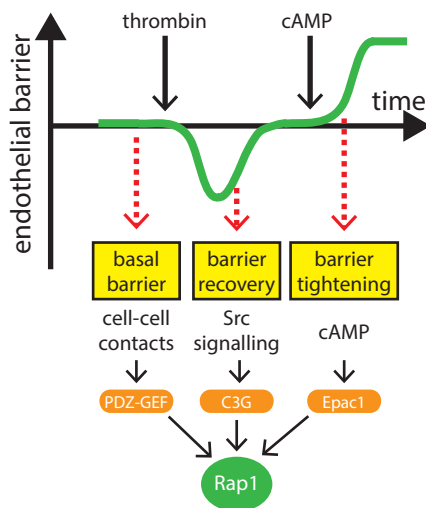


Figure 1: Schematic representation of RapGEF function during different stages of barrier control.

At steady-state, endothelial monolayers confer a certain level of barrier function, termed basal barrier function, during which Rap1 is continuously activated by PDZ-GEFs, possibly downstream of VE-cadherin engagement at cell-cell contacts. After induction of hyperpermeability, for instance by thrombin, barrier function is actively restored to basal levels, termed barrier recovery, during which Rap1 is activated by Src-activated C3G. High levels of barrier function (barrier tightening) are induced by cAMP via activation of the RapGEF Epac1.

GEF does affect basal barrier function²⁵⁹. Activation of Epac1 induces high levels of barrier tightening and desensitizes monolayers to PDZ-GEF depletion²⁵⁹. However, one could imagine that when barrier measurements are performed under conditions with low PDZ-GEF1 activity and abundant growth factors (cAMP present) some Epac1-dependency of basal barrier function could be measured. Indeed, an Epac1-dependent effect on basal barrier function of HUVEC has been reported²³⁹. In vivo, similar differences in PDZ-GEF1-responsiveness and cAMP-induction might exist between different endothelial cells along the vascular tree. Epac1 deletion in mice is claimed to enhance basal permeability in skin, muscle and fat tissue²⁶⁷, although it remains to be determined to what extent this phenotype reflects basal barrier function rather than failure to respond to cAMP-inducing agents. Therefore, it is important to stress that our definition of basal barrier function is a state of intrinsic, Rap1-dependent, barrier regulation when cAMP levels are low.

Basal barrier function: PDZ-GEF

Motivated by the finding that basal barrier function required Rap1 activity but not the cAMP-regulated endothelial RapGEF Epac1, the PDZ-GEFs were identified to control Rap1 activity under basal conditions²⁵⁹. PDZ-GEF1 and PDZ-GEF2 are two RapGEFs that are highly similar in domain architecture and which are both implicated in the regulation of epithelial cell-cell junctions²⁵⁵. In the control of endothelial barrier function, PDZ-GEF1 is the main isoform²⁵⁹. PDZ-GEF1 deletion causes embryonic lethality as a result of defective yolk sac vasculogenesis^{268,269}, which can be attributed to defective cell-cell adhesion²⁷⁰. Given the permeabilizing effects of PDZ-GEF1 depletion or Rap1 depletion under basal conditions, we envision that PDZ-GEF1-Rap1 functions to prevent excessive barrier leakage during steady-state, probably in response to a stimulus that is constitutively present. Importantly, this stimulus is not cAMP. Although PDZ-GEF1 resembles Epac1 in the sense that it bears a cyclic-nucleotide-binding domain, in vitro activation of Rap1 by PDZ-GEF1 cannot be induced by cyclic nucleotides^{271,272}. Alternatively, the presence of cell-cell contacts could confer constitutive PDZ-GEF1 activation. Rap1 is activated at cell-cell contacts upon engagement of VE-cadherin in a manner dependent on MAGI-1, which is a junctional scaffold protein that binds beta-catenin and PDZ-GEF1⁸⁰. It remains unclear whether MAGI-1 binding is sufficient for PDZ-GEF1 activation or whether it is merely required for PDZ-GEF1 activation. In case of the latter, other junctional proteins could be participating. VE-cadherin engagement activates the GTPase Rac1²⁷³, which stabilizes the endothelial barrier through its effector cortactin²⁷⁴. Interestingly, cortactin depleted HUVEC monolayers display decreased basal levels of Rap1 activity. This coincides with increased permeability under basal conditions, but not upon activation of Epac1-Rap1, perfectly mimicking the effect of PDZ-GEF depletion²⁷⁵. Clearly, the molecular details on PDZ-GEF1 activation await further research.

Barrier recovery: C3G

Upon request of the underlying tissue, the endothelial barrier can be decreased to allow passage of solutes or cells. Thrombin and VEGF are examples of such permeabilizing factors. Restoration of basal barrier function after hyperpermeability is not just dependent on these factors diminishing, but can be actively induced²⁶⁶. Thrombin induces activation of the key permeability-inducing protein Rho. Following the Rho-induced permeability increase, Rap1 becomes activated to restore basal barrier function. Indeed, inhibition of Rap1 signaling does prolong the duration of barrier recovery²⁶⁶. Barrier recovery is similarly affected by inhibition of Src signaling. Interestingly, Rap1 activation during barrier recovery coincides with enhanced Src phosphorylation and increased Src-mediated phosphorylation of C3G²⁶⁶, which is known to relieve C3G autoinhibition²⁷⁶. These results were obtained using thrombin to challenge the monolayer, but C3G-mediated activation of Rap1 has also been suggested upon the permeability-inducing proteins VEGF and TIMP-2²⁷⁷⁻²⁷⁹. Technically, the effect of C3G depletion

on barrier recovery remains to be shown, although it is encouraging that C3G is similarly implicated in barrier recovery of epithelial monolayers: Rap1 becomes activated when an epithelial monolayer is challenged to restore the monolayer, which correlates with C3G binding to E-cadherin^{82,280}. Here, dominant negative C3G does prevent AJ reassembly after monolayer challenge²⁸⁰.

Barrier tightening: Epac1

When vascular leakage exceeds the need of the underlying tissues, additional tightening of the endothelial monolayer can be induced by agents like adrenomedullin and prostaglandin E2^{281,282}. These vasoactive agents function by increasing intracellular levels of cAMP. The main cAMP targets are PKA and the Epac proteins, which function in concert to tighten the endothelial barrier^{237,283}. Epac is of particular importance here, as its key function is to activate Rap signaling upon binding of cAMP²⁸⁴⁻²⁸⁶. The generation of an Epac-selective analogue of cAMP (named 007) boosted the identification of processes induced by Epac activation, amongst which is endothelial barrier tightening. Actually, the aforementioned reports that implicated Rap1 to be involved in endothelial barrier function all made use of 007, thereby simultaneously implicating Epac1 in endothelial barrier function. Hence, Epac1-Rap1 induces tightening in cultured monolayers and isolated rat venules and *in vivo* protects against VEGF-induced dermal leakage and ventilator-induced lung injury^{31,167,228,231,238,261}. Epac exists as two isoforms: Epac1 and Epac2, but only Epac1 is expressed in endothelial cells, which is in agreement with barrier tightening being sensitive to Epac1 depletion and the vascular leakage defects observed in Epac1-/- mice^{31,239,267,287}. It should be noted that although Epac1 activates Rap1, not all Epac1 effects can be attributed to the activation of Rap1: whereas depletion of Epac1 completely abolishes the effect of 007 on barrier tightening, depletion of Rap1 only has a partial effect²⁵⁹. This cannot be simply explained by inefficient Rap1 knockdown, as depletion of the downstream pathway Rasip1-Radil-ArhGAP29 (see below) completely prevents barrier tightening induced by an active mutant of Rap1, but simultaneously allows a similar partial increase by 007⁷¹. This cAMP-induced, Rap1-independent barrier tightening effect of Epac1 is mediated by microtubules (MTs)²³⁹. How Epac1 regulates MTs is still elusive. Interestingly, cAMP induces Epac1 translocation independent of its effect on Epac1 auto-inhibition²⁸⁸. As such, Epac1 could function as a cAMP-regulated adaptor protein to recruit binding partners, such as AKAP9. AKAP9 is required for Epac1-induced MT growth. In addition, AKAP9 is required for adhesion of HUVEC on surfaces coated with the Fibronectin peptide RGD, but not on Fc-VE-cadherin-coated surfaces, suggesting Epac1-MT functions to activate integrins²⁸⁹. These activated integrins do not induce barrier tightening by enhancing cell-matrix interactions, as integrin-mediated adhesion to matrix is dispensable for 007-induced barrier tightening²³⁷. Instead, these integrins are suggested to function at cell-cell contacts²⁸⁹. Indeed, 007 induces α v and α 5 integrin relocation to cell-cell contacts, where they are required for 007-induced barrier tightening²⁸⁹.

RAP1 RELEASES CYTOSKELETAL TENSION

Rap1 tightens the endothelial barrier in a manner dependent of AJs^{31,259} and induces adhesion of HUVEC on Fc-VE-cadherin-coated surfaces^{167,290}. Using immunofluorescence, the intensity of VE-cadherin staining at cell-cell contacts seems increased upon Rap1 activation^{167,228,231}, although this is not accompanied by increased VE-cadherin staining using flow cytometry²³⁷, suggesting that Rap1 does not function to increase VE-cadherin transport to the plasma membrane, but rather changes the morphology or dynamics of cell junctions to make VE-cadherin staining appear more intense. This is supported by FRAP analysis on VE-cadherin, which indicate that the lateral mobility of VE-cadherin in cell-cell junctions is impaired by 007⁸⁵. Junction morphology and dynamics are tightly controlled by the actin cytoskeleton²⁹¹. Indeed, Rap1-induced barrier tightening is accompanied by gross changes in the actin cytoskeleton: the amount and intensity of radial stress fibers (RSFs) decrease, whereas

increased amounts of F-actin colocalize with VE-cadherin (referred to as 'junctional actin'). These Rap1-induced actin changes are independent of AJ presence³¹, whereas the Rap1-induced lateral mobility decrease of VE-cadherin in cell-cell junctions and Rap1-mediated barrier tightening are sensitive to actin-depolymerizing agents^{85,239}. Hence, Rap1 regulates the actin cytoskeleton to control endothelial barrier function.

The actin cytoskeleton dynamically regulates the AJ by applying a physical force on the junction²⁹¹. When permeability is induced, RSFs localize in bundles perpendicular to the cell-cell contacts and confer high tension on the junction, causing the AJs to appear discontinuous (also referred to as punctuate, zipper-like or focal AJs)^{91,291}. When cytoskeletal tension declines, AJs will become linear and actin fibers will run parallel to or even colocalize with the cell-cell contact²⁹¹. Cytoskeletal tension is conferred by the sliding of Myosin motors along the actin filaments²⁹². To enable sliding, regulatory Myosin Light Chain 2 (MLC2) needs to be phosphorylated on its T18 and S19 residues, which can be induced by the kinase ROCK²⁹³. ROCK in turn is activated by the Rho proteins. As such, the activity of Rho can be considered the key gatekeeper of cytoskeletal tension.

It has been suggested in a multitude of cellular contexts that Rap1 functions to control Rho-mediated cytoskeletal tension in both positive and negative ways²⁹⁴⁻²⁹⁸. In the endothelium, the situation seems clear-cut: Rap1-depleted monolayers display clear RSFs and discontinuous AJs (indicative of high radial tension), whereas monolayers stimulated with O07 are largely devoid of RSFs, but rather have junctional actin and linear AJs (low radial tension)^{259,283}. This has initiated the search to how Rap1 inhibits Rho signaling. Currently, two different molecular mechanisms have been identified.

Tension reduction by KRIT1

KRIT1 is a FERM-domain containing adaptor protein that was first identified as a Rap1 interacting protein²⁹⁹, and subsequently shown to act downstream of Rap1 in endothelial barrier function²³⁶. The molecular mechanism is largely elucidated: KRIT1 binds to MTs, but when active Rap1 binds the FERM domain, KRIT1 translocates to AJs, where it binds beta-catenin^{236,300,301}. In accordance, a KRIT1 mutant protein with decreased affinity for Rap1 displays increased MT binding and decreased junction localization, the latter being rescued by MT disruption⁹⁶. This same mutant is unable to rescue the decreased endothelial barrier function upon KRIT1 depletion *in vitro* and fails to rescue the dilated heart phenotype found in KRIT1-morphant zebrafish *in vivo*. KRIT1 inhibits Rho activity, which was revealed by mice with heterozygous loss of KRIT1 or the KRIT1 interacting protein CCM2. These mice display increased vascular permeability, which coincides with increased levels of phosphorylated MLC2^{96,104,150}. In both mice, the vascular leakage defect can be completely restored by treatment with fasudil, an inhibitor of the Rho effector ROCK¹⁰⁴. In humans, mutations in KRIT1 and CCM2 are known to cause cerebral cavernous malformations (CCMs), which are vascular malformations in the central nervous system characterized by dilated vessels that are prone to leakage^{302,303}. Although KRIT1+/- mice show increased vascular permeability, these mice lack the typical malformations observed in the human disease. However, these lesions can be induced by simultaneously compromising DNA mismatch repair, suggesting a two-hit model for the human disease³⁰⁴. Importantly, the prevalence of these CCM lesions can be decreased by the fasudil³⁰⁵.

It is unclear how KRIT1 and CCM2 control Rho signaling. KRIT1 deletion was shown to change Rho activity but not Rho protein levels¹⁰⁴. In contrast, depletion of KRIT1 or CCM2 in cultured endothelial cells does not only increase the amount of active Rho, but also increases overall Rho protein levels^{105,150}. KRIT1 depletion causes nuclear translocation of its binding partner beta-catenin to increase beta-catenin-

mediated transcription¹⁴⁸. In addition, KRIT1 itself can also translocate to the nucleus³⁰⁶. Hence, KRIT1 may control endothelial barrier function via either direct control of Rho activity or by transcriptionally controlling Rho proteins or even Rho regulators. Clearly, both of these putative mechanisms need further exploration.

Tension reduction by Rasip1

Rasip1 is a recently characterized effector of Rap1^{71,307}, the expression of which co-clusters with endothelial specific genes³⁰⁸. During development, Rasip1 is essential for blood vessel formation, as shown using Rasip1^{-/-} mice and morpholino's in *Xenopus*^{101,118,307}. In human, a SNP in the Rasip1 locus is associated with retinal venular caliber³⁰⁹, indicating the importance of Rasip1 for endothelial function. Rasip1 binds the RhoGAP ArhGAP29 to regulate Rho and the downstream phosphorylation of MLC2, which likely underlies the defective blood vessel formation in animal models, as impaired lumen formation of Rasip1-depleted or ArhGAP29-depleted HUVEC in matrigel can be rescued by dominant negative RhoA¹⁰¹. Concomitantly, HUVEC monolayers depleted of Rasip1 show discontinuous AJs and increased RSFs, resulting in decreased basal barrier function³⁰⁷. Thus, Rasip1 depletion is sufficient to affect basal barrier function of HUVEC, but this phenotype is enhanced by simultaneous depletion of the Rasip1 homologue Radil⁷¹, which has also been shown to bind ArhGAP29¹⁰⁰. The effects of Radil/Rasip1 depletion on barrier function and RSFs are phenocopied by depletion of ArhGAP29⁷¹ and impairment of basal barrier function by ArhGAP29 depletion is relieved by simultaneous depletion of Rho, suggesting that Rap1 functions by reducing Rho activity through Rasip1 and ArhGAP29⁷¹. In line with this, increased Rho-GTP levels are observed upon depletion of Rasip1 or ArhGAP29¹⁰¹, although others could not find changes in Rho activity upon Rasip1 depletion³⁰⁷ or Rap1 activation⁷¹. Further research on this issue is required.

Rasip1 was originally claimed to be an effector of Ras, although less efficient binding to Rap1 was also observed²⁴⁰. However, its depletion phenotype on HUVEC strikingly resembles Rap1 depletion, suggesting Rasip1 to be regulated by Rap1. Indeed, activation-dependent binding of Rap1 to Rasip1 can be convincingly shown using GST-pull-down or FRET assays^{71,307}. Furthermore, Rap1 signaling is required for junctional localization of Rasip1³⁰⁷. Hence, the Rasip1/Radil-ArhGAP29-Rho module constitutes a signaling cascade by which Rap1 reduces radial tension to increase endothelial barrier function.

6

RAP1 INCREASES JUNCTIONAL TENSION

Activation of Rap1 dissolves RSFs and induces linear junction cables to tighten the barrier. Importantly, this effect is not entirely phenocopied by inhibition of radial tension: tension inhibitors cause RSFs to disappear and junctional actin increase, but this junctional actin is not organized in straight, linear cables, but rather takes a curved, winding appearance (figures 2A and B, middle panels)^{90,259,310}. This winding actin phenotype coincides with decreased endothelial barrier function, as opposed to the increased endothelial barrier function when junctional actin appears straight²⁵⁹. This suggests that while barrier tightening requires radial tension to be released, some tension should be present within the junction for proper barrier function (figure 2A). In this case, the direction of the tension runs along the cell-cell contact rather than perpendicular to it, which is very similar to force generation at the zonula adherens in fully polarized epithelia²⁹¹. We call this 'junctional tension', which was recently shown to be regulated by Rap1: while Rap1 relieves radial tension by inhibiting the Rho/ROCK pathway, resulting in decreased levels of phosphorylated MLC2 on T18 and S19, Rap1 simultaneously activates Cdc42 and its effector MRCK, which induces monophosphorylation of MLC2 on S19 (figure 2B). Whereas phospho-T18-S19-MLC2 appears at RSFs, phospho-S19-MLC2 appears at cell-cell contacts,

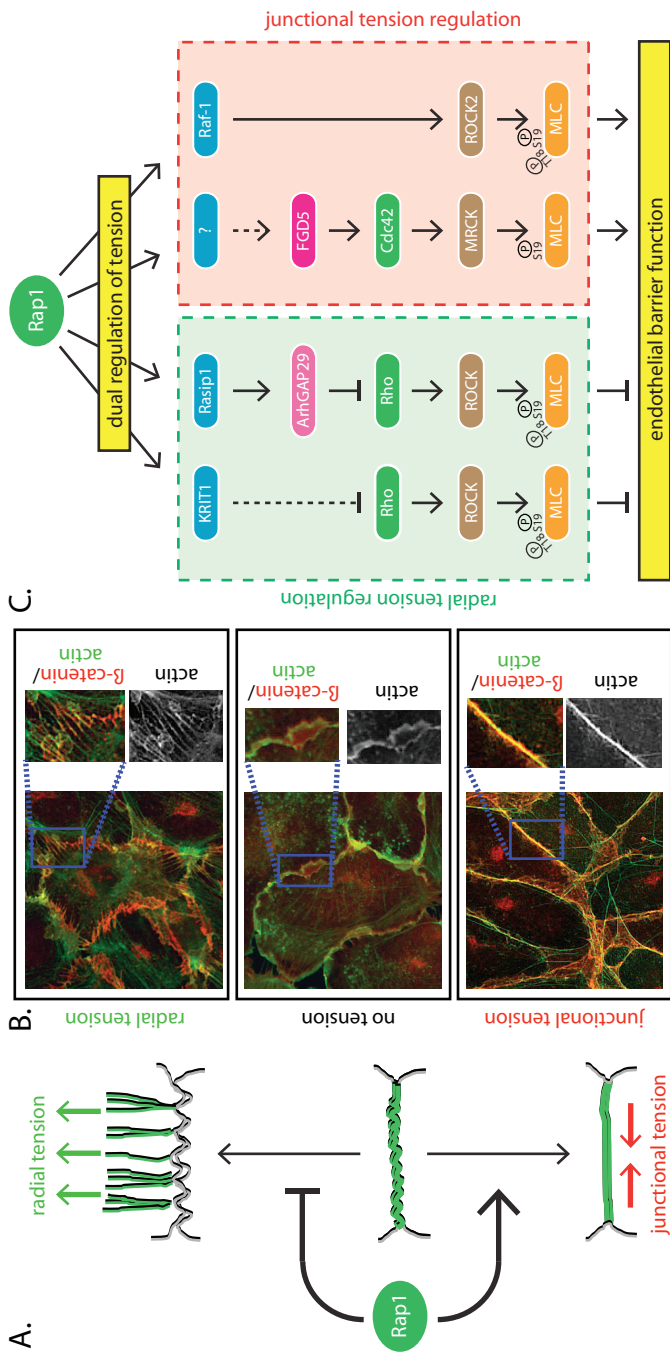


Figure 2: Dual regulation of tension by Rap1. (A) Rap1 regulates endothelial barrier by a twofold regulation of cytoskeletal tension.

First, Rap1 relieves tension on radial stress fibers, thereby decreasing the radial tension on the junction (upper cartoon). Second, Rap1 induces tension in linear actin cables along the cell-cell contact (junctional tension, lower cartoon). The middle cartoon is a normally non-existent, intermediate state (winding actin) when no tension is present, which can be induced by inhibiting Myosin. Cell-cell contacts are shown in grey, actin cables are shown in green. (B) Immunofluorescence pictures showing the different actin morphologies depicted in 2A, which were induced by ArhGAP29 depletion (upper box), blebbistatin treatment (100uM, 30 mins) (middle box) or 007 treatment (1uM, 10 mins) (lower box). Actin is shown in green, whereas the AI marker beta-catenin is shown in red. (C) Molecular mechanisms of tension regulation employed by Rap1 to regulate endothelial barrier function, comprising both regulation of radial tension (left box, green) and regulation of junctional tension (right box, red). See text for details.

suggesting monophosphorylation of MLC2 regulates junctional tension³¹⁰. Hence, Rap1 exerts a dual regulation of tension: radial tension on the AJs is decreased, whereas junctional tension is increased (figure 2A). The latter effect requires Cdc42 and MRCK, although it has to be noted that the induction of phospho-S19-MLC2 at cell-cell contacts by O07 is still partially sensitive to inhibition of Rho and ROCK³¹⁰. Indeed, in immortalized mouse endothelial cells, O07 induces diphosphorylated MLC2 at cell-cell contacts in a manner dependent on Raf-1 and ROCK2³¹¹. Considering the differences in MLC2 phosphorylation status at cell-cell contacts in these reports, further research is required on junctional tension and the underlying signaling mechanisms, but the novel concept of dual tension regulation by Rap1 offers a very intriguing new view on Rap1 function.

ADDITIONAL OR SECONDARY EFFECTS OF RAP1 ACTIVATION

The dual-tension-regulation mechanism that Rap1 exerts on the actin cytoskeleton would be sufficient to explain the effects Rap1 has on the lateral mobility of VE-cadherin and endothelial barrier function (figure 2). However, additional effects and effectors have been suggested. For instance, oxidized phospholipids induce barrier tightening by creating cross-interactions between AJs and TJs in a Rap1-dependent manner³¹². These Rap1-induced AJ-TJ interactions depend on the Rap1 effector AF6, which is also the suggested Rap1 effector in barrier recovery^{266,313}. Intriguingly, AF6 depletion causes sustained levels of phosphorylated MLC2 during barrier recovery²⁶⁶. Hence, AF6 might also fulfill a role in the dual-tension mechanism. Another important role in Rap1-mediated barrier regulation may be fulfilled by Rac. Barrier tightening by prostaglandin E2, prostacyclin and ANP coincides with Rap1-dependent activation of Rac and Rac is also activated upon Epac1 induction with O07^{238,283,314}. Rac activity is of vital importance for endothelial barrier function, as both dominant negative and constitutively active mutants increase HUVEC permeability⁷⁵. Its function in endothelial junctions is multifaceted: cadherin trafficking, stabilization of the cadherin-catenin complex and polymerization of junctional actin are controlled by Rac³¹⁵. Furthermore, dynamic interplay exists between Rac and Rho signaling³¹⁶, suggesting that Rac could add an additional layer of control to the dual tension mechanism. It remains to be determined which of these Rac effects on barrier function occurs under the control of Rap1, and whether this occurs directly or indirectly.

CONCLUDING REMARKS

Rap1 is a master regulator in endothelial barrier function. Multiple activation signals, mediated by various RapGEFs, confer the activation of Rap1, which then activates a variety of signaling cascades to induce endothelial barrier function. Here, we have discussed how these activators and effectors function together. Clearly, several RapGEFs are involved in different aspects of endothelial barrier regulation (figure 1). Here, the molecular mechanisms of Epac1 activation are well understood, but little is known on how and where PDZ-GEF and C3G are activated. Also, additional levels of Rap1 regulation may exist. For instance, RapGAPs may be involved in barrier regulation⁷³, but how they contribute to endothelial barrier function is unclear. A critical event in the regulation of endothelial barrier by Rap1 is the control of cytoskeletal tension. Importantly, Rap1 exerts a dual control on tension: whereas radial tension is decreased by Rap1, tension in the junction is induced (figure 2). The molecular mechanism through which Rap1 differentially regulates tensions is partially elucidated, but many questions remain. For instance, which other Rap1 effectors are required for barrier function and how do these pathways interact with each other? Do different Rap1-effector pools exist in space or in time? And what is the function of Rap2 proteins in endothelial barrier function? They have a Rap1-opposing effect⁷³, the mechanism of which remains to be determined. Is this effect also achieved by modulating tension?

Hyperpermeability of endothelial monolayers results in edema formation during thermal injury, acute lung injury and reperfusion injury. Furthermore, hyperpermeability underlies the microvascular defects in Diabetes Mellitus³¹⁷. Epac1 is a dominant activator of Rap1, which potently increases endothelial barrier function. As such, Epac1-Rap1 offers a very suitable therapeutic target to treat aforementioned pathologies. WS® 1442 is a standardized, safe proven, extract from the Crataegus hawthorn, which in vitro tightens endothelial barrier by activating Epac1-Rap1, and in vivo prevents inflammation-induced hyperpermeability in the mouse cremaster muscle³¹⁸, paving a road to target Epac1-Rap1 in the treatment of hyperpermeability. 007 seems to be the most promising way to achieve this: 007 specifically activates Epac1-Rap1³¹⁹, significantly limiting putative side-effects that would result from general cAMP inducers. Furthermore, 007 induces superactivation of Epac1, meaning that the maximal activity of Epac1 obtainable with saturating concentrations of 007 is much higher than the maximal activity of Epac1 stimulated with cAMP³²⁰. Hence, if you are to treat hyperpermeability, 007 seems the way to go. How to get 007 in your endothelium? The ball is up to the pharmacists!

CHAPTER

7

RESTRICTION OF APICAL BRUSH BORDER
LOCALIZATION BY PTPL1

A. Post, M.Y. Kapteijn, M. J. Vliem, J. L. Boss

ABSTRACT

Microvilli or brush borders at the apical membrane of intestinal cells increase the surface area necessary for efficient nutrient uptake. The small GTPase Rap2A has been demonstrated to induce brush border formation through the activation of the kinases TNIK and Mst4, resulting in the activation of the actin-binding protein Ezrin. Actin cytoskeletal dynamics underlie brush border formation. Although actin dynamics are at the mercenary of the small GTPase Rho, a role for Rho in brush border formation has not been confirmed. Here we propose that there is a positive feedback loop between Rap2A and Rho at the brush border, parallel to the activation of TNIK by Rap2A. For this feedback loop, PTPL1 functions as a scaffold at the apical membrane, by interacting with both Rap2A and Rho up- and downstream effectors. We suggest that PTPL1 restricts the localization of these effectors, and thus of this feedback loop, at the plasma membrane, thereby restricting where brush borders are formed.

INTRODUCTION

Cellular polarization is a fundamental process during both embryogenesis and adult tissue homeostasis. Whereas apico-basal polarization of epithelial cells is frequently described to succeed cell-cell contact formation, polarization of intestinal epithelial cells can occur even in the absence of cell-cell or cell-extracellular matrix adhesions. Through the actions of the serine/threonine kinase LKB1, and its cofactors Strada and Mo25, apico-basal polarity is established in single cells³²¹⁻³²³. Subsequently, microvilli, or brush borders, form at the apical membrane to increase the surface area^{322,324}, which in the intestine is necessary to allow fast nutrient uptake.

The phosphoinositide PI(4,5)P2 is enriched at the apical membrane and creates a docking site for several proteins necessary for proper homeostasis of the apical patch^{325,326}. In intestinal cells, PLD1 is localized to the apical membrane by binding PI(4,5)P2 where it locally generates phosphatidic acid (PA)³²⁷. In turn, PA recruits the RapGEF, PDZ-GEF, resulting in local Rap2A activation. Activation of Rap2A plays a critical role in brush border establishment. Through its effector TNIK, Rap2A recruits and activates Mst4, resulting in Ezrin phosphorylation³²⁷. Phosphorylation of Ezrin induces its open, active conformation. Once open, Ezrin can bind PI(4,5)P2 through its FERM-domain and actin through its actin binding domain (ABD), thereby linking the plasma membrane (PM) to the actin cytoskeleton, a critical step in brush border formation¹⁹⁸. Importantly, Rap2A does not interfere with cellular polarity³²⁷.

Also localized to the apical membrane is the tyrosine phosphatase PTPL1³²⁸. Similar to Ezrin, PTPL1 contains a FERM-domain that can interact with PI(4,5)P2, which is targets it to the apical membrane³²⁹. Besides a FERM-domain, PTPL1 contains five PDZ-domains and a C-terminal tyrosine phosphatase domain³²⁸. Intriguingly, the second PDZ-domain on PTPL1 interacts with the C-terminus of PDZ-GEF³³⁰, possibly linking PTPL1 to brush border formation. Furthermore, the fourth PDZ-domain of PTPL1 interacts with the C-terminus of the RhoGAP ArhGAP29²⁴¹. Interestingly, ArhGAP29 is a Rap2-effector whose RhoGAP activity is proposed to be inhibited by Rap2³³¹.

Although the actin cytoskeleton underlies brush border formation, a clear role for Rho in this process has not been established. Possibly, PTPL1 functions as a scaffold for a signaling module at the apical membrane of intestinal cells, through which active Rap2A can increase Rho activity, to reinforce brush border formation.

An intriguing feature of brush border formation in intestinal cells devoid of cell-cell contacts is that their brush borders are still restricted to a small area of the cell surface. This implies that the brush border-inducing signals are restricted to one part of the plasma membrane. We suggest that through its binding to PI(4,5)P2 and its interaction with both Rap2A and Rho up- and downstream effectors, PTPL1 restrict brush border formation to the apical membrane.

RESULTS

PTPL1 restricts brush border localization

Doxycyclin stimulation of Ls174T-W4 intestinal epithelial cells induces the expression of Flag-Strada, which results in the cytosolic localization and activation of LKB1. Activation of LKB1 subsequently induces polarization and brush border formation in an adhesion-independent manner³²². To investigate a possible link between PTPL1 and brush border formation we first visualized the localization of PTPL1 in these intestinal cells. For this Ls174T-W4 cells were transfected with mCherry-tagged PTPL1, fixed and stained with phalloidin to visualize the F-actin cytoskeleton. In unstimulated cells PTPL1 uniformly localized to the plasma membrane (PM) (Fig. 1a). In doxycycline-treated cells, PTPL1 was enriched at the brush border (Fig. 1a). Introduction of point mutations in the FERM-domain of PTPL1 (PTPL1 KN1-2), rendering it incapable of binding PI(4,5)P2³²⁹, abolished its PM localization both in unstimulated, as well as doxycyclin-treated cells (fig. 1b). Intriguingly, PTPL1 KN1-2 expression resulted in a marker

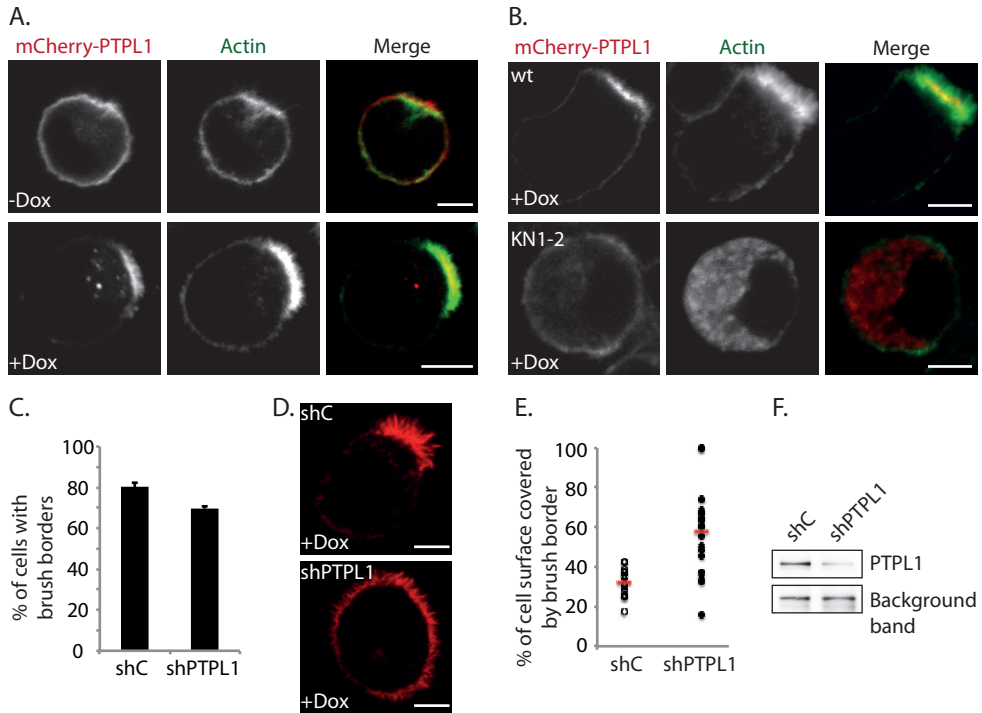


Figure 1: PTPL1 restricts brush border localization.

(A) Visualization of mCherry-PTPL1 localization in Ls174T-W4 cells with or without doxycyclin stimulation. Cells were fixed and the actin cytoskeleton was stained with phalloidin. (B) Visualization of the brush border with phalloidin in wild type mCherry-PTPL1 or mCherry-PTPL1 KN1-2 expressing Ls174T-W4 cells stimulated with doxycyclin. (C) Quantification of the number of cells with brush borders upon doxycyclin stimulation of Ls174T-W4 cells infected with control shRNA (shC) or shRNA targeting PTPL1 (shPTPL1). (D) Immunofluorescent image of the brush borders of Ls174T-W4 cells upon doxycyclin stimulation of Ls174T-W4 cells infected with control shRNA (shC) or shRNA targeting PTPL1 (shPTPL1). (E) Quantification of the cell surface area covered with brush border upon doxycyclin stimulation of Ls174T-W4 cells infected with control, scrambled shRNA (shC) or shRNA targeting PTPL1 (shPTPL1). (F) Western blot showing PTPL1 expression levels in Ls174T-W4 cells infected with either control shRNA (shC) or shRNA targeting PTPL1 (shPTPL1). Scale bar, 10 μ m.

reduction of brush border formation (Fig. 1b). This suggests that PM localization of PTPL1 may be essential for brush border formation. To confirm this, we depleted PTPL1 from Ls174T-W4 cells using shRNA. Surprisingly, depletion of PTPL1 did not reduce the number of cells forming brush borders (Fig. 1c). In contrast, PTPL1 depletion resulted in an enlarged portion of the surface area to be covered by brush border (Fig. 1d and e).

These findings may point toward a scaffolding function for PTPL1 in brush border formation. By interacting with proteins involved in brush border formation, expression of PTPL1 KN1-2 may sequester them to a cytoplasmic pool, preventing their PM localization. In contrast, the results from the PTPL1 knock down experiments suggest that its interaction partners still localize to the PM in the absence of PTPL1, where they induce brush border formation, however that they are no longer restricted to the apical patch.

PTPL1 directly binds PDZ-GEF and anchors it to the plasma membrane

PTPL1 contains five consecutive PDZ-domains, of which the second one has been crystallized in

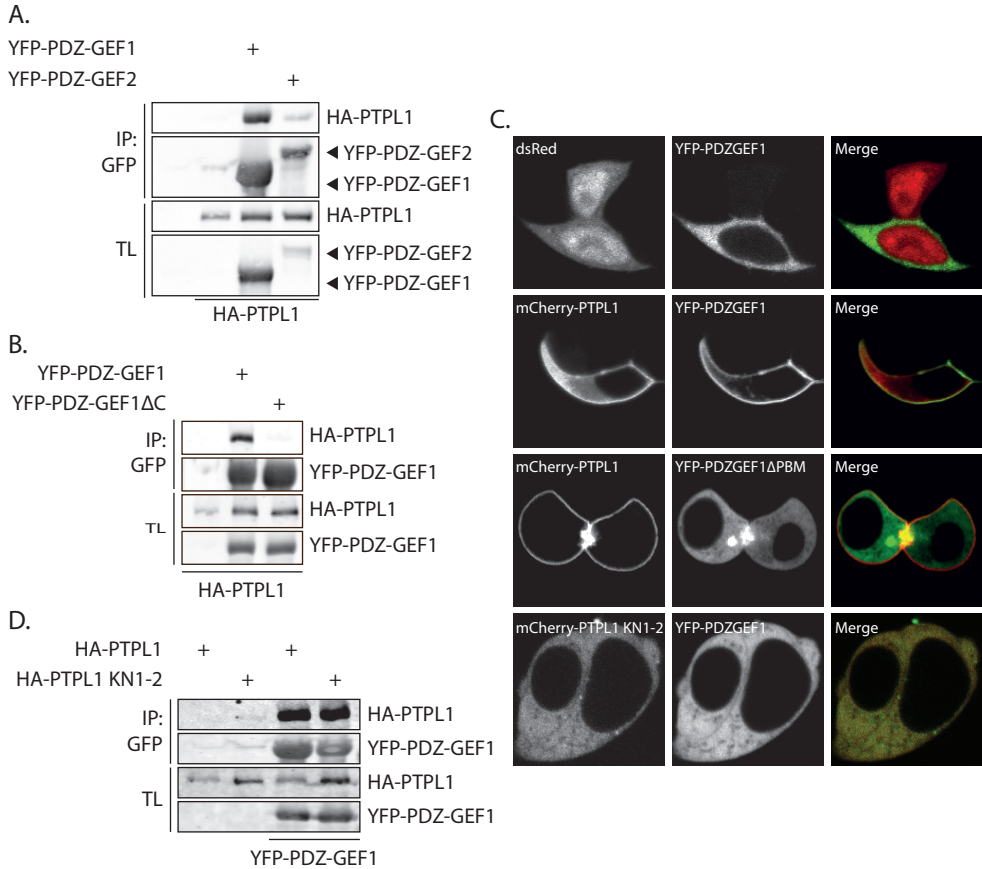


Figure 2: PTPL1 directly binds PDZ-GEF and anchors it to the plasma membrane.

(A) Co-immunoprecipitation of HA-PTPL1 with YFP-PDZGEF1 or YFP-PDZGEF2 expressed in HEK293T cells. (B) Co-immunoprecipitation of HA-PTPL1 with YFP-PDZGEF1 or YFP-PDZGEF1ΔC expressed in HEK293T cells. (C) Live imaging of HEK293T cells expressing mCherry-PTPL1 wt or mCherry-PTPL1 KN1-2, together with YFP-PDZGEF1 or YFP-PDZGEF1ΔC. (D) Co-immunoprecipitation of HA-PTPL1 or HA-PTPL1 KN1-2 with YFP-PDZGEF1 expressed in HEK293T cells.

complex with the 15 most C-terminal amino acids of PDZ-GEF2³³⁰. PDZ-GEF2 together with PDZ-GEF1 is essential for brush border formation³²⁷. Since PDZ-GEF1 and PDZ-GEF2 display high sequence similarity, with an identical C-terminal sequence, we first investigated whether PTPL1 could interact with both full length PDZ-GEF1 and PDZ-GEF2. Precipitation of YFP-PDZ-GEF1 or YFP-PDZ-GEF2 from HEK293T cells readily coprecipitated HA-PTPL1 (Fig. 2a). Since PTPL1 interacts with both PDZ-GEF1 and PDZ-GEF2, and the GEFs function redundantly in brush border formation³²⁷, we used PDZ-GEF1 for further functional analysis.

PDZ-GEF1 contains a PDZ-binding motif at its C-terminus, consisting V-S-A-V. Introduction of a premature stop codon at the C-terminus of PDZ-GEF1 (PDZ-GEF1ΔC), resulting in a truncation mutant lacking the last four amino acids, completely abolished the interaction with HA-PTPL1, confirming the interaction of PTPL1 with the C-terminus of PDZ-GEF1 (Fig. 2b). Next we investigated whether PTPL1 affected the localization of PDZ-GEF1. YFP-PDZ-GEF1 was localized to the cytoplasm in HEK293T cells. Cotransfection with mCherry-PTPL1 readily localized YFP-PDZ-GEF1 to the PM (Fig. 2c). In contrast, cotransfection with mCherr-PTPL1 KN1-2 resulted in cytoplasmic localization of YFP-PDZ-GEF1 (fig. 2c),

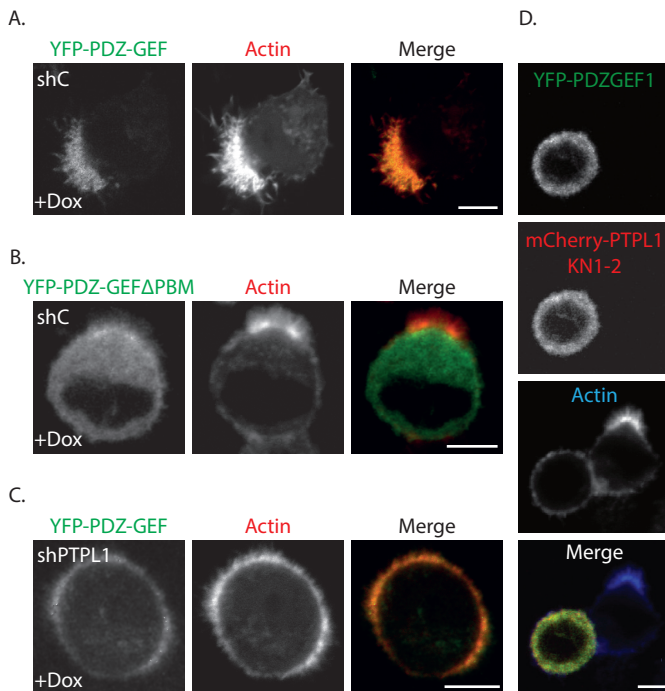


Figure 3: Regulation of PDZ-GEF1 localization at the BB by PTPL1.

(A) Visualization of YFP-PDZGEF1 localization in Ls174T-W4 cells infected with control shRNA (shC) upon doxycyclin stimulation. Cells were fixed and the actin cytoskeleton was stained with phalloidin. (B) Visualization of YFP-PDZGEF1ΔC localization in Ls174T-W4 cells infected with control shRNA (shC) upon doxycyclin stimulation. Cells were fixed and the actin cytoskeleton was stained with phalloidin. (C) Visualization of YFP-PDZGEF1 localization in Ls174T-W4 cells infected with shRNA targeting PTPL1 (shPTPL1) upon doxycyclin stimulation. Cells were fixed and the actin cytoskeleton was stained with phalloidin. (D) Visualization of YFP-PDZGEF1 localization in Ls174T-W4 cells coexpressing mCherry-PTPL1 KN1-2. Scale bar, 10µm.

even though this PTPL1 mutant was still capable of interacting with PDZ-GEF1 (Fig. 2d).

Thus, PTPL1 interacts with the C-terminus of PDZ-GEF1 and PDZ-GEF2, and through this interaction PDZ-GEF is localized to the plasma membrane.

Regulation of PDZ-GEF localization at the BB by PTPL1

Previously, we determined that PDZ-GEF localizes to the brush border by interacting with phosphatidylic acid, which is enriched at the apical membrane³²⁷, however our current findings suggest that PTPL1 could also be involved in localizing PDZ-GEF at the brush border. As we reported previously, stimulation of Ls174T-W4 cells with doxycycline induces the brush border localization of PDZ-GEF⁽³²⁷⁾, (Fig. 3a). Surprisingly, mutant YFP-PDZ-GEF1 lacking its C-terminus was still capable of localizing to the brush border, although to a lesser extent (Fig. 3b), suggesting that PDZ-GEF1 can localize to the brush border in a PTPL1-independent manner, most likely through its interaction with PA. Next we investigated the localization of YFP-PDZ-GEF1 in PTPL1-depleted Ls174T-W4 cells. Intriguingly, whereas YFP-PDZ-GEF1 was still capable of localizing to the brush border in the absence of PTPL1, it was localized to a much larger area of the PM (Fig. 3c), correlating to the extended brush border in these cells. In contrast, whereas full length PTPL1 and PDZ-GEF1 colocalized at the brush border in Ls174T-W4 cells, PDZ-GEF1 was completely cytoplasmic in PTPL1 KN1-2 expressing cells (Fig. 3d), possibly explaining why these cells do not form brush borders.

In conclusion, whereas PTPL1 interacts with PDZ-GEF1 at the brush border, this interaction is not essential for the localization of PDZ-GEF1 to the brush border. However, loss of PTPL1 results in PDZ-GEF1 localizing to a broader PM area, correlating to an extended brush border.

PTPL1 anchors ArhGAP29 at the BB

Whereas the second PDZ-domain of PTPL1 interacts with PDZ-GEF1, which activates Rap2A at the

brush border, the fourth PDZ-domain of PTPL1 interacts with the RhoGAP ArhGAP29²⁴¹, a downstream effector of Rap2A³³¹. This prompted us to investigate the role of ArhGAP29 in brush border formation. First we investigated the localization of ArhGAP29 in Ls174T-W4 cells. Interestingly, whereas YFP-ArhGAP29 localized to the brush border in cells expressing low amounts of YFP-ArhGAP29, moderate or high expression of YFP-ArhGAP29 resulted in a mostly cytoplasmic localization (Fig. 4a). Surprisingly, moderate or high amounts of ArhGAP29 completely blocked brush border formation (Fig. 4a), suggesting that inhibition of Rho is detrimental to brush border formation.

To investigate the role of PTPL1 in the brush border localization of ArhGAP29 we first confirmed the interaction between the two proteins. As expected, precipitation of YFP-ArhGAP29 from HEK293T cells readily coprecipitated HA-PTPL1 (Fig. 4b). Furthermore, a truncation mutant of ArhGAP29 lacking the last four amino acids (ArhGAP29 Δ C), a PDZ-binding motif, was incapable of interacting with PTPL1 (Fig. 4c). YFP-ArhGAP29 was cytoplasmic in HEK293T cells. As was found for PDZ-GEF1, YFP-ArhGAP29 localized to the PM in HEK293T cells cotransfected with wild type PTPL1, whereas cotransfection with PTPL1 KN1-2 kept ArhGAP29 in the cytoplasm (Fig. 4d). Again, PTPL1 KN1-2 was still capable of interacting with ArhGAP29 (Fig. 4e).

Moderate to high expression of the ArhGAP29 truncation mutant, lacking its last four amino acids, in Ls174T-W4 cells, still inhibited brush border formation (Fig. 4f). Lower expression levels of this ArhGAP29 mutant, however, revealed that it could still partially localize to the brush border, although a significant amount was also cytoplasmically localized (Fig.4f). This could either be due to incomplete knock down of PTPL1 or, as suggested for PDZ-GEF1, through a PTPL1-independent anchoring mechanism. ArhGAP29 contains an N-terminal BAR-domain, capable of interacting with phospholipids (Fig. 4g). This could possibly be responsible for its PTPL1-independent localization at the brush border. Alternatively, ArhGAP29 may be recruited to active Rap2A at the brush borders. Active Rap2A has been demonstrated to interact with the N-terminal region of ArhGAP29, where the BAR-domain is located³³¹. BAR-domains in some other proteins have been demonstrated to not only be able to interact with phospholipids, but also with active small GTPases³³²⁻³³⁵. To determine whether Rap2A interacts specifically with the BAR-domain of ArhGAP29 we cloned various regions of ArhGAP29 and expressed these in HEK293T cells, together with Rap2AV12 and Rap1AV12 as a control. Indeed, only Rap2AV12 and not Rap1AV12 interacted with ArhGAP29 (Fig. 4h). Moreover, Rap2AV12 interacted with full length ArhGAP29 as well as with the BAR-domain only. Expression of a C-terminal construct lacking the BAR-domain was incapable of interacting with Rap2AV12, suggesting that active Rap2A interacts directly with the BAR-domain of ArhGAP29.

In summary, whereas PTPL1 is capable of interacting with the C-terminus of ArhGAP29 and localizes it to the PM, this interaction is not essential for brush border localization of ArhGAP29 in Ls174T-W4 cells. Importantly, substantial expression of ArhGAP29 abrogates brush border formation, suggesting that Rho activity is essential for brush border formation. Interestingly, it has been suggested that Rap2A inhibits the activity of ArhGAP29³³¹. Through this, activation of Rap2A at the brush border may result in increased Rho activity there.

Cyclical activation of Rho is necessary for BB formation

Although the actin cytoskeleton is fundamental to brush border formation, and Rho has a well-known role in actin dynamics, a role for Rho in brush border formation has not been established. As overexpression of ArhGAP29 inhibits brush border formation, this implies that Rho may be involved in brush border formation. To investigate this we depleted Ls174T-W4 cells of all three Rho isoforms simultaneously (RhoA, RhoB and RhoC). Indeed, depletion of Rho greatly reduced the number of cells forming brush borders (Fig. 5a). Since overexpression of ArhGAP29 also abrogates brush border formation, we investigated whether depletion of ArhGAP29 would enhance brush border formation.

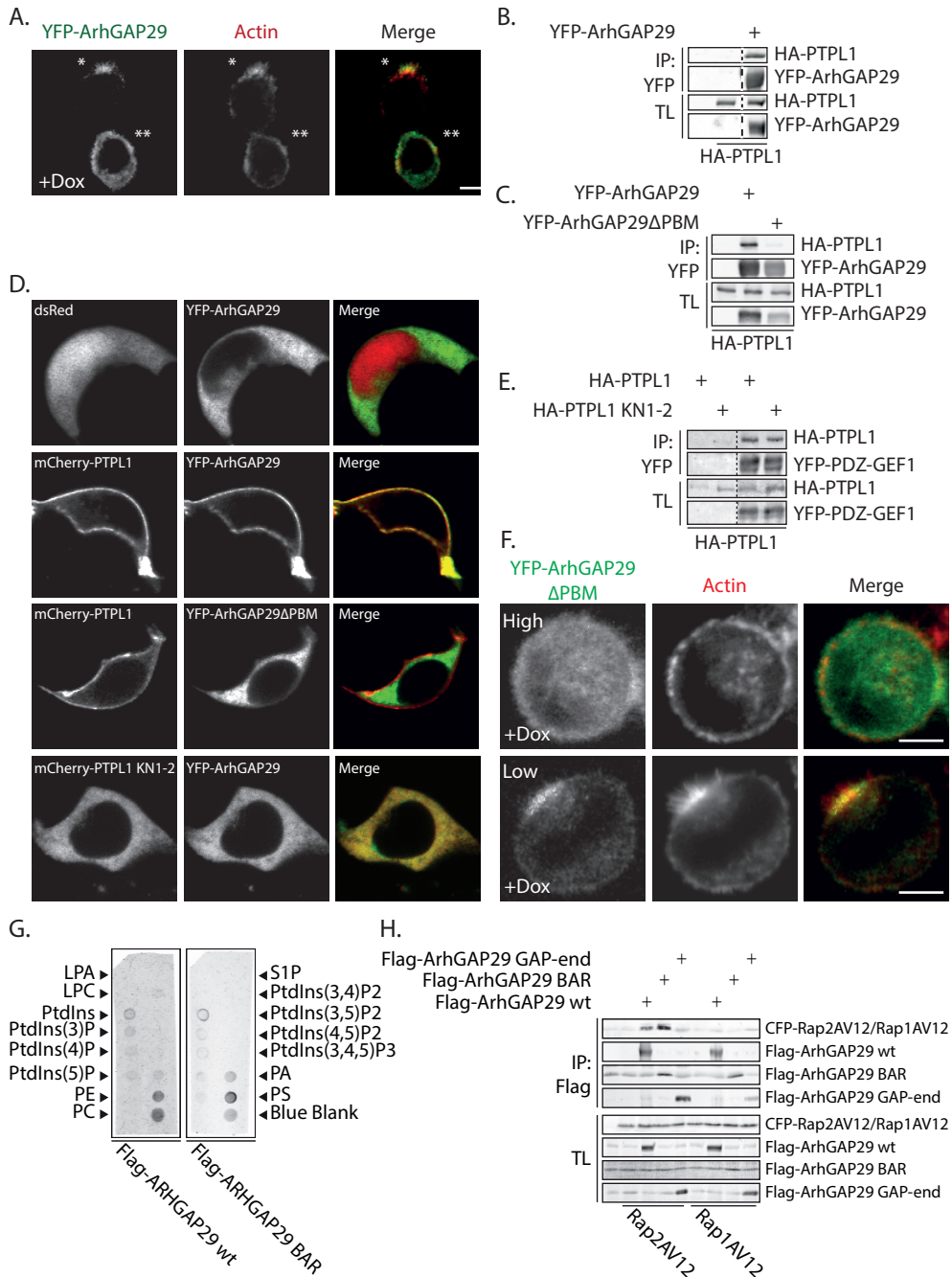


Figure 4: PTPL1 directly binds ArhGAP29 and anchors localizes it to the brush border.

(A) Visualization of YFP-ArhGAP29 localization in Ls174T-W4 cells upon doxycyclin stimulation. Cells were fixed and the actin cytoskeleton was stained with phalloidin. * = low YFP-ArhGAP29 expression, ** = high YFP-ArhGAP29 expression. (B) Co-immunoprecipitation of HA-PTPL1 with YFP-ArhGAP29 expressed in HEK293T cells. (C) Co-immunoprecipitation of HA-PTPL1 with YFP-ArhGAP29 or YFP-ArhGAP29ΔC expressed in HEK293T cells. (D) Live

Surprisingly, depletion of ArhGAP29 abrogated brush border formation (Fig. 5b). These findings possibly reflect that cyclical activation of Rho is necessary for brush border formation. To investigate this we expressed either constitutively active or inactive RhoA (RhoAQ63 or RhoAN19, respectively) in Ls174T-W4 cells. Indeed, both mutants inhibited brush border formation (Fig. 5c), suggesting that Rho must cycle between its active and inactive conformation to induce brush border formation.

Several effectors of Rho have been discovered. One of them, PKN2, interacts with the third PDZ-domain of PTPL1, making it a likely effector through which Rho regulates brush border formation. Indeed, depletion of PKN2 greatly inhibited brush border formation of Ls174T-W4 cells (Fig. 5d), suggesting that Rho regulates brush border formation through PKN2. Interestingly, it has been demonstrated that whereas the C-terminal amino acids of PKN2, which interact of PTPL1, are dispensable for its activation by RhoA *in vitro*, they are essential for its full activation by RhoA *in vivo* ³³⁶.

DISCUSSION

Here we identify PTPL1 as a scaffold, integrating both Rap2A and Rho up- and downstream signaling, thereby coupling the two GTPases in brush border formation. By binding PDZ-GEF, ArhGAP29 and PKN2 we propose that PTPL1 functions as a platform for a positive feedback loop, reinforcing brush border formation, which we discuss below. We propose that PTPL1 not only integrates these signals, but also restricts them to the brush border.

How the loss of PTPL1 results in an extended brush formation is currently unclear. It is plausible that PTPL1 restricts the localization of PDZ-GEF, ArhGAP29 and PKN2 to the apical membrane. Loss of PTPL1 may allow these proteins to diffuse over the membrane, resulting in extended brush border formation. Indeed, PDZ-GEF, ArhGAP29 and PKN2 all contain lipid-binding domains, possibly allowing them to interact with the plasma membrane in the absence of PTPL1. Alternatively, PTPL1 itself may inhibit brush border formation. Loss of PTPL1, and thus loss of the inhibitory signal on brush border formation, will result in an extended brush border. Future research will be needed to confirm these models, however our current findings, combined with previous reports, support the prior model.

Establishment of apico-basal polarity, involving the asymmetrical distribution of plasma membrane components, can be induced in single cells by the serine/threonine kinase LKB1 ³²². The subsequent asymmetric distribution of phosphatidyl inositides has been identified as a spatial cue for polarity in a variety of cell types, necessary for both the induction as well as the maintenance of polarity ^{325,326}. The phosphatidyl inositide PI(4,5)P2 is enriched at the apical membrane, creating a docking site for various proteins ³²⁵, including PTPL1. Through its FERM-domain, which interacts with PI(4,5)P2 ³²⁹, PTPL1 is localized to the brush border. Here it interacts with PDZ-GEF, previously demonstrated to be responsible for the activation of Rap2A at the apical membrane, resulting in brush border formation ³²⁷. Surprisingly, we found that PTPL1 is not essential for targeting PDZ-GEF to the apical membrane, indicating that there are other docking sites for PDZ-GEF at the apical membrane, most likely phosphatidic acid (PA) ³²⁷. Previously, we have demonstrated that PLD1 is recruited to the apical membrane ³²⁷, which is achieved through its interaction with PI(4,5)P2. There, PLD1 increases the local PA production. Whereas the binding of PI(4,5)P2 may induce PLD1 activation ^{337,338}, others have

imaging of HEK293T cells expressing wild type mCherry-PTPL1 or mCherry-PTPL1 KN1-2, together with YFP-ArhGAP29 or YFP-ArhGAP29ΔC. (E) Co-immunoprecipitation of HA-PTPL1 or HA-PTPL1 KN1-2 with YFP-ArhGAP29 expressed in HEK293T cells. (F) Visualization of YFP-ArhGAP29ΔC localization in Ls174T-W4 cells upon doxycyclin stimulation. Cells were fixed and the actin cytoskeleton was stained with phalloidin. (G) Protein-lipid overlay assay with Flag-ArhGAP29 or the BAR-domain only of ArhGAP29 (Flag-ArhGAP29 BAR) purified from HEK293T cells. (H) Co-immunoprecipitation of CFP-Rap2AV12 or CFP-Rap1AV12 with wild type ArhGAP29 (Flag-ArhGAP29 wt), the BAR-domain of ArhGAP29 (Flag-ArhGAP29 BAR) or the C-terminal half of ArhGAP29 lacking the BAR domain (Flag-ArhGAP29 GAP-end) expressed in HEK293T cells.

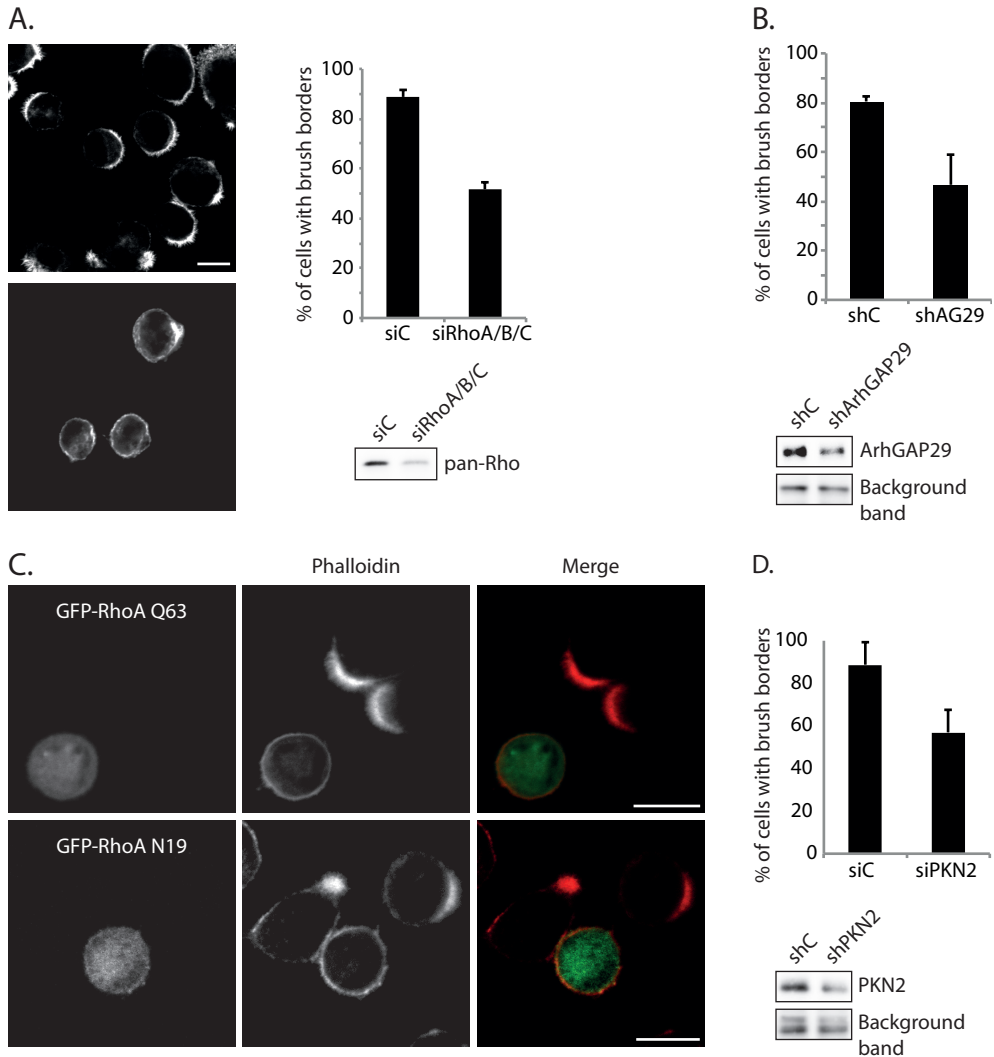


Figure 5: Cyclical activation of Rho is necessary for BB formation.

(A) Left panel: Immunofluorescent image of the brush borders in Ls174T-W4 cells upon doxycyclin stimulation, transfected with control siRNA (siC) or siRNA targeting RhoA, RhoB and RhoC (siRhoA/B/C). Right panel: Quantification of the number of cells with brush borders upon doxycyclin stimulation of Ls174T-W4 cells transfected with control siRNA (siC) or siRNA targeting RhoA (siRhoA), RhoB (siRhoB), RhoC (siRhoC) or all three simultaneously (siRhoA/B/C). (B) Quantification of the number of cells with brush borders upon doxycyclin stimulation of Ls174T-W4 cells transfected with control siRNA (siC) or siRNA targeting ArhGAP29 (siArhGAP29). (C) Visualization of the brush border with phalloidin in GFP-RhoA Q63 or GFP-RhoA N19 expressing Ls174T-W4 cells stimulated with doxycyclin. (D) Quantification of the number of cells with brush borders upon doxycyclin stimulation of Ls174T-W4 cells transfected with control siRNA (siC) or siRNA targeting PKN2 (siPKN2). Scale bar, 20 μ m.

demonstrated that direct interaction of PLD1 with PKN family proteins enhances its activity³³⁹. This points towards a feed forward signaling loop, for which PTPL1 functions as a scaffold at the apical membrane. Localization of PTPL1 at the apical membrane may restrict PKN2 localization at the apical membrane. In turn, activation of PLD1 by PKN2 would result in increased local PA production. Binding of PDZ-GEF to this pool of PA induces the activation of Rap2A, which, through TNIK, Mst4 and Ezrin

induces brush border formation³²⁷. Simultaneously, binding of ArhGAP29 by active Rap2A inhibits its RhoGAP activity³³¹, which may result in increased Rho activity. Rho in turn may further activate PKN2, thereby reinforcing this signaling cascade (For this working model see figure 2 of chapter 8). However, further research confirming this feed forward mechanism is necessary.

Whereas overexpression of ArhGAP29 inhibits brush border formation, suggesting that its activity must be restricted, depletion of ArhGAP29 also inhibits brush border formation. This suggests that cyclical activation of Rho is essential for brush border formation. Indeed, both constitutively active and inactive RhoA mutants abrogate brush border formation. Interestingly, further down the signaling cascade, local cycling of the phosphorylation status of Ezrin has been demonstrated to be essential for Ezrin to localize to and support microvilli³⁴⁰. How Ezrin is dephosphorylated in this process is unclear, however cyclical regulation of the signaling cascade inducing the phosphorylation may be one aspect of the process.

In conclusion, we find that PTPL1 may function as a platform for the crosstalk between Rap2A and Rho. As such it restricts the localization of brush border formation, in a currently unknown manner. Whether, besides its scaffolding capacity, the tyrosine phosphatase activity of PTPL1 plays a role in this process has not been addressed. Currently, most reports on PTPL1 have either focused on its tyrosine phosphatase activity or its scaffolding capacity, and it would be intriguing to find a process in which both are involved.

MATERIAL AND METHODS

Reagents and antibodies

Antibodies were from Invitrogen (fluorescently-labeled Phalloidin), Roche (GFP), Chemicon (α -tubulin), Sigma-Aldrich (Flag; M2), Novus Biologicals (Rho GTPase-activating protein 29 (ArhGAP29)), BD biosciences (Rho and PKN2), Santa Cruz Biotechnology (PTPL1; H-300) and Covance (HA; HA11). All knockdowns were performed using ON-Target Plus siRNA (Dharmacon). siRNA SMARTpools were used for RhoA, RhoB, RhoC and PKN2. shRNA pools of the TRC1 library (Sigma-Aldrich) were used for PTPL1 and ArhGAP29. Doxycycline ($1 \mu\text{g ml}^{-1}$) was from Sigma-Aldrich.

DNA constructs

PTPL1 was cloned into the Gateway system (Invitrogen) from cDNA, which was a kind gift from Prof. J. H. Lee (Stanford, USA). Subsequently it was N-terminally cloned to an mCherry tag in a modified pLV-CMVbc vector or an HA tag in a pMT2 vector. Using site-directed mutations, PTPL1 KN 1-2 was generated (K645, 646, 647N (KN1) and K824, 825, 830, 831, 832N (KN2)). Rap1AV12 and Rap2A were previously described in²⁴⁷ and³²⁷. YFP-ArhGAP29, YFP-PDZGEF1 and YFP-PDZGEF2 were previously described in⁷¹ and³²⁷, respectively. Site-directed mutagenesis was used to create YFP-ArhGAP29 Δ C (P1258*) and YFP-PDZGEF1 (V1496*). ArhGAP29 BAR (190-473) and ArhGAP29 GAP-end (662-1261) were cloned into the Gateway system (Invitrogen) and were N-terminally tagged with a Flag-His tag in a pcDNA3 vector. GFP-RhoAQ63L was a gift from J. de Rooij (Hubrecht Institute, the Netherlands). GFP-RhoAN19 was a kind gift P. L. Hordijk.

Cell culture, transfections and lentiviral transductions

Ls174T-W4 cells were grown in RPMI medium supplemented with 10% fetal bovine serum and antibiotics. HEK293T cells were grown in DMEM medium supplemented with 10% fetal bovine serum and antibiotics. Cells were transfected with expression plasmids using X-tremeGENE 9 (Roche), according to the manufacturers' protocols. For lentiviral knockdown experiments in Ls174T-W4 cells, the cells were infected with lentiviral shRNAs pools from the TRC1 library (produced in HEK293T cells) and subsequently selected with puromycin. Two days after the infection, cells were seeded overnight in the absence or presence of doxycycline. siRNA transfections were performed 72 hours before experiments with 40 nM ON-TARGETplus SMARTpools siRNAs (Dharmacon Inc.) targeting indicated proteins using HiPerfect (Qiagen).

Confocal imaging

Ls174T-W4 cells were seeded overnight in the absence or presence of doxycycline. Cells were fixed with 3.8% formaldehyde, permeabilized using 0.1% Triton X-100 and incubated with the indicated primary and Alexa-

conjugated phalloidin (Invitrogen) to visualize brush borders. For live cell imaging of 293T cells were seeded overnight in WillCo wells (WillCo Wells BV) and imaged in L-15 Leibovitz medium (Invitrogen) under temperature-controlled conditions. All microscopic analyses were performed on an inverted Zeiss LSM510 confocal microscope equipped with 63× magnification objective lens (N.A. 1.4; Leica). Images were processed using ImageJ software (NIH) and Adobe Photoshop.

Co-immunoprecipitations

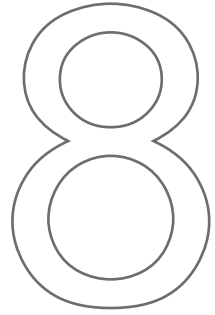
HEK293T cells were cultured in 6-cm dishes and lysed 48h after transfection. Lysates were made using a buffer containing 0,5% NP-40, 20 mM Tris, pH 7.5, 150 mM NaCl, 20 mM MgCl₂, 10% glycerol and protease and phosphatase inhibitors. Cell lysates were cleared by centrifugation, and lysates were incubated with protein A-agarose beads (Pharmacia) coupled to the appropriate antibody. After extensive washing with lysis buffer, bound proteins were eluted in Laemmli buffer and analyzed by SDS-PAGE.

Protein-lipid overlay assays

Flag-ArhGAP29 and Flag-ArhGAP29 BAR-domain, expressed in HEK293T cells, were immunoprecipitated from cell lysates using a monoclonal Flag M2 antibody as described for the co-immunoprecipitation assay, and eluted with 200 μg ml⁻¹ 3×Flag-peptide (Sigma) according to the manufacturer's protocol. Nitrocellulose membranes spotted with 100pmol of different lipids (Echelon Biosciences) were blocked for 1 h in blocking buffer (3% fatty-acid-free BSA, 50 mM Tris-HCl (pH 7.5), 150 mM NaCl and 0.1% Tween 20) and then incubated with the eluted proteins for 1h in blocking buffer. Bound protein was detected with either the Flag M2 antibody.

CHAPTER

SUMMARY & DISCUSSION



SUMMARY

Small GTPases of the Rap family are involved in a plethora of actin cytoskeleton-linked biological processes. The small GTPase Rap1 does so by regulating the Rho small GTPase family, the master regulators of actin cytoskeletal dynamics (discussed in chapter 1). In this thesis we have investigated how active Rap1 regulates actin cytoskeleton driven processes, by modulating Rho. Most importantly, we have identified the RhoGAP ArhGAP29 as a downstream effector of Rap1 signaling. Through ArhGAP29 Rap1 regulates Rho signaling and thus actin cytoskeletal dynamics.

In **chapter 2** we developed an siRNA screen to identify downstream effectors of Rap1 involved in Rap1-induced cell spreading and adhesion. Through this screening method we identified Ezrin as a downstream effector of Rap1. Ezrin belongs to the ERM family of proteins, which comprises Ezrin, Radixin and Moesin. Although all three proteins show high sequence similarity, Ezrin mediated Rap1-induced cell spreading in a non-redundant manner. Previously, we identified that ERM proteins function as anchors for the RapGEF Epac1. In **chapter 2** we demonstrate that Ezrin also functions downstream of Rap1 in cell spreading. Cell spreading depends on both cell-extracellular matrix adhesion as well as plasma membrane protrusion, induced by the actin cytoskeleton. Rap1 induces both processes. We found that Ezrin is only involved in the latter, demonstrating that the two processes can be uncoupled. Apart from Ezrin, we identified the Rap1-effector Radil to be necessary for Rap1-induced cell spreading. This was the only RA-domain containing protein tested, mediating Rap1-induced cell spreading in this screen.

In **chapter 3** we investigated the link between Ezrin and Radil in Rap1-induced cell spreading. Here we found that Radil is in complex with Ezrin. We found that Ezrin in its active conformation can recruit Radil to the plasma membrane. This occurs in an Epac1-Rap1-dependent manner. Once at the plasma membrane, Radil co-clusters with active Ezrin at the plasma membrane. Thus Ezrin integrates Rap1 up- and downstream signaling by recruiting both Epac1 and Radil.

Using cell spreading as a read-out, in **chapter 4**, we identified Rasip1, a family member of Radil, as a novel Rap1-effector. Moreover, we identified that the Rasip1 and Radil interactor ArhGAP29 functions downstream of Rap1, mediating Rap1-regulation of Rho signaling and actin cytoskeletal dynamics. Whereas Rasip1, Radil and ArhGAP29 mediate Rap1-induced cell spreading, they are not involved in Rap1-induced cell adhesion. Moreover, we found that the regulation of Rho signaling through this pathway was essential for Rap1-induced endothelial barrier potentiation. Through this pathway Rap1 reduced radial stress fiber content, known to induce endothelial barrier permeability.

In **chapter 5** we explored how Rap1 regulated Rasip1, Radil and ArhGAP29. We found that upon Rap1 activation, all three proteins translocate to the plasma membrane in a highly dynamic manner. ArhGAP29 does so by forming a stable complex with Radil, which binds to active Rap1 at the plasma membrane through its RA-domain. Rasip1 is recruited by Rap1 independent of Radil and ArhGAP29. However, activation of Rap1 does induce the formation of a ternary complex, incorporating Rasip1, Radil and ArhGAP29. This led us to conclude that once all three proteins are located at the plasma membrane, they form a functional complex. Indeed, all members are essential for Rap1-induced endothelial barrier potentiation.

In **chapter 6** we have discussed a Rap1-regulated dual tension mode. Whereas the inhibition of Rho through ArhGAP29 reduced radial stress fibers, Rap1 simultaneously activates Cdc42 to potentiate endothelial barrier function. Cdc42 results in the formation of a junctional actin ring. This junctional actin is also subjected to tension. However, in contrast to Rho-regulated radial stress fibers, which exert tension perpendicular to the junction, the tension of junctional actin is orientated parallel to the junction. This tension is thought to be necessary for endothelial barrier function.

Finally, in **chapter 7** we identified a Rap1-Radil-Rasip1-independent regulation system of ArhGAP29. Here, PTPL1 functions as a scaffold, integrating both Rap and Rho up- and downstream signaling

components, which we find to be important for brush border formation in intestinal epithelial cells. Through direct interaction, PTPL1 localizes PDZGEF and ArhGAP29 to the plasma membrane. At the brush border PDZGEF activates Rap2A. Active Rap2A directly binds ArhGAP29, which has been proposed to inhibit its activity. Furthermore, ArhGAP29 also interacts with the Rho-effector PKN2, which we also demonstrate to be necessary for brush border formation. Thus PTPL1 integrates Rap2 and Rho signaling at the brush border. By binding PIP2, which is enriched at the apical membrane, PTPL1 restricts the localization and thus signaling of PDZGEF, ArhGAP29 and PKN2, thereby restricting the localization of the brush border. Therefore, loss of PTPL1 results in an extended brush border. From the results presented in this thesis and previous reports, we have created a picture in which Rap1 translates cortical spatial cues into localized regulation of Rho signaling through ArhGAP29, resulting in actin cytoskeletal modulation. Recognition of these spatial cues happens through Epac1, recognizing phosphatidic acid, in the case of the dynamic spatial regulation reported in **chapter 5**, ERM proteins, recognizing PIP2, in the case of cell spreading reported in **chapter 3**, and PTPL1, also recognizing PIP2 in the case of brush border formation presented in **chapter 7**. We will discuss our findings in the next section, and discuss how the different spatial anchors for this Rap-Rho axis may be implicated in endothelial barrier control.

DISCUSSION

Rap1 was originally identified as a K-Ras revertant, capable of suppressing the oncogenic capacity of mutant Ras²⁵. Whereas this feature of Rap1 was first thought to be achieved through the sequestration of Ras-effectors by Rap1³⁴¹, this view had to be adjusted by the discovery that Rap1-signaling induced cell adhesion. Rather, it was through the increased cell adhesion that Rap1 could prevent the transforming capacity of oncogenic K-Ras in tissue culture. Further research demonstrated that activation of Rap1 resulted in both increased integrin-mediated cell-ECM adhesion⁴⁻⁶, as well as cadherin-mediated cell-cell adhesion^{31,81,211,228,232}. Activation of Rap1 has been demonstrated to result in increased integrin activity and avidity, thus it is thought that Rap1 can directly affect the conformational status of integrins⁵⁻⁷. For cadherin-based cell-cell contact it is thought that Rap1 can increase the amount of cadherin at the junction through both targeting it to the plasma membrane, as well as preventing its endocytosis once it is at the plasma membrane^{84,252}. From research over the past decade, including that described in this thesis, we might have to change our view on Rap1-signaling once again. Although we do not want to exclude the above described processes being regulated by Rap1, we here demonstrated that various of the known biological effects of Rap1 can be ascribed to it modulating the actin cytoskeleton through controlling Rho activity, including endothelial barrier control, cell spreading and brush border formation.

Cell spreading as a read out for Rap1-induced actin dynamics

In chapter 2 we have developed a screening method for identifying signaling cascades regulated downstream of Rap1. This led to the discovery of Ezrin as a mediator of Rap1-induced cell spreading. Furthermore, we identified that the Rap1-effector Radil mediated Rap1-induced cell spreading. We later demonstrated that Radil links Rap1 to Rho regulation (Chapters 4 and 5). Moreover, Ezrin is known to link the actin cytoskeleton to the plasma membrane, emphasizing the importance of actin cytoskeletal dynamics during Rap1-induced cell spreading. Interestingly, both Ezrin and Radil depletion did not affect Rap1-induced cell adhesion, but specifically abrogated Rap1-induced cell spreading, demonstrating that these two processes can be uncoupled. Although inhibition of integrin-mediated adhesion does prevent cell spreading on extracellular matrices⁴⁹, Rap1 can induce cell spreading in an integrin-independent manner when plated on poly-L-lysine coated surfaces⁶⁵, to which cells adhere through electrostatic interactions. Thus, Rap1 can induce cell spreading in the absence of integrin-mediated adhesion, however spread surfaces do require physical linkage to a matrix to sustain the spread area.

How Rap1 induces cell adhesion is still unclear, but the Rap1-effectors RapL⁵² and Riam^{50,51} have been implicated in this. Whether Rho GTPases also play a role in Rap1-induced cell adhesion is currently unknown, but intriguingly, only those integrin complexes linked to the actin cytoskeleton are subjective to Rap1-modulation^{3,4,6,7,342,343}. Linkage of integrin-based cell-ECM adhesion to the actin cytoskeleton stabilizes the newly forming adhesions. Possibly, Rap1 increases cell adhesion by increasing the stabilization of new adhesions through modulation of the actin cytoskeleton they are linked to, rather than increasing the activity of integrins themselves.

Making use of cell spreading as a read-out, we identified that the Radil family member Rasip1, is a Rap1-effector (Chapter 4). Rasip1 mediates cell spreading in a similar manner as Radil and Ezrin do, e.g. depletion of Rasip1 reduces Rap1-induced cell spreading without affecting cell-ECM adhesion. We demonstrated in chapter 4 that this is achieved through reduction of Rho activity, mediated by the RhoGAP ArhGAP29. Indeed, depletion of ArhGAP29 also prevents Rap1-induced cell spreading without affecting cell-ECM adhesion. Regulation of Rho and subsequent modulation of the actin cytoskeleton through this signaling cascade accounts for the potentiation of the endothelial barrier function, described in the next section.

Rap1 controls endothelial barrier function through modulation of Rho activity and the actin cytoskeleton

Drastic changes to the actin cytoskeleton occur upon Rap1-activation in endothelial monolayers. Radial stress fibers, thought to exert tension on the cell junctions and increase endothelial permeability, disappear, whereas junctional actin increases, thought to stabilize cell-cell junctions^{31,228}. Through these changes in the actin cytoskeleton, Rap1 is capable of increasing the endothelial barrier function. As reviewed in chapter 6, Rap1 is thought to achieve this through inhibiting Rho, while activating Rac1 and Cdc42. Supporting a model in which Rap1 tips the balance of Rho GTPase signaling toward Rac1 and Cdc42, endothelial barrier potentiating factors, usually decrease Rho activity, while increasing Rac1 and Cdc42 activity. In contrast, endothelial permeabilizing factors affect Rho GTPases in the opposite manner^{95,99,344-347}.

Two types of actin structures are linked to VE-cadherin at cell-cell junctions. Radial stress fibers are orientated perpendicular to the junction and are thought to exert tension on the cell-cell junction, resulting in increased endothelial permeability. These radial stress fibers are controlled by Rho, and activation of Rap1 results in their disappearance⁷¹. Secondly, a junctional actin ring oriented parallel to the junction, is regarded to potentiate the endothelial barrier function. Rap1 induces the formation of this actin ring through activation of Cdc42⁸⁸. Although Rap1 has been proposed to increase VE-cadherin levels at the junction, this is not supported by flow cytometry experiments²³⁷. Rather, Rap1 reduces the lateral mobility of VE-cadherin, which is proposed to be due to its linkage to the junctional actin ring^{85,88}.

The adherens junctional component nectin, as well as the tight junctional components occludin, claudin and JAM (Junctional Adhesion Molecule), are also linked to actin cytoskeleton. Apart from cadherin-based cell-cell adhesion, Rap1 has been reported to be involved in both nectin-based cell-cell junction as well as in tight junctions. However, the latter has been generally ascribed to be mediated through the effects of Rap1 on cadherin-based junctions. By regulating Rho GTPase activity, and thus modulating the actin cytoskeleton, Rap1 may indeed be capable of regulating all these junctional components. However, rather than regulating the junctional proteins themselves, Rap1 regulates the actin cytoskeleton that they are linked to.

The Rap1-effector KRIT1 has been implicated in mediating the inhibition of RhoA by Rap1 in endothelial monolayers^{103,104}, however the molecular mechanism for this is still elusive. Furthermore, under the circumstance used in chapters 4 and 5, KRIT1 does not mediate Rap1-induced endothelial barrier potentiation²²⁹. We have resolved that Rap1 instead regulates Rho activity by spatially regulating the RhoGAP ArhGAP29, resulting in increased endothelial barrier function. This is mediated through the Rap1-effectors Radil and Rasip1. Through this signaling cascade, Rap1 regulates Rho activity, resulting in reduced phospho-MLC2 levels and subsequent radial stress fibers, as described in chapter 4⁷¹.

As described in chapter 5, whereas Radil and ArhGAP29 form a stable complex, the interaction of Rasip1 with this complex is regulated by Rap1, which is necessary for its functionality. The architecture of this complex is still unknown, however possibly the interaction between Rasip1 and ArhGAP29 is mediated through Radil. Indeed, we find that the interaction between Rasip1 and ArhGAP29 is increased in the presence of Radil. Rasip1 is phosphorylated upon stimulation of endothelial cells with 007³⁴⁸. Moreover, Radil contains a putative FHA-domain, which are classified as phosphoprotein binding domains, creating a possible interaction interface between the two proteins. Supporting this, we found an interaction between Rasip1 and Radil in the absence of ArhGAP29 (A. Post and J.L. Bos, unpublished results). Alternatively, Rasip1 may directly interact with ArhGAP29. Supporting this, we found that very high expression of Rasip1 in 293T cells could recruit ArhGAP29 to the plasma membrane, although this was not consistent. Possibly the interaction between Rasip1 and ArhGAP29 is too weak for Rasip1 to target ArhGAP29 to the plasma membrane.

Spatial regulation of the Rap1-Rho signaling axis

1. Spatially restricting Rho signaling in a dynamic manner

In chapter 5 we have demonstrated that upon elevated Rap1 activity, be it through activation of Epac1 or overexpression of an active Rap1 mutant (Rap1AV12), Radil, Rasip1 and ArhGAP29 translocate to the plasma membrane. The translocation of ArhGAP29 depends on the presence of Radil, whereas Rasip1 is dispensable for this.

Previously, we have demonstrated that Rap1 regulates endothelial barrier function under both basal conditions, as well as potentiates endothelial barrier function when necessary. PDZ-GEF regulates the activity of Rap1 under basal conditions, keeping it at a steady state, whereas endothelial barrier potentiating agents, through production of cAMP, induce Epac1 activity resulting in increased Rap1 activity²²⁹. Intriguingly, the effect of depletion of ArhGAP29 on endothelial barrier function closely resembles that of Rap1, affecting both basal and enhanced barrier function. In contrast, the effects of Radil and Rasip1 depletion on basal barrier function are less severe, especially that of Radil (chapter 4,⁷¹). One explanation may be that Radil is only necessary to increase the amount of ArhGAP29 at the plasma membrane when barrier tightening is required. This would imply that there is a pool of ArhGAP29 linked to the plasma membrane in a Radil-independent manner and that Rap1 regulates this pool of ArhGAP29 independent of Radil, possibly through Rasip1. Upon increased activation of Rap1, recruitment of ArhGAP29 through Radil would then increase the pool of ArhGAP29 at the plasma membrane.

Especially in endothelial barrier control, fast responses to vasoactive agents are necessary to quickly adjust its permeability to the need of underlying tissues. The dynamic translocation of Epac1 and ArhGAP29 may allow the cell to quickly increase barrier integrity in response to such extracellular stimuli, which for ArhGAP29 is mediated by Radil. In contrast the functionality of ArhGAP29 is regulated by Rasip1, Rasip1 should be capable of interacting with ArhGAP29 independent of Radil. In this light, in contrast to that suggested in the previous section, the increased interaction of Rasip1 and ArhGAP29 in the presence of Radil may be explained by the two only interacting with each other at the plasma membrane. Increased expression of Radil will increase the amount of ArhGAP29 at the plasma membrane capable of interacting with Rasip1.

Radil seems to be mainly cytoplasmic in 293T cells. Upon activation of Rap1 by Epac1 signaling, stimulated by the Epac1-specific cAMP analogue 8-CPT-2'OMe-cAMP-AM (007-AM), Radil uniformly translocates to the plasma membrane (Chapter 5). This correlates to the distribution of Epac1 over the plasma membrane upon binding of 007-AM²²¹. Also in HUVECs we found that upon activation of Rap1 Radil translocates to the plasma membrane. This translocation coincides with an increase in the endothelial barrier function, since depletion of Radil abolishes Rap1-induced endothelial barrier function. Uniform localization of Radil, and thereby ArhGAP29, at the plasma membrane may be sufficient for modulating endothelial barrier function. After all, Rho is also anchored to the plasma membrane. However, intriguingly, we find in a subset of cells that at discontinuous junctions, thought endure tension, Radil displays a punctate phenotype, which colocalizes VE-cadherin (chapter 5; Fig. 6b). This points toward an interaction between Radil and the junctional complex. How this interaction is mediated is currently unclear, however there could potentially be a role for ADIP. ADIP has previously been demonstrated to interact with junctional α -actinin and with Afadin, a family member of Radil. More specifically, ADIP interacts with the Dilute-domain of Afadin, which is also present in Radil. Indeed, we have found Radil to interact with ADIP (A. Post, J.L. Bos, unpublished data). Thus, possibly ADIP directly links Radil to the junctional complex through α -actinin. Whether this interaction is essential for endothelial barrier potentiation remains to be investigated.

2. ERM proteins create focal points where they integrate Rap1 up- and downstream signaling

Previously, we have reported that activation of Epac1 by 007-AM and subsequent Rap1-activation can inhibit HGF-induced cell scattering in a 2D system¹⁶⁹. However, increased Rap1 activity has also been reported to increase cell migration, rather than inhibit it³³⁻³⁶. Cell migration relies on the induction of cell protrusion in a polarized manner. Based on the uniform redistribution of Epac1 to the plasma membrane upon activation with 007-AM, Rap1 is most likely activated all over the membrane. Indeed, upon Epac1-Rap1 signaling, Radil is also uniformly distributed over the plasma membrane (chapter 3). Subsequently, cell protrusion is induced in a non-polarized manner, thus in all directions, resulting in cell spreading. Likely it is this simultaneous induction of cell protrusions in opposing directions that inhibits HGF-induced cell scattering. This emphasizes the importance of spatial regulation of Rap1 signaling. This can be achieved through the localization of its GEFs and GAPs, determining where Rap1 is activated. In addition, this can be enhanced by spatial regulation of its downstream effectors. There may be a role for ERM proteins in this by clustering both Epac1 and Radil to microdomains at the plasma membrane (chapter 3). Therefore, localized activation of ERM proteins may determine the net outcome on cell migration. Indeed, ERM proteins have been found to localize at the protruding edge of migration cells^{349,350}. Whether ERM proteins not only cluster Epac1 and Radil at the plasma membrane, but also directly link the two by simultaneously binding them remains to be determined. RhoA signaling has a prominent role in ERM activation. Both direct phosphorylation of the actin-binding domain (ABD) through the Rho-effector Rock^{185,187,324}, as well as increased PI(4,5)P₂ production, via activation of PIP5K²²⁴, results in the open conformation of ERM proteins. This results in the recruitment of Epac1 and, subsequently, Radil. The translocation of Radil to the plasma membrane upon activation of Epac1 007-AM, a selective agonist for Epac1²⁴⁶, co-recruits ArhGAP29 to the plasma membrane (chapter 5). Furthermore, we have demonstrated that ArhGAP29 is essential for Rap1-induced cell spreading (chapter 4)⁷¹.

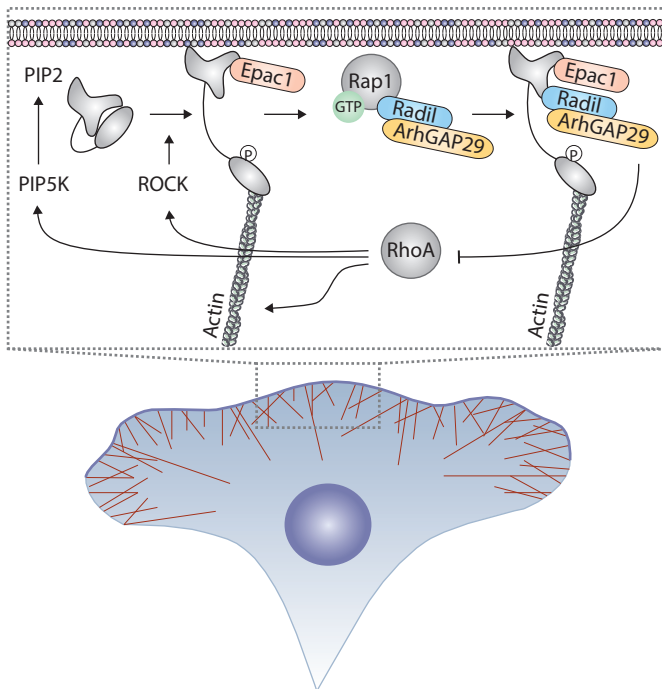


Figure 1: Working model – ERM proteins integrate Rap1 up- and downstream signaling for efficient cell spreading.

Activation of ERM proteins, regulated by RhoA-effectors, induces the open, active conformation of ERM proteins. Subsequently, ERM proteins form docking sites for Epac1 at the plasma membrane. Through activation of Rap1 Radil and ArhGAP29 are recruited to the plasma membrane, where Radil may interact with the open ERM proteins. ArhGAP29 can subsequently inactivate RhoA. This will release actomyosin contraction, allowing membrane protrusion. Simultaneously, this will result in reduced Rock activity, creating a negative feedback loop.

Therefore, the scaffolding function of ERM proteins in Rap1-signaling may comprise a direct negative feedback loop, reducing RhoA activity and ERM phosphorylation.

Cyclical phosphorylation of Ezrin has been suggested to be necessary for proper cell spreading ²²⁶. Supporting this, we found that whereas a phospho-mimicking mutant of Ezrin, thus in a constitutively active conformation, does induce cell spreading, it does so in a distinctive manner from Rap1-induced cell spreading ⁴⁸. This could possibly be due to the continuous linkage of the plasma membrane to the actin cytoskeleton, thereby restricting the protrusive capacity of the plasma membrane. Supporting such a model, expression of an actin-binding mutant of Ezrin in A549-Epac1 cells, greatly increases cell spreading in a morphological manner resembling Rap1-induced cell spreading (S.H. Ross and J.L. Bos, unpublished data). Thus, dephosphorylating Ezrin may be necessary for proper cell spreading. Negative feedback toward Rho, through recruitment of Radil and ArhGAP29 may thereby increase cell spreading. Actin binding, and thus linkage of the plasma membrane to the actin cytoskeleton, on the other hand, is essential for proper cell migration ³⁵¹. This suggests that waves of ERM protein activation and inactivation are necessary for proper cell migration, in which ERM proteins have a triple function: 1) localizing the Rap1-Rho axis for local tension inhibition, resulting in membrane protrusion, 2) this simultaneously creates a feedback loop, inactivating ERM proteins, and thereby uncoupling the plasma membrane from the underlying actin cytoskeleton to allow membrane protrusion and 3) linking the protruded membrane to the actin cytoskeleton to stabilize it and induce tension needed for cell migration (Fig. 1).

Cycling of the phosphorylation status of ERM proteins has been demonstrated to be necessary for various biological processes ³⁵². Moreover, other examples exist in which ERM proteins function as a scaffold to negatively regulate Rho activity ³⁵³. Thus, this dual role for ERM proteins, in which it functions as a scaffold, simultaneously creating a negative feedback loop, may be a conserved function in ERM protein signaling.

Interestingly, this two-step targeting model of Radil to the plasma membrane is not the only example. Previously it has been demonstrated that upon G-protein activation, Rap1 is activated and recruits Radil to the plasma membrane. Subsequently, Radil interacts with the G β / γ subunits of this G-protein, which are thought to stabilize it at the plasma membrane ¹⁸². Thus, again the upstream signal determining where Radil is recruited to, also produces the anchor for Radil, stabilizing its localization there.

3. PTPL1 functions as an alternative plasma membrane localizing anchor for ArhGAP29 – regulating Rho by a Rap2 module

PTPL1 interacts with the C-terminus of ArhGAP29 ²⁴¹, the same region that interacts with Radil. By doing so, PTPL1 localizes ArhGAP29 to the plasma membrane in 293T cells, by interacting with PI(4,5)P2 through its FERM-domain ^{328,329}. Therefore, it seems that PTPL1 functions analogues to the Rap1-Radil module, by tethering ArhGAP29 to the plasma membrane. How the activity of ArhGAP29 is regulated is currently unknown. However, for several other BAR-domain containing GAPs it has been demonstrated that the BAR-domain interacts with the GAP-domain, autoinhibiting its function ^{354,355}. Binding of phospholipids to this BAR-domain releases the autoinhibitory function ³⁵⁵. Thus, recruitment of ArhGAP29 to the plasma membrane, whether it is through PTPL1 or Rap1-Radil signaling, bringing ArhGAP29 in proximity to phospholipids, may induce the activation of ArhGAP29. Active Rap2A, on the other hand, directly interacts with the BAR-domain of ArhGAP29 (chapter 7) and is suggested to inhibit its activity ³³¹. Possibly, binding of Rap2A to the BAR-domain prevents it from interacting with phospholipids, keeping it in an autoinhibited state, thereby inhibiting its activity.

Interestingly, PDZGEF, which activates Rap2A at the brush border ³²⁷, also interacts with PTPL1 ³³⁰, thereby coupling Rap2A up- and downstream signaling.

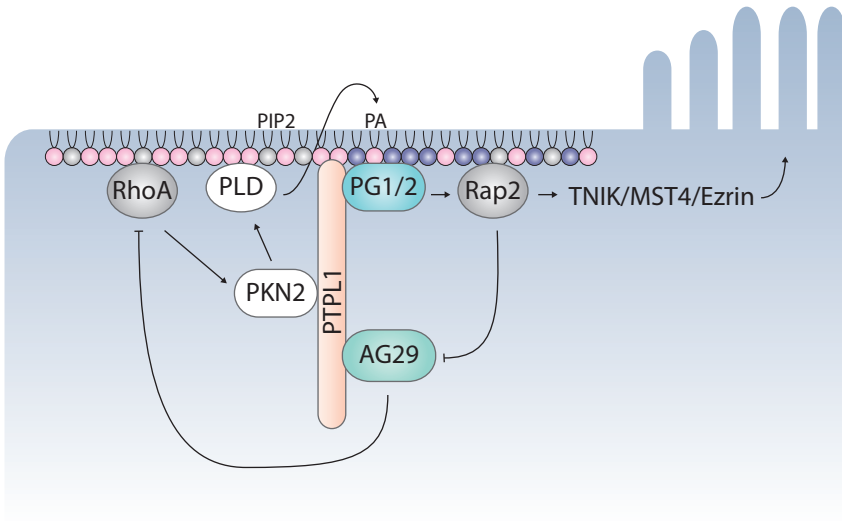


Figure 2: Working model – PTPL1 restricts brush border localization.

Depicted is an intestinal cell showing part of the inner leaflet of the plasma membrane and an area forming a brush border. By binding PI(4,5)P2 PTPL1 is recruited to the plasma membrane. Through its second PDZ-domain PTPL1 restricts PDZGEF at the apical membrane. PDZGEF, in turn, activates Rap2A at the apical membrane, resulting in brush border formation through the TNIK-Mst4-Ezrin signaling cascade. Simultaneously, Rap2A binds and inhibits ArhGAP29, bound to the fourth PDZ-domain of PTPL1. Inhibition of ArhGAP29 will result in increased Rho activity, which may then activate PKN2, bound to the third PDZ-domain of PTPL1. Active PKN2 can interact and activate PLD1, known to increase phosphatidic acid levels at the brush border, and induce PDZGEF signaling. Thus, PTPL1 functions as a platform for a positive feedback loop, and restricts its localization to the apical membrane, thereby reinforcing and localizing brush border formation.

Whereas Rap1 modulates Rho GTPase signaling and subsequent actin dynamics in various biological processes (chapter 1), Rap2 mainly has kinases as effectors³⁵⁶⁻³⁵⁸, through which it may also regulate actin dynamics, as demonstrated in intestinal brush border formation³²⁷. Its regulation of the activity of ArhGAP29 also links Rap2 to Rho GTPase regulation.

In chapter 7 we proposed that by accumulating at the apical membrane in intestinal cells, PTPL1 may concentrate its interaction partners there. The PTPL1-interacting proteins PDZGEF, ArhGAP29 and PKN2 are all necessary for brush border formation. We proposed in chapter 7 that concentrating their localization at the apical membrane, restricts where the brush border is formed (Fig. 2). Alternatively, rather than forming a positive feedback loop, PTPL1 may be part of a negative feedback loop. Although PI(4,5)P2 is enriched at the apical membrane, it is not absent from the basolateral membrane. Supporting this, we did see a small amount of PTPL1 localizing to the basolateral membrane. Possibly through its tyrosine phosphatase activity, PTPL1 inhibits brush border formation there. Inhibition of its activity at the apical membrane would result in brush border formation.

Interestingly, apart from ArhGAP29 and PDZ-GEF all players in this feed forward system have also been implicated in cytokinesis³⁵⁹⁻³⁶¹ and it is an intriguing thought that this module may also regulate cytoskeletal dynamics during cytokinesis. Furthermore, both the Mst4 homologue svkA in *Dictyostelium discoideum* and ERM proteins are involved in cytokinesis, further strengthening a potential role for this signaling module in cytokinesis. RhoA plays a prominent role in regulating the actin ring at the cytokinetic cleft and is under tight regulation, both spatially and temporally (reviewed in³⁶²). Moreover, cyclical activation of RhoA at the cleavage furrow is essential for cytokinesis to occur, emphasized by the finding that both constitutively active and inactive RhoA abrogates cytokinesis.

Indeed, both RhoGEFs and GAPs have been localized to and implicated in cytokinesis^{362,363}. Possibly the PTPL1 module restricts the localization of RhoA activity at the cleavage furrow. Also the well-known centralspindlin-Ect2 module, responsible for the activation of RhoA at the cleavage furrow, has recently been demonstrated to have an extramitotic function at the epithelial zonula adherens²⁴³, indicating that there is dual functionality for signaling modules involved in regulating the actin cytoskeleton at the cleavage furrow and elsewhere.

If there is indeed a dual role for PTPL1 in cytokinesis and apical brush border formation, it is of note that PTPL1 is thought to capture microtubules at the cleavage furrow³⁵⁹. It would be of interest to determine whether it also does so at the apical membrane since polarized vesicle trafficking, regulated by Cdc42 and depending on microtubules, is a key process in the establishment and maintenance of apical polarity.

4. Integrating the anchors in endothelial barrier control

As discussed before, whereas depletion of Radil has only a minor effect on basal endothelial barrier function, ArhGAP29 depletion affects both basal and enhanced endothelial barrier function, much like Rap1 does. We proposed that this could be explained by Radil being mostly important during enhanced endothelial barrier function. It would do so by increasing the amount of ArhGAP29 at the plasma membrane. This would imply that there is another anchor for ArhGAP29, localizing a basal amount of ArhGAP29 to the plasma membrane under basal conditions. Possibly, this anchor is PTPL1. Recall that ArhGAP29 also binds PDZGEF, the RapGEF responsible for Rap1 activity and endothelial barrier integrity under basal conditions. Thus, possibly PTPL1 forms the platform for Rap1-induced endothelial barrier function under basal conditions. Interestingly, in epithelial cells, PKN2 is important for cell-cell junction formation in a Rho-dependent manner³⁶⁴. Extrapolating this to endothelial barrier control, under basal conditions ArhGAP29-regulated Rho activity may not only serve to release tension through inhibition of ROCK and MLC2, but may also PKN2 signaling for endothelial barrier control. However, how PKN2 regulates cell-cell adhesion is currently unknown. Moreover, although PKN2 has most commonly been reported to be regulated by RhoA, it may also be regulated by Rac1 and Cdc42³⁶⁵. Although not confirmed *in vivo*, PTPL1 can dephosphorylate β -catenin *in vitro*³⁶⁶, possibly reflecting a second function of PTPL1 in endothelial barrier control.

In chapter 7 we suggested that at the apical brush border of intestinal cells PTPL1 functions as a scaffold for a Rap2-Rho module, in which PDZGEF activates Rap2A.

In endothelial cells Rap2 counteracts the effects of Rap1 on endothelial barrier function, reducing the endothelial barrier function. This was suggested to be regulated through its effector MAP4K4⁷³. Possibly, inhibition of ArhGAP29 by Rap2³³¹ may contribute to this.

Thus possibly, PTPL1 and its interactors PDZGEF and ArhGAP29 form a Rap1-signaling module under basal conditions, whereas Radil, binding to ArhGAP29 and responding to Epac1-induced Rap1 activation, forms the signaling module for enhanced endothelial barrier function. Intriguingly, Radil does follow the biological patterns of Epac1 signaling, having only a minor effect on basal barrier function, dynamically translocating to the plasma membrane upon cAMP-stimulation and being anchored to ERM proteins.

Importantly, ERM proteins have also been linked to endothelial barrier regulation³⁶⁷⁻³⁶⁹. Here, they seem to serve opposing functions. As we found for Radil, depletion of ERM proteins has only a minor effect on the basal barrier³⁶⁹. Endothelial barrier potentiation, however, by stimulating with sphingosine-1-phosphate (S1P), depends on the presence of ERM proteins. ERM proteins were suggested to mediate S1P-induced Rac1 activation, resulting in endothelial barrier potentiation³⁶⁸. However, the molecular mechanism for this was not elucidated. Possibly the activation of Rac1 was indirect through inhibition of Rho activity. In this sense, Radil may be involved in this by recruiting ArhGAP29, thus inhibiting Rho.

Intriguingly, depletion of ERM proteins also reduces thrombin-induced endothelial permeability³⁶⁷. Thrombin induces endothelial permeability by activating RhoA. In turn, the RhoA-effector ROCK induces stress fiber formation and actomyosin contraction, resulting in endothelial barrier permeability. Simultaneously, ROCK can phosphorylate ERM proteins, resulting in their active, open conformation. Hereby, ERM proteins may link the actin cytoskeleton to the plasma membrane, transducing the actomyosin-generated tension to the junctions. Radil may also be involved in this process.

CONCLUDING REMARKS

From the research on Rap1-biology over the past decade, including that presented in this thesis, a picture emerges in which Rap GTPases are necessary for the establishment and fine-tuning of cell architecture through modulation of the actin cytoskeleton. As such, Rap1 translates cortical landmark cues into localized modulation of the actin cytoskeleton by spatially and temporally regulating the Rho GTPase family, the master regulators of the actin cytoskeleton. Recognition of these landmarks may occur directly through RapGEFs and GAPs, or alternatively, through scaffolds for the RapGEFs or GAPs, such as ERM proteins for Epac1 and PTPL1 for PDZGEF. However, once activated, Rap1 needs to cope with the fact that it has a vast amount of effector proteins and needs to couple the input signal to the appropriate effector. Scaffolds such as ERM proteins and PTPL1, which bind Radil and ArhGAP29 respectively, may play a key role in this, by also interacting with downstream effectors. Moreover, directly linking a particular input signal to a specific downstream signaling cascade may explain why the cell would put multiple GEFs or GAPs for the same GTPase in place, regulating the same biological outcome.

By having such scaffold proteins integrating up- and downstream signaling, we may start to understand how specific input signals are linked to specific biological outcomes.

APPENDICES

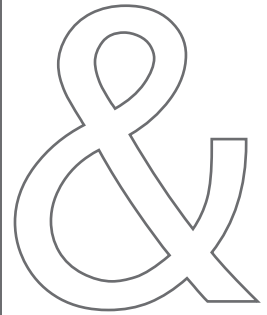
REFERENCES

NEDERLANDSE SAMENVATTING

CURRICULUM VITAE

PUBLICATIONS

DANKWOORD



REFERENCES

- 1 Bos, J. L., Rehmann, H. & Wittinghofer, A. GEFs and GAPs: critical elements in the control of small G proteins. *Cell* **129**, 865-877, doi:10.1016/j.cell.2007.05.018 (2007).
- 2 Wennerberg, K., Rossman, K. L. & Der, C. J. The Ras superfamily at a glance. *Journal of cell science* **118**, 843-846, doi:10.1242/jcs.01660 (2005).
- 3 Bertoni, A. *et al.* Relationships between Rap1b, affinity modulation of integrin alpha IIb beta 3, and the actin cytoskeleton. *The Journal of biological chemistry* **277**, 25715-25721, doi:10.1074/jbc.M202791200 (2002).
- 4 Caron, E., Self, A. J. & Hall, A. The GTPase Rap1 controls functional activation of macrophage integrin alpha M beta 2 by LPS and other inflammatory mediators. *Current biology : CB* **10**, 974-978 (2000).
- 5 Katagiri, K. *et al.* Rap1 is a potent activation signal for leukocyte function-associated antigen 1 distinct from protein kinase C and phosphatidylinositol-3-OH kinase. *Molecular and cellular biology* **20**, 1956-1969 (2000).
- 6 Reedquist, K. A. *et al.* The small GTPase, Rap1, mediates CD31-induced integrin adhesion. *The Journal of cell biology* **148**, 1151-1158 (2000).
- 7 Sebzda, E., Bracke, M., Tugal, T., Hogg, N. & Cantrell, D. A. Rap1A positively regulates T cells via integrin activation rather than inhibiting lymphocyte signaling. *Nature immunology* **3**, 251-258, doi:10.1038/nri765 (2002).
- 8 Pizon, V., Chardin, P., Lerosey, I., Olofsson, B. & Tavitian, A. Human cDNAs rap1 and rap2 homologous to the Drosophila gene Dras3 encode proteins closely related to ras in the 'effector' region. *Oncogene* **3**, 201-204 (1988).
- 9 Bivona, T. G. *et al.* Rap1 up-regulation and activation on plasma membrane regulates T cell adhesion. *The Journal of cell biology* **164**, 461-470, doi:10.1083/jcb.200311093 (2004).
- 10 Takahashi, M. *et al.* Sequential activation of Rap1 and Rac1 small G proteins by PDGF locally at leading edges of NIH3T3 cells. *Genes to cells : devoted to molecular & cellular mechanisms* **13**, 549-569, doi:10.1111/j.1365-2443.2008.01187.x (2008).
- 11 Ohba, Y., Kurokawa, K. & Matsuda, M. Mechanism of the spatio-temporal regulation of Ras and Rap1. *The EMBO journal* **22**, 859-869, doi:10.1093/emboj/cdg087 (2003).
- 12 Mor, A. *et al.* Phospholipase D1 regulates lymphocyte adhesion via upregulation of Rap1 at the plasma membrane. *Molecular and cellular biology* **29**, 3297-3306, doi:10.1128/MCB.00366-09 (2009).
- 13 Hisata, S. *et al.* Rap1-PDZ-GEF1 interacts with a neurotrophin receptor at late endosomes, leading to sustained activation of Rap1 and ERK and neurite outgrowth. *The Journal of cell biology* **178**, 843-860, doi:10.1083/jcb.200610073 (2007).
- 14 Pizon, V., Desjardins, M., Bucci, C., Parton, R. G. & Zerial, M. Association of Rap1a and Rap1b proteins with late endocytic/phagocytic compartments and Rap2a with the Golgi complex. *Journal of cell science* **107 (Pt 6)**, 1661-1670 (1994).
- 15 Pizon, V., Mechali, F. & Baldacci, G. RAP1A GTP/GDP cycles determine the intracellular location of the late endocytic compartments and contribute to myogenic differentiation. *Experimental cell research* **246**, 56-68, doi:10.1006/excr.1998.4284 (1999).
- 16 York, R. D. *et al.* Role of phosphoinositide 3-kinase and endocytosis in nerve growth factor-induced extracellular signal-regulated kinase activation via Ras and Rap1. *Molecular and cellular biology* **20**, 8069-8083 (2000).
- 17 Brock, T. G., Serezani, C. H., Carstens, J. K., Peters-Golden, M. & Aronoff, D. M. Effects of prostaglandin E2 on the subcellular localization of Epac-1 and Rap1 proteins during Fc gamma-receptor-mediated phagocytosis in alveolar macrophages. *Experimental cell research* **314**, 255-263, doi:10.1016/j.yexcr.2007.10.011 (2008).
- 18 Liu, C. *et al.* The interaction of Epac1 and Ran promotes Rap1 activation at the nuclear envelope. *Molecular and cellular biology* **30**, 3956-3969, doi:10.1128/MCB.00242-10 (2010).
- 19 Beranger, F., Goud, B., Tavitian, A. & de Gunzburg, J. Association of the Ras-antagonistic Rap1/Krev-1 proteins with the Golgi complex. *Proceedings of the National Academy of Sciences of the United States of America* **88**, 1606-1610 (1991).
- 20 Nomura, K., Kanemura, H., Satoh, T. & Kataoka, T. Identification of a novel domain of Ras and Rap1 that directs their differential subcellular localizations. *The Journal of biological chemistry* **279**, 22664-22673, doi:10.1074/jbc.M314169200 (2004).
- 21 Wienecke, R. *et al.* Co-localization of the TSC2 product tuberlin with its target Rap1 in the Golgi

- apparatus. *Oncogene* **13**, 913-923 (1996).
- 22 Wright, L. P. & Philips, M. R. Thematic review series: lipid posttranslational modifications. CAAAX modification and membrane targeting of Ras. *Journal of lipid research* **47**, 883-891, doi:10.1194/jlr.R600004-JLR200 (2006).
- 23 Rundell, C. J., Repellin, C. E. & Yarwood, S. J. Protease inhibitors prevent the protein kinase A-dependent loss of Rap1 GTPase from the particulate fraction of COS1 cells. *Biochemical and biophysical research communications* **315**, 1077-1081, doi:10.1016/j.bbrc.2004.01.161 (2004).
- 24 Medeiros, R. B. *et al.* Protein kinase D1 and the beta 1 integrin cytoplasmic domain control beta 1 integrin function via regulation of Rap1 activation. *Immunity* **23**, 213-226, doi:10.1016/j.immuni.2005.07.006 (2005).
- 25 Kitayama, H., Sugimoto, Y., Matsuzaki, T., Ikawa, Y. & Noda, M. A ras-related gene with transformation suppressor activity. *Cell* **56**, 77-84 (1989).
- 26 Noda, M. *et al.* Detection of genes with a potential for suppressing the transformed phenotype associated with activated ras genes. *Proceedings of the National Academy of Sciences of the United States of America* **86**, 162-166 (1989).
- 27 Cook, S. J., Rubinfeld, B., Albert, I. & McCormick, F. RapV12 antagonizes Ras-dependent activation of ERK1 and ERK2 by LPA and EGF in Rat-1 fibroblasts. *The EMBO journal* **12**, 3475-3485 (1993).
- 28 Lin, Y., Mettling, C. & Chou, C. Rap1-suppressed tumorigenesis is concomitant with the interference in ras effector signaling. *FEBS letters* **467**, 184-188 (2000).
- 29 Vossler, M. R. *et al.* cAMP activates MAP kinase and Elk-1 through a B-Raf- and Rap1-dependent pathway. *Cell* **89**, 73-82 (1997).
- 30 Bos, J. L., de Rooij, J. & Reedquist, K. A. Rap1 signalling: adhering to new models. *Nature reviews. Molecular cell biology* **2**, 369-377, doi:10.1038/35073073-35073073 [pii] (2001).
- 31 Kooistra, M. R., Corada, M., Dejana, E. & Bos, J. L. Epac1 regulates integrity of endothelial cell junctions through VE-cadherin. *FEBS Lett* **579**, 4966-4972, doi:S0014-5793(05)00949-X [pii]10.1016/j.febslet.2005.07.080 (2005).
- 32 Pannekoek, W. J., Kooistra, M. R. H., Zwartkruis, F. J. T. & Bos, J. L. Cell-cell junction formation: The role of Rap1 and Rap1 guanine nucleotide exchange factors. *Bba-Biomembranes* **1788**, 790-796, doi:DOI 10.1016/j.bbamem.2008.12.010 (2009).
- 33 Bailey, C. L., Kelly, P. & Casey, P. J. Activation of Rap1 promotes prostate cancer metastasis. *Cancer research* **69**, 4962-4968, doi:10.1158/0008-5472.CAN-08-4269 (2009).
- 34 Itoh, M., Nelson, C. M., Myers, C. A. & Bissell, M. J. Rap1 integrates tissue polarity, lumen formation, and tumorigenic potential in human breast epithelial cells. *Cancer research* **67**, 4759-4766, doi:10.1158/0008-5472.CAN-06-4246 (2007).
- 35 Freeman, S. A. *et al.* Preventing the activation or cycling of the Rap1 GTPase alters adhesion and cytoskeletal dynamics and blocks metastatic melanoma cell extravasation into the lungs. *Cancer research* **70**, 4590-4601, doi:10.1158/0008-5472.CAN-09-3414 (2010).
- 36 Lin, K. B. *et al.* The Rap GTPases regulate the migration, invasiveness and in vivo dissemination of B-cell lymphomas. *Oncogene* **29**, 608-615, doi:10.1038/onc.2009.345 (2010).
- 37 Schwamborn, J. C. & Püschel, A. W. in *Nat. Neurosci.* Vol. 7 923-929 (2004).
- 38 Heasman, S. J. & Ridley, A. J. Mammalian Rho GTPases: new insights into their functions from in vivo studies. *Nature reviews. Molecular cell biology* **9**, 690-701, doi:10.1038/nrm2476 (2008).
- 39 Bustelo, X. R., Sauzeau, V. & Berenjeno, I. M. GTP-binding proteins of the Rho/Rac family: regulation, effectors and functions in vivo. *BioEssays : news and reviews in molecular, cellular and developmental biology* **29**, 356-370, doi:10.1002/bies.20558 (2007).
- 40 Lock, F. E., Ryan, K. R., Poulter, N. S., Parsons, M. & Hotchin, N. A. Differential regulation of adhesion complex turnover by ROCK1 and ROCK2. *PLoS one* **7**, e31423, doi:10.1371/journal.pone.0031423 (2012).
- 41 Goode, B. L. & Eck, M. J. Mechanism and function of formins in the control of actin assembly. *Annual review of biochemistry* **76**, 593-627, doi:10.1146/annurev.biochem.75.103004.142647 (2007).
- 42 Takenawa, T. & Suetsugu, S. The WASP-WAVE protein network: connecting the membrane to the cytoskeleton. *Nature reviews. Molecular cell biology* **8**, 37-48, doi:10.1038/nrm2069 (2007).
- 43 Delorme, V. *et al.* Cofilin activity downstream of Pak1 regulates cell protrusion efficiency by organizing lamellipodium and lamella actin networks. *Developmental cell* **13**, 646-662, doi:10.1016/j.devcel.2007.08.011 (2007).
- 44 Wilkinson, S., Paterson, H. F. & Marshall, C. J. Cdc42-MRCK and Rho-ROCK signalling cooperate in myosin phosphorylation and cell invasion. *Nature cell biology* **7**, 255-261, doi:10.1038/ncb1230 (2005).
- 45 Guilluy, C., Garcia-Mata, R. & Burridge, K. Rho protein crosstalk: another social network? *Trends in cell*

- biology **21**, 718-726, doi:10.1016/j.tcb.2011.08.002 (2011).
- 46 Carey S, J. C. J., and Reinhart-Kin C.A. in *Tissue Engineering and Biomaterials: Cellular and Biomolecular Mechanics and Mechanobiology* (ed Gefen A.) (Springer, 2011).
- 47 Parsons, J. T., Horwitz, A. R. & Schwartz, M. A. Cell adhesion: integrating cytoskeletal dynamics and cellular tension. *Nature reviews. Molecular cell biology* **11**, 633-643, doi:10.1038/nrm2957 (2010).
- 48 Ross, S. H. *et al.* Ezrin is required for efficient Rap1-induced cell spreading. *J Cell Sci* **124**, 1808-1818, doi:jcs.079830 [pii] 10.1242/jcs.079830 (2011).
- 49 Ross, S. H. *et al.* Rap1 can bypass the FAK-Src-Paxillin cascade to induce cell spreading and focal adhesion formation. *PLoS one* **7**, e50072, doi:10.1371/journal.pone.0050072 (2012).
- 50 Lafuente, E. M. *et al.* RIAM, an Ena/VASP and Profilin ligand, interacts with Rap1-GTP and mediates Rap1-induced adhesion. *Developmental cell* **7**, 585-595, doi:10.1016/j.devcel.2004.07.021 (2004).
- 51 Lee, H. S., Lim, C. J., Puzon-McLaughlin, W., Shattil, S. J. & Ginsberg, M. H. RIAM activates integrins by linking talin to ras GTPase membrane-targeting sequences. *The Journal of biological chemistry* **284**, 5119-5127, doi:10.1074/jbc.M807117200 (2009).
- 52 Katagiri, K., Maeda, A., Shimonaka, M. & Kinashi, T. RAPL, a Rap1-binding molecule that mediates Rap1-induced adhesion through spatial regulation of LFA-1. *Nature immunology* **4**, 741-748, doi:10.1038/ni950 (2003).
- 53 Nobes, C. D. & Hall, A. Rho, rac, and cdc42 GTPases regulate the assembly of multimolecular focal complexes associated with actin stress fibers, lamellipodia, and filopodia. *Cell* **81**, 53-62 (1995).
- 54 Ridley, A. J. & Hall, A. The small GTP-binding protein rho regulates the assembly of focal adhesions and actin stress fibers in response to growth factors. *Cell* **70**, 389-399 (1992).
- 55 Arthur, W. T. & Burridge, K. RhoA inactivation by p19RhoGAP regulates cell spreading and migration by promoting membrane protrusion and polarity. *Molecular biology of the cell* **12**, 2711-2720 (2001).
- 56 Flevaris, P. *et al.* A molecular switch that controls cell spreading and retraction. *The Journal of cell biology* **179**, 553-565, doi:10.1083/jcb.200703185 (2007).
- 57 Vega, F. M., Fruhwirth, G., Ng, T. & Ridley, A. J. RhoA and RhoC have distinct roles in migration and invasion by acting through different targets. *The Journal of cell biology* **193**, 655-665, doi:10.1083/jcb.201011038 (2011).
- 58 Arthur, W. T., Petch, L. A. & Burridge, K. Integrin engagement suppresses RhoA activity via a c-Src-dependent mechanism. *Current biology : CB* **10**, 719-722 (2000).
- 59 Ren, X. D., Kiosses, W. B. & Schwartz, M. A. Regulation of the small GTP-binding protein Rho by cell adhesion and the cytoskeleton. *The EMBO journal* **18**, 578-585, doi:10.1093/emboj/18.3.578 (1999).
- 60 Ren, X. D. *et al.* Focal adhesion kinase suppresses Rho activity to promote focal adhesion turnover. *Journal of cell science* **113 (Pt 20)**, 3673-3678 (2000).
- 61 Feng, H. *et al.* Activation of Rac1 by Src-dependent phosphorylation of Dock180(Y1811) mediates PDGFRalpha-stimulated glioma tumorigenesis in mice and humans. *The Journal of clinical investigation* **121**, 4670-4684, doi:10.1172/JCI58559 (2011).
- 62 Filipenko, N. R., Attwell, S., Roskelley, C. & Dedhar, S. Integrin-linked kinase activity regulates Rac- and Cdc42-mediated actin cytoskeleton reorganization via alpha-PIX. *Oncogene* **24**, 5837-5849, doi:10.1038/sj.onc.1208737 (2005).
- 63 Miranti, C. K., Leng, L., Maschberger, P., Brugge, J. S. & Shattil, S. J. Identification of a novel integrin signaling pathway involving the kinase Syk and the guanine nucleotide exchange factor Vav1. *Current biology : CB* **8**, 1289-1299 (1998).
- 64 Tkachenko, E. *et al.* Protein kinase A governs a RhoA-RhoGDI protrusion-retraction pacemaker in migrating cells. *Nature cell biology* **13**, 660-667, doi:10.1038/ncb2231 (2011).
- 65 Arthur, W. T. in *The Journal of cell biology* Vol. 167 111-122 (2004).
- 66 Stefanini, L. *et al.* in *Arterioscler. Thromb. Vasc. Biol.* Vol. 32 434-441 (2012).
- 67 Krugmann, S., Williams, R., Stephens, L. & Hawkins, P. T. in *Current Biology* Vol. 14 1380-1384 (2004).
- 68 Stacey, T. T. I. in *Journal of cell science* Vol. 117 6071-6084 (2004).
- 69 Krugmann, S., Andrews, S., Stephens, L. & Hawkins, P. T. in *Journal of cell science* Vol. 119 425-432 (2006).
- 70 Miyata, M. *et al.* Localization of nectin-free afadin at the leading edge and its involvement in directional cell movement induced by platelet-derived growth factor. *Journal of cell science* **122**, 4319-4329, doi:10.1242/jcs.048439 (2009).
- 71 Post, A. *et al.* Rasip1 mediates Rap1 regulation of Rho in endothelial barrier function through ArhGAP29. *Proc Natl Acad Sci U S A* **110**, 11427-11432, doi:10.1073/pnas.1306595110 (2013).
- 72 Myagmar, B.-E. *et al.* in *Biochem. Biophys. Res. Commun.* Vol. 329 1046-1052 (2005).

- 73 Pannekoek, W. J., Linnemann, J. R., Brouwer, P. M., Bos, J. L. & Rehmann, H. Rap1 and Rap2 antagonistically control endothelial barrier resistance. *PLoS one* **8**, e57903, doi:10.1371/journal.pone.0057903 (2013).
- 74 Broman, M. T. *et al.* Cdc42 regulates adherens junction stability and endothelial permeability by inducing alpha-catenin interaction with the vascular endothelial cadherin complex. *Circulation research* **98**, 73-80, doi:10.1161/01.RES.0000198387.44395.e9 (2006).
- 75 Wojciak-Stothard, B., Potempa, S., Eichholtz, T. & Ridley, A. J. Rho and Rac but not Cdc42 regulate endothelial cell permeability. *Journal of cell science* **114**, 1343-1355 (2001).
- 76 Wojciak-Stothard, B., Tsang, L. Y. & Haworth, S. G. Rac and Rho play opposing roles in the regulation of hypoxia/reoxygenation-induced permeability changes in pulmonary artery endothelial cells. *American journal of physiology. Lung cellular and molecular physiology* **288**, L749-760, doi:10.1152/ajplung.00361.2004 (2005).
- 77 Baumer, Y., Drenckhahn, D. & Waschke, J. in *Histochem. Cell Biol.* Vol. 129 765-778 (2008).
- 78 Hage, B., Meinel, K., Baum, I., Giehl, K. & Menke, A. Rac1 activation inhibits E-cadherin-mediated adherens junctions via binding to IQGAP1 in pancreatic carcinoma cells. *Cell communication and signaling : CCS* **7**, 23, doi:10.1186/1478-811X-7-23 (2009).
- 79 van Nieuw Amerongen, G. P. *et al.* Involvement of Rho kinase in endothelial barrier maintenance. *Arteriosclerosis, thrombosis, and vascular biology* **27**, 2332-2339, doi:10.1161/ATVBAHA.107.152322 (2007).
- 80 Sakurai, A. *et al.* MAGI-1 is required for Rap1 activation upon cell-cell contact and for enhancement of vascular endothelial cadherin-mediated cell adhesion. *Molecular biology of the cell* **17**, 966-976, doi:10.1091/mbc.E05-07-0647 (2006).
- 81 Hogan, C. *et al.* in *Molecular and cellular biology* Vol. 24 6690-6700 (2004).
- 82 Asuri, S., Yan, J., Paranavitana, N. C. & Quilliam, L. A. E-cadherin dis-engagement activates the Rap1 GTPase. *Journal of cellular biochemistry* **105**, 1027-1037, doi:10.1002/jcb.21902 (2008).
- 83 Hogan, B. M., Bussmann, J., Wolburg, H. & Schulte-Merker, S. ccm1 cell autonomously regulates endothelial cellular morphogenesis and vascular tubulogenesis in zebrafish. *Human molecular genetics* **17**, 2424-2432, doi:10.1093/hmg/ddn142 (2008).
- 84 Hoshino, T. *et al.* Regulation of E-cadherin endocytosis by nectin through afadin, Rap1, and p120ctn. *The Journal of biological chemistry* **280**, 24095-24103, doi:10.1074/jbc.M414447200 (2005).
- 85 Noda, K. *et al.* Vascular endothelial-cadherin stabilizes at cell-cell junctions by anchoring to circumferential actin bundles through alpha- and beta-catenins in cyclic AMP-Epac-Rap1 signal-activated endothelial cells. *Molecular biology of the cell* **21**, 584-596, doi:E09-07-0580 [pii] 10.1091/mbc.E09-07-0580 (2010).
- 86 Kovacs, E. M. *et al.* N-WASP regulates the epithelial junctional actin cytoskeleton through a non-canonical post-nucleation pathway. *Nature cell biology* **13**, 934-943, doi:10.1038/ncb2290 (2011).
- 87 Yamada, S., Pokutta, S., Drees, F., Weis, W. I. & Nelson, W. J. Deconstructing the cadherin-catenin-actin complex. *Cell* **123**, 889-901, doi:10.1016/j.cell.2005.09.020 (2005).
- 88 Ando, K. *et al.* in *The Journal of cell biology* Vol. 202 901-916 (2013).
- 89 Cullere, X. *et al.* in *Blood* Vol. 105 1950-1955 (2005).
- 90 Huveneers, S. *et al.* Vinculin associates with endothelial VE-cadherin junctions to control force-dependent remodeling. *The Journal of cell biology* **196**, 641-652, doi:10.1083/jcb.201108120 (2012).
- 91 Millan, J. *et al.* Adherens junctions connect stress fibres between adjacent endothelial cells. *BMC biology* **8**, 11, doi:10.1186/1741-7007-8-11 (2010).
- 92 le Duc, Q. *et al.* Vinculin potentiates E-cadherin mechanosensing and is recruited to actin-anchored sites within adherens junctions in a myosin II-dependent manner. *The Journal of cell biology* **189**, 1107-1115, doi:10.1083/jcb.201001149 (2010).
- 93 Mangold, S. *et al.* Hepatocyte growth factor acutely perturbs actin filament anchorage at the epithelial zonula adherens. *Current biology : CB* **21**, 503-507, doi:10.1016/j.cub.2011.02.018 (2011).
- 94 Birukova, A. A. *et al.* in *Microvascular research* 1-11 (Elsevier B.V., 2009).
- 95 Birukova, A. A., Zagranichnaya, T., Alekseeva, E., Bokoch, G. M. & Birukov, K. G. in *J. Cell. Physiol.* Vol. 215 715-724 (2008).
- 96 Liu, J. J. *et al.* A mechanism of Rap1-induced stabilization of endothelial cell-cell junctions. *Molecular biology of the cell* **22**, 2509-2519, doi:10.1091/mbc.E11-02-0157 (2011).
- 97 Fukuyama, T. *et al.* in *The Journal of biological chemistry* Vol. 280 815-825 (2005).
- 98 Sato, T. *et al.* in *The Journal of biological chemistry* Vol. 281 5288-5299 (2006).
- 99 Birukova, A. A. *et al.* in *Experimental Cell Research* Vol. 313 2504-2520 (2007).
- 100 Ahmed, S. M. *et al.* KIF14 negatively regulates Rap1a-Radil signaling during breast cancer progression. *J Cell Biol* **199**, 951-967, doi:10.1083/jcb.201206051 (2012).

- 101 Xu, K. *et al.* Blood vessel tubulogenesis requires Rasip1 regulation of GTPase signaling. *Dev Cell* **20**, 526-539, doi:S1534-5807(11)00079-7 [pii] 10.1016/j.devcel.2011.02.010 (2011).
- 102 Wilson, C. W. *et al.* Rasip1 regulates vertebrate vascular endothelial junction stability through Epac1-Rap1 signaling. *Blood* **122**, 3678-3690, doi:10.1182/blood-2013-02-483156 (2013).
- 103 Glading, A., Han, J., Stockton, R. A. & Ginsberg, M. H. in *The Journal of cell biology* Vol. 179 247-254 (2007).
- 104 Stockton, R. A., Shenkar, R., Awad, I. A. & Ginsberg, M. H. Cerebral cavernous malformations proteins inhibit Rho kinase to stabilize vascular integrity. *J Exp Med* **207**, 881-896, doi:jem.20091258 [pii] 10.1084/jem.20091258 (2010).
- 105 Borikova, A. L. *et al.* Rho kinase inhibition rescues the endothelial cell cerebral cavernous malformation phenotype. *The Journal of biological chemistry* **285**, 11760-11764, doi:10.1074/jbc.C109.097220 (2010).
- 106 Fukuyama, T., Ogita, H., Kawakatsu, T., Inagaki, M. & Takai, Y. in *Oncogene* (2005).
- 107 Ogita, H. & Takai, Y. in *Meth. Enzymol.* Vol. 406 415-424 (2006).
- 108 Pertz, O., Hodgson, L., Klemke, R. L. & Hahn, K. M. Spatiotemporal dynamics of RhoA activity in migrating cells. *Nature* **440**, 1069-1072, doi:10.1038/nature04665 (2006).
- 109 Nellore, A. *et al.* Loss of Rap1GAP in papillary thyroid cancer. *The Journal of clinical endocrinology and metabolism* **94**, 1026-1032, doi:10.1210/jc.2008-1042 (2009).
- 110 Tsygankova, O. M. *et al.* Downregulation of Rap1GAP contributes to Ras transformation. *Molecular and cellular biology* **27**, 6647-6658, doi:10.1128/MCB.00155-07 (2007).
- 111 Tsygankova, O. M., Wang, H. & Meinkoth, J. L. Tumor cell migration and invasion are enhanced by depletion of Rap1 GTPase-activating protein (Rap1GAP). *The Journal of biological chemistry* **288**, 24636-24646, doi:10.1074/jbc.M113.464594 (2013).
- 112 Yan, J., Li, F., Ingram, D. A. & Quilliam, L. A. in *Molecular and cellular biology* Vol. 28 5803-5810 (2008).
- 113 Wu, B. *et al.* in *J. Struct. Biol.* Vol. 180 84-95 (2012).
- 114 Miyata, M. *et al.* Regulation by afadin of cyclical activation and inactivation of Rap1, Rac1, and RhoA small G proteins at leading edges of moving NIH3T3 cells. *The Journal of biological chemistry* **284**, 24595-24609, doi:10.1074/jbc.M109.016436 (2009).
- 115 Fournier, G. *et al.* Loss of AF6/afadin, a marker of poor outcome in breast cancer, induces cell migration, invasiveness and tumor growth. *Oncogene* **30**, 3862-3874, doi:10.1038/onc.2011.106 (2011).
- 116 Liu, L. *et al.* Radil controls neutrophil adhesion and motility through beta2-integrin activation. *Molecular biology of the cell* **23**, 4751-4765, doi:10.1091/mbc.E12-05-0408 (2012).
- 117 Smolen, G. A. *et al.* A Rap GTPase interactor, RADIL, mediates migration of neural crest precursors. *Genes & development* **21**, 2131-2136, doi:10.1101/gad.1561507 (2007).
- 118 Xu, K., Chong, D. C., Rankin, S. A., Zorn, A. M. & Cleaver, O. Rasip1 is required for endothelial cell motility, angiogenesis and vessel formation. *Developmental biology* **329**, 269-279, doi:10.1016/j.ydbio.2009.02.033 (2009).
- 119 Minard, M. E., Kim, L. S., Price, J. E. & Gallick, G. E. The role of the guanine nucleotide exchange factor Tiam1 in cellular migration, invasion, adhesion and tumor progression. *Breast cancer research and treatment* **84**, 21-32, doi:10.1023/B:BREA.0000018421.31632.e6 (2004).
- 120 Yamanaka, T. *et al.* PAR-6 regulates aPKC activity in a novel way and mediates cell-cell contact-induced formation of the epithelial junctional complex. *Genes to cells : devoted to molecular & cellular mechanisms* **6**, 721-731 (2001).
- 121 Gotta, M., Abraham, M. C. & Ahringer, J. CDC-42 controls early cell polarity and spindle orientation in *C. elegans*. *Current biology : CB* **11**, 482-488 (2001).
- 122 Kay, A. J. & Hunter, C. P. CDC-42 regulates PAR protein localization and function to control cellular and embryonic polarity in *C. elegans*. *Current biology : CB* **11**, 474-481 (2001).
- 123 Yu, W. *et al.* Involvement of RhoA, ROCK I and myosin II in inverted orientation of epithelial polarity. *EMBO reports* **9**, 923-929, doi:10.1038/embor.2008.135 (2008).
- 124 Nakayama, M. *et al.* Rho-kinase phosphorylates PAR-3 and disrupts PAR complex formation. *Developmental cell* **14**, 205-215, doi:10.1016/j.devcel.2007.11.021 (2008).
- 125 Choi, W., Harris, N. J., Sumigray, K. D. & Peifer, M. Rap1 and Canoe/afadin are essential for establishment of apical-basal polarity in the *Drosophila* embryo. *Molecular biology of the cell* **24**, 945-963, doi:10.1091/mbc.E12-10-0736 (2013).
- 126 Lampugnani, M. G. *et al.* CCM1 regulates vascular-lumen organization by inducing endothelial polarity. *Journal of cell science* **123**, 1073-1080, doi:10.1242/jcs.059329 (2010).
- 127 Iden, S. *et al.* A distinct PAR complex associates physically with VE-cadherin in vertebrate endothelial cells. *EMBO reports* **7**, 1239-1246, doi:10.1038/sj.embor.7400819 (2006).

- 128 Qin, Y., Capaldo, C., Gumbiner, B. M. & Macara, I. G. The mammalian Scribble polarity protein regulates epithelial cell adhesion and migration through E-cadherin. *The Journal of cell biology* **171**, 1061-1071, doi:10.1083/jcb.200506094 (2005).
- 129 Imai, F. *et al.* Inactivation of aPKCλ results in the loss of adherens junctions in neuroepithelial cells without affecting neurogenesis in mouse neocortex. *Development* **133**, 1735-1744, doi:10.1242/dev.02330 (2006).
- 130 Pinheiro, E. M. & Montell, D. J. Requirement for Par-6 and Bazooka in Drosophila border cell migration. *Development* **131**, 5243-5251, doi:10.1242/dev.01412 (2004).
- 131 Harris, T. J. & Peifer, M. Adherens junction-dependent and -independent steps in the establishment of epithelial cell polarity in Drosophila. *The Journal of cell biology* **167**, 135-147, doi:10.1083/jcb.200406024 (2004).
- 132 Mandai, K. *et al.* Afadin: A novel actin filament-binding protein with one PDZ domain localized at cadherin-based cell-to-cell adherens junction. *The Journal of cell biology* **139**, 517-528 (1997).
- 133 Takaishi, K., Sasaki, T., Kotani, H., Nishioka, H. & Takai, Y. in *The Journal of cell biology* Vol. 139 1047-1059 (1997).
- 134 Komura, H. *et al.* Establishment of cell polarity by afadin during the formation of embryoid bodies. *Genes to cells : devoted to molecular & cellular mechanisms* **13**, 79-90, doi:10.1111/j.1365-2443.2007.01150.x (2008).
- 135 Ooshio, T. *et al.* Cooperative roles of Par-3 and afadin in the formation of adherens and tight junctions. *Journal of cell science* **120**, 2352-2365, doi:10.1242/jcs.03470 (2007).
- 136 Gerard, A., Mertens, A. E. E., van der Kammen, R. A. & Collard, J. G. in *The Journal of cell biology* Vol. 176 863-875 (2007).
- 137 Arimura, N. & Kaibuchi, K. Neuronal polarity: from extracellular signals to intracellular mechanisms. *Nature reviews. Neuroscience* **8**, 194-205, doi:10.1038/nrn2056 (2007).
- 138 Yamada, T., Sakisaka, T., Hisata, S., Baba, T. & Takai, Y. in *The Journal of biological chemistry* Vol. 280 33026-33034 (2005).
- 139 Jeon, C.-Y. *et al.* in *Experimental & molecular medicine* Vol. 42 335 (2010).
- 140 Jeon, C.-Y. *et al.* in *J. Cell. Physiol.* Vol. 224 786-794 (2010).
- 141 Krugmann, S. *et al.* Identification of ARAP3, a novel PI3K effector regulating both Arf and Rho GTPases, by selective capture on phosphoinositide affinity matrices. *Molecular cell* **9**, 95-108 (2002).
- 142 Shi, S. H., Jan, L. Y. & Jan, Y. N. Hippocampal neuronal polarity specified by spatially localized mPar3/mPar6 and PI 3-kinase activity. *Cell* **112**, 63-75 (2003).
- 143 Kang, P. J., Beven, L., Hariharan, S. & Park, H. O. The Rsr1/Bud1 GTPase interacts with itself and the Cdc42 GTPase during bud-site selection and polarity establishment in budding yeast. *Molecular biology of the cell* **21**, 3007-3016, doi:10.1091/mbc.E10-03-0232 (2010).
- 144 Park, H. O., Kang, P. J. & Rachfal, A. W. Localization of the Rsr1/Bud1 GTPase involved in selection of a proper growth site in yeast. *The Journal of biological chemistry* **277**, 26721-26724, doi:10.1074/jbc.C200245200 (2002).
- 145 Jaffe, A. B., Hall, A. & Schmidt, A. Association of CNK1 with Rho guanine nucleotide exchange factors controls signaling specificity downstream of Rho. *Current biology : CB* **15**, 405-412, doi:10.1016/j.cub.2004.12.082 (2005).
- 146 Manser, E. *et al.* PAK kinases are directly coupled to the PIX family of nucleotide exchange factors. *Molecular cell* **1**, 183-192 (1998).
- 147 Terry, S. J. *et al.* Spatially restricted activation of RhoA signalling at epithelial junctions by p114RhoGEF drives junction formation and morphogenesis. *Nature cell biology* **13**, 159-166, doi:10.1038/ncb2156 (2011).
- 148 Glading, A. J. & Ginsberg, M. H. Rap1 and its effector KRIT1/CCM1 regulate beta-catenin signaling. *Dis Model Mech* **3**, 73-83, doi:10.1242/dmm.003293 (2010).
- 149 Zhang, J., Clatterbuck, R. E., Rigamonti, D., Chang, D. D. & Dietz, H. C. Interaction between krit1 and icap1alpha infers perturbation of integrin beta1-mediated angiogenesis in the pathogenesis of cerebral cavernous malformation. *Human molecular genetics* **10**, 2953-2960 (2001).
- 150 Whitehead, K. J. *et al.* The cerebral cavernous malformation signaling pathway promotes vascular integrity via Rho GTPases. *Nature medicine* **15**, 177-184, doi:10.1038/nm.1911 (2009).
- 151 Hart, M. J., Callow, M. G., Souza, B. & Polakis, P. IQGAP1, a calmodulin-binding protein with a rasGAP-related domain, is a potential effector for cdc42Hs. *The EMBO journal* **15**, 2997-3005 (1996).
- 152 Jeong, H.-W., Li, Z., Brown, M. D. & Sacks, D. B. in *The Journal of biological chemistry* Vol. 282 20752-20762 (2007).

- 153 Joyal, J. L. *et al.* Calmodulin modulates the interaction between IQGAP1 and Cdc42. Identification of
IQGAP1 by nano-electrospray tandem mass spectrometry. *The Journal of biological chemistry* **272**,
15419-15425 (1997).
- 154 Kortholt, A. *et al.* A Rap/phosphatidylinositol 3-kinase pathway controls pseudopod formation
[corrected]. *Molecular biology of the cell* **21**, 936-945, doi:10.1091/mbc.E09-03-0177 (2010).
- 155 Murga, C., Zohar, M., Teramoto, H. & Gutkind, J. S. Rac1 and RhoG promote cell survival by the activation
of PI3K and Akt, independently of their ability to stimulate JNK and NF-kappaB. *Oncogene* **21**, 207-216,
doi:10.1038/sj.onc.1205036 (2002).
- 156 Montresor, A. *et al.* JAK tyrosine kinases promote hierarchical activation of Rho and Rap modules of
integrin activation. *The Journal of cell biology* **203**, 1003-1019, doi:10.1083/jcb.201303067 (2013).
- 157 Caloca, M. J., Zugaza, J. L., Vicente-Manzanares, M., Sanchez-Madrid, F. & Bustelo, X. R. F-actin-
dependent translocation of the Rap1 GDP/GTP exchange factor RasGRP2. *The Journal of biological
chemistry* **279**, 20435-20446, doi:10.1074/jbc.M313013200 (2004).
- 158 Maheshwari, G., Brown, G., Lauffenburger, D. A., Wells, A. & Griffith, L. G. Cell adhesion and motility
depend on nanoscale RGD clustering. *Journal of cell science* **113 (Pt 10)**, 1677-1686 (2000).
- 159 Geiger, B., Bershadsky, A., Pankov, R. & Yamada, K. M. Transmembrane crosstalk between the
extracellular matrix-cytoskeleton crosstalk. *Nature reviews. Molecular cell biology* **2**, 793-805,
doi:10.1038/35099066 (2001).
- 160 Ginsberg, M. H., Partridge, A. & Shattil, S. J. Integrin regulation. *Current opinion in cell biology* **17**, 509-
516, doi:10.1016/j.ceb.2005.08.010 (2005).
- 161 Luo, B. H., Carman, C. V. & Springer, T. A. Structural basis of integrin regulation and signaling. *Annual
review of immunology* **25**, 619-647, doi:10.1146/annurev.immunol.25.022106.141618 (2007).
- 162 Caron, E. Cellular functions of the Rap1 GTP-binding protein: a pattern emerges. *Journal of cell science*
116, 435-440 (2003).
- 163 Bos, J. L. *et al.* The role of Rap1 in integrin-mediated cell adhesion. *Biochemical Society transactions* **31**,
83-86, doi:10.1042/ (2003).
- 164 Boettner, B. & Van Aelst, L. Control of cell adhesion dynamics by Rap1 signaling. *Current opinion in cell
biology* **21**, 684-693, doi:10.1016/j.ceb.2009.06.004 (2009).
- 165 Bos, J. L. Linking Rap to cell adhesion. *Current opinion in cell biology* **17**, 123-128, doi:10.1016/j.
ceb.2005.02.009 (2005).
- 166 Kinbara, K., Goldfinger, L. E., Hansen, M., Chou, F. L. & Ginsberg, M. H. Ras GTPases: integrins' friends or
foes? *Nature reviews. Molecular cell biology* **4**, 767-776, doi:10.1038/nrm1229 (2003).
- 167 Fukuhara, S. *et al.* Cyclic AMP potentiates vascular endothelial cadherin-mediated cell-cell contact to
enhance endothelial barrier function through an Epac-Rap1 signaling pathway. *Molecular and cellular
biology* **25**, 136-146, doi:10.1128/MCB.25.1.136-146.2005 (2005).
- 168 Kooistra, M. R., Dube, N. & Bos, J. L. Rap1: a key regulator in cell-cell junction formation. *Journal of cell
science* **120**, 17-22, doi:10.1242/jcs.03306 (2007).
- 169 Lyle, K. S., Raaijmakers, J. H., Bruinsma, W., Bos, J. L. & de Rooij, J. cAMP-induced Epac-Rap activation
inhibits epithelial cell migration by modulating focal adhesion and leading edge dynamics. *Cellular
signalling* **20**, 1104-1116, doi:10.1016/j.cellsig.2008.01.018 (2008).
- 170 Tsukamoto, N., Hattori, M., Yang, H., Bos, J. L. & Minato, N. Rap1 GTPase-activating protein SPA-1
negatively regulates cell adhesion. *The Journal of biological chemistry* **274**, 18463-18469 (1999).
- 171 de Bruyn, K. M., Rangarajan, S., Reedquist, K. A., Figdor, C. G. & Bos, J. L. The small GTPase Rap1 is
required for Mn(2+)- and antibody-induced LFA-1- and VLA-4-mediated cell adhesion. *The Journal of
biological chemistry* **277**, 29468-29476, doi:10.1074/jbc.M204990200 (2002).
- 172 Lafuente, E. & Boussiotis, V. A. Rap1 regulation of RIAM and cell adhesion. *Methods in enzymology* **407**,
345-358, doi:10.1016/S0076-6879(05)07029-1 (2006).
- 173 Watanabe, N. *et al.* Mechanisms and consequences of agonist-induced talin recruitment to platelet
integrin alphaIIb beta3. *The Journal of cell biology* **181**, 1211-1222, doi:10.1083/jcb.200803094 (2008).
- 174 Ebisuno, Y. *et al.* Rap1 controls lymphocyte adhesion cascade and interstitial migration within
lymph nodes in RAPL-dependent and -independent manners. *Blood* **115**, 804-814, doi:10.1182/
blood-2009-03-211979 (2010).
- 175 Katagiri, K., Imamura, M. & Kinashi, T. Spatiotemporal regulation of the kinase Mst1 by binding protein
RAPL is critical for lymphocyte polarity and adhesion. *Nature immunology* **7**, 919-928, doi:10.1038/
ni1374 (2006).
- 176 Kinashi, T. & Katagiri, K. Regulation of lymphocyte adhesion and migration by the small GTPase Rap1 and
its effector molecule, RAPL. *Immunology letters* **93**, 1-5, doi:10.1016/j.imlet.2004.02.008 (2004).

- 177 Miertzschke, M. *et al.* Characterization of interactions of adapter protein RAPL/Nore1B with RAP GTPases and their role in T cell migration. *The Journal of biological chemistry* **282**, 30629-30642, doi:10.1074/jbc.M704361200 (2007).
- 178 Raaijmakers, J. H. *et al.* The PI3K effector Arap3 interacts with the PI(3,4,5)P3 phosphatase SHIP2 in a SAM domain-dependent manner. *Cellular signalling* **19**, 1249-1257, doi:10.1016/j.cellsig.2006.12.015 (2007).
- 179 Arthur, W. T., Quilliam, L. A. & Cooper, J. A. Rap1 promotes cell spreading by localizing Rac guanine nucleotide exchange factors. *The Journal of cell biology* **167**, 111-122, doi:10.1083/jcb.200404068 (2004).
- 180 Boettner, B., Govek, E. E., Cross, J. & Van Aelst, L. The junctional multidomain protein AF-6 is a binding partner of the Rap1A GTPase and associates with the actin cytoskeletal regulator profilin. *Proceedings of the National Academy of Sciences of the United States of America* **97**, 9064-9069 (2000).
- 181 Zhang, Z., Rehmann, H., Price, L. S., Riedl, J. & Bos, J. L. AF6 negatively regulates Rap1-induced cell adhesion. *The Journal of biological chemistry* **280**, 33200-33205, doi:10.1074/jbc.M505057200 (2005).
- 182 Ahmed, S. M., Daulat, A. M., Meunier, A. & Angers, S. G protein betagamma subunits regulate cell adhesion through Rap1a and its effector Radil. *J Biol Chem* **285**, 6538-6551, doi:M109.069948 [pii] 10.1074/jbc.M109.069948 (2010).
- 183 Raaijmakers, J. H. & Bos, J. L. Specificity in Ras and Rap signaling. *J Biol Chem* **284**, 10995-10999, doi:10.1074/jbc.R800061200 (2009).
- 184 Frische, E. W. *et al.* RAP-1 and the RAL-1/exocyst pathway coordinate hypodermal cell organization in *Caenorhabditis elegans*. *EMBO J* **26**, 5083-5092, doi:7601922 [pii] 10.1038/sj.emboj.7601922 (2007).
- 185 Glocier, M. *et al.* Spatial regulation of cyclic AMP-Epac1 signaling in cell adhesion by ERM proteins. *Molecular and cellular biology* **30**, 5421-5431, doi:10.1128/MCB.00463-10 (2010).
- 186 Gautreau, A., Louvard, D. & Arpin, M. Morphogenic effects of ezrin require a phosphorylation-induced transition from oligomers to monomers at the plasma membrane. *The Journal of cell biology* **150**, 193-203 (2000).
- 187 Matsui, T. *et al.* Rho-kinase phosphorylates COOH-terminal threonines of ezrin/radixin/moesin (ERM) proteins and regulates their head-to-tail association. *The Journal of cell biology* **140**, 647-657 (1998).
- 188 Naba, A., Reverd, C., Louvard, D. & Arpin, M. Spatial recruitment and activation of the Fes kinase by ezrin promotes HGF-induced cell scattering. *The EMBO journal* **27**, 38-50, doi:10.1038/sj.emboj.7601943 (2008).
- 189 Srivastava, J., Elliott, B. E., Louvard, D. & Arpin, M. Src-dependent ezrin phosphorylation in adhesion-mediated signaling. *Molecular biology of the cell* **16**, 1481-1490, doi:10.1091/mbc.E04-08-0721 (2005).
- 190 Algrain, M., Turunen, O., Vaheri, A., Louvard, D. & Arpin, M. Ezrin contains cytoskeleton and membrane binding domains accounting for its proposed role as a membrane-cytoskeletal linker. *The Journal of cell biology* **120**, 129-139 (1993).
- 191 Granes, F., Urena, J. M., Rocamora, N. & Vilaro, S. Ezrin links syndecan-2 to the cytoskeleton. *Journal of cell science* **113 (Pt 7)**, 1267-1276 (2000).
- 192 Granes, F. *et al.* Identification of a novel Ezrin-binding site in syndecan-2 cytoplasmic domain. *FEBS letters* **547**, 212-216 (2003).
- 193 Heiska, L. *et al.* Association of ezrin with intercellular adhesion molecule-1 and -2 (ICAM-1 and ICAM-2). Regulation by phosphatidylinositol 4, 5-bisphosphate. *The Journal of biological chemistry* **273**, 21893-21900 (1998).
- 194 Helander, T. S. *et al.* ICAM-2 redistributed by ezrin as a target for killer cells. *Nature* **382**, 265-268, doi:10.1038/382265a0 (1996).
- 195 Hirao, M. *et al.* Regulation mechanism of ERM (ezrin/radixin/moesin) protein/plasma membrane association: possible involvement of phosphatidylinositol turnover and Rho-dependent signaling pathway. *The Journal of cell biology* **135**, 37-51 (1996).
- 196 Tsukita, S. *et al.* ERM family members as molecular linkers between the cell surface glycoprotein CD44 and actin-based cytoskeletons. *The Journal of cell biology* **126**, 391-401 (1994).
- 197 Yonemura, S. *et al.* Ezrin/radixin/moesin (ERM) proteins bind to a positively charged amino acid cluster in the juxta-membrane cytoplasmic domain of CD44, CD43, and ICAM-2. *The Journal of cell biology* **140**, 885-895 (1998).
- 198 Fehon, R. G., McClatchey, A. I. & Bretscher, A. Organizing the cell cortex: the role of ERM proteins. *Nature reviews. Molecular cell biology* **11**, 276-287, doi:10.1038/nrm2866 (2010).
- 199 Fievet, B., Louvard, D. & Arpin, M. ERM proteins in epithelial cell organization and functions. *Biochimica et biophysica acta* **1773**, 653-660, doi:10.1016/j.bbamcr.2006.06.013 (2007).

- 200 Louvet-Vallée, S. ERM proteins: from cellular architecture to cell signaling. *Biology of the cell / under the*
auspices of the European Cell Biology Organization **92**, 305-316 (2000).
- 201 Delon, J., Kaibuchi, K. & Germain, R. N. Exclusion of CD43 from the immunological synapse is mediated
by phosphorylation-regulated relocation of the cytoskeletal adaptor moesin. *Immunity* **15**, 691-701
(2001).
- 202 Faure, S. *et al.* ERM proteins regulate cytoskeleton relaxation promoting T cell-APC conjugation. *Nature*
immunology **5**, 272-279, doi:10.1038/ni1039 (2004).
- 203 Treanor, B. *et al.* The membrane skeleton controls diffusion dynamics and signaling through the B cell
receptor. *Immunity* **32**, 187-199, doi:10.1016/j.immuni.2009.12.005 (2010).
- 204 Hiscox, S. & Jiang, W. G. Ezrin regulates cell-cell and cell-matrix adhesion, a possible role with E-cadherin/
beta-catenin. *Journal of cell science* **112 Pt 18**, 3081-3090 (1999).
- 205 Martin, M. *et al.* Ezrin NH2-terminal domain inhibits the cell extension activity of the COOH-terminal
domain. *The Journal of cell biology* **128**, 1081-1093 (1995).
- 206 Osawa, H., Smith, C. A., Ra, Y. S., Kongkham, P. & Rutka, J. T. The role of the membrane cytoskeleton
cross-linker ezrin in medulloblastoma cells. *Neuro-oncology* **11**, 381-393, doi:10.1215/15228517-2008-
110 (2009).
- 207 Takeuchi, K. *et al.* Perturbation of cell adhesion and microvilli formation by antisense oligonucleotides
to ERM family members. *The Journal of cell biology* **125**, 1371-1384 (1994).
- 208 Wan, X. *et al.* Beta4 integrin promotes osteosarcoma metastasis and interacts with ezrin. *Oncogene* **28**,
3401-3411, doi:10.1038/onc.2009.206 (2009).
- 209 Orian-Rousseau, V. *et al.* Hepatocyte growth factor-induced Ras activation requires ERM proteins linked
to both CD44v6 and F-actin. *Molecular biology of the cell* **18**, 76-83, doi:10.1091/mbc.E06-08-0674
(2007).
- 210 Tremmel, M. *et al.* A CD44v6 peptide reveals a role of CD44 in VEGFR-2 signaling and angiogenesis.
Blood **114**, 5236-5244, doi:10.1182/blood-2009-04-219204 (2009).
- 211 Price, L. S. *et al.* Rap1 regulates E-cadherin-mediated cell-cell adhesion. *The Journal of biological*
chemistry **279**, 35127-35132, doi:10.1074/jbc.M404917200 (2004).
- 212 Zwartkruis, F. J., Wolthuis, R. M., Nabben, N. M., Franke, B. & Bos, J. L. Extracellular signal-regulated
activation of Rap1 fails to interfere in Ras effector signalling. *The EMBO journal* **17**, 5905-5912,
doi:10.1093/emboj/17.20.5905 (1998).
- 213 Schwartz, M. A. & Denninghoff, K. Alpha v integrins mediate the rise in intracellular calcium in endothelial
cells on fibronectin even though they play a minor role in adhesion. *The Journal of biological chemistry*
269, 11133-11137 (1994).
- 214 Medema, R. H., de Laat, W. L., Martin, G. A., McCormick, F. & Bos, J. L. GTPase-activating protein SH2-
SH3 domains induce gene expression in a Ras-dependent fashion. *Molecular and cellular biology* **12**,
3425-3430 (1992).
- 215 Franke, B., Akkerman, J. W. & Bos, J. L. Rapid Ca²⁺-mediated activation of Rap1 in human platelets. *The*
EMBO journal **16**, 252-259, doi:10.1093/emboj/16.2.252 (1997).
- 216 Gloerich, M. & Bos, J. L. Regulating Rap small G-proteins in time and space. *Trends Cell Biol* **21**, 615-623,
doi:S0962-8924(11)00135-8 [pii] 10.1016/j.tcb.2011.07.001 (2011).
- 217 Consonni, S. V., Gloerich, M., Spanjaard, E. & Bos, J. L. cAMP regulates DEP domain-mediated binding of
the guanine nucleotide exchange factor Epac1 to phosphatidic acid at the plasma membrane. *Proc Natl*
Acad Sci U S A **109**, 3814-3819, doi:10.1073/pnas.1117599109 (2012).
- 218 Gloerich, M. *et al.* The nucleoporin RanBP2 tethers the cAMP effector Epac1 and inhibits its catalytic
activity. *J Cell Biol* **193**, 1009-1020, doi:jcb.201011126 [pii] 10.1083/jcb.201011126 (2011).
- 219 Gupta, M. & Yarwood, S. J. MAP1A light chain 2 interacts with exchange protein activated by cyclic AMP
1 (EPAC1) to enhance Rap1 GTPase activity and cell adhesion. *The Journal of biological chemistry* **280**,
8109-8116, doi:10.1074/jbc.M413697200 (2005).
- 220 Mangmool, S., Shukla, A. K. & Rockman, H. A. beta-Arrestin-dependent activation of Ca(2+)/calmodulin
kinase II after beta(1)-adrenergic receptor stimulation. *The Journal of cell biology* **189**, 573-587,
doi:10.1083/jcb.200911047 (2010).
- 221 Ponsioen, B. *et al.* Direct spatial control of Epac1 by cyclic AMP. *Mol Cell Biol* **29**, 2521-2531, doi:10.1128/
MCB.01630-08 (2009).
- 222 Niggli, V. & Rossy, J. Ezrin/radixin/moesin: versatile controllers of signaling molecules and of the
cortical cytoskeleton. *Int J Biochem Cell Biol* **40**, 344-349, doi:S1357-2725(07)00059-3 [pii] 10.1016/j.
biocel.2007.02.012 (2008).
- 223 Fievet, B. T. *et al.* Phosphoinositide binding and phosphorylation act sequentially in the activation

- mechanism of ezrin. *The Journal of cell biology* **164**, 653-659, doi:10.1083/jcb.200307032 (2004).
- 224 Oude Weernink, P. A. *et al.* Stimulation of phosphatidylinositol-4-phosphate 5-kinase by Rho-kinase. *The Journal of biological chemistry* **275**, 10168-10174 (2000).
- 225 Parameswaran, N., Matsui, K. & Gupta, N. Conformational switching in ezrin regulates morphological and cytoskeletal changes required for B cell chemotaxis. *Journal of immunology* **186**, 4088-4097, doi:10.4049/jimmunol.1001139 (2011).
- 226 Treanor, B., Depoil, D., Bruckbauer, A. & Batista, F. D. Dynamic cortical actin remodeling by ERM proteins controls BCR microcluster organization and integrity. *The Journal of experimental medicine* **208**, 1055-1068, doi:10.1084/jem.20101125 (2011).
- 227 Machacek, M. *et al.* Coordination of Rho GTPase activities during cell protrusion. *Nature* **461**, 99-103, doi:10.1038/nature08242 (2009).
- 228 Cullere, X. *et al.* Regulation of vascular endothelial barrier function by Epac, a cAMP-activated exchange factor for Rap GTPase. *Blood* **105**, 1950-1955, doi:10.1182/blood-2004-05-1987 (2005).
- 229 Pannekoek, W. J. *et al.* Epac1 and PDZ-GEF cooperate in Rap1 mediated endothelial junction control. *Cellular Signalling* **23**, 2056-2064, doi:DOI 10.1016/j.cellsig.2011.07.022 (2011).
- 230 Wittchen, E. S., Aghajanian, A. & Burrigide, K. Isoform-specific differences between Rap1A and Rap1B GTPases in the formation of endothelial cell junctions. *Small GTPases* **2**, 65-76, doi:10.4161/sgtp.2.2.15735 (2011).
- 231 Wittchen, E. S. *et al.* Rap1 GTPase inhibits leukocyte transmigration by promoting endothelial barrier function. *The Journal of biological chemistry* **280**, 11675-11682, doi:10.1074/jbc.M412595200 (2005).
- 232 Knox, A. L. & Brown, N. H. Rap1 GTPase regulation of adherens junction positioning and cell adhesion. *Science* **295**, 1285-1288, doi:10.1126/science.1067549 (2002).
- 233 Baluk, P., Hashizume, H. & McDonald, D. M. Cellular abnormalities of blood vessels as targets in cancer. *Current opinion in genetics & development* **15**, 102-111, doi:10.1016/j.gde.2004.12.005 (2005).
- 234 Bazzoni, G. & Dejana, E. Endothelial cell-to-cell junctions: molecular organization and role in vascular homeostasis. *Physiological reviews* **84**, 869-901, doi:10.1152/physrev.00035.2003 (2004).
- 235 Weis, S. M. Vascular permeability in cardiovascular disease and cancer. *Current opinion in hematology* **15**, 243-249, doi:10.1097/MOH.0b013e3282f97d86 (2008).
- 236 Glading, A., Han, J., Stockton, R. A. & Ginsberg, M. H. KRIT-1/CCM1 is a Rap1 effector that regulates endothelial cell cell junctions. *J Cell Biol* **179**, 247-254, doi:jcb.200705175 [pii] 10.1083/jcb.200705175 (2007).
- 237 Lorenowicz, M. J., Fernandez-Borja, M., Kooistra, M. R., Bos, J. L. & Hordijk, P. L. PKA and Epac1 regulate endothelial integrity and migration through parallel and independent pathways. *European journal of cell biology* **87**, 779-792, doi:10.1016/j.ejcb.2008.05.004 (2008).
- 238 Birukova, A. A. *et al.* Rac GTPase is a hub for protein kinase A and Epac signaling in endothelial barrier protection by cAMP. *Microvasc Res* **79**, 128-138, doi:10.1016/j.mvr.2009.11.007 (2010).
- 239 Sehrawat, S., Cullere, X., Patel, S., Italiano, J., Jr. & Mayadas, T. N. Role of Epac1, an exchange factor for Rap GTPases, in endothelial microtubule dynamics and barrier function. *Molecular biology of the cell* **19**, 1261-1270, doi:10.1091/mbc.E06-10-0972 (2008).
- 240 Mitin, N. Y. *et al.* Identification and characterization of rain, a novel Ras-interacting protein with a unique subcellular localization. *J Biol Chem* **279**, 22353-22361, doi:10.1074/jbc.M312867200 M312867200 [pii] (2004).
- 241 Saras, J. *et al.* A novel GTPase-activating protein for Rho interacts with a PDZ domain of the protein-tyrosine phosphatase PTPL1. *J Biol Chem* **272**, 24333-24338 (1997).
- 242 Carey SP, C. J., and Reinhart-King CA. in *Cellular and Biomolecular Mechanics and Mechanobiology* (ed Gefen A.) 29-69 (Springer Berlin Heidelberg, 2011).
- 243 Ratheesh, A. *et al.* Centralspindlin and alpha-catenin regulate Rho signalling at the epithelial zonula adherens. *Nat Cell Biol* **14**, 818-828, doi:10.1038/ncb2532 (2012).
- 244 Kher, S. S. & Worthylake, R. A. Nuanced junctional RhoA activity. *Nat Cell Biol* **14**, 784-786, doi:10.1038/ncb2553 (2012).
- 245 Smutny, M. *et al.* Myosin II isoforms identify distinct functional modules that support integrity of the epithelial zonula adherens. *Nature cell biology* **12**, 696-702, doi:10.1038/ncb2072 (2010).
- 246 Vliem, M. J. *et al.* 8-pCPT-2'-O-Me-cAMP-AM: an improved Epac-selective cAMP analogue. *Chembiochem* **9**, 2052-2054, doi:10.1002/cbic.200800216 (2008).
- 247 van Triest, M. & Bos, J. L. Pull-down assays for guanoside 5'-triphosphate-bound Ras-like guanosine 5'-triphosphatases. *Methods Mol Biol* **250**, 97-102, doi:10.1385/1-59259-671-1:97 (2004).
- 248 Wittchen, E. S. & Hartnett, M. E. The small GTPase Rap1 is a novel regulator of RPE cell barrier function.

- 249 *Investigative ophthalmology & visual science* **52**, 7455-7463, doi:10.1167/iovs.11-7295 (2011).
- Beckers, C. M., van Hinsbergh, V. W. & van Nieuw Amerongen, G. P. Driving Rho GTPase activity in endothelial cells regulates barrier integrity. *Thrombosis and haemostasis* **103**, 40-55, doi:10.1160/TH09-06-0403 (2010).
- 250 Spindler, V., Schlegel, N. & Waschke, J. Role of GTPases in control of microvascular permeability. *Cardiovascular research* **87**, 243-253, doi:10.1093/cvr/cvq086 (2010).
- 251 Szulcek, R. *et al.* Localized RhoA GTPase activity regulates dynamics of endothelial monolayer integrity. *Cardiovascular research* **99**, 471-482, doi:10.1093/cvr/cvt075 (2013).
- 252 Dube, N. *et al.* The RapGEF PDZ-GEF2 is required for maturation of cell-cell junctions. *Cell Signal* **20**, 1608-1615, doi:DOI 10.1016/j.cellsig.2008.05.006 (2008).
- 253 Wohlgemuth, S. *et al.* Recognizing and defining true Ras binding domains I: biochemical analysis. *Journal of molecular biology* **348**, 741-758, doi:10.1016/j.jmb.2005.02.048 (2005).
- 254 Birkenfeld, J. *et al.* GEF-H1 modulates localized RhoA activation during cytokinesis under the control of mitotic kinases. *Developmental cell* **12**, 699-712, doi:10.1016/j.devcel.2007.03.014 (2007).
- 255 Pannekoek, W. J., Kooistra, M. R., Zwartkruis, F. J. & Bos, J. L. Cell-cell junction formation: the role of Rap1 and Rap1 guanine nucleotide exchange factors. *Biochim Biophys Acta* **1788**, 790-796, doi:S0005-2736(08)00403-3 [pii] 10.1016/j.bbamem.2008.12.010 (2009).
- 256 Chrzanoska-Wodnicka, M. Distinct functions for Rap1 signaling in vascular morphogenesis and dysfunction. *Exp Cell Res* **319**, 2350-2359, doi:10.1016/j.yexcr.2013.07.022 (2013).
- 257 Komarova, Y. & Malik, A. B. Regulation of endothelial permeability via paracellular and transcellular transport pathways. *Annual review of physiology* **72**, 463-493, doi:10.1146/annurev-physiol-021909-135833 (2010).
- 258 Dejana, E., Tournier-Lasserre, E. & Weinstein, B. M. The control of vascular integrity by endothelial cell junctions: molecular basis and pathological implications. *Dev Cell* **16**, 209-221, doi:10.1016/j.devcel.2009.01.004 (2009).
- 259 Pannekoek, W. J. *et al.* Epac1 and PDZ-GEF cooperate in Rap1 mediated endothelial junction control. *Cell Signal* **23**, 2056-2064, doi:10.1016/j.cellsig.2011.07.022 (2011).
- 260 Yan, J., Li, F., Ingram, D. A. & Quilliam, L. A. Rap1a is a key regulator of fibroblast growth factor 2-induced angiogenesis and together with Rap1b controls human endothelial cell functions. *Mol Cell Biol* **28**, 5803-5810, doi:10.1128/MCB.00393-08 (2008).
- 261 Adamson, R. H. *et al.* Epac/Rap1 pathway regulates microvascular hyperpermeability induced by PAF in rat mesentery. *American journal of physiology. Heart and circulatory physiology* **294**, H1188-1196, doi:10.1152/ajpheart.00937.2007 (2008).
- 262 Lakshmikanthan, S. *et al.* Rap1 promotes VEGFR2 activation and angiogenesis by a mechanism involving integrin α 5 β 3. *Blood* **118**, 2015-2026, doi:10.1182/blood-2011-04-349282 (2011).
- 263 Prior, I. A. & Hancock, J. F. Ras trafficking, localization and compartmentalized signalling. *Seminars in cell & developmental biology* **23**, 145-153, doi:10.1016/j.semcdb.2011.09.002 (2012).
- 264 Vandenbroucke, E., Mehta, D., Minshall, R. & Malik, A. B. Regulation of endothelial junctional permeability. *Annals of the New York Academy of Sciences* **1123**, 134-145, doi:10.1196/annals.1420.016 (2008).
- 265 Curry, F. R. & Adamson, R. H. Tonic regulation of vascular permeability. *Acta Physiol (Oxf)* **207**, 628-649, doi:10.1111/apha.12076 (2013).
- 266 Birukova, A. A., Tian, X., Tian, Y., Higginbotham, K. & Birukov, K. G. Rap-afadin axis in control of Rho signaling and endothelial barrier recovery. *Mol Biol Cell* **24**, 2678-2688, doi:10.1091/mbc.E13-02-0098 (2013).
- 267 Karlsen, T. V. *et al.* Microvascular permeability in the absence of Epac1 activity *FASEB J* **26** (2012).
- 268 Satyanarayana, A. *et al.* RapGEF2 is essential for embryonic hematopoiesis but dispensable for adult hematopoiesis. *Blood* **116**, 2921-2931, doi:10.1182/blood-2010-01-262964 (2010).
- 269 Wei, P. *et al.* Defective vascular morphogenesis and mid-gestation embryonic death in mice lacking RA-GEF-1. *Biochem Biophys Res Commun* **363**, 106-112, doi:S0006-291X(07)01845-1 [pii] 10.1016/j.bbrc.2007.08.149 (2007).
- 270 Kanemura, H. *et al.* Impaired vascular development in the yolk sac and allantois in mice lacking RA-GEF-1. *Biochem Biophys Res Commun* **387**, 754-759, doi:S0006-291X(09)01469-7 [pii] 10.1016/j.bbrc.2009.07.108 (2009).
- 271 Kuiperij, H. B. *et al.* Characterisation of PDZ-GEFs, a family of guanine nucleotide exchange factors specific for Rap1 and Rap2. *Biochim Biophys Acta* **1593**, 141-149, doi:S0167488902003658 [pii] (2003).
- 272 Pham, N. *et al.* The guanine nucleotide exchange factor CNrasGEF activates ras in response to cAMP and

- cGMP. *Curr Biol* **10**, 555-558 (2000).
- 273 Carey, S. P., Charest, J. M. & Reinhart/King, C. A. *Forces during cell adhesion and spreading: implications for cellular homeostasis*. 1st edition edn, Vol. 4 (2011).
- 274 Jacobson, J. R. *et al.* Endothelial cell barrier enhancement by ATP is mediated by the small GTPase Rac and cortactin. *American journal of physiology. Lung cellular and molecular physiology* **291**, L289-295, doi:10.1152/ajplung.00343.2005 (2006).
- 275 Schnoor, M. *et al.* Cortactin deficiency is associated with reduced neutrophil recruitment but increased vascular permeability in vivo. *J Exp Med* **208**, 1721-1735, doi:10.1084/jem.20101920 (2011).
- 276 Ichiba, T. *et al.* Activation of C3G guanine nucleotide exchange factor for Rap1 by phosphorylation of tyrosine 504. *J Biol Chem* **274**, 14376-14381 (1999).
- 277 Oh, J. *et al.* Tissue inhibitors of metalloproteinase 2 inhibits endothelial cell migration through increased expression of RECK. *Cancer research* **64**, 9062-9069, doi:10.1158/0008-5472.CAN-04-1981 (2004).
- 278 Stoletov, K. V., Gong, C. & Terman, B. I. Nck and Crk mediate distinct VEGF-induced signaling pathways that serve overlapping functions in focal adhesion turnover and integrin activation. *Exp Cell Res* **295**, 258-268, doi:10.1016/j.yexcr.2004.01.008 (2004).
- 279 Tawa, H. *et al.* Role of afadin in vascular endothelial growth factor- and sphingosine 1-phosphate-induced angiogenesis. *Circulation research* **106**, 1731-1742, doi:10.1161/CIRCRESAHA.110.216747 (2010).
- 280 Hogan, C. *et al.* Rap1 regulates the formation of E-cadherin-based cell-cell contacts. *Mol Cell Biol* **24**, 6690-6700, doi:10.1128/MCB.24.15.6690-6700.2004 (2004).
- 281 Farmer, P. J. *et al.* Permeability of endothelial monolayers to albumin is increased by bradykinin and inhibited by prostaglandins. *American journal of physiology. Lung cellular and molecular physiology* **280**, L732-738 (2001).
- 282 Kato, J., Tsuruda, T., Kita, T., Kitamura, K. & Eto, T. Adrenomedullin: a protective factor for blood vessels. *Arteriosclerosis, thrombosis, and vascular biology* **25**, 2480-2487, doi:10.1161/01.ATV.0000184759.91369.f8 (2005).
- 283 Birukova, A. A. *et al.* Prostaglandins PGE(2) and PGI(2) promote endothelial barrier enhancement via PKA- and Epac1/Rap1-dependent Rac activation. *Exp Cell Res* **313**, 2504-2520, doi:10.1006/j.yexcr.2007.03.036 (2007).
- 284 de Rooij, J. *et al.* Epac is a Rap1 guanine-nucleotide-exchange factor directly activated by cyclic AMP. *Nature* **396**, 474-477, doi:10.1038/24884 (1998).
- 285 Rehmann, H. *et al.* Structure of Epac2 in complex with a cyclic AMP analogue and RAP1B. *Nature* **455**, 124-127, doi:10.1038/nature07187 (2008).
- 286 Rehmann, H., Das, J., Knipscheer, P., Wittinghofer, A. & Bos, J. L. Structure of the cyclic-AMP-responsive exchange factor Epac2 in its auto-inhibited state. *Nature* **439**, 625-628, doi:10.1038/nature04468 (2006).
- 287 Fang, Y. & Olah, M. E. Cyclic AMP-dependent, protein kinase A-independent activation of extracellular signal-regulated kinase 1/2 following adenosine receptor stimulation in human umbilical vein endothelial cells: role of exchange protein activated by cAMP 1 (Epac1). *The Journal of pharmacology and experimental therapeutics* **322**, 1189-1200, doi:10.1124/jpet.107.119933 (2007).
- 288 Ponsioen, B. *et al.* Detecting cAMP-induced Epac activation by fluorescence resonance energy transfer: Epac as a novel cAMP indicator. *EMBO reports* **5**, 1176-1180, doi:10.1038/sj.embor.7400290 (2004).
- 289 Sehrawat, S. *et al.* AKAP9 regulation of microtubule dynamics promotes Epac1-induced endothelial barrier properties. *Blood* **117**, 708-718, doi:10.1182/blood-2010-02-268870 (2011).
- 290 Orlova, V. V., Economopoulou, M., Lupu, F., Santoso, S. & Chavakis, T. Junctional adhesion molecule-C regulates vascular endothelial permeability by modulating VE-cadherin-mediated cell-cell contacts. *J Exp Med* **203**, 2703-2714, doi:10.1084/jem.20051730 (2006).
- 291 Huveneers, S. & de Rooij, J. Mechanosensitive systems at the cadherin-F-actin interface. *J Cell Sci* **126**, 403-413, doi:10.1242/jcs.109447 (2013).
- 292 Levayer, R. & Lecuit, T. Biomechanical regulation of contractility: spatial control and dynamics. *Trends Cell Biol* **22**, 61-81, doi:10.1016/j.tcb.2011.10.001 (2012).
- 293 Totsukawa, G. *et al.* Distinct roles of ROCK (Rho-kinase) and MLCK in spatial regulation of MLC phosphorylation for assembly of stress fibers and focal adhesions in 3T3 fibroblasts. *J Cell Biol* **150**, 797-806 (2000).
- 294 Jeon, C. Y. *et al.* p190RhoGAP and Rap-dependent RhoGAP (ARAP3) inactivate RhoA in response to nerve growth factor leading to neurite outgrowth from PC12 cells. *Experimental & molecular medicine* **42**, 335-344 (2010).

295 Riedl, J. A. *et al.* Down-regulation of Rap1 activity is involved in ephrinB1-induced cell contraction. *Biochem J* **389**, 465-469, doi:BJ20050048 [pii] 10.1042/BJ20050048 (2005).

296 Rufanova, V. A., Alexanian, A., Wakatsuki, T., Lerner, A. & Sorokin, A. Pyk2 mediates endothelin-1 signaling via p130Cas/BCAR3 cascade and regulates human glomerular mesangial cell adhesion and spreading. *J Cell Physiol* **219**, 45-56, doi:10.1002/jcp.21649 (2009).

297 Vielkind, S., Gallagher-Gambarelli, M., Gomez, M., Hinton, H. J. & Cantrell, D. A. Integrin regulation by RhoA in thymocytes. *J Immunol* **175**, 350-357 (2005).

298 Yamada, T., Sakisaka, T., Hisata, S., Baba, T. & Takai, Y. RA-RhoGAP, Rap-activated Rho GTPase-activating protein implicated in neurite outgrowth through Rho. *J Biol Chem* **280**, 33026-33034, doi:M504587200 [pii] 10.1074/jbc.M504587200 (2005).

299 Serebriiskii, I., Estojak, J., Sonoda, G., Testa, J. R. & Golemis, E. A. Association of Krev-1/rap1a with Krit1, a novel ankyrin repeat-containing protein encoded by a gene mapping to 7q21-22. *Oncogene* **15**, 1043-1049, doi:10.1038/sj.onc.1201268 (1997).

300 Beraud-Dufour, S., Gautier, R., Albiges-Rizo, C., Chardin, P. & Faurobert, E. Krit 1 interactions with microtubules and membranes are regulated by Rap1 and integrin cytoplasmic domain associated protein-1. *FEBS J* **274**, 5518-5532, doi:EJB6068 [pii] 10.1111/j.1742-4658.2007.06068.x (2007).

301 Francalanci, F. *et al.* Structural and functional differences between KRIT1A and KRIT1B isoforms: a framework for understanding CCM pathogenesis. *Exp Cell Res* **315**, 285-303, doi:10.1016/j.yexcr.2008.10.006 (2009).

302 Clatterbuck, R. E., Eberhart, C. G., Crain, B. J. & Rigamonti, D. Ultrastructural and immunocytochemical evidence that an incompetent blood-brain barrier is related to the pathophysiology of cavernous malformations. *Journal of neurology, neurosurgery, and psychiatry* **71**, 188-192 (2001).

303 Tu, J., Stoodley, M. A., Morgan, M. K. & Storer, K. P. Ultrastructural characteristics of hemorrhagic, nonhemorrhagic, and recurrent cavernous malformations. *Journal of neurosurgery* **103**, 903-909, doi:10.3171/jns.2005.103.5.0903 (2005).

304 McDonald, D. A. *et al.* A novel mouse model of cerebral cavernous malformations based on the two-hit mutation hypothesis recapitulates the human disease. *Hum Mol Genet* **20**, 211-222, doi:ddq433 [pii] 10.1093/hmg/ddq433 (2011).

305 McDonald, D. A. *et al.* Fasudil decreases lesion burden in a murine model of cerebral cavernous malformation disease. *Stroke* **43**, 571-574, doi:STROKEAHA.111.625467 [pii] 10.1161/STROKEAHA.111.625467 (2012).

306 Zhang, J., Basu, S., Rigamonti, D., Dietz, H. C. & Clatterbuck, R. E. Krit1 modulates beta 1-integrin-mediated endothelial cell proliferation. *Neurosurgery* **63**, 571-578; discussion 578, doi:10.1227/01.NEU.0000325255.30268.B0 (2008).

307 Wilson, C. W. *et al.* Rasip1 regulates vertebrate vascular endothelial junction stability through Epac1-Rap1 signaling. *Blood*, doi:10.1182/blood-2013-02-483156 (2013).

308 Wallgard, E. *et al.* Identification of a core set of 58 gene transcripts with broad and specific expression in the microvasculature. *Arteriosclerosis, thrombosis, and vascular biology* **28**, 1469-1476, doi:10.1161/ATVBAHA.108.165738 (2008).

309 Ikram, M. K. *et al.* Four novel Loci (19q13, 6q24, 12q24, and 5q14) influence the microcirculation in vivo. *PLoS genetics* **6**, e1001184, doi:10.1371/journal.pgen.1001184 (2010).

310 Ando, K. *et al.* Rap1 potentiates endothelial cell junctions by spatially controlling myosin II activity and actin organization. *J Cell Biol* **202**, 901-916, doi:10.1083/jcb.201301115 (2013).

311 Wimmer, R., Cseh, B., Maier, B., Scherrer, K. & Baccarini, M. Angiogenic sprouting requires the fine tuning of endothelial cell cohesion by the Raf-1/Rok-alpha complex. *Dev Cell* **22**, 158-171, doi:10.1016/j.devcel.2011.11.012 (2012).

312 Birukova, A. A. *et al.* Association between adherens junctions and tight junctions via Rap1 promotes barrier protective effects of oxidized phospholipids. *J Cell Physiol* **226**, 2052-2062, doi:10.1002/jcp.22543 (2011).

313 Birukova, A. A. *et al.* Afadin controls p120-catenin-ZO-1 interactions leading to endothelial barrier enhancement by oxidized phospholipids. *J Cell Physiol* **227**, 1883-1890, doi:10.1002/jcp.22916 (2012).

314 Birukova, A. A., Zagranichnaya, T., Alekseeva, E., Bokoch, G. M. & Birukov, K. G. Epac/Rap and PKA are novel mechanisms of ANP-induced Rac-mediated pulmonary endothelial barrier protection. *J Cell Physiol* **215**, 715-724, doi:10.1002/jcp.21354 (2008).

315 Popoff, M. R. & Geny, B. Multifaceted role of Rho, Rac, Cdc42 and Ras in intercellular junctions, lessons from toxins. *Biochim Biophys Acta* **1788**, 797-812, doi:10.1016/j.bbamem.2009.01.011 (2009).

316 Burridge, K. & Wennerberg, K. Rho and Rac take center stage. *Cell* **116**, 167-179 (2004).

- 317 Yuan, S. Y. & Rigor, R. R. in *Regulation of Endothelial Barrier Function Integrated Systems Physiology: From Molecule to Function to Disease* (2010).
- 318 Bubik, M. F. *et al.* A novel approach to prevent endothelial hyperpermeability: the Crataegus extract WS(R) 1442 targets the cAMP/Rap1 pathway. *Journal of molecular and cellular cardiology* **52**, 196-205, doi:10.1016/j.yjmcc.2011.10.020 (2012).
- 319 Enserink, J. M. *et al.* A novel Epac-specific cAMP analogue demonstrates independent regulation of Rap1 and ERK. *Nat Cell Biol* **4**, 901-906, doi:10.1038/ncb874 ncb874 [pii] (2002).
- 320 Rehmann, H., Schwede, F., Doskeland, S. O., Wittinghofer, A. & Bos, J. L. Ligand-mediated activation of the cAMP-responsive guanine nucleotide exchange factor Epac. *J Biol Chem* **278**, 38548-38556, doi:10.1074/jbc.M306292200 (2003).
- 321 Baas, A. F. *et al.* Activation of the tumour suppressor kinase LKB1 by the STE20-like pseudokinase STRAD. *The EMBO journal* **22**, 3062-3072, doi:10.1093/emboj/cdg292 (2003).
- 322 Baas, A. F. *et al.* Complete polarization of single intestinal epithelial cells upon activation of LKB1 by STRAD. *Cell* **116**, 457-466 (2004).
- 323 Zeqiraj, E., Filippi, B. M., Deak, M., Alessi, D. R. & van Aalten, D. M. Structure of the LKB1-STRAD-MO25 complex reveals an allosteric mechanism of kinase activation. *Science* **326**, 1707-1711, doi:10.1126/science.1178377 (2009).
- 324 ten Klooster, J. P. *et al.* Mst4 and Ezrin induce brush borders downstream of the Lkb1/Strad/Mo25 polarization complex. *Developmental cell* **16**, 551-562, doi:10.1016/j.devcel.2009.01.016 (2009).
- 325 Martin-Belmonte, F. *et al.* PTEN-mediated apical segregation of phosphoinositides controls epithelial morphogenesis through Cdc42. *Cell* **128**, 383-397, doi:10.1016/j.cell.2006.11.051 (2007).
- 326 Shewan, A., Eastburn, D. J. & Mostov, K. Phosphoinositides in cell architecture. *Cold Spring Harbor perspectives in biology* **3**, a004796, doi:10.1101/cshperspect.a004796 (2011).
- 327 Gloerich, M. *et al.* Rap2A links intestinal cell polarity to brush border formation. *Nature cell biology* **14**, 793-801, doi:10.1038/ncb2537 (2012).
- 328 Cuppen, E. *et al.* A FERM domain governs apical confinement of PTP-BL in epithelial cells. *Journal of cell science* **112** (Pt 19), 3299-3308 (1999).
- 329 Bompard, G., Martin, M., Roy, C., Vignon, F. & Freiss, G. Membrane targeting of protein tyrosine phosphatase PTP11 through its FERM domain via binding to phosphatidylinositol 4,5-bisphosphate. *Journal of cell science* **116**, 2519-2530, doi:10.1242/jcs.00448 (2003).
- 330 Kozlov, G., Banville, D., Gehring, K. & Ekiel, I. Solution structure of the PDZ2 domain from cytosolic human phosphatase hPTP1E complexed with a peptide reveals contribution of the beta2-beta3 loop to PDZ domain-ligand interactions. *Journal of molecular biology* **320**, 813-820 (2002).
- 331 Myagmar, B. E. *et al.* PARG1, a protein-tyrosine phosphatase-associated RhoGAP, as a putative Rap2 effector. *Biochemical and biophysical research communications* **329**, 1046-1052, doi:10.1016/j.bbrc.2005.02.069 (2005).
- 332 Miaczynska, M. *et al.* APPL proteins link Rab5 to nuclear signal transduction via an endosomal compartment. *Cell* **116**, 445-456 (2004).
- 333 Miki, H., Yamaguchi, H., Suetsugu, S. & Takenawa, T. IRSp53 is an essential intermediate between Rac and WAVE in the regulation of membrane ruffling. *Nature* **408**, 732-735, doi:10.1038/35047107 (2000).
- 334 Spitzenberger, F. *et al.* Islet cell autoantigen of 69 kDa is an arfaptin-related protein associated with the Golgi complex of insulinoma INS-1 cells. *The Journal of biological chemistry* **278**, 26166-26173, doi:10.1074/jbc.M213222200 (2003).
- 335 Tarricone, C. *et al.* The structural basis of Arfaptin-mediated cross-talk between Rac and Arf signalling pathways. *Nature* **411**, 215-219, doi:10.1038/35075620 (2001).
- 336 Lim, W. G. *et al.* The C-terminus of PRK2/PKNgamma is required for optimal activation by RhoA in a GTP-dependent manner. *Archives of biochemistry and biophysics* **479**, 170-178, doi:10.1016/j.abb.2008.09.008 (2008).
- 337 Hodgkin, M. N. *et al.* Phospholipase D regulation and localisation is dependent upon a phosphatidylinositol 4,5-bisphosphate-specific PH domain. *Current biology : CB* **10**, 43-46 (2000).
- 338 Sciorra, V. A. *et al.* Identification of a phosphoinositide binding motif that mediates activation of mammalian and yeast phospholipase D isoenzymes. *The EMBO journal* **18**, 5911-5921, doi:10.1093/emboj/18.21.5911 (1999).
- 339 Oishi, K. *et al.* PKN regulates phospholipase D1 through direct interaction. *The Journal of biological chemistry* **276**, 18096-18101, doi:10.1074/jbc.M010646200 (2001).
- 340 Viswanatha, R., Ohouo, P. Y., Smolka, M. B. & Bretscher, A. Local phosphocycling mediated by LOK/SLK restricts ezrin function to the apical aspect of epithelial cells. *The Journal of cell biology* **199**, 969-984,

- doi:10.1083/jcb.201207047 (2012).
- 341 Schmitt, J. M. & Stork, P. J. Cyclic AMP-mediated inhibition of cell growth requires the small G protein
Rap1. *Molecular and cellular biology* **21**, 3671-3683, doi:10.1128/MCB.21.11.3671-3683.2001 (2001).
- 342 Watanabe, S. *et al.* Dietary docosahexaenoic acid but not eicosapentaenoic acid suppresses
lipopolysaccharide-induced interleukin-1 beta mRNA induction in mouse spleen leukocytes.
Prostaglandins Leukot Essent Fatty Acids **62**, 147-152, doi:S0952327800901340 [pii] (2000).
- 343 Arai, A. *et al.* Rap1 is activated by erythropoietin or interleukin-3 and is involved in regulation of beta1
integrin-mediated hematopoietic cell adhesion. *The Journal of biological chemistry* **276**, 10453-10462,
doi:10.1074/jbc.M004627200 (2001).
- 344 Birukova, A. A. *et al.* Role of Rho GTPases in thrombin-induced lung vascular endothelial cells barrier
dysfunction. *Microvascular research* **67**, 64-77 (2004).
- 345 Essler, M. *et al.* Thrombin inactivates myosin light chain phosphatase via Rho and its target Rho kinase
in human endothelial cells. *The Journal of biological chemistry* **273**, 21867-21874 (1998).
- 346 Kobayashi, K. *et al.* Prostaglandin D2-DP signaling promotes endothelial barrier function via the cAMP/
PKA/Tiam1/Rac1 pathway. *Arteriosclerosis, thrombosis, and vascular biology* **33**, 565-571, doi:10.1161/
ATVBAHA.112.300993 (2013).
- 347 Sun, H., Breslin, J. W., Zhu, J., Yuan, S. Y. & Wu, M. H. Rho and ROCK signaling in VEGF-induced microvascular
endothelial hyperpermeability. *Microcirculation* **13**, 237-247, doi:10.1080/10739680600556944 (2006).
- 348 Meijer, L. A. *et al.* Quantitative global phosphoproteomics of human umbilical vein endothelial cells after
activation of the Rap signaling pathway. *Molecular bioSystems* **9**, 732-749, doi:10.1039/c3mb25524g
(2013).
- 349 Castelo, L. & Jay, D. G. Radixin is involved in lamellipodial stability during nerve growth cone motility.
Molecular biology of the cell **10**, 1511-1520 (1999).
- 350 Lamb, R. F. *et al.* Essential functions of ezrin in maintenance of cell shape and lamellipodial extension in
normal and transformed fibroblasts. *Current biology : CB* **7**, 682-688 (1997).
- 351 Saleh, H. S. *et al.* Properties of an ezrin mutant defective in F-actin binding. *Journal of molecular biology*
385, 1015-1031, doi:10.1016/j.jmb.2008.11.051 (2009).
- 352 Zhu, L. *et al.* Comparative study of ezrin phosphorylation among different tissues: more is good; too much
is bad. *American journal of physiology. Cell physiology* **295**, C192-202, doi:10.1152/ajpcell.00159.2008
(2008).
- 353 Hatzoglou, A. *et al.* Gem associates with Ezrin and acts via the Rho-GAP protein Gmip to down-regulate
the Rho pathway. *Molecular biology of the cell* **18**, 1242-1252, doi:10.1091/mbc.E06-06-0510 (2007).
- 354 Eberth, A. *et al.* A BAR domain-mediated autoinhibitory mechanism for RhoGAPs of the GRAF family.
The Biochemical journal **417**, 371-377, doi:10.1042/BJ20081535 (2009).
- 355 Prouzet-Mauleon, V., Lefebvre, F., Thoraval, D., Crouzet, M. & Doignon, F. Phosphoinositides affect both
the cellular distribution and activity of the F-BAR-containing RhoGAP Rgd1p in yeast. *The Journal of
biological chemistry* **283**, 33249-33257, doi:10.1074/jbc.M805161200 (2008).
- 356 Machida, N. *et al.* Mitogen-activated protein kinase kinase kinase 4 as a putative effector of
Rap2 to activate the c-Jun N-terminal kinase. *The Journal of biological chemistry* **279**, 15711-15714,
doi:10.1074/jbc.C300542200 (2004).
- 357 Nonaka, H. *et al.* MINK is a Rap2 effector for phosphorylation of the postsynaptic scaffold protein TANC1.
Biochemical and biophysical research communications **377**, 573-578, doi:10.1016/j.bbrc.2008.10.038
(2008).
- 358 Taira, K. *et al.* The Traf2- and Nck-interacting kinase as a putative effector of Rap2 to regulate actin
cytoskeleton. *The Journal of biological chemistry* **279**, 49488-49496, doi:10.1074/jbc.M406370200
(2004).
- 359 Herrmann, L., Dittmar, T. & Erdmann, K. S. The protein tyrosine phosphatase PTP-BL associates with
the midbody and is involved in the regulation of cytokinesis. *Molecular biology of the cell* **14**, 230-240,
doi:10.1091/mbc.E02-04-0191 (2003).
- 360 Schmidt, A., Durgan, J., Magalhaes, A. & Hall, A. Rho GTPases regulate PRK2/PKN2 to control entry
into mitosis and exit from cytokinesis. *The EMBO journal* **26**, 1624-1636, doi:10.1038/sj.emboj.7601637
(2007).
- 361 Telkoparan, P. *et al.* Coiled-coil domain containing protein 124 is a novel centrosome and midbody
protein that interacts with the Ras-guanine nucleotide exchange factor 1B and is involved in cytokinesis.
PLoS one **8**, e69289, doi:10.1371/journal.pone.0069289 (2013).
- 362 Piekny, A., Werner, M. & Glotzer, M. Cytokinesis: welcome to the Rho zone. *Trends in cell biology* **15**,
651-658, doi:10.1016/j.tcb.2005.10.006 (2005).

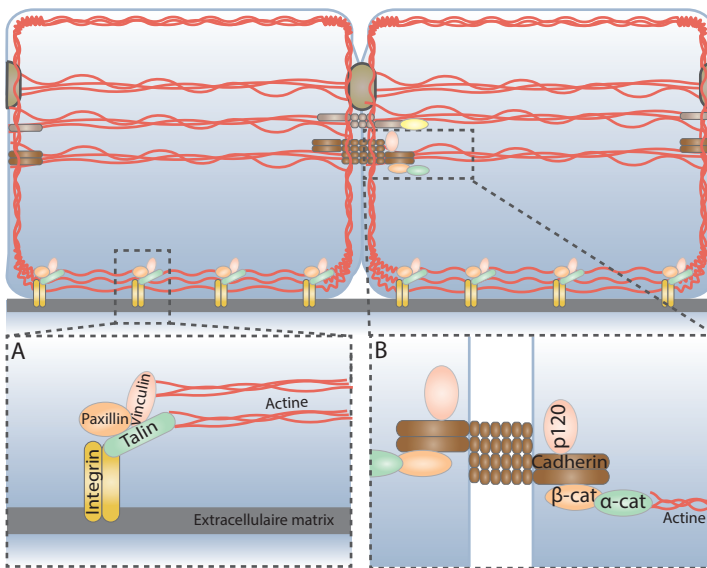
- 363 Miller, A. L. & Bement, W. M. Regulation of cytokinesis by Rho GTPase flux. *Nature cell biology* **11**, 71-77, doi:10.1038/ncb1814 (2009).
- 364 Wallace, S. W., Magalhaes, A. & Hall, A. The Rho target PRK2 regulates apical junction formation in human bronchial epithelial cells. *Molecular and cellular biology* **31**, 81-91, doi:10.1128/MCB.01001-10 (2011).
- 365 Vincent, S. & Settleman, J. The PRK2 kinase is a potential effector target of both Rho and Rac GTPases and regulates actin cytoskeletal organization. *Molecular and cellular biology* **17**, 2247-2256 (1997).
- 366 Erdmann, K. S. *et al.* The Adenomatous Polyposis Coli-protein (APC) interacts with the protein tyrosine phosphatase PTP-BL via an alternatively spliced PDZ domain. *Oncogene* **19**, 3894-3901, doi:10.1038/sj.onc.1203725 (2000).
- 367 Adyshev, D. M. *et al.* Ezrin/radixin/moesin proteins differentially regulate endothelial hyperpermeability after thrombin. *American journal of physiology. Lung cellular and molecular physiology* **305**, L240-255, doi:10.1152/ajplung.00355.2012 (2013).
- 368 Adyshev, D. M., Moldobaeva, N. K., Elangovan, V. R., Garcia, J. G. & Dudek, S. M. Differential involvement of ezrin/radixin/moesin proteins in sphingosine 1-phosphate-induced human pulmonary endothelial cell barrier enhancement. *Cell Signal* **23**, 2086-2096, doi:10.1016/j.cellsig.2011.08.003 (2011).
- 369 Bogatcheva, N. V. *et al.* Ezrin, radixin, and moesin are phosphorylated in response to 2-methoxyestradiol and modulate endothelial hyperpermeability. *American journal of respiratory cell and molecular biology* **45**, 1185-1194, doi:10.1165/rcmb.2011-0092OC (2011).

BEKNOPTE NEDERLANDSE SAMENVATTING (VOOR DE SEMI-LEEK)

Het menselijk lichaam bestaat uit miljarden cellen. Om te zorgen dat ze op hun plek blijven zitten, hechten die cellen aan elkaar en aan een extracellulaire matrix. Dit noemen we celadhesie en daarbij worden celadhesie-complexen gevormd. Er zijn ook cellen die juist door het lichaam bewegen, zoals bloedcellen, maar ook uitzaaiende kankercellen. Ook deze cellen zijn afhankelijk van celadhesie. De celadhesie-complexen kunnen hierbij gezien worden als de handen en voeten van de cel.

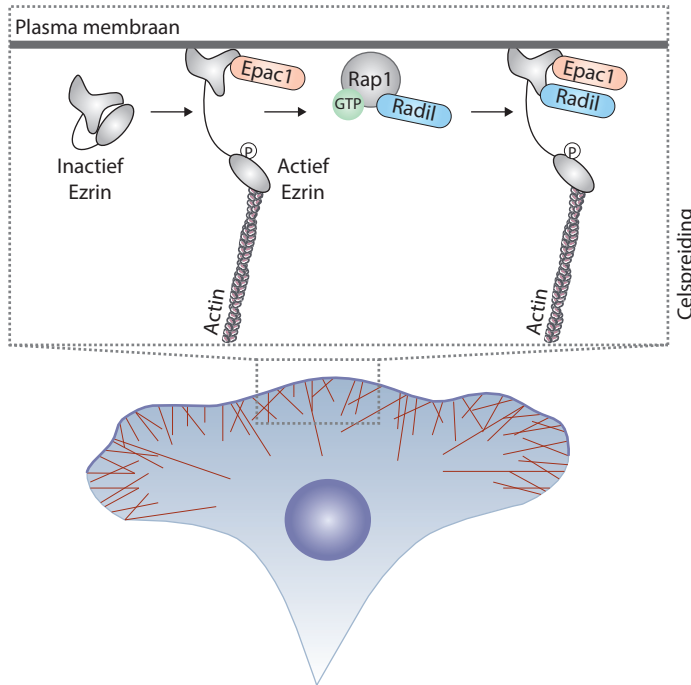
De adhesie van cellen aan elkaar en aan extracellulaire matrices moet gereguleerd worden en daarbij speelt het signaaleiwit Rap een belangrijke rol. De twee belangrijkste celadhesie-complexen die door Rap gereguleerd worden zijn de zogeheten 'focal adhesions', die de adhesie met de extracellulaire matrix aangaan, en 'adherens junctions', die zorgen voor de adhesie tussen twee cellen (Fig. 1). 'Focal adhesions' zijn opgebouwd uit een aantal verschillende eiwitten waarvan integrines de centrale spelers zijn. Integrines zijn eiwitten die door de celmembran heen naar buiten steken en daar direct aan matrixcomponenten kunnen binden. Binnenin de cel vormt zich dan een groot eiwitcomplex rondom de integrine, de 'focal adhesie'.

Ook 'adherens junctions' zijn opgebouwd uit een scala aan eiwitten, waarbij cadherin het belangrijkste eiwit is. Net als integrines steken cadherins door de plasmamembraan naar buiten. Daar kunnen ze binden aan cadherins van naastgelegen cellen. Net als bij integrines, vormt zich binnenin de cel rondom de cadherins een complex van een aantal eiwitten, dat de 'adherens junction' heet. Enkele



Figuur 1: 'Focal adhesie' en 'Adherens junction'.

Bovenste panel: Schematische tekening van twee cellen met daarin het actine cytoskelet (rood), 'focal adhesions' en cel-celadhesie componenten, waaronder 'adherens junctions'. (A) Uitvergroting van een 'focal adhesie' met daarin een aantal eiwitten die daar een belangrijke rol in spelen. Integrines steken door de plasmamembraan heen naar buiten en binden daar met de extracellulaire matrix. Binnenin de cel binden onder andere talin, vinculin en paxillin aan de integrines. Talin en vinculin binden ook aan het actine cytoskelet en verbinden daarmee het actine cytoskelet met de 'focal adhesions'. (B) Uitvergroting van een 'adherens junction' met daarin een aantal eiwitten die daar een belangrijke rol in spelen. Cadherins steken door de plasmamembraan naar buiten en binden daar met cadherins van de naastgelegen cel. Binnenin de cel binden onder andere p120-catenine, β -catenine en α -catenine. α -Catenine bindt ook het actine cytoskelet en verbindt daarmee het actine cytoskelet met de 'adherens junction'.



Figuur 2: Ezrin vormt een platform aan de plasmamembraan waar Epac1 en Radil samenkomen.

Onder invloed van het cytoskelet vindt celspreiding plaats. Wanneer Ezrin actief is kan het aan de plasmamembraan binden. Epac1 kan vervolgens aan actief Ezrin binden. Daardoor kan Epac1 lokaal Rap1 activeren aan de plasmamembraan. Radil bindt actief Rap1 en zal dus naar de plasmamembraan verplaatsen. Eenmaal daar kan Radil ook binden aan actief Ezrin.

eiwitten uit het 'focal adhesie' complex en 'adherens junction' complex kunnen rechtstreeks binden met het actine cytoskelet. De status van het actine cytoskelet beïnvloedt zo de status van de 'focal adhesies' en 'adherens junctions'.

Zoals ons skelet vorm geeft aan ons lichaam, zo heeft ook elke cel een skelet dat vorm geeft aan de cel. Dat noemen we het cytoskelet. Maar in tegenstelling tot het skelet van ons lichaam, is dat van een cel zeer dynamisch. Dit houdt in dat het cytoskelet kan groeien, krimpen en van vorm kan veranderen, afhankelijk van de behoeftes van de cel. Het cytoskelet bestaat uit drie componenten: actine, microtubuli en intermediaire filamenten. Naast het versterken van celadhesie, moduleert actief Rap ook het cytoskelet. Regulering van celadhesie kan door rechtstreeks de celadhesie-eiwitten te reguleren, maar kan ook door regulering van het cytoskelet dat gekoppeld is aan de celadhesie-eiwitten.

Rho GTPases, een familie van eiwitten, reguleren de dynamiek van het cytoskelet. De belangrijkste en best bestudeerde Rho GTPases zijn RhoA, Rac1 en Cdc42. Voor dit proefschrift heb ik onderzocht hoe het signaleiwit Rap het cytoskelet en de daarmee samenhangende celadhesie kan reguleren, door te signaleren naar Rho eiwitten. In het algemeen wordt gedacht dat verhoogde Rho activiteit, via de modulatie van het actine cytoskelet, resulteert in cellulair spanning. Rho doet dit onder andere door het gevormde actine cytoskelet te stabiliseren en te zorgen dat het samentrekt. Rac1 en Cdc42 zorgen er juist voor dat er minder spanning staat op het cytoskelet en dat dit kan groeien.

In **hoofdstuk 1** wordt uitgebreid besproken hoe Rap, met name Rap1, kan communiceren met de Rho GTPases RhoA, Rac1 en Cdc42. Rap1 doet dit in een aantal cellulair processen die allemaal afhankelijk zijn van de dynamiek van het cytoskelet. Onderzoek van de afgelopen 10 jaar wijst erop dat Rap1 de Rho GTPases RhoA, Rac1 en Cdc42 kan reguleren. Rap1 doet dit door ofwel de activiteit van die drie eiwitten te reguleren, of door te bepalen wáár in de cel de activiteit wordt gereguleerd. Het bepalen van de plaats in de cel waar de signaleringsroute plaatsvindt, kan grote implicaties hebben voor het biologische effect. In de literatuur lijkt er consensus te zijn dat Rap1 de activiteit van RhoA verlaagt,

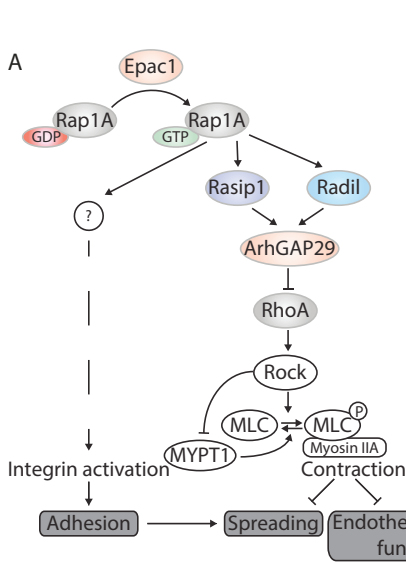
terwijl het de activiteit van Rac1 en Cdc42 verhoogt.

Hoofdstuk 2 beschrijft de resultaten van ons onderzoek naar hoe Rap celadhesie aan een extracellulaire matrix reguleert. Activatie van Rap1 zorgt ervoor dat er zich meer 'focal adhesions' vormen en dat de cel vervolgens gaat spreiden, een proces dat plaatsvindt onder leiding van het cytoskelet. Daarnaast kan het groeiende cytoskelet tegen de plasmamembraan duwen, waardoor de cel nog verder kan spreiden. Om te onderzoeken hoe Rap dit bewerkstelligt, hebben we gescreend naar eiwitten die door Rap1 gereguleerd zouden kunnen worden in dit proces. Hiervoor hebben we eiwitten onderzocht waarvan al bekend was dat het effectoren van Rap zijn, dus gereguleerd worden door Rap, of waarvan al bekend was dat zij een rol kunnen spelen in celadhesie. Door deze screen hebben we een aantal eiwitten kunnen identificeren die belangrijk zijn voor het induceren van celspreiding, maar niet celadhesie. Twee belangrijke eiwitten waren Radil, dat direct aan actief Rap1 kan binden, en Ezrin, een eiwit dat rechtstreeks aan het cytoskelet en de plasmamembraan kan binden.

Aangezien Radil en Ezrin allebei belangrijk bleken te zijn voor celspreiding, hebben we vervolgens gekeken of er een interactie is tussen Radil en Ezrin. De resultaten van dat onderzoek zijn beschreven in **hoofdstuk 3**. Ezrin behoort tot de familie ERM (ezrin/Radixin/Moesin) eiwitten, die allemaal sterk op elkaar lijken. We hebben ontdekt dat Radil onder bepaalde omstandigheden kan binden aan elk van deze eiwitten. Onder normale omstandigheden bevindt Radil zich in het cytosol. Actieve ERM eiwitten bevinden zich aan de plasmamembraan. We hebben sterke aanwijzingen gevonden dat Radil bindt aan actieve ERM eiwitten aan de plasmamembraan. Hier is echter wel eerst actief Rap1 voor nodig aan de plasmamembraan. Dus actief Rap1 aan de plasmamembraan zorgt ervoor dat Radil zich naar de plasmamembraan verplaatst, waarna het kan binden aan actieve ERM eiwitten aan de plasmamembraan. In het verleden is in ons lab aangetoond dat ERM eiwitten ook Epac1 kunnen binden. Epac1 is een activator van Rap1. ERM eiwitten brengen dus Epac1, dat Rap1 activeert, en Radil, dat gerecrueteerd wordt door actief Rap1, bij elkaar. Hierdoor zijn deze signaaleiwitten beter in staat hun signaal aan elkaar door te geven en bepalen de ERM eiwitten ook waar in de cel het signaal wordt doorgegeven (Fig. 2).

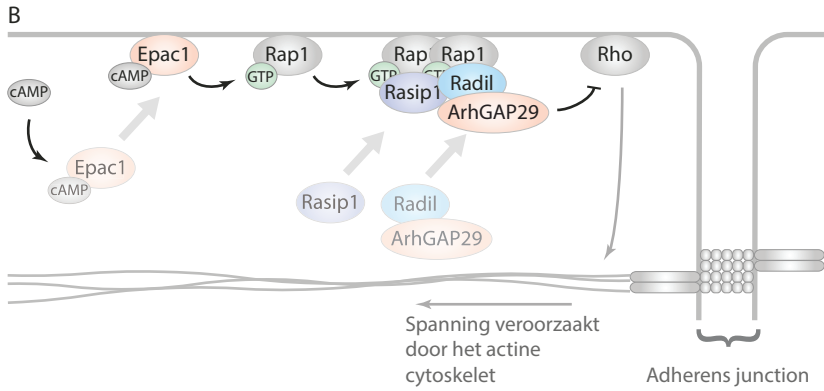
In **hoofdstuk 4** wordt de ontdekking beschreven dat een familielid van Radil, genaamd Rasip1, ook direct kan binden aan Rap1 en hierdoor Rap1-geïnduceerde celspreiding medieert. Daarnaast reguleren Radil en Rasip1 ook cel-celadhesie, wat we lieten zien in endotheelcellen. Deze cellen bekleden de wand van bloedvaten en hun belangrijkste functie is een barrière te vormen waarmee ze de passage van bloedcellen, vloeistoffen en macromoleculen reguleren. Door de cel-celadhesie te verhogen, creëer je een sterkere barrière. Het is al langer bekend dat activatie van Rap1 leidt tot een verhoogde cel-celadhesie en daarmee een versterkte barrièrefunctie. Radil en Rasip1 mediëren Rap1-geïnduceerde celspreiding en cel-celadhesie door aan te grijpen op het cytoskelet. Dit doen ze via hun bindingspartner ArhGAP29. ArhGAP29 is een enzym dat Rho inactiveert en dus het cytoskelet moduleert. Zoals verwacht is ook ArhGAP29 belangrijk voor Rap1-geïnduceerde celspreiding en verhoging van de endotheliale barrière. Wij hebben laten zien dat Rap1, via Radil, Rasip1 en ArhGAP29, zorgt voor verminderde spanning op het cytoskelet. Door deze verminderde spanning is de cel in staat om verder te spreiden en kan het zijn barrièrefunctie verhogen (Fig. 3).

Waar we in het in hoofdstuk 4 beschreven onderzoek de componenten van een signaleringsroute hebben gevonden, beschrijft **hoofdstuk 5** ons onderzoek naar hoe de signaaltransductie mechanistisch tot stand komt. In afwezigheid van actief Rap1 bevindt Radil zich in het cytosol, terwijl Rasip1 een stippenpatroon vormt in het cytosol. Actief Rap1 bevindt zich voornamelijk aan de plasmamembraan. Doordat Radil en Rasip1 rechtstreeks kunnen binden aan actief Rap1 verplaatsen zij zich naar de plasmamembraan wanneer Rap1 geactiveerd wordt. Ook ArhGAP29 verplaatst zich naar de plasmamembraan. De verplaatsing van ArhGAP29 na activatie van Rap1 wordt gemedieerd door Radil, omdat Radil direct bindt aan ArhGAP29. Rasip1 gaat onafhankelijk van Radil en ArhGAP29 naar



Figuur 3: Radil, Rasip1 en ArhGAP29 mediëren Rap1-geïnduceerde celspreiding en endotheliale barrièrefunctie.

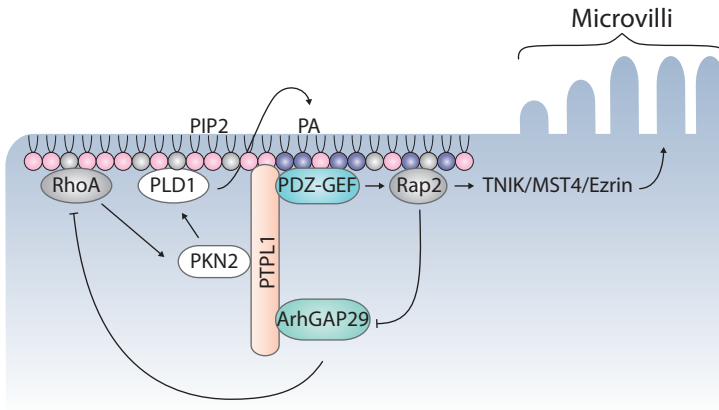
(A) Schematische weergave van de signaleringsroute die door Rap1 wordt geactiveerd. Via Radil en Rasip1 reguleert Rap1 ArhGAP29. Vervolgens inactieveert ArhGAP29 Rho. Door de inactivering van Rho vermindert de hoeveelheid spanning in de cel die door het actine cytoskelet gegenereerd wordt, waardoor de cel kan spreiden en een verhoogde endotheliale barrière vormt. (B) Schematische weergave van de mechanische regulatie van de signaleringsroute weergegeven in A. Doordat Epac1 cAMP bindt, wordt deze geactiveerd en bindt Epac1 aan de membraan. Daar activeert Epac1 Rap1, die aan de membraan zit. Rasip1 en Radil verplaatsen zich onafhankelijk van elkaar naar de plasmamembraan door aan actief Rap1 te binden. Doordat Radil aan ArhGAP29 bindt, verplaatst ArhGAP29 zich ook naar de plasmamembraan. Eenmaal daar vormen Radil, ArhGAP29 en Rasip1 een complex met elkaar. Hierdoor kan ArhGAP29 Rho inactiveren waardoor het actine cytoskelet ontspant.



de plasmamembraan. Daar aangekomen, vormen Radil en ArhGAP29 een complex met Rasip1. Wij vermoeden dat de binding van Rasip1 aan dit complex essentieel is voor de functie van dit complex, omdat alle drie de componenten essentieel zijn voor Rap1-geïnduceerde modificaties van het cytoskelet en cel-celadhesie.

Rap1 speelt dus een essentiële rol in de regulering van de barrière van endotheel-cellen. Er zijn verscheidene inputsignalen die leiden tot de activatie van Rap1 in endotheelcellen. De vertaling van deze verschillende inputsignalen naar de activatie van Rap1 gebeurt dus ook via verschillende Rap1-activatoren. Eenmaal geactiveerd, moet Rap1 het cytoskelet moduleren om de barrièrefunctie van de endotheelcellen te verhogen. Wij hebben laten zien dat dit onder andere gebeurt door Rho te inactiveren. Maar ook activatie van Cdc42 en Rac1 door Rap1 speelt een rol in dit proces. Dit alles hebben wij besproken in **hoofdstuk 6**.

In tegenstelling tot de vorige hoofdstukken hebben we tot slot een cytoskelet-afhankelijk, maar celadhesie-onafhankelijk proces onderzocht, en beschreven in **hoofdstuk 7**. Het lumen van onze darmen wordt hermetisch afgesloten van de onderliggende weefsels door een enkele laag cellen, de intestinale epitheelcellen. Naast het vormen van de scheidingswand tussen het lumen en de onderliggende weefsels, zijn deze epitheelcellen ook verantwoordelijk voor de opname van



Figuur 4: PTPL1 vormt een platform voor Rap2 en Rho communicatie en bepaalt waar microvilli gevormd worden.

Tekening van een intestinale epitheelcel waar schematisch een deel van de binnenzijde van de plasmamembraan en een gebied waar microvilli vormen wordt weergegeven. PTPL1 bindt aan de plasmamembraan daar waar de microvilli gevormd dienen te

worden. PTPL1 bindt PDZ-GEF waardoor deze ook op de plek zit waar microvilli gevormd moeten worden. PDZ-GEF activeert daar Rap2. Actief Rap2 kan via TNIK, Mst4 en Ezrin de vorming van microvilli induceren. Verder bindt en inactieveert Rap2 ArhGAP29. ArhGAP29 bindt ook PTPL1 en bevindt zich dus waar de microvilli gevormd moeten worden. Doordat ArhGAP29 geïnactiveerd wordt door Rap2 zal de Rho activiteit verhoogd zijn. Actief Rho activeert op zijn beurt PKN2, dat ook aan PTPL1 bindt. PLD1 zorgt voor de vorming van fosfatidezuur, wat nodig is voor de activatie van PDZ-GEF.

voedingsstoffen uit ons eten. Om te zorgen dat deze cellen dit op een efficiënte wijze kunnen doen, vergroten ze aan de lumenale kant hun oppervlakte door een heleboel kleine uitstulpingen te maken, microvilli genaamd. Het cytoskelet geeft vorm en stevigheid aan de microvilli en de vorming van deze microvilli is onafhankelijk van celadhesie. Het is al bekend dat Rap2 een essentiële rol speelt bij de vorming van microvilli. Door de activatie van een signaleringsroute bestaande uit TNIK, Mst4 en Ezrin kan actief Rap2 de vorming van microvilli induceren. Activatie van Rap2 in dit proces gebeurt door PDZ-GEF (Fig. 4). Hier hebben we gevonden dat het eiwit PTPL1 een platform vormt voor Rap2 en Rho communicatie. In de intestinale epitheelcel bevindt PTPL1 zich op de plek waar Rap2 geactiveerd dient te worden. PTPL1 bindt rechtstreeks aan PDZ-GEF, de activator van Rap2. Het is dus plausibel dat PTPL1 ervoor zorgt dat PDZ-GEF op de juiste locatie in de cel Rap2 kan activeren. Verder bindt PTPL1 ook ArhGAP29. ArhGAP29 wordt op zijn beurt geïnactiveerd door actief Rap2. Bovendien hebben wij gevonden dat ArhGAP29 belangrijk is voor de vorming van microvilli. ArhGAP29 inactieveert op zijn beurt weer Rho, de masterregulator van het cytoskelet. Wij hebben gevonden dat zowel te veel als te weinig activiteit van Rho de vorming van microvilli voorkomt. Actief Rho kan vervolgens PKN2 reguleren, dat ook bindt aan PTPL1 en nodig is voor de vorming van microvilli. Actief PKN2 activeert het enzym PLD1. PLD1 zorgt voor de vorming van het plasmamembraanlipide fosfatidezuur, dat belangrijk is voor de functie van PDZ-GEF in dit proces. Dus de bindingspartners van PTPL1, PDZ-GEF, ArhGAP29 en PKN2, zijn alle drie nodig voor de vorming van microvilli. Ook de betrokken signaleiwitten Rap2 en Rho zijn essentieel voor microvilli-vorming. Het lijkt erop dat PTPL1, door bij de microvilli te lokaliseren, ervoor zorgt dat deze eiwitten op de juiste plek in de cel samenkomen en dus bepaalt waar de microvilli gevormd worden.

Samenvattend hebben we in dit proefschrift een signaleringsroute ontrafeld via welke Rap1 en Rap2 de activiteit van Rho, en daarmee de dynamiek van het cytoskelet, kunnen reguleren. De resultaten beschreven in de **hoofdstukken 3, 5 en 7** beschrijven tevens manieren waarop de lokalisatie van deze signaleringsroute bepaald kan worden. In **hoofdstuk 8** hebben we de implicaties van onze bevindingen uitgebreid bediscussieerd.

CURRICULUM VITAE

Anneke Post werd geboren op 19 maart 1983 te Boston, MA, Verenigde Staten. In 2001 behaalde zij haar atheneumdiploma aan het Sint Bonifatius Lyceum te Utrecht. Hetzelfde jaar begon zij met de opleiding Geneeskunde aan de Vrije Universiteit van Amsterdam. Na twee jaar besloot zij over te stappen naar de opleiding Biomedische Wetenschappen aan de Universiteit van Utrecht. Na afronding van haar Bachelor, begon zij in 2006 aan de Master Biology of Disease, die ze in 2009 cum laude afrondde. Tijdens deze Masteropleiding heeft Anneke een onderzoekstage van 9 maanden gedaan bij de afdeling Metabole en Endocriene Ziekten in het Wilhelmina Kinderziekenhuis, UMC Utrecht, onder begeleiding van dr. Ellen Jeninga in het lab van dr. Eric Kalkhoven. Anneke heeft een tweede onderzoekstage van 6 maanden gedaan bij de afdeling Obstetrics, Gynecology & Reproductive Sciences aan de University of California San Francisco, in het lab van prof. dr. Susan Fisher. In juli 2009 is Anneke begonnen als onderzoeker in opleiding bij de afdeling Molecular Cancer Research, UMC Utrecht, in het laboratorium van prof. dr. Hans Bos, waar ze gewerkt heeft aan het onderzoek beschreven in dit proefschrift.

PUBLICATION LIST

Post, A., Pannekoek, W.J., Ponsioen, B., Vliem, M.J., Bos, J.L. (2014) Rap1 spatially controls ArhGAP29 to inhibit Rho signaling during endothelial barrier regulation.

To be submitted.

Pannekoek, W.J., **Post, A.**, Bos, J.L. (2014). Rap1 signaling in endothelial barrier control.

Cell Adhesion and Migration 8(2).

Post, A., Pannekoek, W.J., Ross, S.H., Verlaan, I., Brouwer, P.M., Bos, J.L. (2013). Rasip1 mediates Rap1 regulation of Rho in endothelial barrier function through ArhGAP29.

PNAS 110(28): 11427-11432.

Ross, S.H., Spanjaard, E., **Post, A.**, Vliem, M.J., Kristyanto, H., Bos, J.L., de Rooij, J. (2012). Rap1 can bypass the FAK-Src-Paxillin cascade to induce cell spreading and focal adhesion formation.

PLoS ONE 7(11): e50072.

Ross, S.H., **Post, A.**[†], Raaijmakers, J.H.[†], Verlaan, I., Gloerich, M., Bos, J.L. (2011). Ezrin is required for efficient Rap1-induced cell spreading.

Journal of Cell science 124(11): 1808-1818.

[†]These authors contributed equally to this work.

DANKWOORD

Hoe ironisch. Nadat 161 pagina's tekst zo uit mijn digitale pen zijn gevloeid, met nog zo'n vier te gaan, is daar dat onafwendbare moment: een 'writer's block'. Het zal wel iets te maken hebben met de lading van het volgende stuk en omdat, laten we eerlijk zijn, voor de meesten van jullie de volgende vier pagina's de enige pagina's van dit boek zullen zijn die jullie daadwerkelijk gaan lezen. So, without further ado...

Hans, ik moet je opbiechten dat, toen ik voor het eerst bij jou op gesprek kwam, ik niet helemaal door had dat het om een sollicitatiegesprek ging. Ik weet niet wat ik dacht. Ik weet alleen dat ik anderhalf uur later op de fiets naar huis zat met een promotieplek op zak! Maar het is een goede keus gebleken. Je hebt me de vrijheid gegeven om me te ontwikkelen op zowel het wetenschappelijke als het persoonlijke vlak. Geen enkel idee was te gek zolang het maar goed onderbouwd was, en met name de discussies over politiek in de wetenschap waren ontzettend leerzaam. Het was me een genoegen om bij te mogen dragen aan jouw levenswerk: Rap-biologie! (En ook een beetje Rho! Ha!) Dankjewel.

Mijn paranimfen:

SAH!! Fellow coffee and shopping addict! Dr.! It was gr8 being ur default roomm8, whthr it was in d office, @ a meeting or @ a retreat. I'm gonna miss ur funky naivety and habits (yes, Italians can get sunburnt in Holland and I'm pretty sure that solely eating carrots is not what they mean with 'a healthy diet'). GL2U getting settled in Lux and keep your i's on the prize: Australia!!

Jasmin. Crazy hoeveel wij gemeen hebben. Ik mocht het stokje al aan je doorgeven op de basisschool, middelbare school, studie, (SF, soort van) en nu ook met de promotie. En hoe beter je promotie te beginnen dan als paranimf, dan kun je alvast wennen aan hoe het is om daar vooraan te staan. Na vijf jaar luisteren naar mijn verhalen over mijn PhD en alles daaromheen mag ik nu vijf jaar luisteren naar jouw promotieperikelen. Veel succes en plezier bij Hugo en Jacco!

De bosjes! Fried, het is allemaal begonnen bij jou met mijn master thesis. Pas jaren later begreep ik dat ik een onderwerp had bedacht dat echt in jou straatje lag! Aan het eind stelde je voor om eens met Hans te gaan praten. Misschien had ik daarom niet door dat het om een sollicitatiegesprek ging! Dank voor alle input en dat je een oogje in het zeil hield. Veel succes toegewenst! **WJ**, je hebt een plekje in mijn hart veroverd en niet alleen omdat je zo vaak op zondag naar het lab bent gegaan voor mij! Je bent een bijzonder mens. Mijn PhD was lang niet zo leuk geweest zonder jouw galgenhumor, karaoke en uren kleppen met een bakkie koffie. Tof dat ik de laatste twee jaar zo nauw met je heb mogen samenwerken! Keep Radil and Rasip1 alive! **Marjolein**, wat heb ik jou gemist tijdens jouw zwangerschapsverlof! Maar liefst drie van de hoofdstukken uit dit boek zijn er mede dankzij jou en je hebt me veel werk uit handen genomen, dankjewel. Een echt werkpaard en doorzetter! Veel succes met je verdere carrière en veel geluk met je gezin! **Ingrid**, je hebt een prachtige bijdrage geleverd aan dit boek (eindeloos veel spreading en adhesion assays), dankjewel daarvoor. Er zijn weinig analisten (en AIO's!) die zoveel uren maken als jij. Ze mogen in hun handjes knijpen met jou bij de organoid groep! **The coffee club**, a.k.a. **WJ, SAH, Patricia, René** en **Lucas**, drinking coffee will never be the same again ☺. **Patricia**, prachtig om te zien hoe je van een onzekere studente in een zelfverzekerde dame bent veranderd de afgelopen vier jaar. Veel succes bij Genmap! **René**, de schakel in de groep: de enige die Rap met organoids combineert. Succes hier, maar ook met het uitzoeken van wat je in de toekomst wil. **Lucas**, ik heb je ontmaskerd, je bent een nep-autist. Lekker nukkig doen totdat er een paar biertjes in zitten en dan is de uitknop niet meer te vinden! Nu ik mijn proefschrift echt heb afgerond, wordt het tijd dat wij eens gaan babbelen over het PTPL1 project. Kan nog een mooi hoofdstukje voor je worden!

Holger, too bad we never had the chance to explore how ArhGAP29 functions mechanistically. Thanks for all the cloning tips and tricks and all the best for the future! **Bas!** Je komt over als een warhoofd maar bent zo gestructureerd, heerlijk! Dank voor alle uren werk aan de RhoFRET proeven. Helaas hebben ze dit boekje niet gehaald, maar hopelijk wel de publicatie! **Hugo**, pas je een beetje op mijn kleine zusje? Je groep groeit als kool, succes! **Carla**, succes met je organoid werk maar vooral succes met je ‘multi-organoid’ (a.k.a. baby)! **Koen**, als je voetbalcarrière niets wordt, kun je altijd nog actrice worden. Een verborgen talent! Succes met de organoids!

Bos-oldies, **Martijn, Lars, On Ying, Anouk, Marlous, Milicia, Nayara** en **Jorien**. Thanks for all the fun borrels, dinners, retreats, etc. and good luck with all your future careers. Special thanks to **Sarah R.** You introduced me to the world of Rap and cell spreading. I miss your Scottish accent, ‘Ezrin’ never sounds as great when I say it. All the best for the future!!

Maike, mijn beste student ooit! Je moet niet zo streng zijn voor jezelf. Zonder jou was hoofdstuk 7 er niet geweest. Laat je niet gek maken door iedereen om je heen die precies lijkt te weten waar hij heen gaat. Ik doe ook maar wat... Succes!

Vijf jaar Bos betekent ook vijf jaar de **Burgering/Dansen-groep**. Helaas hebben wij de maatschappelijke segregatie niet buiten de deur weten te houden, en zijn we in de afgelopen vijf jaar van de Bos-Burgering groep naar de Bos en Burgering groepen getransformeerd. Maar zoals heel Nederland zich deze zomer zal verenigen tijdens het WK, weten wij elkaar uitstekend te vinden tijdens praatjes, meetings, koekjestijd, en borrels. Dank voor alle gezelligheid! **Boudewijn** en **Tobias**, dank voor alle interesse en input in mijn projecten. **Martin, Marieke, Harmjan** and **Maria**, good luck with your projects! **David**, almost there! Succes met de laatste loodjes! **Astrid, Marrit** en **Maike**, dank voor de gezellige tijd! Succes met jullie post-docs (je bent gek als je dat niet gaat doen, Astrid)! **Evi**, graduating two weeks before me. Good luck! **Lydia, Miranda, Paulien, Maike** en **Kim**, de spullen van de Burgering/Dansen-groep! Succes!

De Rooij groep. De nieuwste aanwinst op onze afdeling en met een onderwerp dat goed aansluit bij onze groep ook een zeer welkome aanwinst! **Johan**, een fanatiekeling tijdens werkbesprekingen. Dank voor je input een feedback, met name tijdens de jaarlijkse OIO-evaluaties. **Emma**, toch ook een beetje Bos. Dank voor de hulp en input de afgelopen jaren. Succes met de allerlaatste loodjes! **Joppe, Mitchel** en **Gerard**, veel succes met jullie projecten.

Marianne, Christina en **Betty**, de dames die alles weten. Jullie zijn onmisbaar! **Marianne**, nu hoef je me eindelijk niet meer met mailtjes te bestoken over mijn vrije dagen 😊 (maar ik zal die humoristische mailtjes wel gaan missen, hoor!).

MEZ-, Kops-, Lens-, Timmers-, Vermeulen-, Holstege-labs en het **DNA-lab**: Dank voor de goede sfeer, gezellige labstapdagen, borrels en input tijdens de BWDs. **Marian, Marjoleine, Cheuk** en **Marcel**, bedankt dat jullie altijd alles zo netjes op orde houden. **Livio**, dank voor alle hulp bij mijn confocal werk. Ik had het niet zonder je gekund! Ik hoop dat je snel werk kunt vinden in Australië, al zal het een aderlating zijn voor het Stratenum! **Rutger**, mister Nespresso! Dit is niet het eerste boekje en zal zeker niet het laatste boekje zijn dat geschreven is onder invloed van een ‘caffeine high’. Thanks for feeding my addiction! **ICT-ers**, dank voor alle keren dat jullie mij uit de brand hebben geholpen (vooral toen de scanner mijn paspoort had opgegeten).

De leden van de leescommissie: **Boudewijn Burgering, René Medema, René Bernards, Hans Clevers** en **Peter Hordijk**, bedankt voor het lezen en beoordelen van mijn proefschrift.

Ook buiten de academische wereld hebben veel mensen indirect bijgedragen aan mijn promotietijd. Helaas heb ik hier niet de ruimte om iedereen persoonlijk te bedanken, want er zijn zoveel lieve vrienden, familie en kennissen om mij heen geweest die altijd met me mee hebben geleefd en interesse hebben getoond in mijn werk (vaak gepaard gaande met een glazige blik zodra ik probeerde uit te leggen wat ik deed). Aan jullie allen, dankjewel daarvoor. Vooral wanneer je zelf even niet meer weet waarom je in godsnaam weken zit te pielen aan de kleinste details, is het ontzettend leuk als mensen om je heen zo enthousiast zijn over je onderzoek.

Expliciet wil ik nog wel mijn vriendinnetjes van **jc Bliksem** bedanken. Jullie waren het beste op de hoogte van al het reilen en zeilen omtrent mijn promotie de afgelopen jaren. Dank voor alle interesse in mijn werk en vooral voor de nodige ontspanning in de vorm van diners, borrels, feestjes, weekendjesweg en vakanties de afgelopen jaren. Onze onvoorwaardelijke vriendschap is van onschatbare waarde.

Boonhouse! Lieve **Janandries**, **Gelske**, **Tjarda**, **Jasper** en **Nikki**, ik denk dat er niemand zo hard voor mij heeft staan juichen als jullie deden toen ik de datum voor mijn verdediging had! Tof! Dankjulliewel voor al het toejuichen, meelevens en de interesse in mijn onderzoek de afgelopen maanden en jaren. **Gelske** en **Janandries**, dankjulliewel dat jullie mij menig maal hebben opgelapt toen ik het eind van mijn Latijn had bereikt. Special thanks to **Jappie**: jouw creativiteit met woorden heeft zijn sporen achtergelaten in mijn boek, zie achterzijde!

Pap en Lodewijk. Eigenlijk hadden we een soort case study moeten maken van onze familie, met Jasmin en mij als proefpersonen. Waren we genetisch gedoemd om de wetenschap in te gaan of heeft de dagelijkse blootstelling aan een labrat ons naar de weg tot de wetenschap geleid (of misschien is het gewoon omdat de weg tot de wetenschap praktisch langs ons ouderlijkhuus loopt)? Wie zal het zeggen? Ik vond het in elk geval fijn dat ik de afgelopen jaren bij jullie beiden af en toe mijn frustraties over het lab kon spuien of juist kon juichen over mijn prestaties (en dat jullie ook echt begrepen waar ik het over had!). Maar wat ik het allermeest waardeer is dat jullie beiden mij aanmoedigen om mijn eigen weg te volgen, of dat nu in de wetenschap is of niet. Lieve **Lodewijk**, dank voor al je steun en hulp (vooral met alle Nederlandse teksten). Lieve **Pap**, dankjewel dat je ervoor hebt gezorgd dat jullie alle drie erbij zijn op 30 juni. Dat betekend ontzettend veel voor mij.

Lieve **Mam**, gelukkig heb je, zoals je zelf zegt, een zwak voor nerds. Anders was het leven voor jou toch een stuk zwaarder geweest met nerds als man en dochters. Juist het feit dat ik alles behalve wetenschap met jou kan delen, vind ik heerlijk. Graag wil ik ook van deze gelegenheid gebruik maken om aan al mijn collega's te laten weten dat het jouw genen zijn die ervoor hebben gezorgd dat ik ALTIJD mijn pinpas kwijt ben!! Love you, xx Cara **Isa**, I've tried to think of another bombshell I could drop on you, but I think I am all out (I mean, really, how many life changing events can one fit in a year??). Although we both fit the geek profile, we mostly bond over fashion, theater and cooking. I think you are a role model of how women can and should combine a top career with having a family. Be proud of that! Lieve **Maarten** en **Sanne**, het feit dat jullie deur altijd open staat is van onschatbare waarde. 'Gezelligheid' is jullie tweede naam! Koester dat. Dank voor alle interesse de afgelopen jaren. **Hugo**, Stefan heeft nog wel wat 'hoe overleef ik de promotie van mijn vriendin'-tips voor je! Succes! And **Alex**, I'm going to do the 'big sister talk' with you. Now that you will be going to uni make sure to get good grades and do enough extracurriculars, one day you might want to get your PhD as well, and on the weekends: party as much as you can!! It'll all be over before you know it! Enjoy!!

En dan tot slot, mijn liefste. **Stefan**. Dit boek had er een stuk minder fraai uitgezien zonder jouw hulp. De afgelopen maanden ben ik thuis gekomen naar een gedekte tafel en gespreid bedje. Wat een luxe!

De afgelopen jaren heb je me aangemoedigd en de ruimte gegeven om mezelf te ontplooiën, met hier en daar een kritische noot om me scherp te houden. Nu is het jouw beurt en ik ben je grootste supporter. Zoals jij laatst zei: Wie had dit gedacht toen we 10 jaar geleden in de Nieuwe Dikke Dries stonden? Er staat ons een groot avontuur te wachten. Ik ben trots dat ik dat avontuur met jou mag aangaan en ben intens gelukkig aan jouw zij. Ik hou van jou.

Anneke